SYNTHESIS, CHARACTERIZATION AND REACTIVITY OF ELECTROPHILIC ORGANOMETALLIC COMPOUNDS OF RUTHENIUM, TANTALUM AND SILICON

A Dissertation

by

RODRIGO RAMIREZ

Submitted to the Office of Graduate and Professional Studies of
Texas A&M University
in partial fulfillment of the requirements for the degree of

DOCTOR OF PHILOSOPHY

Chair of Committee,	Oleg V. Ozerov
Committee Members,	Marcetta Y. Darensbourg
	Kim R. Dunbar
	Sandun Fernando
Head of Department,	François Gabbaï

December 2014

Major Subject: Chemistry

Copyright 2014 Rodrigo Ramírez

ABSTRACT

The work presented herein will discuss the synthesis, characterization and reactivity of electrophilic organometallic compounds of ruthenium, tantalum, and silicon in order to explore unusual properties, reactivity, or structure. Several of the chemical species described are cationic, electronically and coordinatively unsaturated, and require the use of weakly coordinating anions in order to retain their high electrophilic character.

The first study consisted in the devolpment of a method to synthesize C–alkylated carborane anions of the type $[RCB_{11}Cl_{11}]^-$ (R = Me, Et, Pr, Bu, Hex) was developed, in order increase the solubility of its salts in weakly coordinating organic solvents. Salts of these C–alkylated anions form crystalline compounds. On the basis of this work, the possibility of the synthesis of a silylium–like zwitterionic compound was investigated. The compound was designed around the anionic $[CB_{11}Cl_{11}]^-$ fragment, attached covalently via the C–vertex to a silylium–type cation through a methylene linker. Its synthesis was succesfuly achieved, and an X–ray diffraction study of this compound revealed that the cationic silicon center is stabilized intramolecularly by weak coordination to a chlorine atom on the *ortho* B–Cl ring of the anionic fragment. This compound retains the fundamental structural and chemical features of its two–component counterparts, but it is extraordinarily insoluble in weakly coordinating organic solvents. This feature can be traced back to the inherent molecular symmetry and charge distribution.

The synthesis of a family of d^6 ML_5 and d^6 ML_6 ruthenium triflate complexes of the pincer $(P_2C=)Ru(X)$ (X = Cl, H, OAc, acac) architecture by ligand exchange using Me_3SiOTf will be presented. It was speculated that metathesis of chloride with the more weakly coordinating triflate would be a convenient way to generate compounds that could be potential Lewis–acidic precatalysts. These compounds can be regarded as synthetic equivalents of truly cationic complexes, with the added advantage that no need for the isolation of highly reactive species is necessary. Finally, the reactivity of $(\eta^5\text{–}C_5Me_5)Ta(\equiv CPh)(PMe_3)_2Cl$ towards internal and terminal alkynes was investigated. In addition to this, chloride abstraction from $(\eta^5\text{–}C_5Me_5)Ta(\equiv CPh)(PMe_3)_2Cl$ was effected, in order to potentially enhance any reactivity towards internal and terminal alkynes. It was found that, upon chloride abstraction from neutral $(\eta^5\text{–}C_5Me_5)Ta(\equiv CPh)(PMe_3)_2Cl$, a reversible C–H bond activation process at PMe_3 takes place, concomitant with protonation of the carbyne to form two cationic, isomeric alkylidenes of the type $[(\eta^5\text{–}C_5Me_5)Ta(=CHPh)(CH_2PMe_2)(PMe_3)]^+$. In terms of reactivity towards alkynes, it was found that both the neutral and cationic systems form stable tantalacyclobutadienes, one of which was characterized structurally through an X–ray diffraction study.

DEDICATION

I dedicate this work to my family, to the ones who were, are and will be.

ACKNOWLEDGEMENTS

I would like to thank my advisor, Dr. Oleg V. Ozerov, for the opportunity given to join his research group, for his guidance, and all the knowledge acquired from him over the course of my research work.

My gratitude is also extended to my committee members, Dr. Marcetta Y. Darensbourg, Dr. Kim R. Dunbar, and Dr. Sandun Fernando for taking the time to review my work.

Thanks also go to all of my colleagues in the Ozerov group.

I also would like to thank Dr. Nattamai Bhuvanesh for his expert advice, timely help and useful discussion in crystallography, and Dr. Yohannes Rezenom at the Laboratory for Biological Mass Spectrometry for the countless times I received his help.

I want express my gratitude to Sandy Manning for all her abundant help and generous patience through my stay at the Graduate Program in Chemistry.

Thank you to Jessica Wiederkehr for everything she has done for me. I am grateful to you more than I can describe in a few words. Ich liebe dich.

Thank you to all the wonderful people I have met during my years at Texas A&M who opened their lives to me, and who also have become dear to my heart. Meeting them alone has made my experience here worthwhile.

Thank you to Oscar H. Torres, which over the course of my life has become a true brother. Your loyalty is one of the biggest treasures I possess.

Thank you to my grandparents Max and Gloria Ramírez, for all their love, care, and patience throughout my life. I cannot express in words my gratitude and love for you.

Last, but not least, thank you to my parents Max and Tere for their love, support, encouragement, and life lessons throughout these years.

NOMENCLATURE

NMR	Nuclear Magnetic Resonance
VT NMR	Variable Temperature Nuclear Magnetic Resonance
CP	Cross Polarization
MAS	Magic Angle Spinning
Cp	Cyclopentadienyl
Cp*	Pentamethylcyclopentadienyl
THF	Tetrahydrofuran
DFT	Density Functional Theory
HOMO	Highest Occupied Molecular Orbital
LUMO	Lowest Unoccupied Molecular Orbital
WCA	Weakly Coordinating Anion
Acac	Acetylacetonate
OAc	Acetate
OTf	Triflate
OEt_2	Diethyl ether
n–Bu	*n*–Butyl
^{t}Bu	*tert*–Butyl
n–BuLi	*n*–Butyllithium
^{i}Pr	*iso*–Propyl

BARF	$[B(3,5\text{–}C_6H_3(CF_3)_2)_4]^-$
MALDI–MS	Matrix–Assisted Laser Desorption/Ionization Mass Spectrometry
TMS	Tetramethyl silane
DMSO	Dimethylsulfoxide
TPP	5,10,15,20–Tetraphenylporphyrinate dianion
dbbipy	4,4'–di–*tert*–Butyl–2,2'–bipyridine

TABLE OF CONTENTS

Page

LIST OF FIGURES

Page

LIST OF SCHEMES

Page

LIST OF TABLES

Page

CHAPTER I

INTRODUCTION AND OVERVIEW

1.1 Electronic and coordinative unsaturation

One of the most essential rudiments in chemistry necessary to understand structure and bonding is the concept of the octet rule. The rule has its basis on the observation that main–group elements will tend to form compounds that will attain the valence–shell electronic configuration of the closest noble gas, that is, ns^2np^6, or 8 valence electrons.[1] Similarly, organotransition metal complexes also tend to attain the closed shell configuration of the subsequent noble gas $(n+1)s^2(n+1)p^6nd^{10}$, or 18 valence electrons, although metals from the groups 8–11 show a preference for forming 16 valence–electron compounds.[2] In general, once an organotransition metal complex has reached the maximum electron count allowed by occupancy of its bonding and non–bonding orbitals, the compound has become coordinatively saturated and cannot accept any further donor ligands (Figure 1–1).[2,3] Conversely, coordinatively unsaturated compounds have low–lying, vacant orbitals available for coordination and, as a consequence, electron counts less than the maximum possible allowed by its bonding and non–bonding orbital structure.[2,3] Coordinative unsaturation is of prime importance in organometallic chemistry. For instance, oxidative additions cannot take place in coordinatively saturated compounds,[4] and reductive eliminations occur more rapidly from d^6 5–coordinate than from d^6 6–coordinate complexes.[5] Moreover, it is the availability of open coordination sites that allows the fundamental step of β–hydrogen elimination to

occur.[6] It is for these reasons that coordinatively unsaturated compounds are central in most metal–catalyzed reactions.

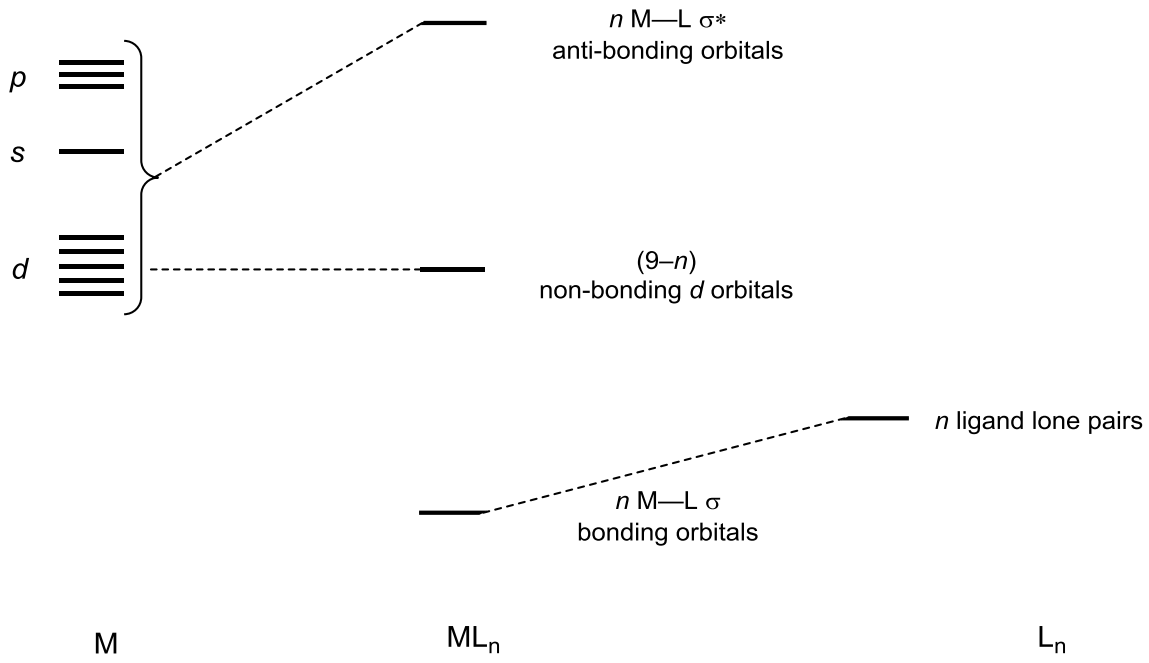

Figure 1–1. Schematic representation of bonding in transition–metal complexes. The solid lines represent multiple orbitals with energy separations dependent on the geometry of the complex. ML_n (n = 4–9).[4]

1.2 Response of transition metal complexes to coordinative unsaturation

To compensate for the loss of a ligand, metal complexes can undergo several types of rearrangements in order to provide additional stabilization of the resulting compound, or

remove the coordinative unsaturation altogether. For instance, a κ^1–coordinated acetate can switch to a κ^2 coordination mode when a coordination site opens *cis* to it. If small ligands with lone pairs of electrons are present, such as halides, these can potentially become bridging ligands and help dimerize unsaturated fragments. Also, intramolecular oxidative addition of a ligand C–H bond (cyclometalation) could take place in a coordinatively unsaturated complex if the metal is electron rich.[7] Solvent molecules could also coordinate to the empty site, especially solvents with lone electron pairs such as haloalkanes, ethers, DMSO, or acetonitrile.

In some instances, complete C–H bond cleavage may not take place. Instead, agostic interactions could appear between the empty coordination site and a ligand C–H bond (intramolecular 3–center, 2–electron M–H–C bond or, more rarely, an M–C–C bond).[8,9] (Figure 1–1). In some instances, σ–complex may also form (intermolecular 3–center, 2–electron bond).[10,11] In the case of agostic and σ–complexes, however, the resulting species are not considered to be truly coordinatively unsaturated, although the still retain a strongly electrophilic character.

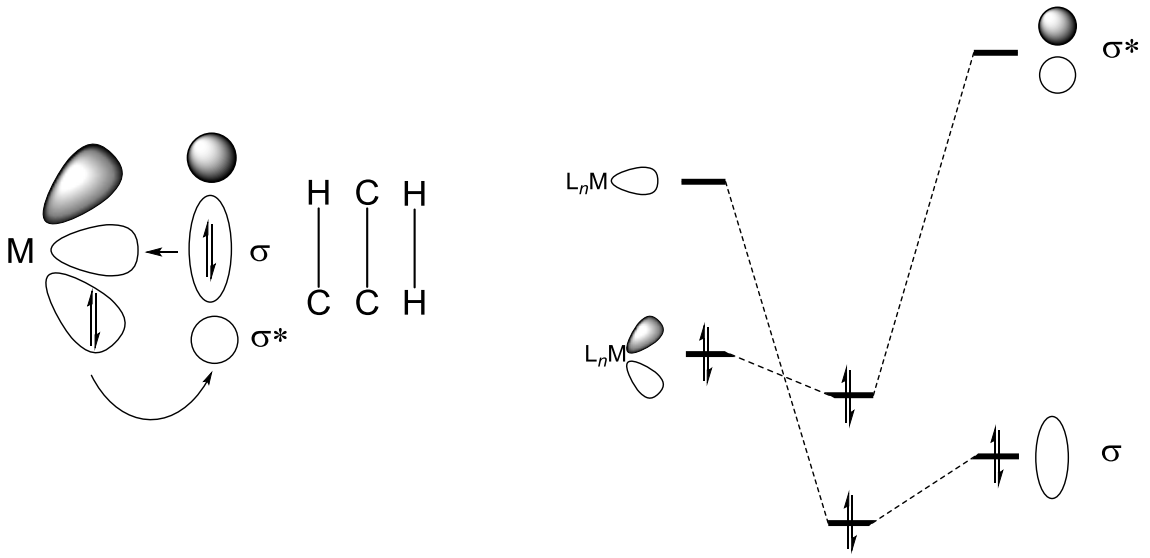

Figure 1–2. Representation of orbital interactions in σ–complexes, and its associated molecular orbital energy diagram. Orbital interactions in agostic complexes are analogous.[5]

In the absence of any of the stabilization mechanisms mentioned above, transition metal complexes can display unusual coordination geometries and electronic configurations. Such is the case of a rare example of a neutral, square planar, paramagnetic, 14–electron Ru(II) complex of the Fryzuk pincer ligand **(101)** (Figure 1–3).[12] In terms of unusual geometries, there are examples of diamagnetic, trigonal pyramidal, 14–electron complexes of Ru(II) supported by P–Si–P tridentate ligands **(102)** (Figure 1–3),[13] and of a distorted trigonal pyramidal, 14–electron Ru(II) imido complex (103) (Figure 1–3).[14]

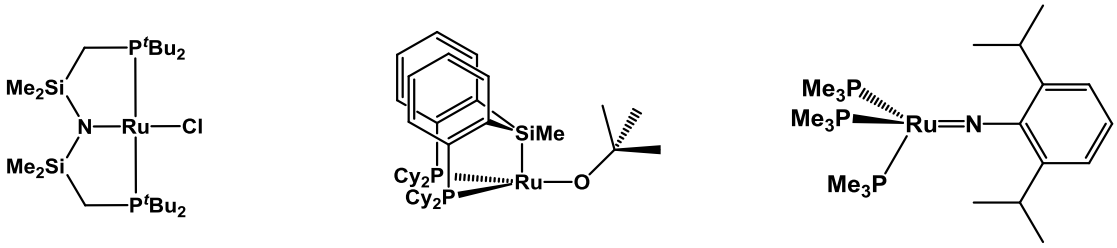

101 **102** **103**

Figure 1–3. Unusual coordination geometries for d^6 ML_4 ruthenium(II) complexes. **101** Square planar.[12] **102** Trigonal pyramidal.[13] **103** Distorted trigonal pyramidal.[14]

In contrast to complexes **101–103**, the geometry preference for the 14–electron, cationic Rh(III) complex **104** is *cis*–divacant octahedral (Figure 1–4).[15a] Complex **104** is a d^6 ML_4 compound stabilized by 4 strong σ–donors, and has a near C_{2v} symmetry in the solid state. A qualitative molecular orbital diagram analysis of the fragment in idealized C_{2v} symmetry, reveals that the presence of strong σ–donors has the effect of destabilizing the LUMO (orbital b_2), which has the effect of reducing its Lewis acidity (Figure 1–4). This was corroborated by an X–ray structural study, where no agostic interactions, or any other close contacts with either solvent molecules or the counter anion were observed. DFT studies conducted on 104 suggested that not only is strong σ–donation responsible in good part for the stabilization of the compound, but also that π–donation into the metal from the NHC (N–heterocyclic carbene) ligands may also play a role **104**.[15b]

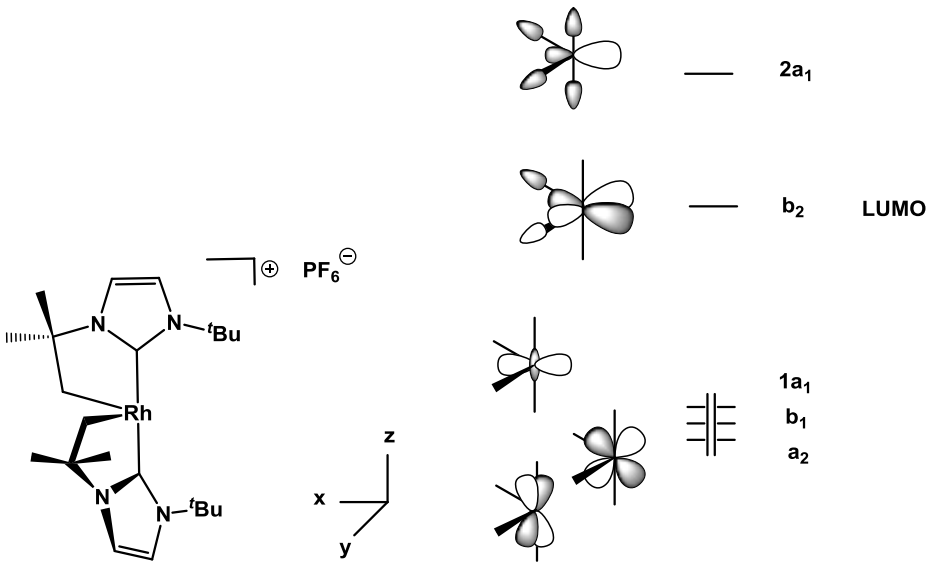

104

Figure 1–4. Qualitative molecular orbital diagram for **104**.[3]

1.3 Cationic, coordinatively unsaturated transition metal complexes

Introduction of coordinative unsaturation could prompt the reactivity described above, but also could be a means to enhance or trigger potentially useful chemistry. A common tactic to achieve coordinative unsaturation is the removal of an X–type ligand from the coordination sphere of a metal complex, and examples of enhanced reactivity by removal of an X–type ligand are numerous. A few interesting examples will be presented in the following section.

1.3.1 Illustrative examples of enhanced reactivity by removal of an X–type ligand

1.3.1.1 Metallocene–mediated olefin polymerization

Notable examples of cationic, coordinatively unsaturated compounds of early transition metals is the family of olefin polymerization catalysts of the type $(\eta^5\text{–Cp})_2M(R)^+$ (M = Ti, Zr, Hf; R = alkyl;).[16] These systems are simpler and more amenable to study than the heterogeneous Ziegler–Natta catalysts, therefore, a number of these homogenous systems have been studied extensively.[16,17] In these systems, the precatalysts $(\eta^5\text{–Cp})_2MCl_2$ treated with methylaluminoxane (MAO = $Al_4O_3(CH_3)_6)_n$), to yield the catalytically active species by rapid alkylation of the metal chloride, followed by dissociation into an ion pair.[18] Due to the amorphous nature of MAO, and the presence of several parallel equilibrium reactions established in solution, structural characterization of the potentially active species has not been possible.[19] On the other hand, structural information has been obtained from the well–defined $[(\eta^5\text{–Cp})_2Zr(Me)(THF)][BPh_4]$ and $[(\eta^5\text{–Cp*})_2Th(Me)][B(C_6H_5)_4]$ systems, both of which are active olefin polymerization catalysts (Scheme 1–1) .[16a, 20]

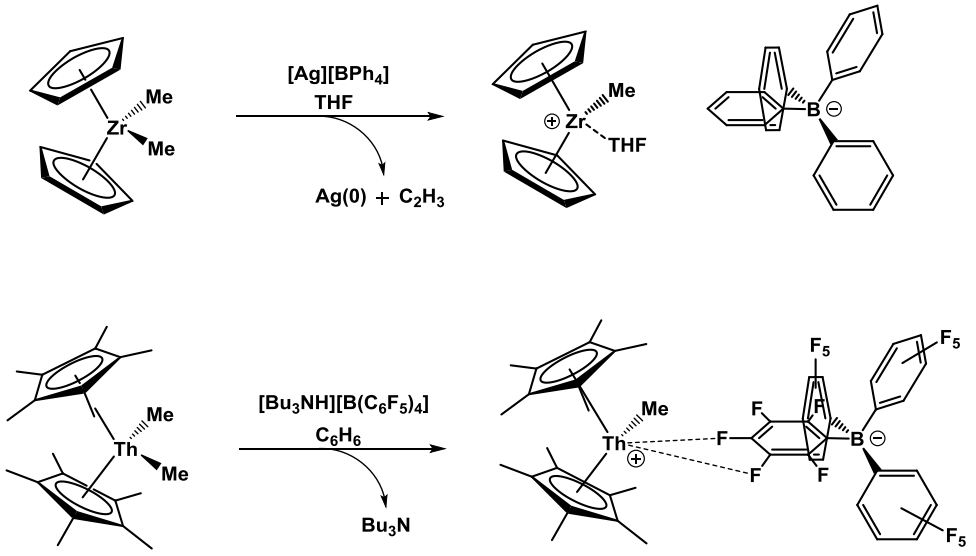

Scheme 1–1. Synthesis of the olefin polymerization catalysts $[(\eta^5\text{–Cp})_2Zr(Me)(THF)][BPh_4]$ and $[(\eta^5\text{–Cp*})_2Th(Me)][B(C_6H_5)_4]$.[16a,20]

1.3.1.2 Facile methane C–H bond activation

Another interesting example of reactivity triggered by a well–defined, cationic, coordinatively unsaturated transition metal compound is the facile activation of aryl C_{sp^3}–H bonds of methane by the Ir(III) complex $[(\eta^5\text{–}C_5Me_5)Ir(CH_3)(PMe_3)(CH_2Cl_2)][B(3,5\text{–}C_6H_3(CF_3)_2)_4]$ reported by Bergman (Scheme 1–2).[21] This compound was prepared by triflate ligand abstraction ($OTf^- = {}^-OSO_2CF_3$) with $Na[B(3,5\text{–}C_6H_3(CF_3)_2)_4]$ in CH_2Cl_2. An X–ray structural study of this compound revealed that it is stabilized by coordination of a molecule of CH_2Cl_2, which is to be expected from a small solvent molecule that possesses free electron pairs. Nevertheless, the coordination of the solvent molecule was not detrimental to the reactivity of the compound.

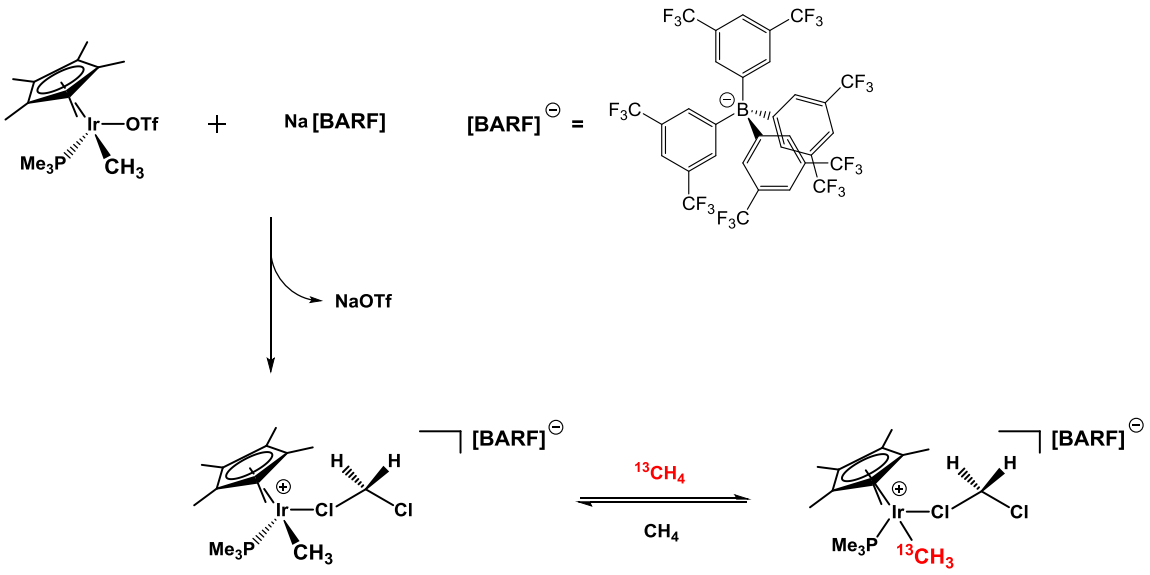

Scheme 1–2. Facile C–H bond activation of methane by $[(\eta^5\text{–Cp*})Ir(CH_3)(PMe_3)][BARF]$.

1.3.1.3 Aryl C–Cl bond activation

X–type ligand removal can allow the operation of reaction mechanisms that otherwise may be blocked. An example of this is the facile C–Cl oxidative addition of chlorobenzene at room temperature into Vaska's complex when its chloride is abstracted.[22] Oxidative addition of aryl chlorides is not a typical reaction for group 9 metals.[22] Removal of the chloride presumably provides access to a concerted oxidative addition mechanism onto a transient three–coordinate Ir(I) fragment (Scheme 1–3).

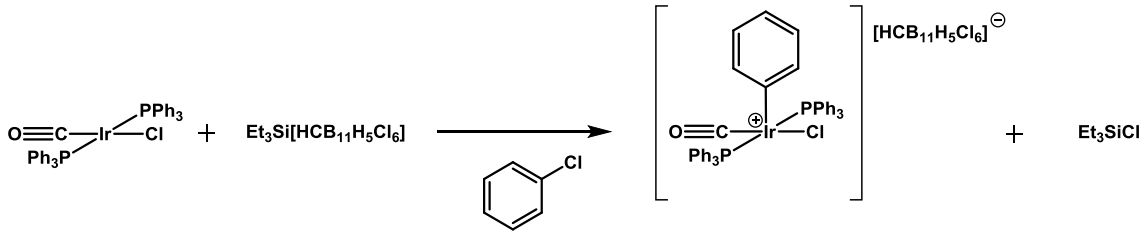

Scheme 1–3. C–Cl oxidative addition of chlorobenzene into Vaska's complex after chloride abstraction.[22]

1.3.1.4 Catalytic Lewis–acid mediated reductions

Another interesting example is the use of silylium–like cations for catalytic silane–fueled hydrodefluorination of C_{sp^3}–F bonds.[23] In this system, $[Ph_3C][HCB_{11}Cl_{11}]$ is used as a precatalyst to generate the catalytically active silylium–like cations ($[R_3Si]^+$ R = ethyl, hexyl) *in situ* by hydride abstraction from alkyl silanes (Scheme 1–4a). A related reaction is the reduction of alkyl halides catalyzed by the pincer compound [POCOP)Ir(H)(Acetone)][$B(C_6F_5)_4$] with Et_3SiH (Scheme 1–4b).[24]

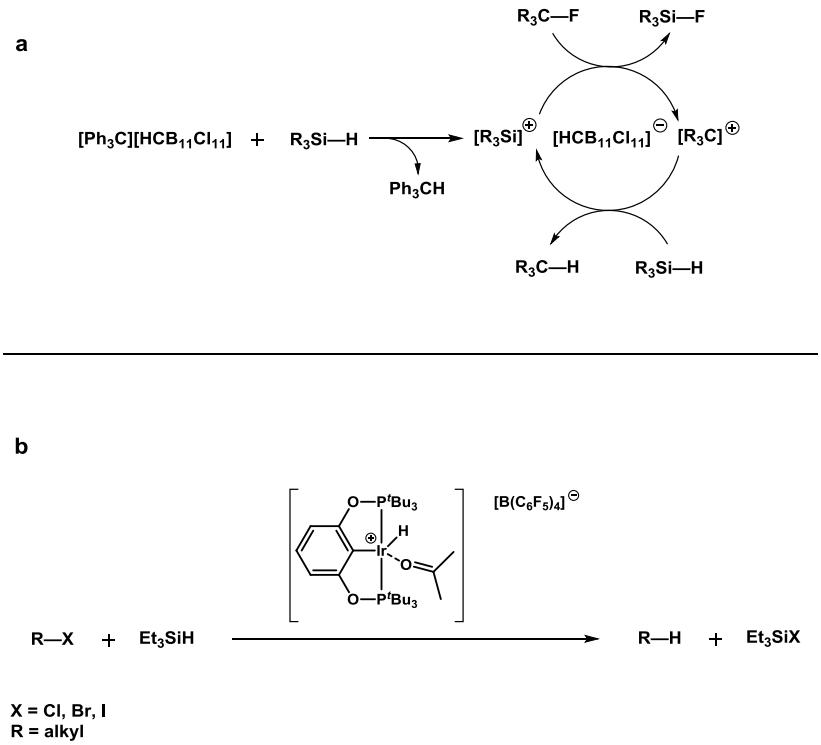

Scheme 1–4. a) Silane fueled, hydrodefluorination catalysis mediated by silylium cations.[23] b) Reduction of alkyl halides mediated by [POCOP]Ir(H)(Acetone)][$B(C_6F_5)_4$].[24]

Even though the chemistry described above spans several, very different, transformations, there is a critical component that is common to all of them. That component is a weakly coordinating anion, which is of critical importance to attain the high reactivity displayed by the electrophilic compounds just described. The following section will delve into the subject of weakly coordinating anions in detail.

1.4 Weakly coordinating anions

Highly Lewis–acidic main group and transition metal species can be prepared by replacement of a coordinated X–type ligand (X = alkyl, hydride, halide) from its coordination sphere with larger, complex anions such as $[ClO_4]^-$, $[BF_4]^-$, $[OSO_2CF_3]^-$, $[AlX_4]^-$ (X = halide, alkoxide). As recently as 25 years ago, these anions were classified as being "non–coordinating", however, there are several factors, of both kinetic and thermodynamic nature, that interplay and ultimately influence the ability of a complex anion to coordinate to a Lewis acidic site, as noted by Rosenthal.[25] For instance, steric hindrance, the nature of the solvent, and the presence of other Lewis bases in the system play an important role, as competition for the open coordination site will be established between all Lewis–basic species present. Anions that were thought to be non–coordinating in the presence of water were later found to be coordinated to the metal when water was excluded.[26] Moreover, X–ray structural data collected for many other coordination compounds revealed that, in numerous cases, the aforementioned "non–coordinating" anions were in fact coordinated to the metal.[25]

In view of these findings, it was proposed that the term "Weakly Coordinating Anions" (WCAs), where weak coordination can be understood as an extremely labile Lewis acid–base interaction, would be a more precise descriptor for these anions.[25,27,28]

Required features of a WCA are a relatively large size and a highly delocalized negative charge, which have the effect of diffusing the density of negative charge, and of hindering the access of the WCA to sterically–congested open coordination sites. As a result, WCAs are both very weakly basic and nucleophilic. These features are in contrast to $[ClO_4]^-$ and

$[OSO_2CF_3]^-$, both of which have a relatively small size, and have resonance structures that place the negative charge on the peripheral oxygen atoms, which also suggests another design parameter of WCAs, which is the incorporation of very weakly basic substituents, such as H or F, on the periphery of the anion. It has been shown that $[BF_4]^-$ is more weakly coordinating than $[ClO_4]^-$ or $[OSO_2CF_3]^-$.[27]

In addition to large size and significant charge delocalization, a critical feature of WCAs is chemical robustness, meaning that these anions should be stable against oxidation and bond cleavage. In this regard $[BF_4]^-$, $[PF_6]^-$, and $[SbF_6]^-$ do not meet this requirement. These anions are adducts of the conjugate Lewis base F^- and the respective Lewis acid $MF_{(5-x)}$ ($n = 1 \equiv M = B$; $n = 0 \equiv M = P, Sb$), and as such, they are only stable in environments where the cationic species present are less fluorophilic than $MF_{(5-x)}$.[29]

Cationic Lewis acidic species paired with WCAs can be seen as synthetic equivalents of true "non–coordinated" cations.[28] It is important to mention that the concept of weak coordination also extends to other chemical species. When highly electron deficient compounds are prepared, the tendency is to compensate for their lack of electrons, and any species present that is capable of acting as an electron donor could, in principle, coordinate to the strong electrophile in order to stabilize it, even the most unlikely molecules. For instance, aromatic solvents are Lewis bases that could coordinate through their π electrons to form complexes of different hapticities, hydrocarbon σ_{C-H} bond electron density could coordinate to empty sites in transition metals, either intramolecularly (agostic interactions)[8] or, intermolecularly (σ–complexes).[11] Examples of σ–Complexes of dihydrogen are numerous,[30]

and a very few examples of C–C σ–complexes can be found in the literature.[31] Preparation of trialkylsilylium salts of WCAs results, in many instances, in the formation of bridging solvent adducts of the type $[R_3Si{-}H{-}SiR_3]^+$, $[R_3Si{-}X{-}SiR_3]^+$, or $[R_3Si \bullet (arene)]^+$ (R = methyl, ethyl, isopropyl; X = halogen, $[OSO_2CF_3]^-$; Arene = benzene, toluene) if the compound is prepared in neat trialkylsilane as the solvent,[32] in the presence of arenes[33] or haloarenes,[34] or halogenated trialkylsilanes.[35] These silylium–like adducts retain a high electrophilic character.[36]

1.4.1 Tetraphenylborate–based WCAs

1.4.1.1 $[B(C_6H_5)_4]^-$ anion

$[B(C_6H_5)_4]^-$ (**105**) anions have been widely used as WCAs, with one of its most notable being the metallocene olefin polymerization catalysis.[37] This anion imparts good solubility to its compounds, but it bears several undesirable characteristics that preclude its use in harsher chemical environments. For instance, it is known that B–C bond cleavage in **105** anions can take place under strongly Brønsted acidic conditions,[38] and that phenyl group transfer occurs in the presence of strongly Lewis acidic cations such as $[Fe(Cp)(CO)_2(THF)]^+$ or $[Fe(TPP)]^+$.[27,39] In terms of stability against oxidation, it is also well known that **105** anions are susceptible to chemical oxidation even in the presence of metals in low oxidations states such as Ni(II) and Co(II).[40,41] In addition to its lack of chemical robustness, the phenyl rings of **105** are good π–electron donors, and several examples of η^2, η^3 and η^6 coordination of **105** to coordinatively unsaturated metal complexes could be found in the literature (Figure 1–5),[42] including an

example of η^6 coordination to the chlorinated $[B(3,5\text{-}C_6H_3Cl_2)_4]^-$ anion.[43] Examples of rather stable η^6 *ansa*–arene complexes of **105** are also known (Figure 1–5).[44]

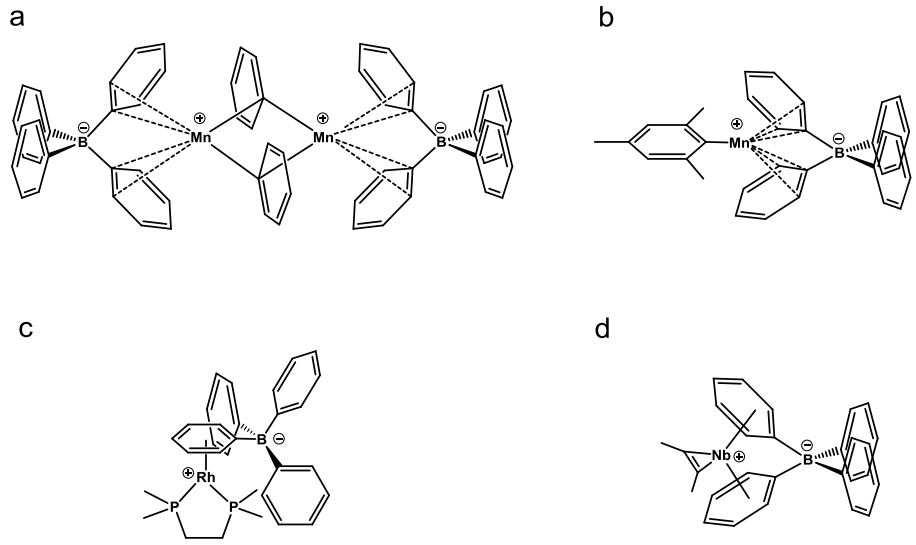

Figure 1–5. Different coordination modes of the $[B(C_6H_5)_4]^-$ **(105)** anion. a) η^2, [42a] b) η^3, [42a] c) η^6, [42c] d) *ansa*–arene.[44]

1.4.1.2 $[B(C_6F_5)_4]^-$ and $[B(3,5\text{-}C_6H_3(CF_3)_2)_4]^-$ anions

In order to reduce the susceptibility of tetraphenylborates to decomposition, the perfluoro– and trifluoromethyl–substituted tetraphenyl borate anions $[B(C_6F_5)_4]^-$ **(106)**, and $[B(3,5\text{-}C_6H_3(CF_3)_2)_4]^-$ **(107)** were synthesized.[45] The presence of electron withdrawing groups has the additional advantage of diminishing the possibility of π–coordination to Lewis acidic centers as a result of the reduced electron density on the phenyl rings.[27] The very weak basicity of the **106** anion is evidenced in the crystal structure of $[(\eta^5\text{-}Cp^*)Th(Me)][B(C_6F_5)_4]$, which

consists of weakly associated cations and anion, as evidenced by F–Th contacts falling outside of the range of the sum of the Th^{4+} and F^{-} ionic radii.[20] This weak coordination was also reflected on its increased reactivity as a catalyst for the hydrogenation of 1–hexene (*ca.* 360:1 TOF), and for the polymerization of ethylene (*ca.* 4500:1 TOF) compared to the analogous compound $[(\eta^5\text{–Cp*})Th(Me)][B(C_6H_5)_4]$ (Figure 1–6).[20]

Another beneficial feature of fluorine substitution is the increased stability of **106** and **107** against oxidation, thus allowing their use as weakly coordinating electrolytes in electrochemistry.[46] Even though these anions show several desirable properties such as good solubility of their salts in organic solvents, and very weak basicity, they still show limitations in their applicability in environments of very high Lewis and Brønsted acidity. For example, the **107** anion is susceptible to decomposition by fluoride abstraction, and B–C bond cleavage in the presence of silylium ions.[47] Additionally, a particular problem is presented by the rotational crystallographic disorder usually encountered around the CF_3 groups when electron density has to be modeled accurately for the purpose of charge–density analysis.[43] It has also been reported that the **106** decomposes in conditions of high Brønsted acidity,[48] and that solvent–free $Ag[B(C_6F_5)_4]$ undergoes pentafluorophenyl group transfer under solvent–free conditions to form $Ag(C_6F_5)$ and $B(C_6F_5)_3$.[49]

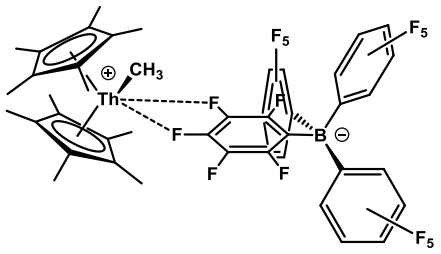

Figure 1–6. Graphic representation of $[(\eta^5\text{–Cp*})\text{Th(Me)}][\text{B}(\text{C}_6\text{H}_5)_4]$. The F–Th contacts fall outside of the range of the sum of the Th_4^+ and F^- ionic radii. [20]

*1.4.2 WCAs based on the carba–*closo*–dodecaborate cluster $[HCB_{11}H_{11}]^-$*

Anions based on the boron cluster carba–*closo*–dodecaborate (carborane for short) framework $[HCB_{11}H_{11}]^-$ (Figure 1–7) have received much attention in recent years because these compounds show many of the desirable properties of an ideal WCA. Carboranes have a large size, highly delocalized electronic density within the cluster (3–dimensional σ–bond aromaticity), and a large HOMO–LUMO gap.[50] These characteristics make carboranes inherently both very weakly basic and nucleophilic, and resistant to electrochemical oxidation. However, the hydrogen atoms on the B–H units on the parent carborane $[HCB_{11}H_{11}]^-$ retain some hydridic character and are, therefore, susceptible to electrophilic substitution. The "*para*" on the cluster is the most susceptible to electrophilic substitution, followed by the "*meta*" positions, while the lowest reactivity is displayed at the "*ortho*" positions.[51]

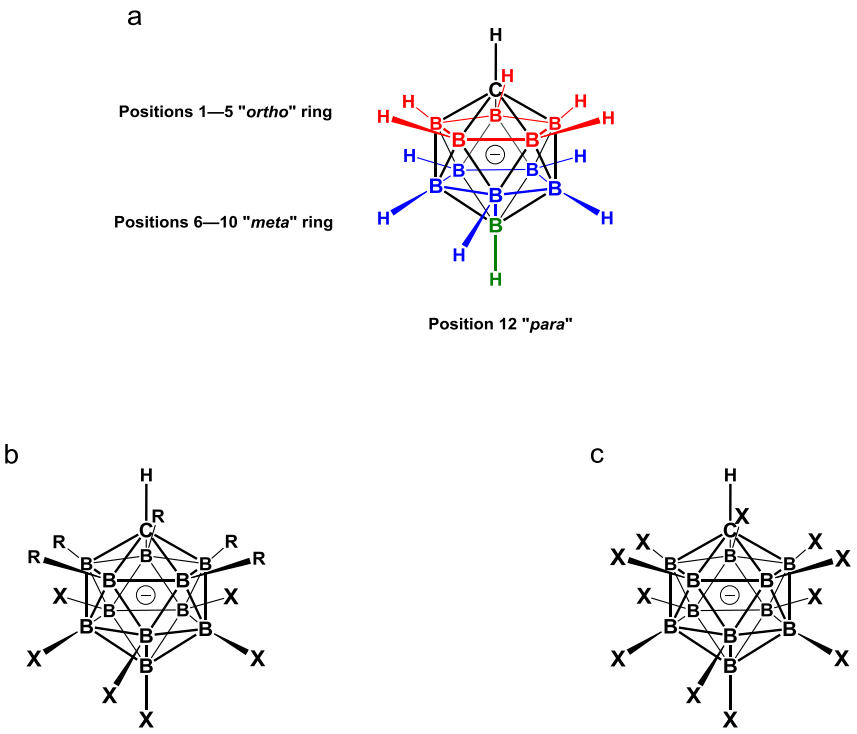

Figure 1–7. (a) Representation of the pseudo–icosahedral parent carba–closo–dodecaborate $[HCB_{11}Cl_{11}]^-$, and identification of the different positions within the anion. (b) Structure of the anions of the type $[HCB_{11}R_5X_6]^-$ (R = Me, H; X = Cl, Br). (c) Structure of the anions of the type $[HCB_{11}X_{11}]^-$ (X = F, Cl, Br, I).

This pattern of reactivity permits different types of substitution around the cluster. Complete, or partial, electrophilic halogenation of the B–H units of the parent carborane leads to species of the type $[HCB_{11}X_{11}]^-$ (X = F, Cl, Br)[52,53] or $[HCB_{11}R_5X_6]^-$ (R = H, Me; X = Cl, Br)[52] (Figure 1–7), that are exceptionally stable in environments of high Brønsted and Lewis acidity where other WCAs would not survive (*vide supra*). In addition to the possibility of functionalizing the B–H units, the C–H moiety in $[HCB_{11}Cl_{11}]^-$ (**108**) and its different

halogenated derivatives, is amenable to deprotonation by *n*–butyllithium, or by much weaker bases. This way, the C vertex can be derivatized by nucleophilic substitution with alkyl halides.[54]

These WCAs have made possible the isolation of highly electrophilic species such as the first free silylium cation.[55] Additionally, a variety of silylium–like compounds stabilized by carborane anions have been prepared[56,57] and used as reagents for different applications, such as halide abstraction from transition metal complexes,[22] and to gain access to the "mighty methyl" reagents $Me[HCB_{11}Me_5Br_6]$ and $Me[HCB_{11}Me_5Cl_6]$, which were prepared from MeOTf and $Et_3Si[HCB_{11}Me_5Br_6]$ and $Me_3Si[HCB_{11}Me_5Cl_6]$.[58] These reagents have been characterized and used to generate tertiary carbocations by hydride abstraction from linear and branched alkanes.[59] Although it was observed that mighty methyl has a significant covalent character, this turned out to be a way to tame the high reactivity of the Me^+ cation, free of any of the complications that decomposition of the anion could pose. Interestingly, $Me[HCB_{11}Cl_{11}]$ could not be isolated because Me^+ reacted rapidly with the alkane solvent used in the synthesis, as a result of the lower basicity of the **108** anion.

The carborane anions **108** and $[HCB_{11}F_{11}]^-$ **(109)** are the least basic WCAs known,[61] a property that has been used to prepare the strangest strongest known Brønsted super acids, $H[CB_{11}Cl_{11}]$ and $H[CB_{11}F_{11}]$.60[b,60] Moreover, **108** has also been employed to support silane–fueled hydrodefluorination of fluoroalkanes.[23]

1.4.3 Various weakly coordination anions

1.4.3.1 Fluoroalkoxyalumintaes $[Al(OR^F)_4]^-$

Fluoroalkoxyaluminates $[Al(OR^F)_4]^-$ (R^F = fluoroalkyl, C_6F_5) are another class of WCAs[61a] that, in contrast to fluorophenyl borates and carboranes, can be easily prepared in large quantities from $LiAlH_4$ and the respective fluorinated alcohol HOR^F. Although alkoxyaluminates could normally be hydrolyzed under mild acidic conditions, the $[Al(OC(CF_3)_3)_4]^-$ anion is stable in 6N nitric acid. Additionally, the large number of C–F units present on the periphery of the anion helps make it one of the most weakly coordinating anions.[61b] It should be noted, however, that the $[Al(OC(CF_3)_3)_4]^-$ can undergo decomposition in the presence of strong fluorophilic cations, such as $[P_2X_5]^+$ (X = Br, I) even at −20 °C.[61c]

1.4.3.2 Pentafluorooxotellurato borates and pnictates

The design principle behind the anions $[B(OTeF_5)_4]^-$,[62a] and $[M(OTeF_5)_n]^-$ (As, Sb, Bi, n = 6)[62b] is the incorporation of the largest number possible of fluorine substituents on the periphery of a large, spherical anion. These anions can be considered to be adducts of $[OTeF_5]^-$ and the corresponding Lewis acid $M(OTeF_5)_n$ (n = 3, 5), and as result, they can only be paired with cations that are weaker Lewis acids than the parent compound $M(OTeF_5)_n$ in order to avoid transfer of $[OTeF_5]^-$, which is a severe limitation to their potential usefulness. In addition, these anions are also prone to hydrolysis, concomitant with release of HF.

1.5 Methods of preparation of coordinatively unsaturated compounds

In general, the synthetic strategies employed to prepare and stabilize complexes of low coordination number include the use of sterically–demanding ligands, electrophilic abstraction of phosphine ligands,[63] anion metathesis with WCAs in the case of the preparation of cationic metal complexes, and the use of weakly coordinating solvents. The anion metathesis reactions rely on electrophilic abstraction of an X–type ligand from the coordination sphere, either with a strong Lewis or Brønsted acid.[27] In the following sections, a brief survey of relevant anion metathesis methods will be presented.

1.5.1 Halide/pseudohalide abstraction

This type of metathesis reaction is by far the most common way to generate cationic species of metal complexes and main group compounds. The most common reagents used for these reactions are Ag(I), Tl(I), and alkali metal salts of WCAs, although in some particular instances these cations are not strongly Lewis acidic enough to abstract the halide.[27] One of such instances is chloride abstraction from Vaska's complex (Scheme 1–3).[22] In this case, halide abstraction was achieved by using the more strongly electrophilic silylium–like compound $Et_3Si[HCB_{11}H_5Cl_6]$.

The use of M[WCA] (M = Na, K) is more convenient because these compounds are more easily synthesized, are not light sensitive, and are free of undesired 1–electron oxidation side reactions, unlike Ag[WCA]. Tl[WCA] has the added disadvantage of being highly toxic. The

synthetically useful triphenylcarbenium salts could be prepared by halide abstraction from Ph_3C–Cl by Na[WCA],[64] or by Ag[WCA],[65]

1.5.2 Hydride and alkyl group abstraction

The most common electrophile for this reaction is $[Ph_3C]^+$ paired with a WCA, which can be prepared by methods described in the preceding section. H^-,[66a] or CH_3^-,[66b,c] could be abstracted directly from the coordination sphere of the metal to form the corresponding cationic complex, or from alkyl ligands to form cationic metal–carbene complexes.[66d] It is know that $[Ph_3C]$[WCA] compounds can also effect one–electron oxidations.[66e,67] Hydride abstraction from trialkyl silanes is the reaction of choice to prepare the highly electrophilic silylium–like cations.[65]

$B(C_6F_5)_3$ is a strong, neutral Lewis acid that can be been used to effect CH_3^- abstraction. Treatment of $(\eta^5\text{–}C_5H_5)_2Al(Me)$ with $B(C_6F_5)_3$ yields $[(\eta^5\text{–}C_5H_5)_2Al][MeB(C_6F_5)_3]$, and active isobutylene polymerization catalyst.[68a] Methide ion abstractions have also been reported for late transition metals. When a solution of $(dbbipy)Pt(Me)_2$ was treated with $B(C_6F_5)_3$ in the presence of CO, quantitative formation of $[(dbbipy)Pt(Me)(CO)][MeB(C_6F_5)_3]$ was observed.[68b] Nevertheless, when precatalysts for olefin polymerization of the type $(\eta^5\text{–}C_5H_5)M(Me)_2$ (M = Ti, Zr, Hf) are treated with $B(C_6F_5)_3$, formation of tight ion pairs takes place.[68c]

Another method of alkyl group removal involves the use of the silylium–like compound $Et_3Si[HCB_{11}Me_5Cl_6]$. This method was used to prepare a free Mes_3Si^+ cation (Mes = mesityl =

2,4,6–$Me_3C_6H_2$) by abstraction of an allyl group from $Mes_3Si(CH_2CH{=}CH_2)$.[36b,69] This strategy relies on the electrophilic attack on the allyl double bond followed by Si–C bond cleavage.

CHAPTER II

C–ALKYLATION OF THE $[HCB_{11}Cl_{11}]^-$ ANION*

2.1 Introduction

The term weakly–coordinating anion (WCA) is typically applied to species that possess a negative charge, but are at the same time very weak bases or nucleophiles. Such species are indispensable in exploring the condensed phase reactivity of Lewis acidic cations.[27,65–72]

Among the various types of WCA, polyhalogenated derivatives of monocarba–*closo*–dodecaborate $[HCB_{11}H_{11}]^-$ anion combine several very desirable properties.[27,65,72] While their low basicity is matched by other WCA classes, their robustness towards strong oxidants, Lewis and Brønsted acids is peerless. As a bonus, halogenated carborane salts tend to form X–ray quality single crystals very readily. These properties of the carborane anions have allowed preparation and characterization of well–defined derivatives of some of the most remarkably reactive cations known.[73–76] Our interest in halogenated carboranes arises in part from their unique suitability for the catalytic C–F activation schemes that employ cationic silicon and aluminum catalysts.[77–80]

Of the halogenated carboranes, fully B–substituted undecahalogeno derivatives $[HCB_{11}X_{11}]^-$ (X = F, Cl, Br, I)[27] are the least basic and the most robust. **108** is particularly attractive because it can be prepared in a scalable and straightforward fashion in a simple

---

* Reproduced in part, and reprinted with permission from "Convenient C–alkylation of the $[HCB_{11}Cl_{11}]^-$ carborane anion" by Ramírez–Contreras, R.; Ozerov, O. V. *Dalton Trans.*, **2012**, *41*, 7842, Copyright 2012 by Royal Society of Chemistry.

experimental setup, without the need for expensive equipment or especially hazardous reagents such as Cl_2, HF or F_2.[81] However, the disadvantage of the use of halogenated carborane anions is the relatively lower solubility of their salts in organic solvents of low polarity in comparison to other commonly used WCA, such as fluorinated tetraarylborates and fluoroalkoxyaluminates.[27,65–72]

It was our hypothesis that alkylation at the C–vertex might provide a route to enhancing the solubility of **108** without impairing its other desirable properties. C–alkylation of **108** has not yet been attempted aside from methylation.[82,83] C–alkylation of carboranes has been carried out previously on carborane anions via deprotonation of the C–H vertex with alkyllithium reagents followed by treatment with alkyl electrophiles.[84–86] Most recently, Nava and Reed have reported a method for C–alkylation of $[HCB_{11}H_5Br_6]^-$, in which $Me_3NH[HCB_{11}H_5Br_6]$ was treated with 2.1 equivalents of *n*–butyllithium in THF followed by an alkyl iodide.[87] Although alkyllithium reagents can lead to successful deprotonation–alkylation, the drawback of their use is the requirement for air–free manipulations and dry solvents. We then sought to develop an alternative procedure free of such requirements.

2.2 Results and discussion

*2.2.1 Bench–top C–alkylation of $[HCB_{11}Cl_{11}]^-$ (**108**)*

We were inspired by a previous report on the C–methylation and C–ethylation of **109** performed with aqueous NaOH–R_2SO_4.[88,89] This result indicated that the C–H vertex in **109** is sufficiently acidic for an oxygenous base to effect deprotonation and we wondered if the

same might be true for **108**. The aqueous NaOH–R_2SO_4 combination is probably limited to R = Me or Et because longer chain alkyl sulfates are not readily available from commercial sources and are likely not soluble in water. As we wished to explore installation of longer alkyl chains, we decided to switch to alkyl iodides as electrophiles, *tert*–butoxide as the base, and *tert*–butyl alcohol as the solvent.

Because separation of the **108** starting material from the C–alkylated products would be impractical, we thought it important to design a reaction that minimizes side reactions of the base with the electrophile or with adventitious Brønsted acids, but nonetheless effects complete conversion even if the side reactions do take place. For that reason, we set out to use a deliberate excess of the base and of the electrophile (Scheme 2–1).

A solution of the trimethylammonium salt of **108** in commercially available 99.5% *tert*–butyl alcohol was treated with 3.5 equivalents of KO^{t}Bu for 30 min at 30 °C, followed by removal of all volatiles *in vacuo* (needed to remove Me_3N, a potential nucleophile), redissolution in *tert*–butyl alcohol and treatment of the reaction mixture with 7 equivalents of an appropriate alkyl iodide (ranging from methyl to hexyl).

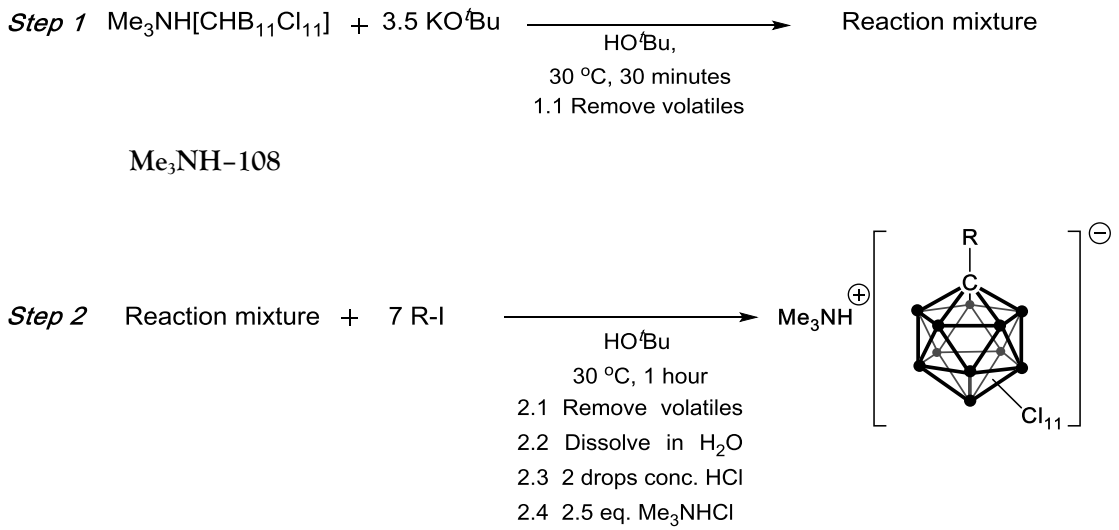

R = Methyl	Ethyl	Butyl	Hexyl
(Me_3NH–201) 83%	**(Me_3NH–202)** 94%	**(Me_3NH–203)** 84%	**(Me_3NH–204)** 93%

Scheme 2–1. General synthetic scheme for C–alkylated carboranes using KO^{t}Bu and alkyl iodides in HO^{t}Bu as solvent. Isolated product yields after precipitation with Me_3NHCl from aqueous solution.

Analysis of an aliquot of the reaction mixture (after 1 h) by negative–ion MALDI mass spectrometry, showed only the expected $[RCB_{11}Cl_{11}]^-$ product in each case. Likewise, $^{11}B\{^1H\}$ NMR spectroscopy detected only one set of signals, assignable to the product. As can be seen from Figure 2–1, the ^{11}B NMR signatures of the $[RCB_{11}Cl_{11}]^-$ products are readily distinguishable from **108**. The workup shown in Scheme 2–1 allowed isolation of the desired anions as trimethylammonium salts in 83–93% yields. Multinuclear NMR spectroscopy (^1H, ^{13}C and ^{11}B), MALDI–MS, and boron elemental analyses support the assigned identity and

the high purity of the isolated materials. Isolated **Me_3NH–201** and **Me_3NH–203**, after drying under vacuum for 12 h at 80 °C, were easily converted to the corresponding sodium salts by treatment with sodium hydride in fluorobenzene (Scheme 2–2). **Na–201** and **Na–203** thus prepared were isolated in yields greater than 90% as analytically pure solids.

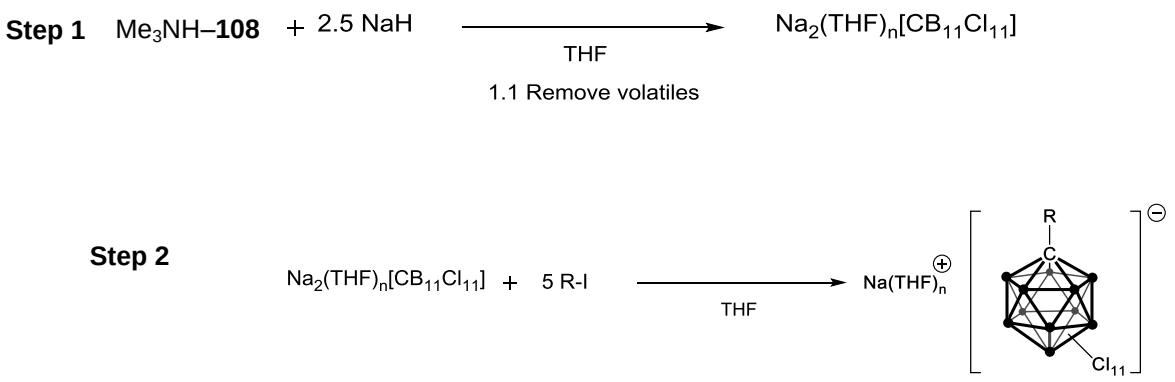

R = Butyl (**Na(THF)–203**); Hexyl (**Na(THF)–204**); Propyl (**Na(THF)–205**)

Scheme 2–2. Air–free synthesis of C–alkylated carboranes from **Me_3NH–108**, using NaH and alkyl iodides. Products can be isolated as trimethylammonium salts from aqueous solution.

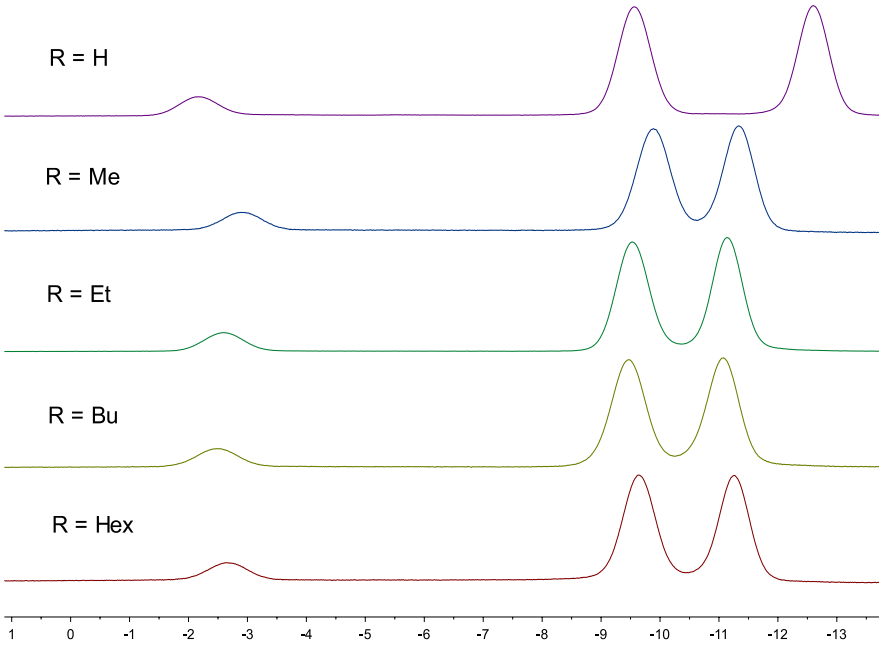

Figure 2–1. $^{11}B\{^{1}H\}$ NMR spectra of aliquots of reaction mixtures taken after 1 h of treatment with the corresponding alkyl electrophile. Spectra were collected in *tert*–butyl alcohol.

We envision that sodium salts of $[RCB_{11}Cl_{11}]^-$ anions may find utility as halide/ pseudo–halide abstraction reagents, analogously to $Na[B(3,5\text{–}C_6H_3(CF_3)_2)_4$ salts.[90,91] **Na–203** is appreciably soluble in fluorobenzene. NaH (2.5 equivalents) in THF can also replace KO^{t}Bu as the base to effect C–alkylation of $[HCB_{11}Cl_{11}]^-$ in an analogous procedure (Scheme 2–2). This protocol, however, requires the use of air– and moisture–free techniques and THF. MALDI–MS and ^{11}B NMR identified only the presence of the desired $[RCB_{11}Cl_{11}]^-$ anions in the products of these reactions. C–alkylation of **108** using the *tert*–butyl alcohol/*tert*–butoxide protocol was also tested using ethyl bromide as the alkyl electrophile. In this case, a

conversion of only *ca.* 50% was observed by ^{11}B NMR and MALDI after 1 h of treatment with the electrophile.

Treatment of **108** with NaH or with *n*–BuLi in dry THF appears to result in complete deprotonation and formation of $Na_2[CB_{11}Cl_{11}]$ (**Na_2–206**) or $Li_2[CB_{11}Cl_{11}]$ (**Li_2–206**) as indicated by a new set of ^{11}B NMR resonances observed. Notably, the boron resonance of the B–Cl unit antipodal to the C–H vertex suffers a large upfield shift, going from δ–2.5 ppm in **108** to δ –5.5 ppm in **206**. Treatment of **108** with KO^{t}Bu in dry THF generated a very similar set of ^{11}B NMR resonances, indicating the formation of $K_2[CB_{11}Cl_{11}]$ (**K_2–206**). Addition of increasing amounts of HO^{t}Bu resulted in the gradual shift of the ^{11}B NMR resonances towards their positions in **108**, while only showing a single set of resonances. This observation is consistent with the pK_a values of **108** and of HO^{t}Bu being similar and the exchange between HO^{t}Bu/$[CB_{11}Cl_{11}]^{2-}$ and **108** being rapid on the NMR timescale. In the presence of excess HO^{t}Bu, the concentration of **206** is small, but evidently kinetically competent to react with alkyl iodides (Figure 2–2).

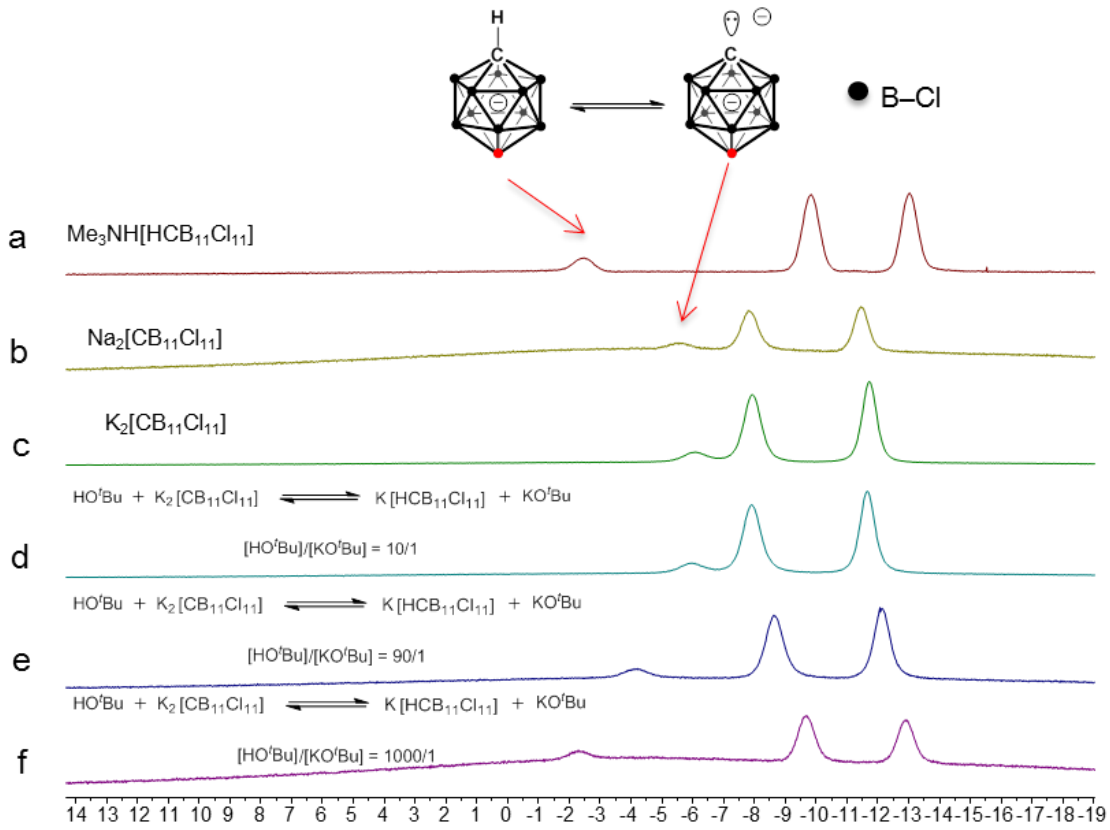

Figure 2–2. (a, b, c) Observation by $^{11}B\{^{1}H\}$ MHz NMR of formation of **206** in THF by deprotonation of **108** with NaH, and KO^{t}Bu. (d, e, f) Observation of equilibration between **K_2–206** and **108** in the presence of varying amounts of HO^{t}Bu.

`

2.2.2 Observation of dechlorination of $[RCB_{11}Cl_{11}]^-$ (R = n–alkyl, H)

It is important to note that excessive heating of the reaction mixture resulting from the Step 1 in Scheme 2–1 is inadvisable. We have found that if such mixtures were heated to 70 °C to facilitate removal of volatiles, MALDI–MS analysis of the residue showed the appearance of a new signal with an apparent intensity of *ca.* 10% relative to that of the main product, and with the *m/z* ratio consistent with the replacement of one chlorine atom with a

hydrogen atom. This decomposition product could not be identified in either $^{11}B\{^1H\}$ or ^1H NMR spectra. Independent experiments, in which *tert*–butyl alcohol solutions of **Me_3NH–202** and **Me_3NH–108** were heated at 70 °C for 2 d in the presence of 5 equivalents of KO^{t}Bu, showed by MALDI–MS that the corresponding decomposition products were indeed forming. Thus, limiting the Step 1 (Scheme 2–1) time to 30 min and the temperature to < 40 °C is crucial for the purity of the product. Interestingly, $[HCB_{11}F_{11}]^-$ was reported to react with aqueous 3 M KOH by displacement of F with OH (not H), forming a mixture of $[HCB_{11}(OH)F_{10}]^-$ and $[HCB_{11}(OH)_2F_9]^-$ anions after 24 h.[88]

*2.2.3 X–ray structural study of [Ag(η^2–C_6H_5F)(H_2O)][$BuCB_{11}Cl_{11}$] (**207**)*

Initially, we were concerned that the $[RCB_{11}Cl_{11}]^-$ anions might be less prone to form crystalline compounds as a result of the presence of the lipophilic and flexible alkyl chain. However, all C–alkylated carborane salts presented in Scheme 2–1 and Scheme 2–2 were isolated as solid powders, with no evidence of oil formation. In addition, we prepared **Ag–203** by analogy with literature syntheses of Ag carborane salts[27,65,72] and were able to obtain a single crystal suitable for an X–ray diffraction study by slow diffusion of hexanes into a fluorobenzene solution of the compound at ambient temperature. Structure solution revealed a compound of the formula [Ag(η^2–C_6H_5F)(H_2O)][$BuCB_{11}Cl_{11}$], (**207**), which consisted of polymeric chains of silver cations motif and the near–symmetrical Ag–(η^2–C_6H_5F) interaction (Ag1–C6 of 2.553(3) Å, and Ag1–C7 of 2.587(3) Å) are analogous to Ag(*closo*–6,7,8,9,10–$Br_5CB_9H_5$)(η^2–C_7H_8).[92] However, in the latter case, distances are slightly longer: 2.618(36) Å

and 2.642(38) Å. Ag–η^2 arene interactions are often dissymmetrical.[93] All chlorine atoms were unambiguously located, in contrast to the reported solid–state structure of **Ag–201** where disorder between all C–Me and B–Br positions was observed.[82] This highlights one of the potential benefits of using an extended alkyl chain. On the other hand, mild disorder of the *n*–butyl group was observed in **207**.

Each anion in **207** has close contacts via some of their chlorine atoms and adjacent silver ions, with distances Ag1–Cl6 of 2.847(1) Å, Ag1–Cl3 of 2.878(1) Å, which are in the upper range of similar interactions observed in [Ag(η^2–*p*–xylene)][$HCB_{11}Cl_6H_5$], where the longest Ag–Cl distance is 2.926(1) Å.[94] A rather long distance Ag1–Cl8 of 3.127(1) Å is also observed in the structure of **207**, and is just below the limit of the sum of the van der Waals radii of Ag and Cl (3.2 Å).[95] The elongation of the Ag–Cl distances in **207** may be attributable to the strong coordination of an adventitious water molecule to the silver ion, with an Ag1–O1 distance of 2.317(2) Å, which is shorter than the Ag–O distances of 2.34(1) and 2.38(1) Å observed in the coordinated water molecules in (naphthalene)$(AgClO_4)_4 \cdot 4H_2O$.[96]

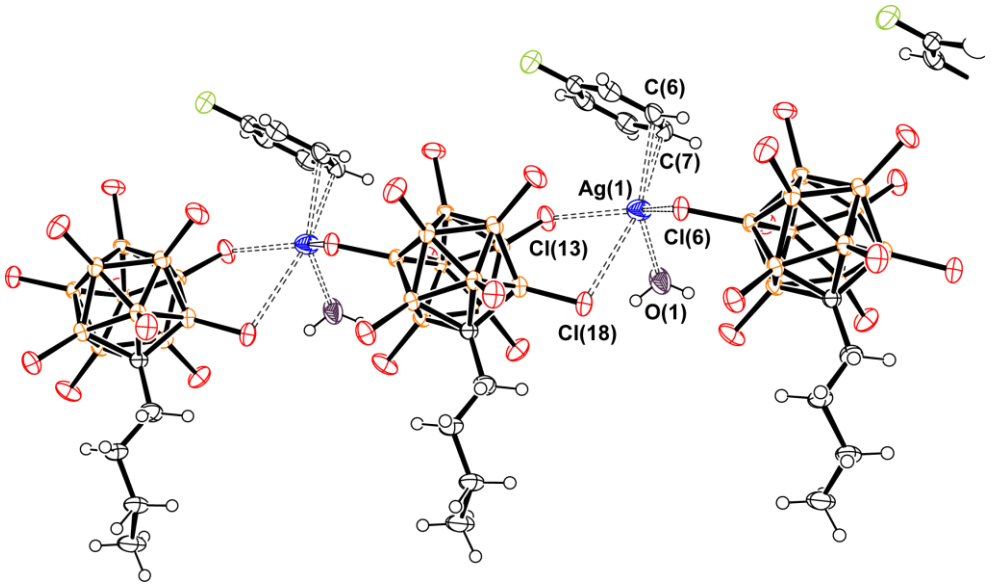

Figure 2–3. ORTEP diagram of **207**, with thermal ellipsoids set to 50% probability. One component of the disorder around the alkyl chain is omitted for clarity.[97]

2.3 Conclusion

In summary, a method for C–alkylation of **108** was developed, using a potassium *tert*–butoxide/*tert*–butyl alcohol system and alkyl iodides, without the need of any special air–free techniques. C–alkylated products can be isolated in good yields as the corresponding trimethylammonium salts. These C–alkylated carboranes may be used to prepare salts of increased solubility that are capable of forming X–ray diffraction quality single crystals.

2.4 Experimental details

2.4.1 General considerations

tert–Butyl alcohol, 99.5% purity, was purchased from Acros Organics, iodo alkyls were purchased from Aldrich or Acros and used without further purification. Potassium *tert*–butoxide was purchased from Strem Chemicals and was used as received. **Me_3NH—108** was prepared from **Cs—108** using the previously published $SbCl_5$ chlorination procedure.[78] All operations were carried out open to air in Schlenk flasks in a fume hood unless otherwise indicated. NMR spectra were collected on Varian Inova 400 (^{11}B NMR, 128.19 MHz) and Varian Inova 500 (^{1}H NMR, 499.43 MHz; ^{13}C NMR, 125.58 MHz) spectrometers using deuterated solvents as indicated. In the case of ^{1}H and ^{13}C NMR, spectra were referenced to residual solvent peaks. For ^{11}B NMR, spectra were referenced externally to δ 0 ppm using $BF_3 \bullet OEt_2$. ^{19}F NMR spectra were referenced externally using 1.0 M CF_3CO_2H in $CDCl_3$ to δ −78.5 ppm. MALDI mass spectrometric analyses of the carborane anions were carried out by the Texas A&M University Laboratory for Biological Mass Spectrometry (LBMS). Elemental analyses were performed by CALI Labs, Inc. (Parsippany, NJ, USA).

2.4.2 Synthetic procedures and characterization data

General Synthesis of $Me_3NH[RCB_{11}Cl_{11}]$ (150 mg scale) using *tert*–butyl alcohol and KO^tBu. Me_3NH–108 (0.15 g, 0.25 mmol) was dissolved in *ca.* 40 mL of *tert*–butyl alcohol in a Schlenk flask and placed in a water bath at 35 °C to prevent crystallization of the solvent. The resulting solution was then treated with 3.5 equivalents of potassium *tert*–butoxide (0.098

g, 0.875 mmol) and the resulting mixture was stirred for 30 min. Once this time was completed, volatiles were removed *in vacuo*. To help remove volatiles, the flask can be placed in a water bath at 35 °C. The resulting residue was suspended in *ca.* 40 mL of butyl alcohol and 7 equivalents of the alkyl iodide (1.7 mmol) were added in a single portion using a Hamilton microliter syringe and the mixture is stirred for one h. The residue was dissolved in *ca.* 10 mL of water and the solution was then acidified with 3 drops of concentrated HCl. This solution was treated with 2 equivalents of solid Me_3NHCl (0.50 mmol) to immediately obtain a white precipitate. The solid was recovered by filtration through a fine fritted funnel, washed with deionized water 2 × 10 mL, dissolved in HPLC grade acetone or dichloromethane and filtered through the same fritted glass funnel into a pre–weighed flask and dried overnight at 80 °C *in vacuo* to obtain white powders. If additional purification is desired, after the final wash with water, the solid should be dissolved in the minimum possible amount of acetone and filtered through a fritted funnel. This mother liquor is then carefully layered on top of *ca.* 20 mL of water and let to slowly diffuse overnight to obtain white crystals.

Me_3NH–201. Yield: 119.0 mg (81%). ^{1}H (499.43 MHz, acetonitrile–d_3) δ 2.80 (s, 9H, HN–$(CH_3)_3^+$), 1.57 (s, 3H, C_{ipso}–CH_3). $^{13}C\{^{1}H\}$ (125.6 MHz, acetonitrile–d_3) δ 12.72 (s, C_{ipso}–CH_3), 46.03 (s, HN–$(CH_3)_3^+$), 51.11 (s br, *ipso*–C). $^{11}B\{^{1}H\}$ (128.19 MHz, acetonitrile–d_3) δ −3.0 (s br, 1B), −9.9 (s br, 5B), −11.3 (s br, 5B). Boron elemental analysis: Calculated (Found) 19.87% (19.84%).

Me_3NH–202. Yield: 148.0 mg (94%). ^1H (499.43 MHz, acetonitrile–d_3) δ 1.30 (t, 3H, C_{ipso}–CH_2–CH_3), 2.40 (m, 2H, C_{ipso}–CH_2–CH_3), 2.80 (d, 9H, HN–$(CH_3)_3^+$). $^{13}C\{^1H\}$ (125.6 MHz, acetonitrile–d_3) δ 10.68 (s, C_{ipso}–CH_2–CH_3), 25.99 (s, C_{ipso}–CH_2–CH_3), 46.06 (s, HN–$(CH_3)_3^+$), 51.69 (bs, C_{ipso}). $^{11}B\{^1H\}$ (128.19 MHz, acetonitrile–d_3) δ −2.6 (s, 1B), −9.5 (s, 5B), −11.1 (s 5B). Boron elemental analysis: Calculated (Found) 19.49% (19.32%).

Me_3NH–203. Yield: 154.0 mg (84%). ^1H NMR (499.43 MHz, acetonitrile–d_3) δ 0.88 (t, 3H, –CH_3, C_{ipso}–*Butyl*), 1.26 (m, 2H, –CH_2–, C_{ipso}–*Butyl*), 1.83 (m, 2H, –CH_2–, C_{ipso}–*Butyl*), 2.26 (filled–in doublet, 2H, –CH_2–, C_{ipso}–*Butyl*), 2.80 (s, 9H, HN–$(CH_3)_3^+$). $^{13}C\{^1H\}$ NMR (125.6 MHz, acetonitrile–d_3) δ 13.75 (s, –CH_3), 23.86 (s, –CH_2–), 27.29 (s, –CH_2–), 31.73 (s, –CH_2–), 46.02 (s, HN–$(CH_3)_3^+$), 51.51 (s br, C_{ipso}). $^{11}B\{^1H\}$ NMR (128.19 MHz, acetonitrile–d_3) δ −2.5 (s br, 1B), −9.5 (s br, 5B), −11.1 (s br, 5B). Elemental analysis: Calculated (Found) C, 15.06% (15.00%); H, 3.00% (2.96%); B, 18.64% (18.53%); Cl, 61.11% (60.97%); N, 2.19% (2.10%).

Me_3NH–204. Yield: 176.5 mg (93%). ^1H NMR (499.43 MHz, acetonitrile–d_3) δ 0.87 (t, 3H, –CH_3, C_{ipso}–*Hexyl*), 1.25 (m, 6H, –$(CH_2)_3$–, C_{ipso}–*Hexyl*), 1.84 (m, 2H, –CH_2–, C_{ipso}–*Hexyl*), 2.25 (filled–in doublet, 2H, –CH_2–, C_{ipso}–*Hexyl*), 2.80 (s, 9H, HN–$(CH_3)_3^+$). $^{13}C\{^1H\}$ NMR (125.6 MHz, acetonitrile–d_3) δ 14.22 (s, –CH_3), 23.08 (s, –CH_2–), 25.15 (s, –CH_2–), 30.32 (s, –CH_2–), 31.72 (s, –CH_2–), 32.02 (s, –CH_2–), 45.97 (s, HN–$(CH_3)_3^+$), 51.62 (s br, C_{ipso}). $^{11}B\{^1H\}$

NMR (128.19 MHz, acetonitrile–d_3) δ −2.5 (s br, 1B), −9.5 (s br, 5B), −11.1 (s br, 5B). Boron elemental analysis: Calculated (Found) 17.85% (17.69%).

General Synthesis of Na[$RCB_{11}Cl_{11}$] (100 mg scale). All procedures were carried out inside an argon–filled glovebox. **Me_3NH–108** (0.10 g, 0.17 mmol) was dissolved in *ca.* 50 mL of dry THF and NaH (0.015 g, 0.44 mmol) was added in a single portion. The mixture was stirred vigorously for one h and volatiles were then removed *in vacuo*. The resulting residue was resuspended in *ca.* 50 mL of dry THF and the corresponding alkyl iodide (0.87 mmol) was added in a single portion using a Hamilton microliter syringe. The resulting mixture was stirred for one h. Volatiles were removed to dryness *in vacuo*, the residue was then suspended in *ca.* 20 mL of THF. This suspension was filtered through a fine frit and dried under vacuum to obtain a white powder.

Na(THF)–203. Yield: 95.0 mg (84.4%) ^{1}H NMR (499.43 MHz, acetonitrile–d_3) δ 0.88 (t, 3H, –CH_3, C_{ipso}–*Butyl*), 1.29 (m, 2H, –CH_2–, C_{ipso}–*Butyl*), 1.85 (m, 2H, –CH_2–, C_{ipso}–*Butyl*), 2.27 (filled–in doublet, 2H, –CH_2–, C_{ipso}–*Butyl*).

Na(THF)–205. Yield: 71.0 mg (69%) ^{1}H NMR (499.43 MHz, acetonitrile–d_3) δ 0.85 (t, 3H, –CH_3, C_{ipso}–*Propyl*), 1.25 (m, 2H, –CH_2–, C_{ipso}–*Propyl*), 1.84 (filled–in doublet, 2H, –CH_2–, C_{ipso}–*Propyl*).

Na(THF)–204. Yield: 107.0 mg (95%) ^{1}H NMR (499.43 MHz, acetonitrile–d_3) δ 0.87 (t, 3H, –CH_3, C_{ipso}–*Hexyl*), 1.26 (m, 6H, –(CH_2)$_3$–, C_{ipso}–*Hexyl*), 1.84 (m, 2H, –CH_2–, C_{ipso}–*Hexyl*), 2.25 (filled–in doublet, 2H, –CH_2–, C_{ipso}–*Hexyl*).

General Synthesis of donor–free Na[RCB$_{11}$Cl$_{11}$] (100 mg scale). All procedures were performed in an argon–filled, dry box. $Me_3NH[RCB_{11}Cl_{11}]$ (0.100 g) was dissolved in enough dry fluorobenzene to effect dissolution. To this solution, 5 equivalents of sodium hydride were added in a single portion and the suspension was stirred for 2 h. Volatiles were removed to obtain a tan powder that was resuspended in *ca.* 20 mL of dry fluorobenzene. This suspension was filtered through a fine–fritted funnel, the mother liquor collected and dried *in vacuo* to obtain white powders.

Na–201. Yield 0.095g (98%). Boron elemental analysis: Calculated (Found) 21.28% (20.95%).

Na–203. Yield 0.137g (90.5%). Boron elemental analysis: Calculated (Found) 19.79% (19.69%).

Synthesis of K–202 using ethyl bromide. 0.113 g (0.194 mmol) of **Me$_3$NH–108** were charged in a Schlenk flask, dissolved in *ca.* 40 mL of *tert*–butyl alcohol and placed in a water bath at 35 °C to prevent crystallization of the solvent. The resulting solution was then treated

with 0.044 g (0.679 mmol) of potassium *tert*–butoxide and the resulting mixture was stirred for 30 min. Once this time was completed, volatiles were removed *in vacuo*. The resulting residue was suspended in *ca.* 40 mL of *tert*–butyl alcohol and 7 equivalents of the ethyl bromide (1.358 mmol) were added in a single portion using a Hamilton microliter syringe and the mixture is stirred for one h. At the end of this time an aliquot of reaction mixture was taken and analyzed by $^{11}B\{^{1}H\}$ NMR (Figure 2–4) and MALDI mass spectrometry (negative ion detection) (Figure 2–5) showing *ca.* 50% conversion.

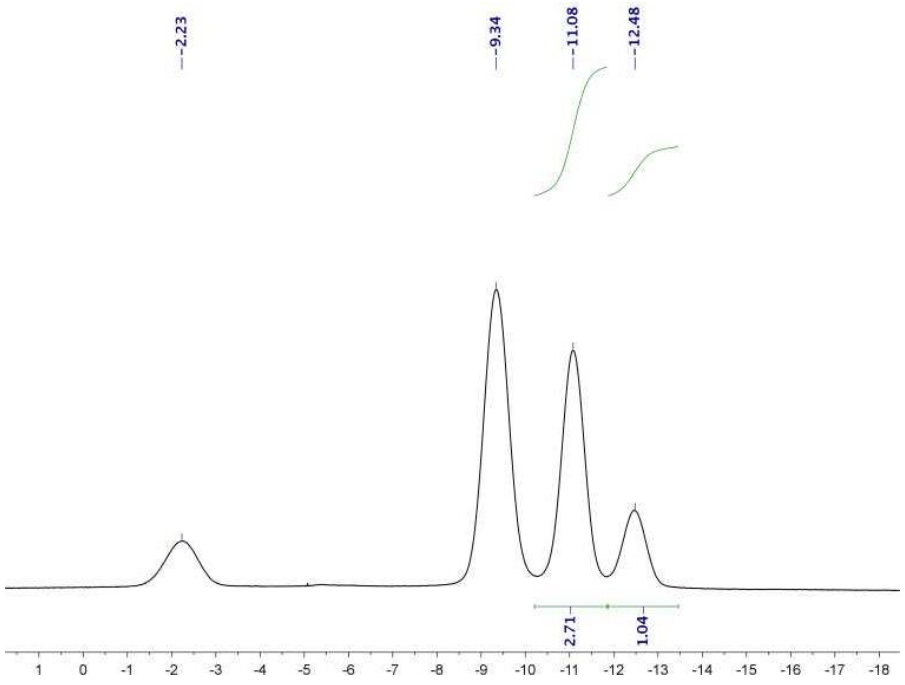

Figure 2–4. Attempted synthesis of **202** using ethyl bromide as the electrophile. $^{11}B\{^{1}H\}$ 128.19 MHz NMR spectrum of an aliquot of the reaction mixture in *tert*–butyl alcohol solution after 1 h of treatment with ethyl bromide.

Observation of dechlorination of 108. 0.072 g (0.124 mmol) of **Me_3NH–108** were charged in a round bottom flask equipped with a PTFE valve and were dissolved in *ca.* 40 mL of *tert*–butyl alcohol. 0.071 g (0.633 mmol) of potassium *tert*–butoxide were charged and the flask was closed, placed in a silicon oil bath set at 70 °C for 2 d. The resulting solution had the appearance of egg yolk. An aliquot of the reaction mixture was analyzed by MALDI mass spectrometry. Analysis of the spectrum revealed a signal at signal with m/z = 488 consistent with formation of an anion with the formula $[HCB_{11}Cl_{10}H]^-$.

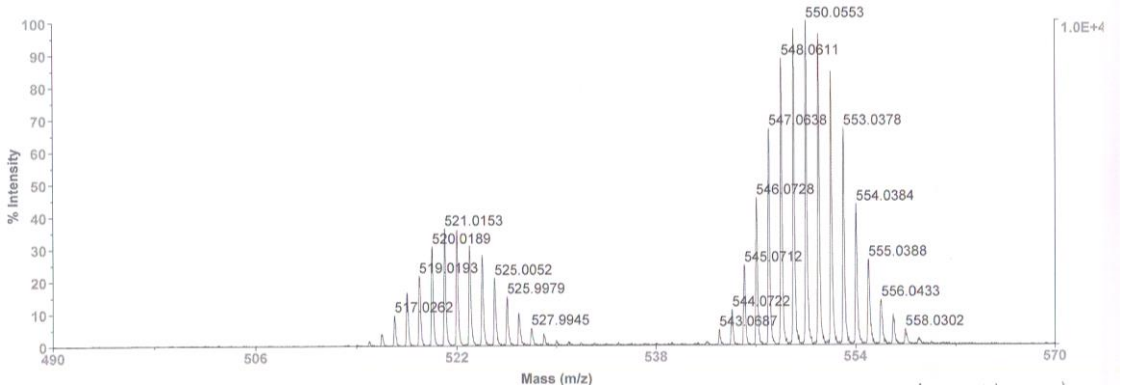

Figure 2–5. Attempted synthesis of **202** using ethyl bromide as the electrophile. MALDI mass spectrum of an aliquot of the reaction mixture after 1 h of treatment with ethyl bromide. Signals at m/z 521 and 550 correspond to **108** and **202** respectively.

Observation of dechlorination of 202. 0.060 g (0.098 mmol) of **202**, purified by crystallization as explained above, were charged in a round bottom flask equipped with a PTFE–lined valve and were dissolved in *ca.* 40 mL of *tert*–butyl alcohol. 0.055 g (0.492 mmol)

of potassium *tert*–butoxide were charged, the flask was closed and then was placed in a silicon oil bath set at 70 °C for two d, after which the solution had turned dark yellow. An aliquot of the reaction mixture was analyzed by MALDI mass spectrometry (Figure 2–6).

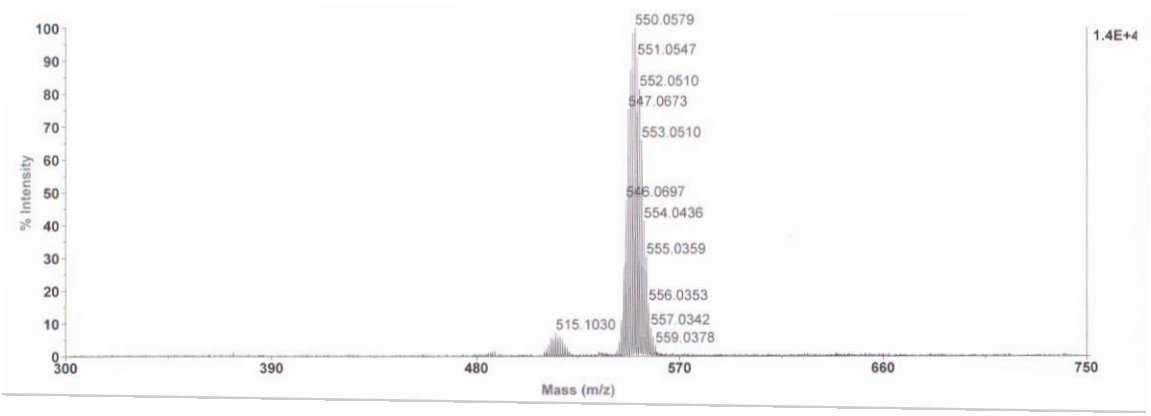

Figure 2–6. MALDI mass spectrum of the solution of **202** and potassium *tert*–butoxide in *tert*–butyl alcohol after heating at 70 °C for 2 d. Signal at m/z = 515 consistent with an anion of formulation $[EtCB_{11}Cl_{10}H]^-$.

Synthesis of 207. Me_3NH–203 was crystallized from acetone/water as described above to eliminate any traces of halides that may be present from previous synthetic steps. **Me_3NH–203** (0.224 g, 0.35 mmol) was charged in a Schlenk flask and suspended in deionized water, then was treated with 0.52 mL of a 2.03 N NaOH aqueous solution (1.05 mmol). Once complete dissolution was effected, Me_3N was removed with under vacuum by reducing the

original volume of solution by a half. The resulting solution is acidified with enough $HOSO_2CF_3$ to achieve red color on litmus paper. To this solution, solid $AgNO_3$ (0.119 g, 0.70 mmol) is added and stirred until it is completely dissolved. Formation of a white colloidal suspension is observed shortly thereafter. **Ag–207** is extracted from this suspension with 3 × 25 mL portions of toluene. The organic extracts were collected and the solvent removed *in vacuo* to obtain a tan solid. This solid was used directly to grow crystals for X–ray diffraction studies by diffusion of hexanes into a solution of **Ag–203** at room temperature avoiding contact with light. Yield: 132 mg (56%). ^{1}H NMR (499.43 MHz, acetonitrile–d_3) δ 0.88 (t, 3H, –C*H*$_3$, C$_{ipso}$–*Butyl*), 1.25 (m, 2H, –C*H*$_2$–, C$_{ipso}$–*Butyl*), 1.83 (m, 2H, –C*H*$_2$–, C$_{ipso}$–*Butyl*), 2.26 (filled–in doublet, 2H, –C*H*$_2$–, C$_{ipso}$–*Butyl*), 2.80 (s, 9H, HN–(C*H*$_3$)$_3^+$). ^{13}C{^{1}H} NMR (125.6 MHz, acetonitrile–d_3) δ 13.78 (s, –CH_3), 23.90 (s, –CH_2–), 27.38 (s, –CH_2–), 31.79 (s, –CH_2–), 51.44 (s br, C$_{ipso}$). ^{11}B{^{1}H} NMR (128.19 MHz, acetonitrile–d_3) δ −3.4 (s br, 1B), −10.3 (s br, 5B), −12.0 (s br, 5B).

Observation of equilibration between 206 and 108 in solution. In a dry box, 50.6 mg (0.087 mmol) of **Me$_3$NH–108** were charged in a J. Young NMR tube and 510 μL of dry THF were added to effect dissolution. To this solution, 34.0 mg of KO^{t}Bu (0.304 mmol, 3.5 equivalents) were added and a ^{11}B{^{1}H} NMR spectrum was collected, showing complete conversion to **K$_2$–206**. Dilution 1: To the previous solution, 290 μL of HO^{t}Bu (3.04 mmol, 10 × |KO^{t}Bu|) were added and a ^{11}B{^{1}H} NMR spectrum was collected. Dilution 2: An aliquot of 100 μL of dilution 1 and 290 μL of HO^{t}Bu (3.04 mmol, 90 × |KO^{t}Bu|) were

charged in an NMR tube and a $^{11}B\{^1H\}$ NMR spectrum was collected. Dilution 3: An aliquot of 10 μL of dilution 1 and 290 μL of HO^{t}Bu (3.04 mmol, 810 × |KO^{t}Bu|) were charged in an NMR tube and a $^{11}B\{^1H\}$ NMR spectrum was collected. Typical reaction mixture: An aliquot of 500 μL was taken from a mixture of **Me$_3$NH–108** (0.081 g, 0.14 mmol), KO^{t}Bu (0.056 g, 0.50 mmol) and 30.0 mL (0.50 mol) of HO^{t}Bu.

Preparation of Na$_2$–206. In a dry box, 51.2mg (0.088 mmol) of **Me$_3$NH–108** and 6.2 mg (0.258 mmol) of NaH were charged in a J. Young NMR tube, and 700 μL of dry THF were added. $^{11}B\{^1H\}$ NMR (128.19 MHz, THF–h_8) δ–5.6 (b1H), –7.8 (b, 5H), –11.5 (b, 5).

Preparation of Li$_2$–206. In a dry box, 48.7 mg (0.084 mmol) of **Me$_3$NH–108** were charged in a J. Young NMR tube and 700 μL of dry THF were added to effect complete dissolution. To this solution, 84.0 μL (0.210 mmol) of a 2.5 M *n*–butyllithium solution in hexanes were added. $^{11}B\{^1H\}$ NMR (128.19 MHz, THF–h_8) δ–5.8 (b, 1H), –8.0 (b, 5H), –11.6 (b, 5).

2.4.3 X–ray structural determinations

X–Ray data collection, solution, and refinement for 207. Crystals of this compound were grown by diffusion of hexanes into a saturated fluorobenzene solution of **207**. A colorless, multi–faceted crystal suitable size and quality (0.46 × 0.15 × 0.13 mm) was selected using an optical microscope and mounted onto a nylon loop. Low temperature (150 K) X–ray

data were obtained on a Bruker APEXII CCD based diffractometer (Mo sealed X–ray tube, K_α = 0.71073 Å). All diffractometer manipulations, including data collection, integration and scaling were carried out using the Bruker APEXII software.[98] An absorption correction was applied using SADABS.[99] The structure was solved in the monoclinic C_c space group using XS (incorporated in SHELXTL).[100] The solution was refined by full–matrix least squares on F^2. No additional symmetry was found using ADDSYMM incorporated into the PLATON program.[101] All non–hydrogen atoms were refined with anisotropic thermal parameters. All hydrogen atoms were placed in idealized positions and refined using a riding model. The structure was refined (weighted least squares refinement on F^2) and the final least–squares refinement converged to R_1 = 0.0225 ($I > 2\sigma(I)$, 6241 data) and wR_2 = 0.0561 (F^2, 14456 data, 335 parameters). Disorder around the alkyl carbon atoms was modeled by dividing the disordered sites into two components, restraining the carbon atom distances to be 1.54 Å and by constraining their anisotropic displacement parameters to be identical. ORTEP–II was used to prepare the final structure plots.[102]

Crystallographic information is summarized in Table 2–1, and is also available in the form of a CIF file (CCDC 859566) from the Cambridge Crystallographic Data Centre (www.ccdc.com.ac.uk).

Table 2–1. Crystallographic information for **207**.

Empirical formula	C_{11} H_{16} Ag B_{11} Cl_{11} F O	
Formula weight	799.97	
Temperature	150(2) K	
Wavelength	0.71073 Å	
Crystal system	Monoclinic	
Space group	C_c	
Unit cell dimensions	a = 8.931(5) Å	α = 90°.
	b = 16.763(9) Å	β = 91.830(5)°.
	c = 18.452(10) Å	γ = 90°.
Volume	2761(2) $Å^3$	
Z	4	
Density (calculated)	1.924 g cm^{-3}	
Absorption coefficient	1.813 mm^{-1}	
F(000)	1552	
Crystal size	0.46 × 0.15 × 0.13 mm^3	
Theta range for data collection	2.21 to 27.50°	
Index ranges	$-11 \le h \le 11$, $-21 \le k \le 21$, $-23 \le l \le 23$	
Reflections collected	14456	
Independent reflections	6241 [R_{int} = 0.0272]	
Completeness to theta = 27.50°	99.60%	
Absorption correction	Semi–empirical from equivalents	
Max. and min. transmission	0.8395 and 0.6124	
Refinement method	Full–matrix least–squares on F^2	
Data / restraints / parameters	6241 / 8 / 335	
Goodness–of–fit on F^2	1.03	
Final R indices [$I > 2\sigma(I)$]	R_1 = 0.0225, wR_2 = 0.0561	
R indices (all data)	R_1 = 0.0233, wR_2 = 0.0566	
Largest diff. peak and hole	0.546 / −0.343 $eÅ^{-3}$	

CHAPTER III

SYNTHESIS OF A SILYLIUM ZWITTERION*

3.1 Introduction

The pursuit of isolable silylium cations (R_3Si^+, where R is an alkyl, aryl, or a similar univalent substituent) has challenged the boundaries of existing chemical concepts and the boundaries of the known synthetic methods.[103–105] Silylium cations are some of the strongest Lewis acids known. Their similarity to their lighter congener carbocations (R_3C^+) had spurred the intrigue but they turned out to be more resistant to isolation than carbocations.[103] Only at the turn of the last century was it possible to prepare compounds that can be viewed as R_3Si^+ salts or their close approximations.[104–109]

The key to the success in R_3Si^+ preparation is the recognition of the need for a weakly coordinating anion (WCA) that is maximally inert and minimally basic.[110] The class of anions that has so far best fulfilled these requirements is comprised of the various halogenated carborane anions ($[HCB_{11}X_{11}]^-$, where X = halogen, H, or alkyl), which are remarkably robust and versatile WCAs.[105,111,112] Only very bulky triaryl silylium cations, such as Mes_3Si^+ have been unambiguously characterized as a discrete three–coordinate cation planar at Si, with the $[HCB_{11}Me_5Br_6]^-$ counter ion for the only solid–state structure.[109,113] Trialkylsilylium cations have only been isolated as very weak adducts, coordinated typically to a halogen atom on the

* Reproduced in part, and with permission from "Synthesis of a Silylium Zwitterion" by Ramírez–Contreras, R.; Bhuvanesh, N.; Zhou, J.; Ozerov, O. V. *Angew. Chem. Int. Ed.*, **2013**, *52*, 10313, copyright 2013 by Wiley–VCH Verlag GmbH & Co.

carborane anion, an arene solvent molecule, or a trialkylsilane.[106–108,114–116] These salt–like compounds $[R_3Si][HCB_{11}X_{11}]$ have some of the highest levels of acidity achievable in well–defined systems under preparatory laboratory conditions and their full potential is yet to be exploited.[117] As an example of their unique capacity, they have recently been utilized as catalysts for the very challenging C–F conversion reactions of aliphatic and aromatic compounds.[118,119]

Silylium cations can be particularly useful in synthesis where abstraction of a halide or pseudohalide is critical for generation of a new highly unsaturated cation.[105,120,121] Their chloride–abstracting ability is far superior to that of the commonly used Ag^+ and is free of redox complications.[104]

To contrast with the two–component cation–anion combinations, we wished to explore the possibility of a single–component, neutral molecule endowed with the Lewis acidity of a silylium cation. Preferably, such a molecule would cleanly convert into a robust WCA upon halide abstraction and not generate another by–product. There are currently no neutral Lewis acids of silylium–class strength that fit this description. Classical strong inorganic Lewis acids (for example, $AlCl_3$, SbF_5) result in anions that are relatively coordinating, prone to rearrangements, and/or are redox non–innocent. Tris(pentafluorophenyl)boron $[B(C_6F_5)_3]$ is a notable non–oxidizing Lewis acid that has found widespread use,[122,123] but it does not have the Lewis acidity of a silylium–like cation. The tris(perfluoroalkoxy)aluminum Lewis acid $Al(OC(CF_3)_3)_3$ is a powerful example,[124,125] although this construction is not immune to degradation and redistribution.

3.2 Results and discussion

We envisaged a zwitterion in which the silylium cation site is connected to the anionic carborane core by an inert covalent linker. The silane precursor anion $[HSiMe_2CH_2CB_{11}Cl_{11}]^-$ (**301** (Scheme 3–1) was synthesized by deprotonation of the carbon vertex of the known **Me_3NH–108** followed by alkylation with $ClCH_2SiMe_2H$. We have reported previously similar alkylation reactions of **108** with simple alkyl iodides.[97] The desired precursor anion **301** was isolated as its tetrabutylammonium salt ***n*–Bu_4N–301** in excellent yield.

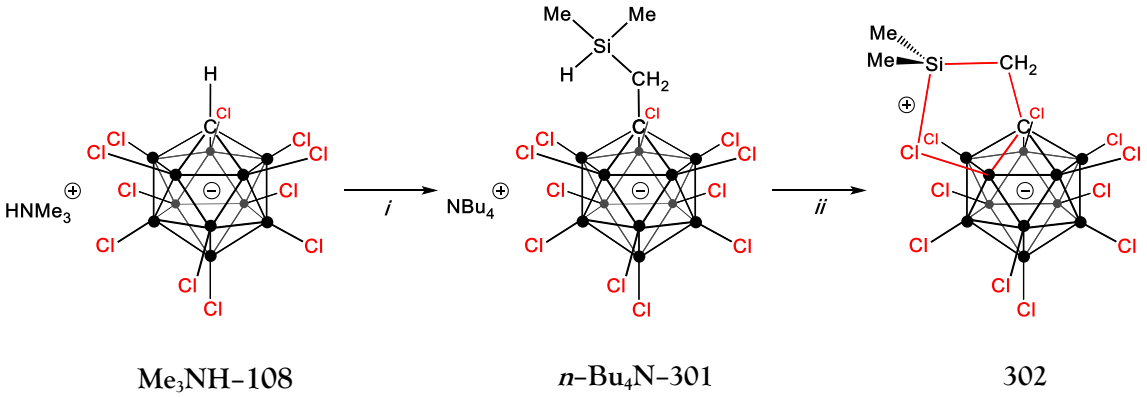

Scheme 3–1. (i) Treatment of **Me_3NH–108** with NaH and $ClCH_2SiMe_2H$ in THF for 48 h at 40 °C followed by precipitation of 301 with $[n\text{–}Bu_4N]Cl$. (ii) $[Ph_3C][B(C_6F_5)_4]$ in a 3:2 toluene/1,2–difluorobenzene mixture with precipitation of **302**.

An X–ray diffraction study was conducted on a single crystal of compound ***n*–Bu_4N–301**, obtained by diffusion of pentane into a solution of the compound in fluorobenzene at −32 °C (Figure 3–1).

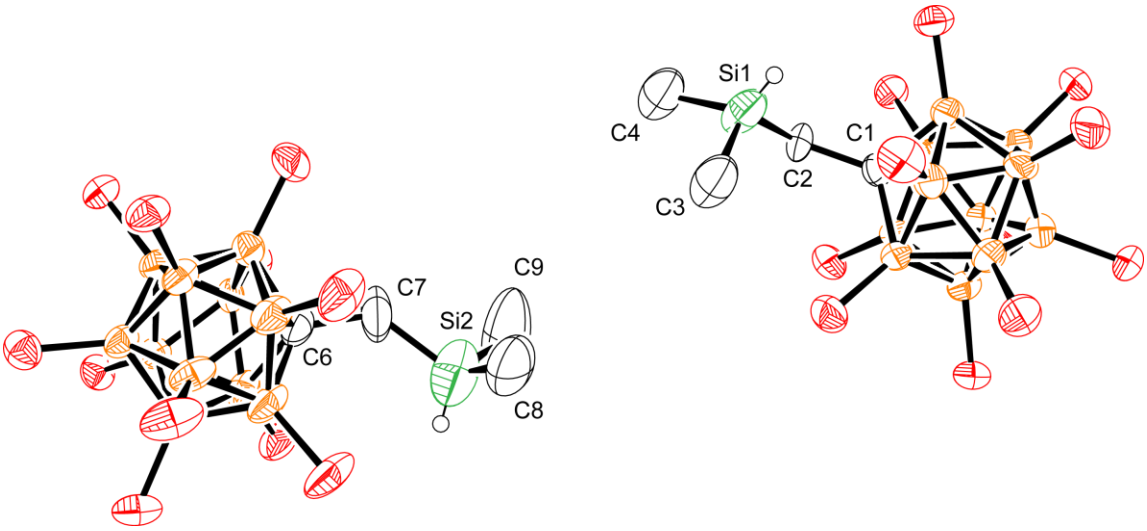

Figure 3–1. ORTEP diagram of the structure of ***n*–Bu$_4$N–301** in the solid state, with methyl and methylene hydrogen atoms, and [*n*–Bu$_4$N]$^+$ counter cations omitted for clarity. Thermal ellipsoids set to 50% probability. Two crystallographically–independent ***n*–Bu$_4$N–301** ion pairs are present in the asymmetric unit. Disorder around C4 omitted for clarity. Hydrogen atoms on Si–H moieties are shown at idealized positions.[126]

Compound ***n*–Bu$_4$N–301** crystalized in the orthorhombic space group P_{bca}. The asymmetric unit contains two independent anions that show mild disorder around the alkyl chains of their respective [*n*–Bu$_4$N]$^+$ counter cations. The silicon atoms of both crystallographically independent molecules show a slightly distorted tetrahedral coordination geometry. The C–Si–C angles fall in the range between 95.8(13) ° and 118.1(5) ° for Si1, and 104.3(8) ° and 110.9(6) °around Si2. The sums of C–Si–C angles are 317.5(19) ° and 322.5(13) °, around Si1 and Si2 respectively. C–Si bond lengths fall within expected values, and within the ranges of 1.853(10) Å–1.900(8) Å for Si1 and 1.794(19)–1.834(11) for Si2.

Treatment of ***n*–Bu$_4$N–301** with $[Ph_3C][B(C_6F_5)_4]$ in a toluene/1,2–difluorobenzene mixture resulted in the abstraction of the silicon–bound hydride by the $[Ph_3C]^+$ cation and precipitation of the desired zwitterion **302**, which was isolated in 46% yield upon workup. Under slow diffusion conditions, this reaction produced a single crystal suitable for a structural study by X–ray diffractometry (XRD). The solid–state structure contained crystallographic disorder derived from the random swapping of the C1–C2–Si1(C3)2 and B1–Cl1–Si1(C3)2 moieties (Figure 3–2 A, B). The silylium center in **302** is stabilized by the weak coordination of a proximal chlorine atom located at a distance of 2.304(8) Å. The significant silylium character of **302** is supported by only modest pyramidalization at Si: sum of C–Si–C angles around Si is 351(2)°. These parameters are similar to those found in adducts of R_3Si^+ cations with chlorocarboranes.[105] For example, the Si–Cl distance was found to be 2.3044(13) Å or 2.2815(11) Å (two crystallographically independent ion pairs) in $Et_3Si[HCB_{11}H_5Cl_6]$,[127] 2.323(3) Å in $^iPr_3Si[HCB_{11}H_5Cl_6]$[114] and 2.334(3) Å in $Et_3Si[HCB_{11}Cl_{11}]$,[115] whereas the values for the sum of the C–Si–C angles in these compounds fall into 345–351° range. Compound **302** proved to be unexpectedly poorly soluble in 1,2–difluorobenzene, a solvent that is typically quite capable of dissolving organic salts of carborane anions. Density functional theory (DFT) calculations performed by Dr. Jia Zhou on an isolated gas–phase molecule of **302** were able to shed light on the low solubility, and on the observed disorder in the solid–state. The calculated structure matched the XRD structure closely (Table 3–1), lending extra credence to the model of the crystallographic disorder, and revealed a nearly C_{2v}–symmetric distribution of charge density in **302** (Figure 3–2 C).

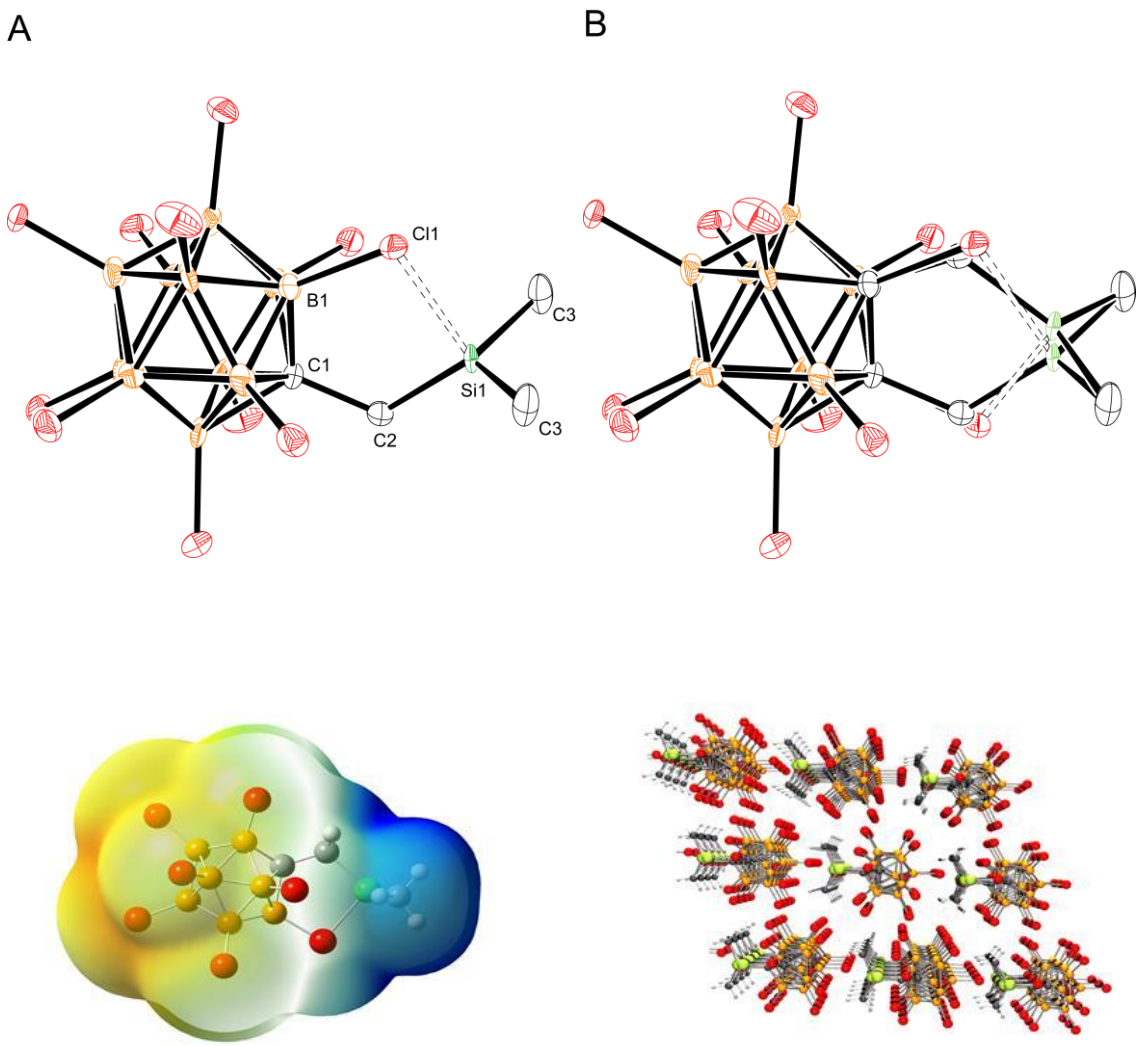

Figure 3–2. A) ORTEP diagram of the structure of **302** in the solid state. Thermal ellipsoids shown at 50% probability. Si1···Cl1 2.304(8) Å; sum of C–Si–C angles 351(2)°. B) ORTEP diagram of the observed disorder in the crystal, consisting of two superimposed orientations of the molecule related by a 180° rotation around a pseudo–C2 axis passing through the center of the cage and the silicon site. In both instances the ellipsoids were set at 50% probability, with the hydrogen atoms omitted for clarity. C) Charge density plot for **302**. D) Three–dimensional packing diagram of **302** in the crystal.[126]

We posit that it is the origin of the crystallographic disorder: **302** packs in the crystal as though it were a C_{2v}–symmetric molecule. The dipole moment of **302** is very high (15.2 D, by DFT) and the "head–to–tail" packing with alternating stacking of layers (Figure 3–2 D) presumably results in a high lattice energy that disfavors dissolution.

DFT calculations on the gas phase **302** also accurately predicted its ^{29}Si NMR chemical shift. **302** resonated at δ 137.4 ppm in the ^{29}Si NMR CP/MAS spectrum; DFT calculation yielded δ 140.7 ppm. The degree of the downfield ^{29}Si NMR chemical shift has been used to characterize the degree of silylium character.[128] The **302** value is farther downfield than the values for adducts of R_3Si^+ with chlorocarboranes and is comparable to $[Me_3Si][EtCB_{11}F_{11}]$ (δ 138ppm), for which ionicity was demonstrated in the melt.[129] Consistent with the postulated significant silylium character, the lowest unoccupied molecular orbital (LUMO) of **302** is predominantly based on silicon (Figure 3–3).

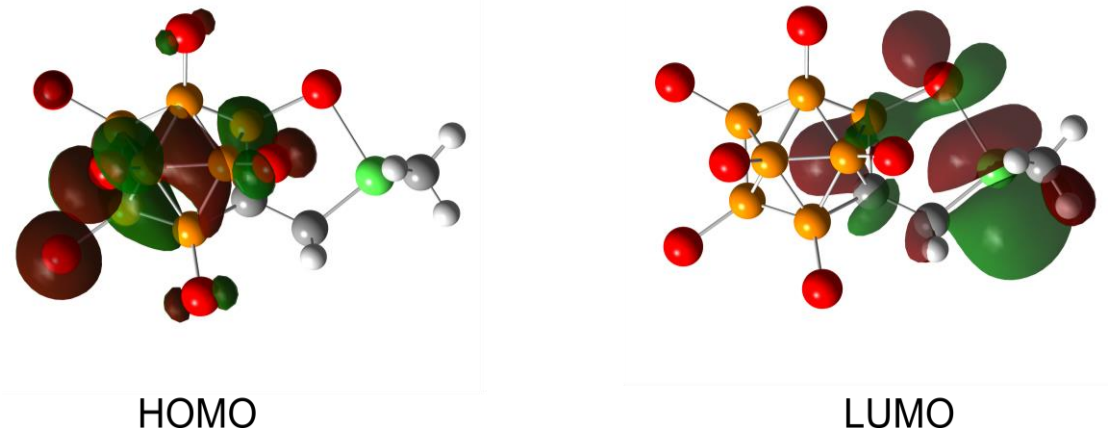

Figure 3–3. HOMO and LUMO of **302** plotted at an isovalue of 0.03.126

Table 3–1. Selected DFT–calculated and experimental bond lengths (Å) and angles (deg) for **302**.

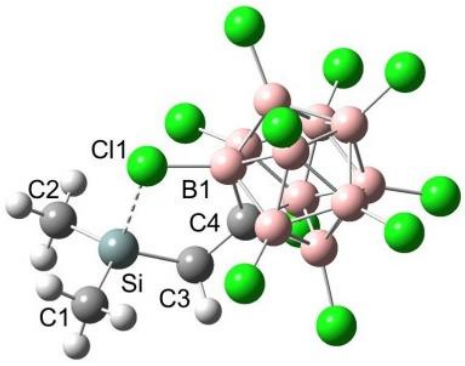

Bond Lengths (Å)		Bond Angles (deg)	
Calculated (Experimental)		Calculated (Experimental)	
Si–Cl1	2.308 (2.304(8))	C1–Si–C3	117.3 (118.5(12))
Cl1–B1	1.873 (1.864(9))	C1–Si–C2	112.4 (113.8(5))
Si–C1	1.857 (1.811(14))	C2–Si–C3	117.3 (122.0(13))
Si–C2	1.857 (1.854(14))		
Si–C3	1.897 (1.85(3))		

Compound **302** reacted rapidly with $(CH_3)_3CCl$ in liquid SO_2 at −70 °C to produce the $[(CH_3)_3C]^+$ cation complemented by the $[ClSiMe_2CH_2CB_{11}Cl_{11}]^-$ (**$(CH_3)_3C$–303**) anion (compound **304**, Scheme 3–2). The identity of the anion was confirmed by independent syntheses (Scheme 3–2): **Ph_4P–303** was cleanly obtained in the reaction of **302** with

[Ph_4P][Cl], while the reaction of ***n*–Bu$_4$N–301** with N–chlorosuccinimide produced ***n*–Bu$_4$N–303**. Compounds **(CH$_3$)$_3$C–303**, **Ph$_4$P–303**, and ***n*–Bu$_4$N–303** were quite soluble in liquid SO_2 or dichloromethane (for **Ph$_4$P–303** and ***n*–Bu$_4$N–303**). The *tert*–butyl cation in **(CH$_3$)$_3$C–303** was identified in SO_2 solution at −60 °C or below based on the characteristic resonances[130,131] in the $^{13}C\{^1H\}$ (δ 334.5 and 49.0 ppm) and ^1H (δ 4.53 ppm) NMR spectra. Warming up the SO_2 solution of **(CH$_3$)$_3$C–303** to ambient temperature resulted in decomposition, although the diminished ^1H NMR resonance of $[(CH_3)_3C]^+$ could still be observed at 20 °C. Apparently, strong acid formation takes place, from the similarity of new downfield signals to the spectrum of $HOSO_2CF_3$ in liquid SO_2. Independent X–ray structural studies performed on the $[(CH_3)_3]^+$ cation by Reed and Laube[130,133] have shown short C_{sp^2}–C_{sp^3} distances within the range of 1.429(4)–1.459(4) Å, in contrast to the average C_{sp^2}–CH_3 distance of 1.**503** Å,[132] suggestive of a significant degree of hyperconjugation of the methyl $\sigma_{C\text{-}H}$ bonds with the empty p_C orbital. This phenomenon can facilitate proton abstraction by an external base, resulting in formation of *iso*–butylene ethylene, with concomitant cationic polymerization, processes that can be slowed down at low temperatures. However, in our case it is not clear whether degradation is a result of interactions with SO_2, adventitious impurities, or the anion itself. Laube has also observed the decomposition of $[(CH_3)_3C][Sb_2F_{11}]$ by ^1H NMR spectroscopy of the crystalline material in SO_2 upon warming up from −60 °C.[133] Kato and Reed[130] also only observed $[(CH_3)_3C][HCB_{11}Me_5Br_6]$ in solution at −60 °C.

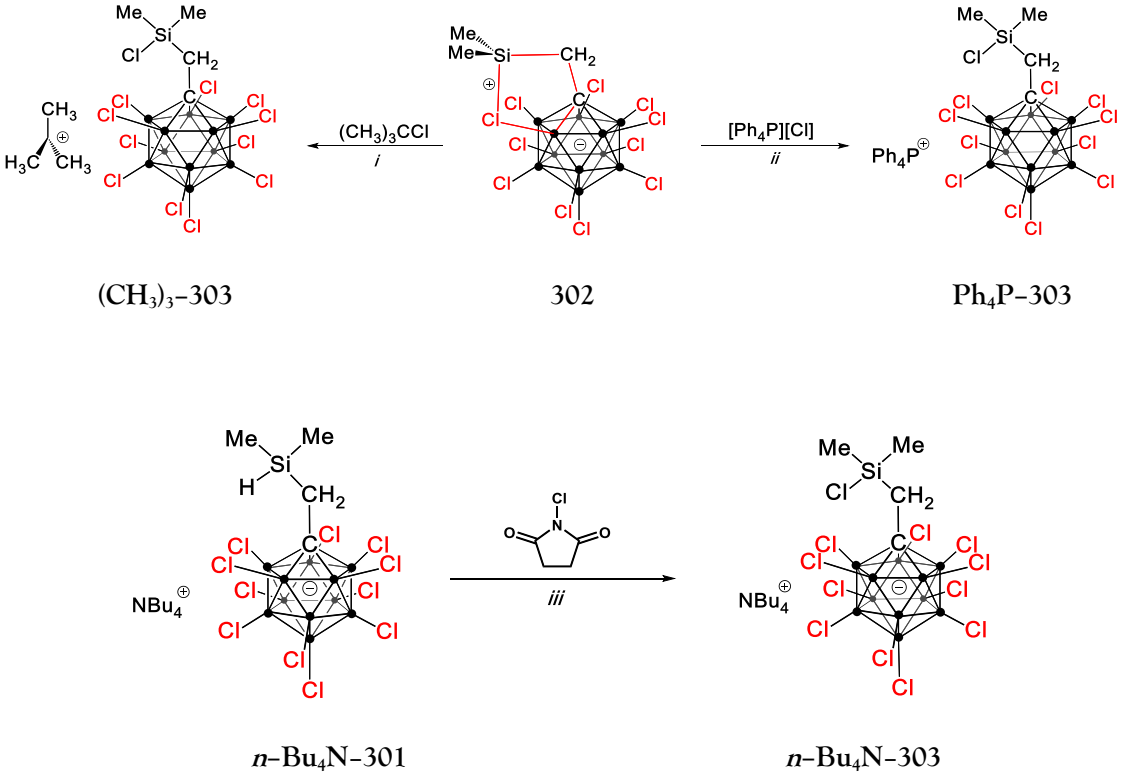

Scheme 3–2. *i*) Treatment of **302** with *tert*–butyl chloride in liquid SO_2 at −70 °C. *ii*) Trapping of **302** with $[Ph_4P][Cl]$ in dichloromethane to form **303**. *iii*) Independent synthesis of the **303** anion by treatment of ***n*–Bu$_4$N–301** with N–chlorosuccinimide in dichloromethane.

This reaction demonstrates the prowess of **302** as a powerful Lewis acid and that the WCA generated from **302** upon chloride abstraction is compatible with a reactive carbocation.

3.3 Conclusion

Our findings demonstrate the potential for design of powerful charge–neutral Lewis acids based on zwitterionic construction with the carborane cage as the anionic component. This approach is conceptually related to the use of neutral carborane radical $MeCB_{11}Me_{11}$ as a one–electron oxidant that converts to a weakly coordinating anion upon accepting an electron.[134,135]

3.4 Experimental details

3.4.1 General considerations

(Chloromethyl)dimethylsilane, and (chloromethyl)chlorodimethylsilane were purchased from Aldrich and used without any further purification. Sodium hydride was purchased from Aldrich as a dispersion in oil and was washed exhaustively with pentane over a fritted funnel to remove all oil and then dried *in vacuo*. **Me_3NH–108** was prepared from **Cs–108** using the previously published $SbCl_5$ chlorination procedure.[81] Halogenated solvents were dried over calcium hydride for 48 h and then vacuum transferred. Hydrocarbon and ether solvents were dried over and distilled from Na/K/Ph_2CO/18–crown–6. Solution. NMR spectra were collected on Varian Inova 400 (^{11}B NMR, 128.19 MHz; ^{29}Si NMR, 79.43 MHz) and Varian Inova 500 (^{1}H NMR, 499.43 MHz; ^{13}C NMR, 125.58 MHz) spectrometers using deuterated solvents as indicated. In the case of ^{1}H and ^{13}C NMR, spectra were referenced to residual solvent peaks. For ^{11}B NMR, spectra were referenced externally to δ 0 ppm using $BF_3 \cdot OEt_2$, and ^{29}Si NMR spectra to δ 0 ppm using tetramethylsilane. Solid state CP/MAS NMR spectra

were collected on a Bruker Avance 400 spectrometer (^{29}Si NMR, 79.49 MHz). A standard cross polarization pulse sequence was utilized, with a contact time of 6 ms and a recycling delay of 5 s. The solid sample was charged into a 4 mm rotor and spun at a rate of 10 kHz. The sample was referenced externally using $Si(SiMe_3)_4$ to the farthest downfield signal to a chemical shift δ −9.82 ppm. MALDI mass spectrometric analyses of the carborane anions were carried out by the Texas A&M University Laboratory for Biological Mass Spectrometry (LBMS). Elemental analyses were performed by CALI Labs, Inc. (Parsippany, NJ, USA).

3.4.2 Synthetic procedures and characterization data

Synthesis of (chloromethyl)dimethylsilane. In an argon–filled dry box, solid $LiAlH_4$ (6.0 g, 0.156 mol), 100 mL of dry THF, and 250 mL of dry OEt_2 were charged in a 3–neck, 1 liter flask equipped with a PTFE stir bar. An addition funnel, charged with (chloromethyl)chlorodimethylsilane (75 g, 0.524 mol) and 20 mL of dry OEt_2, was assembled on the center neck of the flask. A hose adaptor was assembled on another neck, and a glass stopper was placed in the remaining neck. The assembly was taken outside from the dry box and connected to a Schlenk line to provide a positive pressure of argon. The flask was then placed in an acetone/dry ice bath and cooled to −35 °C. The solution of (chloromethyl)chlorodimethylsilane was added dropwise over 30 min to the cooled suspension of $LiAlH_4$. Once addition was complete, the mixture was allowed to warm to room temperature, at which point it was stirred for 1 h. The reaction mixture was poured into a slurry of 200 mL of 10% HCl and crushed ice. The organic phase was extracted with three

portions of 150 mL of OEt_2, the extracts were collected, dried over $MgSO_4$, and filtered through Celite. The product was purified by distillation at atmospheric pressure (b.p. 78– 80 °C). Yield: 17.7 g (31%). ^1H (399.52 MHz, $CDCl_3$) δ 0.19 (d, 6H, $^3J_{H-H}$ = 3.6 Hz, $(CH_2)Si(CH_3)_2H$, silicon satellites $^2J_{H-Si}$ = 120.4 Hz), 2.84 (d, 2H, $^3J_{H-H}$ = 2.5 Hz, $–CH_2–Si(CH_3)_2H$, silicon satellites $^2J_{H-Si}$ = 138.9 Hz), 4.03 (AM_2X_6 multiplet, , $^3J_{H-H}$ = 3.6 Hz, $^3J_{H-H}$ = 2.5 Hz, $Cl(CH_2)Si(CH_3)_2H$, silicon satellites $^2J_{H-Si}$ = 192.4 Hz).

Synthesis of butylchloro(chloromethyl)(methyl)silane. Inside an argon–filled dry box, dichloro(chloromethyl)(methyl)silane (6.0 g, 36.0 mmol), 2.0 M BuMgCl in OEt_2 (18.0 mL, 36.0 mmol) and 10 mL of dry OEt_2 were charged in Schlenk flask equipped with a PTFE–coated magnetic stir bar and a PTFE valve. Next, the flask was placed overnight in an oil bath set to 50 °C, and the solution was stirred overnight. The next morning a copious amount of white solid material was observed. The reaction mixture was filtered through a fritted funnel protected with Celite. The solids left over in the flask and the Celite, were washed 3 × 10 mL portions of dry OEt_2, volatiles were removed *in vacuo* to obtain an oil that was purified by vacuum distillation to obtain a clear oil. Yield 4.2 g (64%) ^1H NMR (499.43 MHz, $CDCl_3$) δ 0.52 (s, 3H, $Si–CH_3$), 0.91 (t, 3H, $^3J_{H-H}$ = 7.1 Hz, $Si–(CH_2)_3–CH_3$), 0.97 (m, 2H, $–CH_2–$), 1.40 (m, 4H, $Si–(CH_2)_2–$), 2.95 (AB quartet, 2H, calculated coupling constants (using MestReNova™ version 8.1.2): $^2J_{H-H}$ = 14.0 Hz, Δδ = 0.035 ppm, $Cl–CH_2–Si$).

Synthesis of butyl(chloromethyl)(methyl)silane. Inside an argon–filled dry box butylchloro(chloromethyl)(methyl)silane (5.8 g, 31.4 mmol) and 20 mL of dry OEt_2 were charged in a Schlenk flask equipped with a PTFE–coated magnetic stir bar. Next, the mixture was placed for 1 h in a freezer set at −30 °C, then a 2.0 M solution of $LiAlH_4$ in THF (3.5 mL, 7.0 mmol) was added via syringe over 1 min under constant stirring. The resulting mixture was stirred for an h, over the course of which a copious amount of white precipitate formed. The reaction mixture was filtered through a fritted funnel protected with Celite. The solids left over in the flask and the Celite, were washed 3 × 10 mL portions of dry OEt_2. The volatiles were removed *in vacuo*, and the resulting oil was purified by vacuum distillation to obtain a clear, oily compound. Yield: 4.4 g (93%). ^{1}H NMR (499.43 MHz, $CDCl_3$) δ 0.19 (d, 3H, $^3J_{Si-H}$ = 3.7 Hz, SiH–C*H*$_3$), 0.73 (m, 2H, butyl–C*H*$_2$–), 0.89 (m, 3H, butyl–C*H*$_3$), 1.36 (m, 4H, butyl–(C*H*$_2$)$_2$–), 2.87 (d, 2H, $^3J_{H-H}$ = 2.5 Hz, Cl–C*H*$_2$–SiH), 3.96 (AM_2X_3 multiplet, 1H, $^3J_{H-H}$ = 2.5 Hz, $^3J_{Si-H}$ = 3.7 Hz, Si–*H*).

Synthesis of butyl(iodomethyl)(methyl)silane. Manipulations were performed without the use of air–free techniques. Butyl(chloromethyl)(methyl)silane (3.0 g, 20.0 mmol), NaI (3.8 g, 25.0 mmol) and 50 mL of HPLC–grade acetone were charged in a Schlenk flask equipped with a PTFE–coated stir bar. A reflux condenser was assembled on top of the flask and the mixture was heated to reflux temperature for 1 h, over the course of which the reaction mixture developed a yellow color. The reaction mixture was filtered through a short path of silica gel, the silica was washed with acetone, and the mother liquor was distilled *in vacuo* to

obtain a clear oil. Yield 2.1 g (43%). ^{1}H NMR (499.43 MHz, $CDCl_3$) δ 0.19 (d, 3H, $^{3}J_{Si-H}$ = 3.6 Hz, SiH–C*H*$_3$), 0.72 (m, 2H, butyl–C*H*$_2$–), 0.89 (m, 3H, butyl–C*H*$_3$), 1.35 (m, 4H, butyl–(C*H*$_2$)$_2$–), 2.05 (AB multiplet, 2H, calculated coupling constants (using MestReNova™ version 8.1.2): $^{2}J_{H-H}$ = 14.0 Hz, $^{3}J_{H-H}$ = 3.1 Hz, Δδ = 0.015 ppm, I–C*H*$_2$–SiH), 4.04 (oct, 1H, $^{3}J_{Si-H}$ = 3.8 Hz, satellites $^{1}J_{Si-H}$ = 191.4 Hz, Si–*H*).

Synthesis of [((butyl)(methyl)SiH)CH$_2$CB$_{11}$Cl$_{11}$]$^-$. Me$_3$NH–108 (0.05 g, 85.9 μmol) was charged in a Schlenk flask equipped with a PTFE–lined stir bar, and dissolved in 30 mL of dry THF. To the resulting solution, NaH (0.008 g, 344.0 μmol) was added in one portion. The suspension was stirred for 1 h at room temperature and the volatiles were removed *in vacuo* to obtain a white solid residue that was resuspended in 30 mL of dry THF. The suspension was treated with butyl(iodomethyl)(methyl)silane (0.13 g, 515.0 μmol), and the resulting mixture was stirred at room temperature for 48 h. An aliquot of the reaction mixture was obtained and analyzed by MALDI mass spectrometry, showing complete conversion. The reaction mixture was dried *in vacuo* to obtain a white residue that was dissolved in 5 mL of deionized water, and the product was then precipitated with [*n*–Bu$_4$N][Cl] (0.05 g, 172.0 μmol). The crude product was recovered by filtration through a fine fritted funnel, and was washed several times with deionized water. Yield 0.04 g (53%). ^{1}H NMR (399.52 MHz, 3:2 toluene–d_8/1,2–difluorobenze) δ 0.24 (d, 3H, $^{3}J_{H-H}$ = 3.5 Hz, SiH–C*H*$_3$), 0.56 (m, 1H, Si butyl–C*H*$_2$–), 0.70 (m, 1H, Si butyl–C*H*$_2$–), 0.80 (m, 3H, Si butyl–CH$_3$), 0.85 (m, 12H, *n*–Bu$_4$N$^+$–CH$_3$), 1.17 (m, 16H, *n*–B*u*$_4$N$^+$ –(C*H*$_2$)$_2$–), 1.27 (m, 4H, Si butyl–

(CH_2)$_2$–), 1.79 (dd, 1H, $^2J_{H-H}$ = 15.8 Hz, $^3J_{H-H}$ = 4.1 Hz, C_{carb}–CH_2–Si), 1.93 (dd, 1H, $^2J_{H-H}$ = 15.7 Hz, $^3J_{H-H}$ = 2.1 Hz, C_{carb}–CH_2–Si), 2.57 (m, 8H, *n*–Bu_4N^+N–(CH_2)–), 4.75 (m, 1H, Si–*H*). $^{11}B\{^1H\}$ NMR (128.19 MHz, 3:2 toluene–d_8/1,2–difluorobenze) δ– 3.0 (b, 1B), –9.9 (b, 5B), –10.9 (b, 5B). MALDI–MS *m*/*z* = 636.

Synthesis of *n*–*B*u$_4$N–301. Air–free manipulations for this procedure were performed in an argon–filled dry box. **Me$_3$NH–108** (0.403 g, 0.69 mmol), previously purified by crystallization from acetone/water and dried, was charged in a round–bottom Schlenk flask equipped with a PTFE valve and a stir bar, and dissolved in *ca.* 20 mL of THF. To this solution NaH (0.066 g, 2.77 mmol) was added in a single portion, resulting in immediate evolution of H_2. This mixture was stirred vigorously for 20 min, and a $^{11}B\{^1H\}$ NMR spectrum of an aliquot of the reaction mixture was collected to confirm that complete formation of the **Na$_2$–206** had been effected. Volatiles were then removed to dryness *in vacuo* to obtain a white residue that was suspended in *ca.* 20 mL of THF and (chloromethyl)chlorodimethylsilane (0.48 g , 4.15 mmol) was added in a single portion. Once all components were mixed, the flask was removed from the box and placed in an oil bath set to a temperature of 40 °C for 48 h. An aliquot of the reaction mixture was taken and a MALDI mass spectrum was obtained showing clean, complete conversion. All volatiles were removed *in vacuo* to obtain a white solid that was dissolved in *ca.* 5 mL of water. To this solution, [*n*–Bu_4N][Cl] (0.288 g, 1.03 mmol) was added in single portion resulting in immediate formation of a white precipitate that was collected by filtration through a fine fritted funnel, washed five times with water and

dissolved in HPLC grade acetone in the same fritted funnel. The resulting solution was filtered and collected in a clean Schlenk flask and all volatiles were removed *in vacuo* to obtain a white solid. The resulting solid was dried *in vacuo* at 180 °C for 12 h and then taken into an argon–filled dry box that has not been used to store or work with any volatile materials besides hydrocarbons and halogenated hydrocarbons. In this dry box, ***n*–Bu$_4$N–301** was crystallized by slow diffusion of pentane into a fluorobenzene solution of the compound. Yield: 0.51 g (88%). ^{1}H NMR (399.52 MHz, 3:2 toluene–d_8/1,2–difluorobenze) δ 0.17 (d, 6H, $^3J_{H-H}$ = 3.5Hz, (C*H*$_3$)$_2$–SiH, silicon satellites $^2J_{H-Si}$ = 120.3 Hz), 0.86 (m, –C*H*$_3$, *n*–Bu$_4$N$^+$), 1.19 (m, –(C*H*$_2$)$_2$–, *n*–Bu$_4$N$^+$), 1.84 (d, 2H, *J* = 5.0 Hz, C$_{ipso}$–C*H*$_2$–Si), 2.57 (m, *n*–N–C*H*$_2$–, Bu$_4$N$^+$), 4.78 (m, 1H, $^3J_{H-H}$ = 3.5 Hz, silicon satellites $^1J_{Si-H}$ = 205.7 Hz, Si–*H*). ^{11}B{^{1}H} NMR (128.19 MHz, 3:2 toluene–d_8/1,2–difluorobenze) δ −11.0 (s br, 5B), −9.9 (s br, 5B), −3.0 (s, br, 1B). ^{29}Si NMR (79 MHz, 3:2 toluene–d_8/1,2–difluorobenze) δ −11.82 (dm, $^1J_{Si-H}$ = 206.6 Hz, *Si*–H). ^{13}C{^{1}H} NMR (100.46 MHz, 3:2 toluene–d_8/1,2–difluorobenze) δ −0.69 (–SiH–(C*H*$_3$)$_2$), 13.69 (–C*H*$_3$, *n*–Bu$_4$N$^+$), 17.58 (C$_{ipso}$–C*H*$_2$–SiMe$_2$H), 20.06 (–C*H*$_2$–CH$_3$, *n*–Bu$_4$N$^+$), 24.08 (–C*H*$_2$–, *n*–Bu$_4$N$^+$), 59.02 (N–C*H*$_2$–, *n*–Bu$_4$N$^+$). Elemental analysis: Calculated (Found) C, 28.71% (28.62%); H, 5.42% (5.30%); B, 14.07% (14.22%).

Synthesis of 302. Manipulations in this procedure were performed in an argon–filled dry box which has not been used to store or work with any volatile materials besides hydrocarbons and halogenated hydrocarbons. [Ph$_3$C][B(C$_6$F$_5$)$_4$] (0.220 g, 0.244 mmol) and ***n*–Bu$_4$N–303** (0.204 g, 0.244 mmol) were placed into a vial and dissolved in 1.0 mL of a 3:2

mixture of toluene and 1,2–difluorobenzene to form a deep orange solution. A lemon yellow solid precipitated out of the solution after a few moments. The orange color of the solution persisted. The solid was filtered off using a fine fritted funnel and washed with 2 × 2 mL portions of 1,2–dichlorobenzene, 1 × 2 mL of fluorobenzene and finally 2 × 2 mL portions of pentane. The solid was then transferred to a Schlenk flask and dried *in vacuo* for 3 h at ambient temperature. These washes were critical in obtaining a high purity product. Yield: 0.067 g (46%). ^{29}Si CP/MAS (79.46 MHz, 10 kHz MAS) (Figure 3–4 and 3–5) δ 137.39. Elemental analysis. Calculated (Experimental): C, 8.10% (8.19%); H, 1.36 (2.13%); B, 20.05 (19.87%).

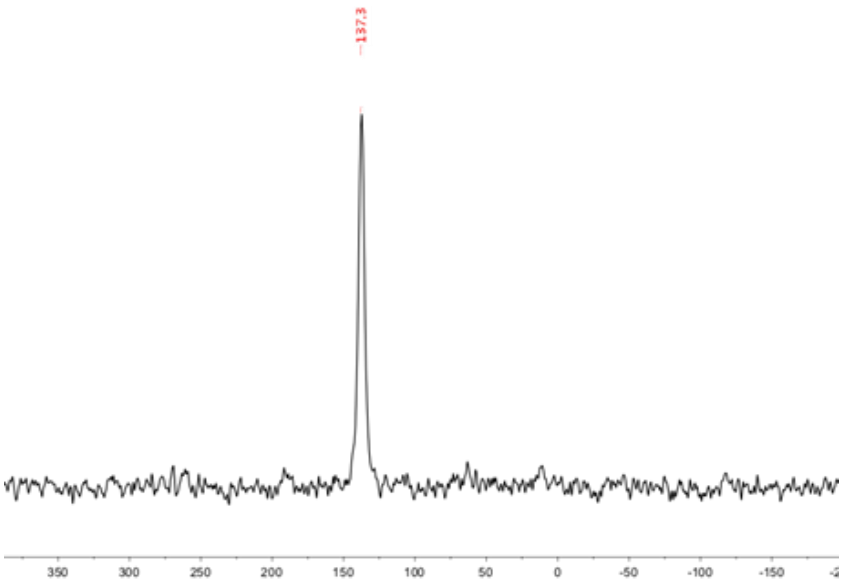

Figure 3–4. ^{29}Si CP/MAS NMR (79 MHz) spectrum of **302**. Neat solid.

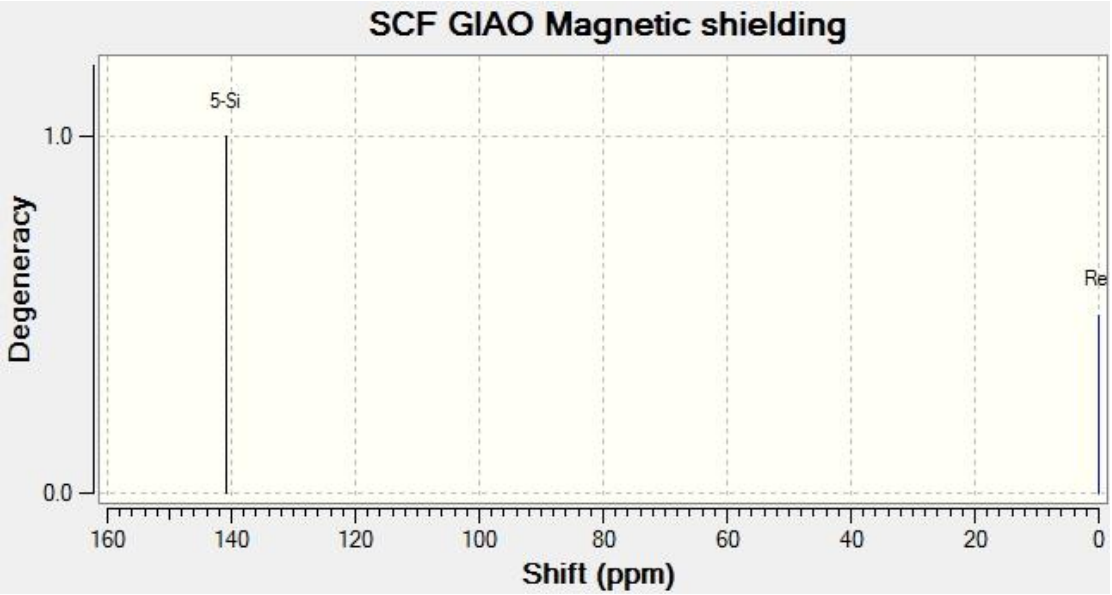

Figure 3–5. Calculated ^{29}Si NMR spectrum for **302**.

Trapping of 302 with Ph_4PCl (Experiment 1). [Ph_4P][Cl] was pre–dried by heating to 130 °C overnight *in vacuo*. **302** (0.010 g, 0.016 mmol) and [Ph_4P][Cl] (0.006 g, 0.016 mmol) were charged in a J. Young NMR tube and CD_2Cl_2 was added resulting in formation of a clear, colorless solution. ^{1}H NMR (399.52 MHz, CD_2Cl_2) δ 0.75 (s, 6H, –Si(CH_3)$_2$Cl), 1.81 (s, 2H, C_{ipso}–CH_2–$SiMe_2Cl$), 7.62–7.93 (m, 20H, Ph_4P^+).

Trapping of 302 with Ph_4PCl (Experiment 2). [Ph_4P][Cl] was pre–dried by heating to 130 °C overnight *in vacuo*. **302** was prepared by treating a solution of [Ph_3C][$B(C_6F_5)_4$] (0.019 g, 0.020 mmol) in a 3:2 mixture of toluene and 1,2–difluorobenzene in a vial with ***n*–Bu_4N–301** (0.017 g, 0.02 mmol). A lemon yellow solid precipitated out of the solution after a few moments. The remaining yellow solution was decanted and the solid was washed once with 2

mL of dry fluorobenzene. The solvent was removed with a pipette and $[Ph_4P][Cl]$ (0.008 g, 0.02 mol) was charged into the vial and 1 mL of fluorobenzene was added. The contents were vigorously stirred for 5 min, the solid was allowed to settle and the supernatant was collected with a pipette and transferred into a J. Young tube. Volatiles were removed *in vacuo* to obtain a white residue. Dry SO_2 was vacuum transferred into the tube and the ^1H NMR spectrum was collected. ^1H NMR (399.52 MHz, SO_2) δ 1.31 (s, 6H, –Si(*C*H_3)$_2$Cl), 2.36 (s, 2H, C_{ipso}–*C*H_2–SiMe$_2$Cl), 8.33–8.48 (m, 20H, Ph_4P^+).

Independent synthesis of 303. ***n*–Bu$_4$N–301** (0.04 g, 0.048 mmol) and N–chlorosuccinimide (0.009 g, 0.067 mmol) were charged in a J. Young NMR tube and dichloromethane–d_2 was added. The NMR tube was placed in an oil bath set to 80 °C for 24 h. NMR analysis of the reaction mixture showed complete, clean conversion. ^1H NMR (399.52 MHz, dichloromethane–d_2) δ 0.75 (s, 6H, –Si(*C*H_3)$_2$Cl), 1.03 (t, 12H, –*C*H_3, *n*–Bu$_4$N$^+$), 1.44 (m, 8H, –*C*H_2–CH$_3$, Bu$_4$N$^+$), 1.61 (m, 8H, –(*C*H_2)–, *n*–Bu$_4$N$^+$), 1.82 (s, 2H, C_{ipso}–*C*H_2–SiMe$_2$Cl), 3.08 (m, 8H, N–*C*H_2–, *n*–Bu$_4$N$^+$). $^{11}B\{^1H\}$ NMR (128.19 MHz, dichloromethane–d_2) δ −11.7 (s br, 5B), −10.7 (s br, 5B), −3.5 (s, br, 1B). $^{29}Si\{^1H\}$ (79 MHz, dichloromethane–d_2) δ −29.26 (–*Si*Me$_2$Cl).

Synthesis of 303. In a base–free dry box, **302** (0.031 g, 50.6 μmol) was charged in a J. Young NMR tube. Using a 10 μL Hamilton syringe, $(CH_3)_3CCl$ (6 μL, 52 μmol) was deposited on the inside wall of the same tube. This tube was taken out from the box, and the

alkyl chloride was frozen by immersing the tube in liquid nitrogen. With the tube immersed in liquid nitrogen at all times, it was connected to a vacuum line and evacuated for 10 min. SO_2 was then distilled into the NMR tube, then closed and placed in an acetone/dry ice cold bath to let the frozen contents slowly thaw. Spectra were then collected in an NMR spectrometer pre-cooled to −70 °C. ^{1}H NMR (399.52 MHz, −70 °C, SO_2) (Figure 3-6) δ 1.30 (s, 6H, -Si(CH_3)$_2$Cl), 2.33 (s, 2H, -C_{ipso}-CH_2-SiMe$_2$Cl), 4.53 (s, 9H, (CH_3)$_3$C$^+$). ^{13}C{^{1}H} (100.46 MHz, −70 °C, SO_2) (Figure S14) δ 7.34, (s, -Si(CH_3)$_2$Cl), 20.84, (s, -C_{ipso}-CH_2-SiMe$_2$Cl), 48.98, (s, (CH_3)$_3$C$^+$), 55.11 (s, C_{ipso}-CH_2-), 334.50 (s, (CH_3)$_3$C$^+$).

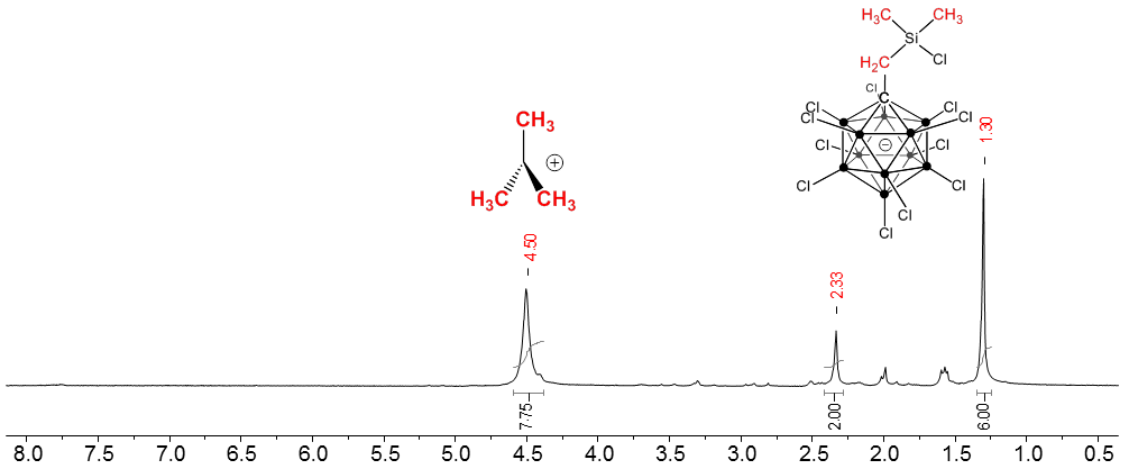

Figure 3-6. ^{1}H NMR spectrum (399.52 MHz) of **(CH$_3$)$_3$C-303** collected in SO_2 at −70 °C. Incipient peak *ca.* δ 9.3 ppm corresponds to the HOSO$^+$ cation. Aromatic resonances can be observed *ca.* δ 7.5 ppm and 8.5 ppm due to arene solvent contamination.

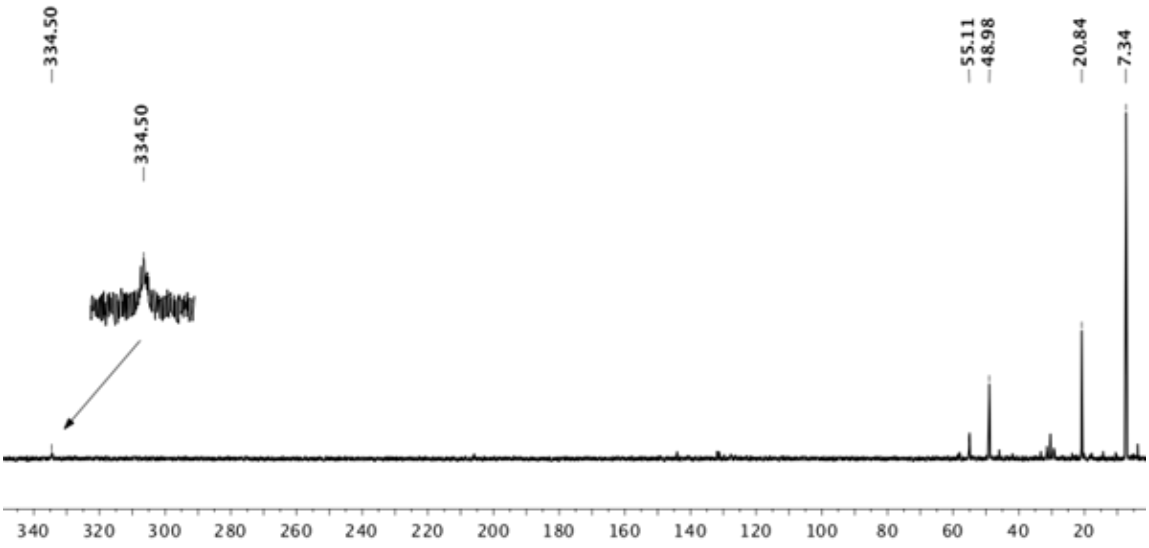

Figure 3–7. $^{13}C\{^{1}H\}$ NMR spectrum (100.46 MHz) of **$(CH_3)_3C$–303** collected in SO_2 at −70 °C.

Synthesis of $(CH_3)_3C$–303 (Experiment 2, excess 302). In a base–free dry box, Si–Zwi (0.030 g, 50.6 μmol) was charged in a J. Young NMR tube. Using a 10 μL Hamilton syringe, $(CH_3)_3CCl$ (3.5 μL, 30.4 μmol) was deposited on the inside wall of another J. Young tube and the taken out of the box and the contents were frozen in a liquid N_2 bath and the contents evacuated *in vacuo*. Dry SO_2 was vacuum transferred into this tube and the contents were thawed to make a solution. This solution was vacuum transferred to the J. Young tube containing 302, pre–cooled in a liquid N_2 bath. Once the solution was transferred, the tube was placed in an acetone/dry ice bath to let the frozen contents slowly thaw. The sample was then warmed up to room temperature and spectra were collected (Figure 3–8).

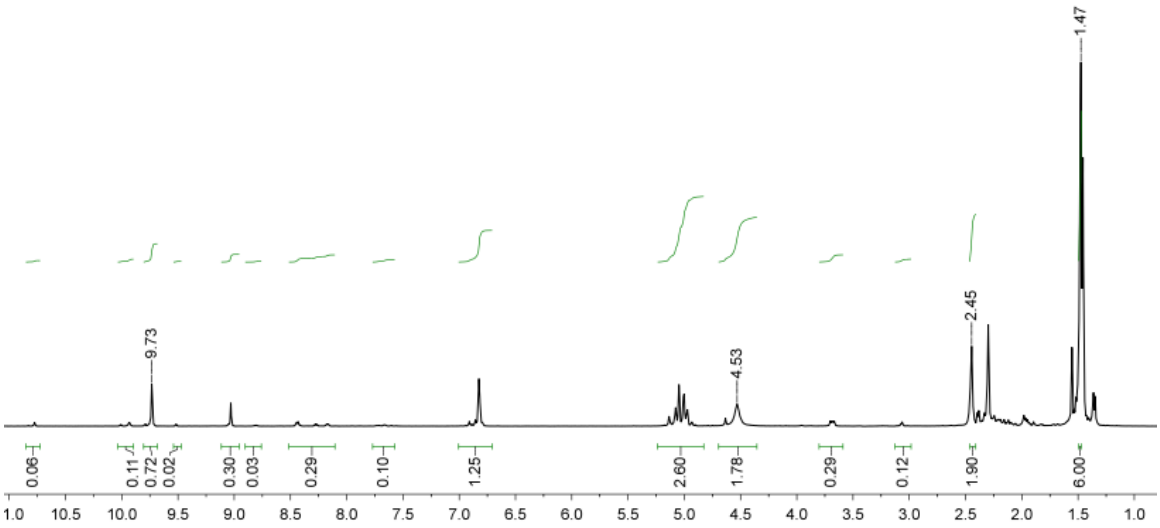

Figure 3–8. ^{1}H NMR spectrum (499.43 MHz) of $(CH_3)_3C$–303 collected in SO_2 collected at 20 °C. 40% excess 302 was used. The sum of integrals is 15.57 (sum of integrals for **$(CH_3)_3C$–303** should be 17.00). Resonances at δ 2.16 and 3.15 ppm correspond to 303. The small resonance at δ 5.34 ppm is a small amount of the $[C(CH_3)_3]^+$ cation.

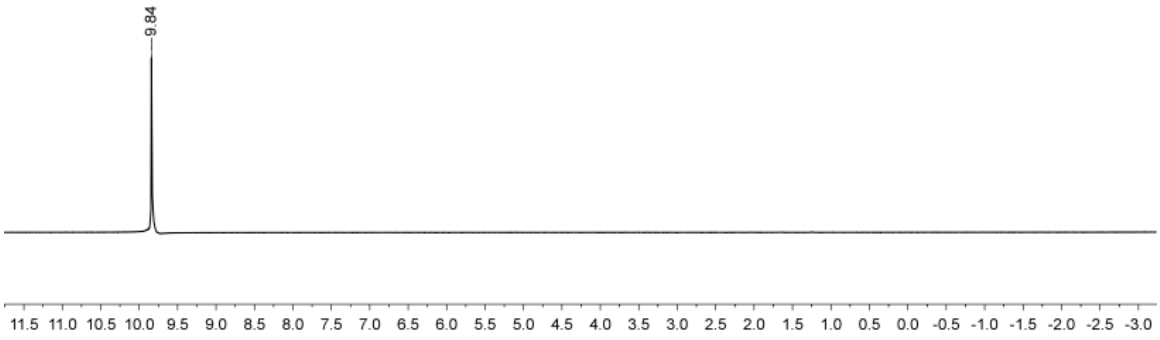

Figure 3–9. ^{1}H NMR spectrum (399.52 MHz) of triflic acid in SO_2 ($HOSO^+$ ion) at 20 °C.

Observation of formation of H–D. $[Ph_3C][B(C_6F_5)_4]$ (0.017 g, 17.9 μmol) and ***n*–Bu_4N–301** (0.030 g, 35.8 μmol) were charged in a J. Young NMR tube dissolved *ca.* 700 μL of a 3:2

mixture of toluene–d_8 and 1,2–difluorobenzene to form a deep orange solution, which quickly turned clear, concomitant with formation of a white precipitate. Bubbling was observed at this point. The ^{1}H NMR spectrum revealed the formation of H–D (δ 4.43, $^1J_{H-D}$ = 42.0 Hz) and H_2 (δ 4.46).

3.4.3 X–ray structural determinations

X–Ray data collection, solution, and refinement for 302. (Solved by Dr. Nattamai Bhuvanesh). Crystals of **302** were grown by diffusion of a saturated solution of ***n*–Bu$_4$N–301** in a toluene/1,2–difluorobenzene 3:2 mixture, into a saturated solution of $[Ph_3C][B(C_6F_5)_4]$ in the same solvent mixture at room temperature. A Leica MZ 75 microscope was used to identify a suitable lemon–yellow block with very well defined faces with dimensions (max, intermediate, and min) 0.12 mm × 0.08 mm × 0.02 mm from a representative sample of crystals of the same habit. The crystal mounted on a nylon loop was then placed in a cold nitrogen stream (Oxford) maintained at 110 K. A BRUKER GADDS X–ray (three–circle) diffractometer was employed for crystal screening, unit cell determination, and data collection. The goniometer was controlled using the FRAMBO software, v.4.1.05.[136] The sample was optically centered with the aid of a video camera such that no translations were observed as the crystal was rotated through all positions. The detector was set at 5.0 cm from the crystal sample. The X–ray radiation employed was generated from a Cu sealed X–ray tube (K_α = 1.5418 Å with a potential of 40 kV and a current of 40 mA) fitted with a graphite monochromator in the parallel mode (175 mm collimator with 0.5 mm pinholes). 180 data

frames were taken at widths of 0.5°. These reflections were used to determine the unit cell using Cell_Now.[137] A suitable cell was found and refined by nonlinear least squares and Bravais lattice procedures. The unit cell was verified by examination of the *h k l* overlays on several frames of data. No super–cell or erroneous reflections were observed. After careful examination of the unit cell, an extended data collection procedure (19 sets) was initiated using omega and phi scans.

Integrated intensity information for each reflection was obtained by reduction of the data frames with APEX2.[98] The integration method employed a three dimensional profiling algorithm and all data were corrected for Lorentz and polarization factors, as well as for crystal decay effects. Finally the data was merged and scaled to produce a suitable data set. SADABS[98] was employed to correct the data for absorption effects.

Systematic reflection conditions and statistical tests indicated the space group $C2$. A solution was obtained readily using SHELXTL (SHELXS).[99] Hydrogen atoms bound to carbon were placed in idealized positions, and were refined using riding model. All non–hydrogen atoms were refined with anisotropic thermal parameters. Atoms B1–Cl1 and C1–C2 were found disordered. Also, elongated thermal ellipsoids of Si1A indicated disorder, and the disorder was modeled successfully. The structure was refined (weighted least squares refinement on F^2) to convergence.[100] ORTEP–II was employed for the final data presentation and structure plots.[102] Crystallographic information for **302** is summarized in Table 3–2 and Table 3–3 and is also available in the form of a CIF file (CCDC 908265) from the Cambridge Crystallographic Data Centre (www.ccdc.cam.ac.uk).

Table 3–2. Selected bond lengths [Å] and angles [deg] for **302**.

B(1)–C(1)#1	1.670(17)
B(1)–Cl(1)	1.864(9)
C(2)–Si(1A)	1.85(3)
Si(1A)–C(3)#1	1.811(14)
Si(1A)–C(3)	1.854(14)
Si(1A)–Cl(1)#1	2.304(8)
C(3)–Si(1A)#1	1.811(14)
C(2)–B(1)–C(1)#1	112.5(11)
C(2)–B(1)–B(1)#1	112.5(11)
C(1)#1–B(1)–B(1)#1	0.0(6)
C(1)#1–B(1)–Cl(1)	117.4(3)
B(1)#1–B(1)–Cl(1)	117.4(3)
B(1)–C(2)–Si(1A)	119.1(16)
C(3)#1–Si(1A)–C(2)	118.5(12)
C(3)#1–Si(1A)–C(3)	113.8(5)
C(2)–Si(1A)–C(3)	122.0(13)
C(3)#1–Si(1A)–Cl(1)#1	99.4(5)
C(2)–Si(1A)–Cl(1)#1	96.8(6)
C(3)–Si(1A)–Cl(1)#1	97.6(4)
Si(1A)#1–C(3)–Si(1A)	17.0(3)

Symmetry transformations used to generate equivalent atoms:
#1 –x, y, –z+2

Table 3–3. Crystallographic information for **302**.

Empirical formula	$C_4 H_8 B_{11} Cl_{11} Si$	
Formula weight	593.05	
Temperature	110(2) K	
Wavelength	1.54178 Å	
Crystal system	Monoclinic	
Space group	C_2	
Unit cell dimensions	a = 13.6825(14) Å	α = 90°.
	b = 11.1604(11) Å	β = 124.793(4)°.
	c = 8.7634(9) Å	γ = 90°.
Volume	1098.95(19) $Å^3$	
Z	2	
Density (calculated)	1.792 g cm^{-3}	
Absorption coefficient	13.182 mm^{-1}	
F(000)	576	
Crystal size	0.12 × 0.08 × 0.02 mm^3	
Theta range for data collection	5.59 to 59.99°.	
Index ranges	$-15 \le h \le 14, -11 \le k \le 12, -9 \le l \le 9$	
Reflections collected	6896	
Independent reflections	1475 [R_{int} = 0.0584]	
Completeness to theta = 59.99°	98.0%	
Absorption correction	Semi–empirical from equivalents	
Max. and min. transmission	0.7785 and 0.3007	
Refinement method	Full–matrix least–squares on F^2	
Data / restraints / parameters	1475 / 8 / 130	
Goodness–of–fit on F^2	1.069	
Final R indices [$I > 2\sigma(I)$]	R_1 = 0.0441, wR_2 = 0.1127	
R indices (all data)	R_1 = 0.0500, wR_2 = 0.1148	
Largest diff. peak and hole	0.519 / −0.424 e.$Å^{-3}$	

X–Ray data collection, solution, and refinement for *n*–Bu_4N–301. (Solved by Dr. Nattamai Bhuvanesh.) Single crystals of ***n*–Bu_4N–301** were grown by diffusion of pentane into a solution of the compound in fluorobenzene at −32 °C. A Leica MZ 75 microscope was used to identify a suitable colorless blocks with very well defined faces with dimensions (max, intermediate, and min) 0.23 mm × 0.15 mm × 0.09 mm from a representative sample of crystals of the same habit. The crystal mounted on a nylon loop was then placed in a cold nitrogen stream (Oxford) maintained at 110 K. A BRUKER APEX2 X–ray (three–circle) diffractometer was employed for crystal screening, unit cell determination, and data collection. The goniometer was controlled using the APEX2 software suite, v2008–6.0.[98] The sample was optically centered with the aid of a video camera such that no translations were observed as the crystal was rotated through all positions. The detector was set at 6.0 cm from the crystal sample (APEX2, 512 × 512 pixel). The X–ray radiation employed was generated from a Mo sealed X–ray tube (K_α = 0.70173Å with a potential of 40 kV and a current of 40 mA) fitted with a graphite monochromator in the parallel mode (175 mm collimator with 0.5 mm pinholes). Sixty data frames were taken at widths of 0.5°. These reflections were used in the auto–indexing procedure to determine the unit cell. A suitable cell was found and refined by nonlinear least squares and Bravais lattice procedures. The unit cell was verified by examination of the *h k l* overlays on several frames of data. No super–cell or erroneous reflections were observed. After careful examination of the unit cell, a standard data collection procedure was initiated using omega scans. Integrated intensity information for each reflection was obtained by reduction of the data frames with the program APEX2.[98] The

integration method employed a three dimensional profiling algorithm and all data were corrected for Lorentz and polarization factors, as well as for crystal decay effects. Finally the data was merged and scaled to produce a suitable data set. The absorption correction program SADABS[99] was employed to correct the data for absorption effects. Systematic reflection conditions and statistical tests of the data suggested the space group P_{bca}. A solution was obtained readily using SHELXTL (XS).[100] The structure has two molecules in the asymmetric unit Z' = 2, Z = 16. Thermal ellipsoids for the carbon atoms on both the *n*–N–butylammonium groups indicated these carbon atoms are significantly disordered. They were modeled successfully between two positions with sufficient restraints to keep the bond distances and thermal ellipsoids meaningful. Also thermal ellipsoids for C4 indicated significant elongation and it was split disordered between two positions. No reflections with reasonable intensity were observed above 1.0 Å. Accordingly, the final refinement was restricted to this solution. Terminal C9 attached to Si shows large thermal ellipsoids indicating possible disorder. Our efforts to model this disorder did not improve the refinement. Given the large unit cell, and the disorder described above, the bond precisions on C–C bonds were low. Hydrogen atoms were placed in idealized positions and were set riding on the respective parent atoms. All non–hydrogen atoms were refined with anisotropic thermal parameters. The structure was refined (weighted least squares refinement on F^2) to convergence.[100,138] ORTEP–II was employed for the final data presentation and structure plots.[102] Crystallographic information for ***n*–Bu$_4$N–301** is summarized in Table 3–4 and 3–5,

and is also available in the form of a CIF file (CCDC 914776) from the Cambridge Crystallographic Data Centre (www.ccdc.cam.ac.uk).

Table 3–4. Selected bond lengths [Å] and angles [deg] for ***n*–Bu$_4$N–301.**

Si(1)–C(4A)	1.836(15)
Si(1)–C(3)	1.853(10)
Si(1)–C(4)	1.883(15)
Si(1)–C(2)	1.900(8)
B(1)–C(1)	1.753(12)
B(1)–Cl(1)	1.763(10)
C(6)–C(7)	1.561(13)
Si(2)–C(9)	1.794(19)
Si(2)–C(7)	1.834(11)
Si(2)–C(8)	1.838(14)
C(1)–C(2)	1.551(11)
C(4A)–Si(1)–C(3)	111.7(12)
C(4A)–Si(1)–C(4)	20.9(12)
C(3)–Si(1)–C(4)	103.6(13)
C(4A)–Si(1)–C(2)	106.9(14)
C(3)–Si(1)–C(2)	118.1(5)
C(4)–Si(1)–C(2)	95.8(13)
C(1)–B(1)–Cl(1)	120.8(6)
C(6)–C(7)–Si(2)	131.3(9)

Table 3–5. Crystallographic information for ***n*–Bu$_4$N–301**.

Empirical formula	C_{20} H_{43} B_{11} Cl_{11} N Si	
Formula weight	834.50	
Temperature	110(2) K	
Wavelength	0.71073 Å	
Crystal system	Orthorhombic	
Space group	P_{bca}	
Unit cell dimensions	a = 21.166(4) Å	α = 90°.
	b = 21.532(4) Å	β = 90°.
	c = 36.164(7) Å	γ = 90°.
Volume	16482(5) Å^3	
Z	16	
Density (calculated)	1.345 g cm^{-3}	
Absorption coefficient	0.788 mm^{-1}	
F(000)	6816	
Crystal size	0.23 × 0.15 × 0.09 mm^3	
Theta range for data collection	2.14 to 21.00°.	
Index ranges	$-21 \le h \le 21$, $-21 \le k \le 21$, $-36 \le l \le 36$	
Reflections collected	104729	
Independent reflections	8841 [R_{int} = 0.0810]	
Completeness to theta = 21.00°	99.8%	
Absorption correction	Semi–empirical from equivalents	
Max. and min. transmission	0.9325 and 0.8395	
Refinement method	Full–matrix least–squares on F^2	
Data / restraints / parameters	8841 / 939 / 1032	
Goodness–of–fit on F^2	1.074	
Final R indices [$I > 2\sigma(I)$]	R_1 = 0.0736, wR_2 = 0.1936	
R indices (all data)	R_1 = 0.0943, wR_2 = 0.2086	
Largest diff. peak and hole	1.498 / −0.879 e.Å^{-3}	

3.4.4 DFT computational studies

Geometry optimization, natural population analysis, and ^{29}Si NMR chemical shift calculation. (Performed by Dr. Jia Zhou). All computations were carried out with the Gaussian09 program.[139] The B3LYP density functional along with 6–311G(d,p)[140] basis set was used for geometry optimization. The harmonic vibrational frequency calculations were performed to ensure that a minimum was obtained. Larger basis set 6–311+G(2d,p) was then used for the NMR calculation using the GIAO method relatively to TMS. The electrostatic potential is mapped onto the total electron density of the silylium zwitterion.

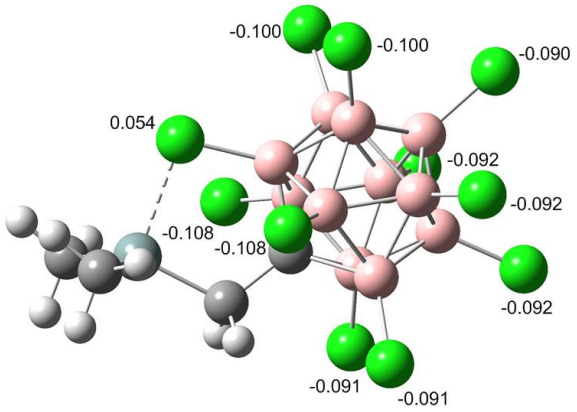

Figure 3–10. DFT–calculated structure of **302** with natural population analysis charges shown for each chlorine atom (in green).

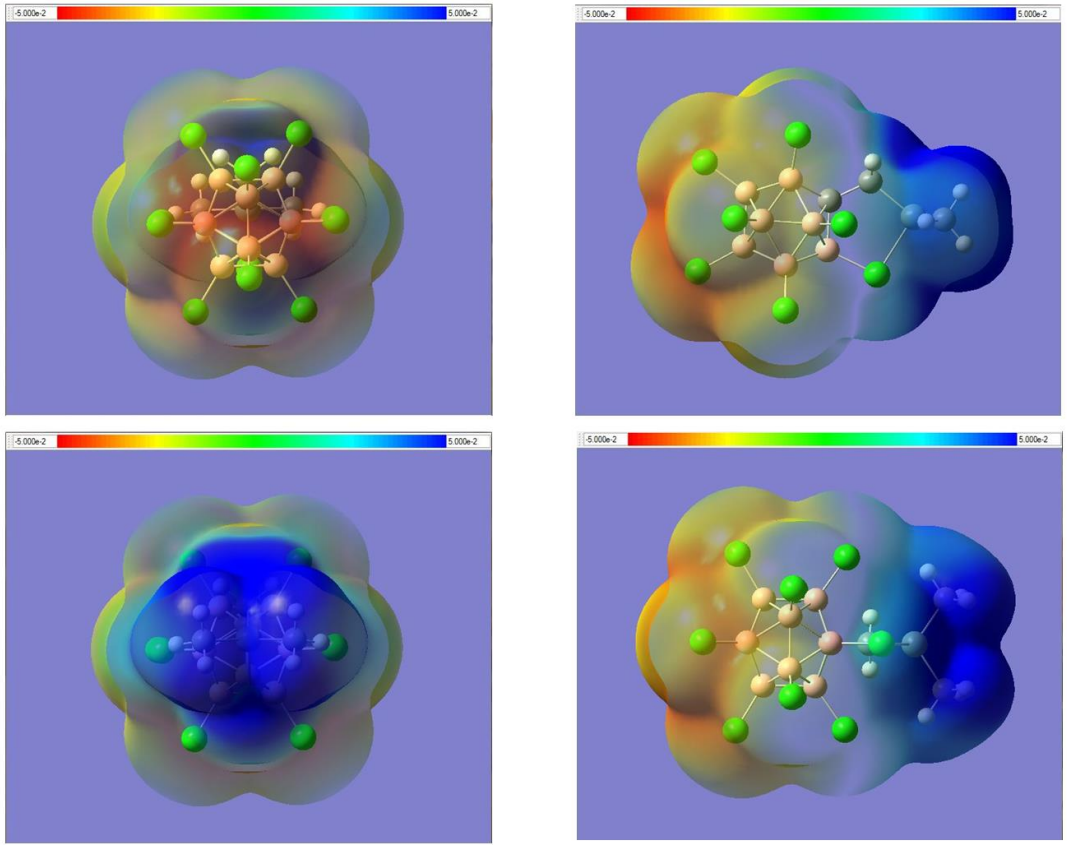

Figure 3–11. Perpendicular views of the electrostatic potential plot of **302**. Blue = negative, red = positive. Isosurface value = 0.01.

CHAPTER IV

SYNTHESIS OF TRIFLUOROMETHANESULFONATE COMPLEXES OF A RUTHENIUM CARBENE–PINCER SYSTEM

4.1 Introduction

The chemistry of transition metal–based Lewis acids has seen intense exploration and advancement during the past decade,[141] leading to the development of systems capable of catalyzing a wide variety of organic transformations, ranging from aldol condensations, Michael additions and hydrosilylation of ketones and aldehydes,[142,143] to chemoselective hydrosilylation of nitriles, Diels–Alder cycloadditions,[144,145] and coupling of alkyl nitriles to carbonyl compounds,[146,147] to name just a few.

Transition metal–based Lewis acids are coordinatively unsaturated species, that in terms of catalysis, display several advantages over their main group element analogues. For instance, the Lewis acidity of transition metal–based acids can be modified and fine–tuned by changing the arrangement and nature of the ligands around the metal center. Transition metal Lewis acids also offer a greater diversity of soft acids and the possibility of having more than one empty orbital within the same metal center, in contrast to their main group counterparts. Moreover, the possibility of ligand modification also gives a great amount of flexibility in the design of the catalyst, allowing for highly specialized systems such as highly stereoselective Lewis acidic catalysts.[148]

The rich catalytic chemistry of this class of compounds is not the only fascinating aspect to them. Coordinatively unsaturated, electron deficient species show unusual and interesting electronic and structural features when taken to extremes of electron deficiency.[12–15]

Coordinative unsaturation of transition metal species is a prerequisite for the fundamental organometallic processes, such as reductive elimination and oxidative addition, to take place.[4–6] In many organometallic catalyst systems, one of the steps along the mechanistic pathway is the loss of a ligand from the coordination sphere of the metal to yield the catalytically active species. One of many examples is Grubbs' alkene metathesis catalysts,[149] where the catalytically active species appears to be a 4–coordinate, 14–electron species formed by loss of phosphine from the d^6 ML_5 precatalyst.[150]

Ligands weakly bound to the metal could, in principle, contribute to lowering the energy barrier associated with ligand displacement, or ligand loss, and may help enhance or even discover new reactivity.[27] These compounds could be thought of as being synthetic equivalents of *bona fide* electron deficient, coordinatively unsaturated species.[151]

4.1.1 Pincer ligands

Pincer ligands are rigid, tridentate, chelating ligands that enforce meridional coordination geometry around the metal center, restricting the accessible geometries to octahedral (ML_6), square pyramidal or trigonal bipyramidal (ML_5), or T–shaped (ML_3) (Figure 4–1 and 4–2). This class of compounds is extraordinarily thermally stable, thus offering a balance between stability and reactivity that can be fine-tuned by systematically modifying the ligand framework

and the metal center itself.[152] These compounds are categorized depending on the identity of the axial donors and the central donor (EXE), for example, PCP, POCOP and PNP. These ligands can be subdivided into two classes: neutral ligands and anionic ligands. Anionic ligands may not exist in the free state, but rather the anionic character is formally assigned once the metallated ligand is formed upon installation on the metal. Such is the case of POCOP, PCP and PNP (Figure 4–2). Examples of neutral pincer ligands are the pyridine based PNP and the P_2C= ligands (Figure 4–2).

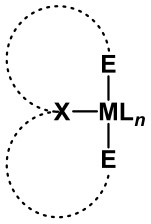

Figure 4–1. General structure of a pincer complex. (M = transition metal; E , X = O, S, N, P).

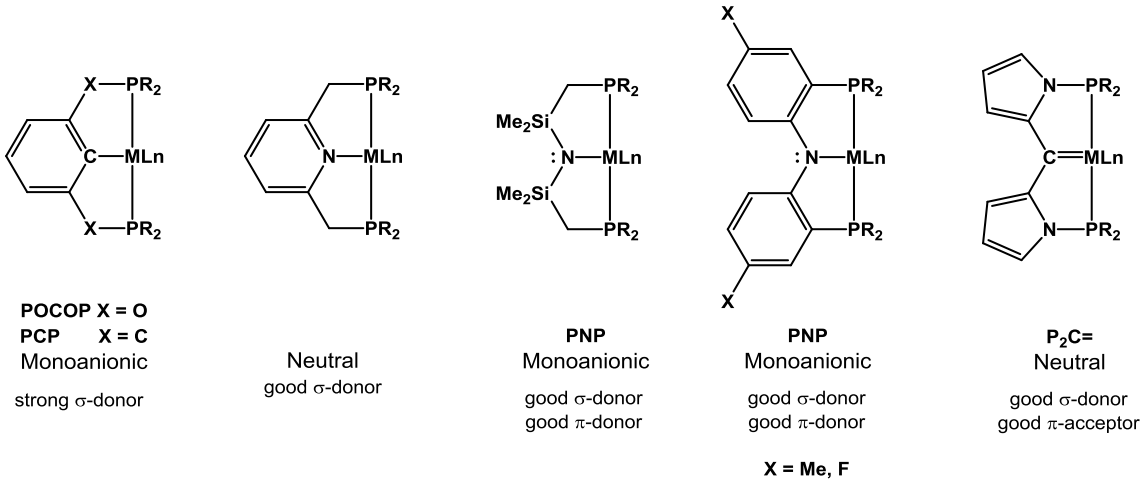

Figure 4–2. Examples of different types of pincer ligands**.**

An important difference among these ligands is the σ donor, π donor/acceptor properties of the central atom (with constant E). For instance, while PCP, POCOP and PNP are all anionic ligands, the first two show negligible π acceptor properties on the central atom, while the central amido moiety of both PNP ligands has an orbital occupied by a lone electron pair, and could act as a π donor. Pyridine based PNP and P_2C= are also neutral, but while the pyridine central moiety shows negligible π acceptor character, P_2C= shows a stronger π acceptor character.[153]

4.1.2 Ruthenium complexes of the pyrrole–based pincer–carbene ligand system

The pyrrole–based pincer carbene ligand system $P_2C=$ (Figure 4–3.) was developed by Wei Weng in the Ozerov group with the objective of incorporating both σ–donors and a π–acceptor to the same ligand framework (Figure 4–3.).[153] The central methylene group of the proto–ligand undergoes double C–H bond activation that results in the formation *in situ* of the central carbene anchor point of the ligand, while two phosphines axially coordinated to the metal, resulting in a meridional coordinated geometry (Scheme 4–1). This coordination pattern is similar to the *mer*–$CO(PR_3)_2$ motif, which is encountered in complexes of group 8 and 9 metals, and other catalyst systems such as Vaska's complex,[154] and is also analogous to that of the Grubbs olefin metathesis catalyst[149] (Figure 4–3). In this last case, the difference with our systems resides in the fact that the alkylidene ligand in the Grubbs catalyst participates in the metathesis reaction, whereas in our system the carbene ligand is only intended to be a spectator ligand. This ligand design is directly relevant to catalysis for the reason that the π acidity of the central coordination site enables the transfer of electron density from the coordinated metal towards the ligand, allowing for a fine modulation of the reactivity of the metal center, while preserving the structural rigidity of a *mer* coordinated pincer ligand.

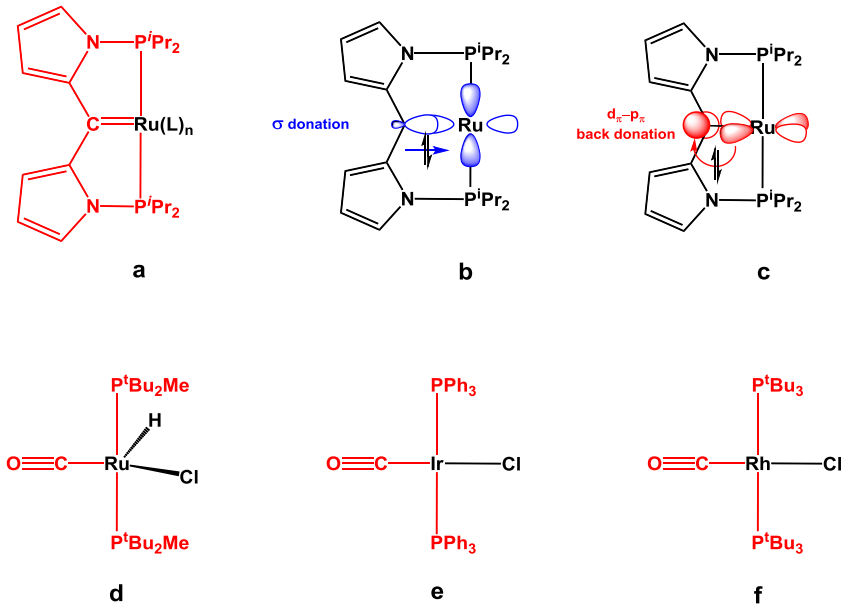

Figure 4–3. a) Structure of the P_2C= ligand architecture.153 b) σ–Donation into a ruthenium d orbital from the ligand central C_{sp^2} orbital. c) Back donation from a filled ruthenium orbital into the ligand central empty Cp orbital. d), [155] e), [156] and f)[154], Examples of the *mer*–(CO)PR_3 coordination motif.

4.1.3 Previous work on the $(P_2C=)Ru(L)_n$ system

In previous work by Wei Weng in the Ozerov group, Y–shaped, and square pyramidal d^6 ML_5 complexes $(P_2C=)$Ru (H)(OTf) (**401**) and $(P_2C=)RuCl_2$ (**402**), and octahedral d^6 ML_6 complexes *trans*–$(P_2C=)Ru(Cl)_2(CO)$ (**403**) and *cis*–$(P_2C=)Ru(Cl)_2(CO)$ (**404**) were prepared (Scheme 4–1).[153] The geometries displayed by these complexes are expected for the coordination numbers and ligand types associated. As explained in previous chapters, coordinative unsaturation is a prerequisite for potential catalytic activity, and it is for this reason that compound **401** was coordinatively unsaturated, it was tested as a precatalyst for the transfer hydrogenation of ketones, using 2–propanol as the hydrogen source, and KO^{i}Pr.

Although the performance of **401** did not challenge that of other Ru pincer catalysts,[157] it showed the ability of the P_2C= ligand scaffold to support catalytic processes.[153]

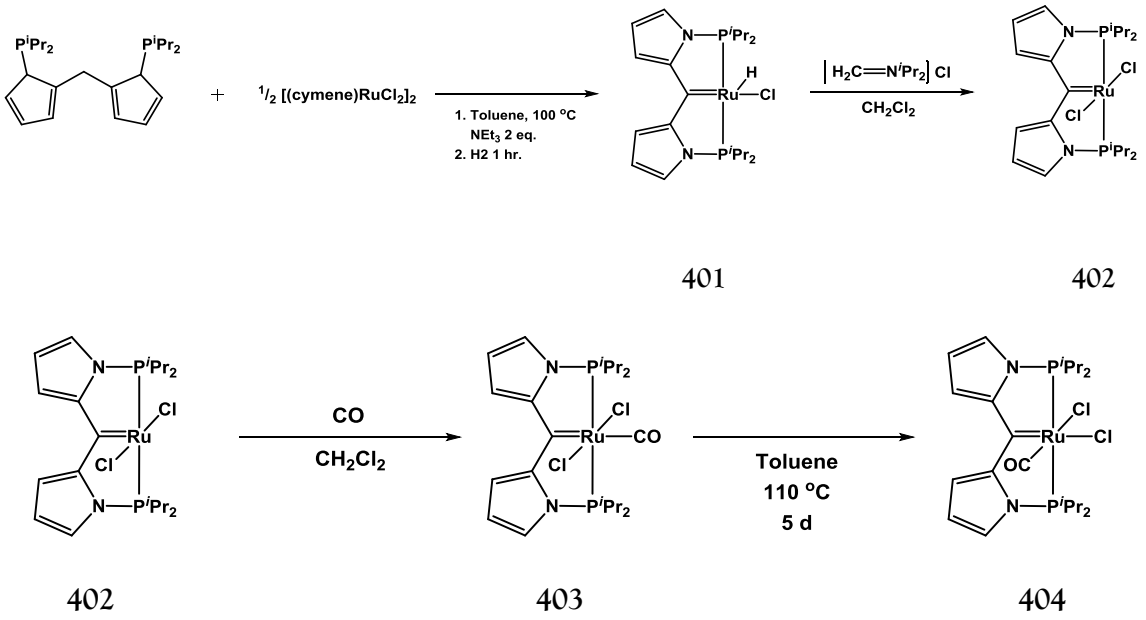

Scheme 4–1. Syntheses of d^6 ML_5 $(P_2C=)Ru(H)(Cl)$ (**401**), and $(P_2C=)RuCl_2$ (**402**), and d^6 ML_6 trans–$(P_2C=)Ru(Cl)_2(CO)$ (**403**) and *cis*–$(P_2C=)Ru(Cl)_2(CO)$ (**404**), previously prepared in the Ozerov group.[153]

4.1.4 Triflate complexes of the $(P_2C=)Ru(L)_n$ system

Compounds **403** and **404** are coordinatively saturated, and although they could be thought of as catalyst precursors, it is to be expected that they show very low, if any, catalytic activity under mild conditions due to the presence of ligands on their coordination sphere that are not easily displaced. We surmised that metathesis of chloride with the more weakly

coordinating triflate would be a convenient way to generate compounds that could be potential Lewis–acidic precatalysts. These compounds can be regarded as synthetic equivalents of truly cationic complexes, with the added advantage that no need for the isolation of highly reactive species is necessary. We speculated that the same reasoning would apply to the d^6 ML_5 compounds **401** and **402**. Given their coordination geometries, these systems could in principle generate open coordination sites *trans* to a variety of ligands with different strengths of *trans* influence, ranging from the strongly *trans* influencing hydride and carbene, to the weaker chloride. We also envisaged the introduction of the oxygen containing ligands acetate and acetylacetonate to the coordination sphere of these complexes, in order to cover a larger range of *trans* influence (Figure 4–4). It was decided to create a library of triflate precatalysts covering a range of coordination geometries such that displacement of a triflate ligand leads to a virtual coordination site *trans* to donors with different strengths of *trans* influence, using **401**, **402**, and **404**. This library could lead to the discovery of new catalyst systems (Figure 4–5).

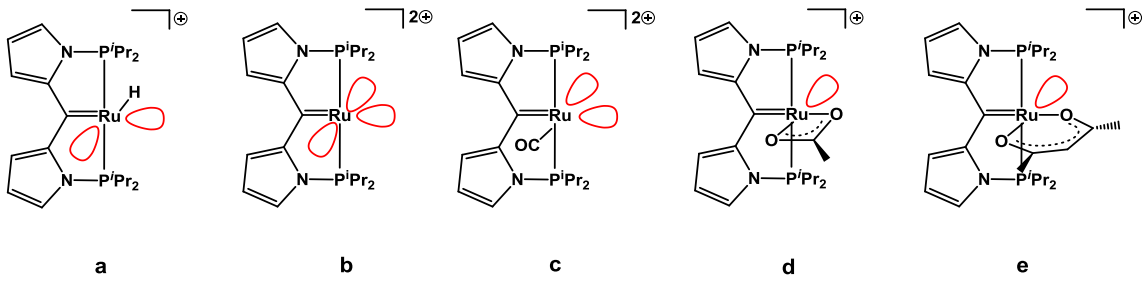

Figure 4–4. Graphic representation of the possible virtual open coordination sites.

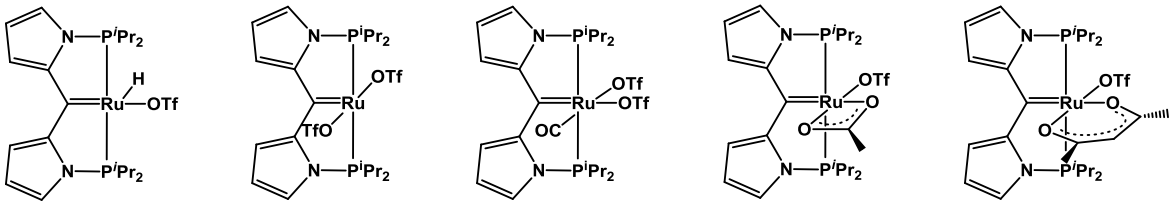

Figure 4–5. Projected library of $(P_2C=)Ru(L)_n$ compounds.

4.2 Results and discussion

4.2.1.1 General NMR spectral features of the family of $(P_2C=)Ru(L)_n$ complexes

The ^1H NMR features of the pyrrole ligand backbone remain essentially constant in all compounds, exhibiting three multiplets in the aromatic region each integrating to two protons. The signals from the methyl groups on the phosphine ligands appear in the aliphatic region usually as perfectly overlapping doublets of virtual triplets, giving the appearance of a quartet (apparent quartets), or closely overlapping A_3BXY multiplets (Figure 4–6). Such multiplicity is indicative of two isopropyl phosphines bound *trans* to each other.[158] Methine signals appear as either one or two multiplets in the region around δ 2 to 3.5 ppm depending on the symmetry of the molecule. For instance, compound **402** is C_{2V} symmetric, and only shows one methine multiplet, and two sets of very closely overlapping signals for the isopropyl methyl groups. Loss of this symmetry could be used as an indicator that ligand exchange at the metal has taken place.

Hydride resonances are indicative of the geometry of the compound in solution. For ruthenium compounds, hydrides located *trans* to empty coordination sites in square

pyramidal RuL_5 complexes have rather upfield chemical shifts within the range of δ −30 ppm to δ −40 ppm,[159] while in RuL_5 complexes with distorted trigonal bipyramidal geometry (Y shape) hydride resonances appear in the range of δ −12 to δ −17 ppm.[160]

The presence of a carbon−metal double bond can be ascertained by the observation of the characteristic downfield resonances in the region of δ 250–260 ppm in the ^{13}C NMR spectrum. Spectral data are summarized in Table 4–1.

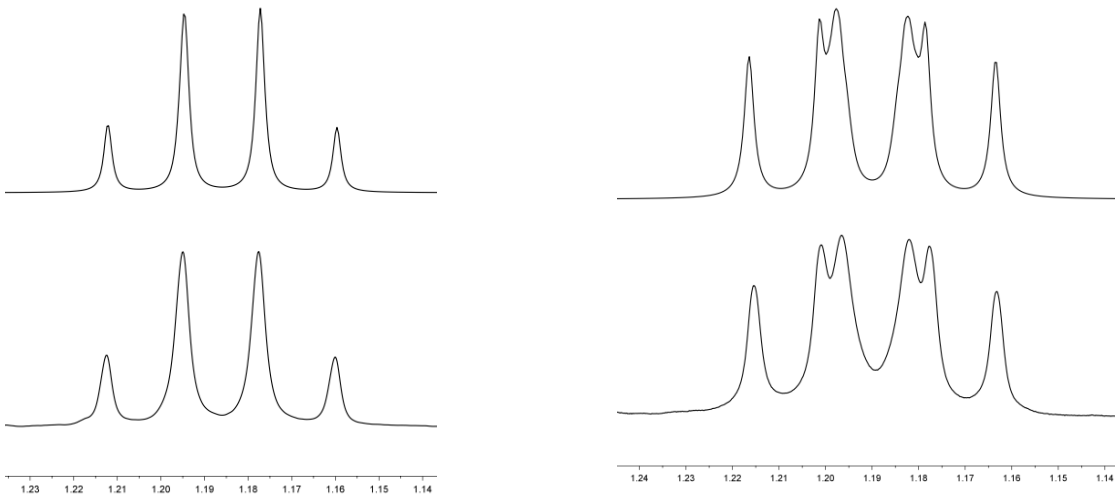

Figure 4–6. Representative ^1H NMR signal types from the methyl groups of mutually *trans* diisopropyl phosphine ligands in compounds of the type $(P_2C=)Ru(L)_n$. *Top*: simulations using MestReNova™ version 8.1.2. *Bottom*: experimental spectra. a) Doublet of virtual triplet (apparent quartet) b) A_6BXY multiplet . Calculated coupling constants are provided in the experimental section.

Table 4–1. Summary of relevant spectroscopic data for 5– and 6–coordinate $(P_2C=)RuL_n$ compounds (n = 2, 3).

	Complex	$\delta(^{13}C)$ Ru=C	$\delta(^{1}H)$ Ru–H	IR $_{CO}$ (cm^{-1})
401[153]	$(P_2C=)Ru(H)(Cl)$	253.4	–15.41	
402[153]	$(P_2C=)RuCl_2$	255.1		
405	$(P_2C=)Ru(H)(OTf)$	268.2	–16.44	
407*	*cis*–$(P_2C=)Ru(CO)(OTf)_2$	226.4		1979 (solid)
410	$(P_2C=)Ru(H)(OAc)$	256.8	–11.05	
411	$(P_2C=)Ru(acac)(Cl)$	265.6		
412	$(P_2C=)Ru(OAc)(Cl)$	268.2		
404[153]	*cis*–$(P_2C=)Ru(CO)(Cl)_2$	239.9		1967 (CH_2Cl_2)
[153]	*trans*–$(P_2C=)Ru(CO)(Cl)_2$	258.4		1991 (CH_2Cl_2)

NMR spectra collected in C_6D_6.
*Collected in $CDCl_3$.

4.2.2 Synthesis of d^6 ML_5 triflate complexes

4.2.2.1 Synthesis of $(P_2C=)Ru(H)(OTf)$ (405)

$(P_2C=)Ru(H)(OTf)$ (**405**) was prepared by either of two different routes (Scheme 4–2). The first route consists of treatment of a fluorobenzene solution of **401** with excess Me_3SiOTf to obtain **405** quantitatively by ^1H NMR spectroscopy. The ^1H NMR spectrum of compound **405** displayed two different methine resonances, and four different methyl resonances, consistent with C_S symmetry in solution. A hydride resonance was observed at δ –16.44 ppm (t, $^2J_{H-P}$ = 19.7 Hz), suggestive of a distorted trigonal bipyramidal geometry of the compound in solution. A new resonance in the ^{19}F NMR spectrum was observed at δ –77.2 ppm, which

is consistent with a metal–bound triflate. The $^{13}C\{^1H\}$ NMR spectrum revealed a downfield resonance at δ 268.2 ppm (t, $^2J_{C-P}$ = 8.5 Hz), which confirmed the presence of a carbon–ruthenium double bond. Compound **405** was isolated as a golden–brown powder in good yield. A second route to access compound **405** was devised to avoid using excess Me_3SiOTf, and it relies on the driving force provided by the formation of a strong Si–O bond to generate Me_3SiOAc, resulting in the substitution of the acetate ligand from $(P_2C=)Ru(H)(OAc)$ (**410**) with triflate (Scheme 4–2). Compound **410** was prepared by treatment of a solution of **401** with excess NaOAc.

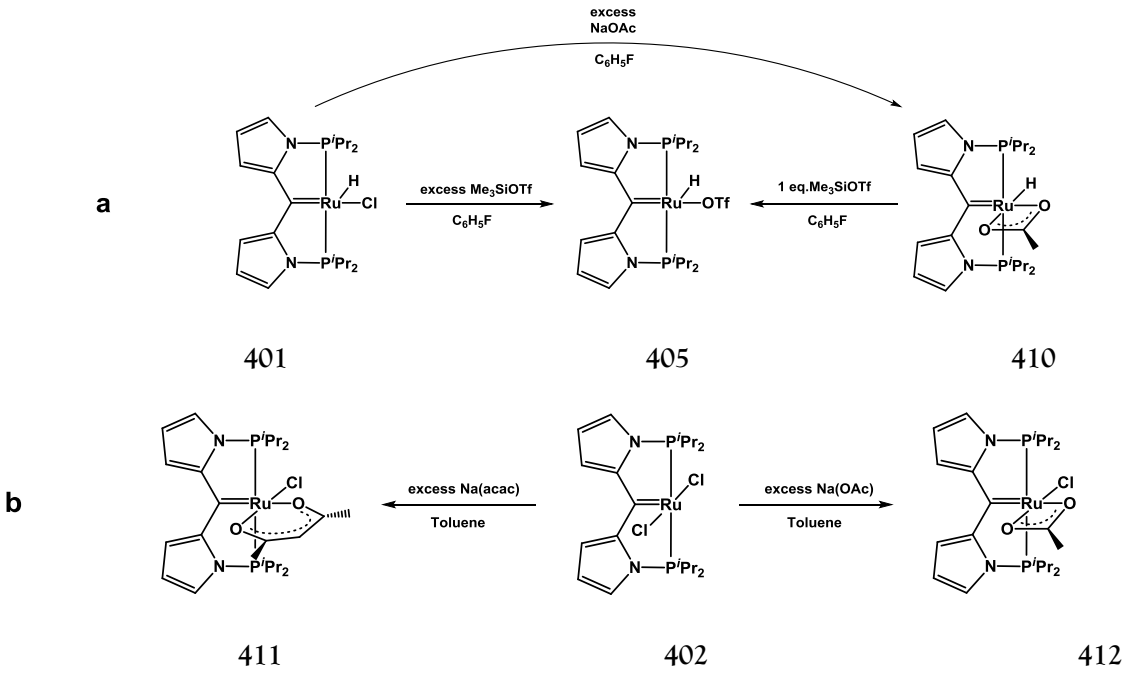

Scheme 4–2. a) Syntheses of (P_2C=)Ru(H)(OTf) (**405**). b) Syntheses of κ^2 complexes of oxygen–based ligands acetylacetonate (acac) (**411**), and acetate (OAc) (**410** and **412**).

^{1}H NMR spectroscopic analysis of **410** revealed the presence of a new methyl resonance at δ 1.97 ppm, consistent with the incorporation of one acetate ligand. A hydride resonance is found at δ −11.04 ppm (t, $^2J_{H-P}$ = 20.3 Hz), in contrast with the hydride resonance of resonance of **401** observed at δ −15.41 ppm, which suggests weak *trans* coordination of one of the acetate oxygen atoms. Consistent with this configuration, four different methyl resonances and two different methine resonances from the isopropyl groups are observed. The presence of the Ru–carbene moiety in compound **410** was confirmed in the ^{13}C{^{1}H} NMR spectrum by the observation of a downfield resonance at δ 256.8 ppm (t, $^2J_{C-P}$ = 10.5 Hz). Therefore, bidentate chelation of the acetate ligand provides extra stabilization of the

resulting complex, which favors the displacement of one of the chloride ligands. In the case of (P_2C=)Ru(Cl)(OAc) (**412**), where two chloride ligands are present, further displacement of the second chloride by another acetate molecule cannot provide this stabilization since there are no more open coordination sites available to form a second κ^2 interaction with the metal. Addition of 1.0 equivalent of Me_3SiOTf to a solution of **410** in fluorobenzene cleanly afforded **405** within the time of mixing. Following this method, **405** could be isolated in good yield as well. The possibility of preparing compound **405** by using AgOTf was also examined. Treatment of a solution of compound **401** in CH_2Cl_2 with AgOTf followed by workup afforded **405**, albeit not cleanly. NMR spectroscopic analysis of the product revealed the presence of multiple signals in the region around δ −78 ppm in the ^{19}F NMR spectrum. The aliphatic region of the ^1H NMR spectrum revealed multiple, intractable signals in the region between δ 0.5 and 1.7 ppm. The reasons for the lack of a clean transformation were not established, however, the presence of traces of water in AgOTf, or oxidation of the pyrrole–based ligand backbone by Ag (I) could be suspected.

It is worth noting that the synthesis of compound **405** was attempted before by Wei Weng in our research group by treatment of a solution of compound **401** in CH_3CN with Me_3SiOTf, affording the cationic solvent adduct [(P_2C=)Ru(H)($NCCH_3$)$_2$]OTf, which is the product of chloride abstraction, and displacement of OTf^- from the coordination sphere of the metal by the more strongly donating CH_3CN solvent molecule. In this case, compound **405** was not isolated, or observed intact in solution.[161]

4.2.2.2 Attempted synthesis of $(P_2C=)Ru(OTf)_2$ (406)

A solution of **402** in benzene was treated with excess Me_3SiOTf (Scheme 4–3). Analysis of the mixture revealed an absence of any new signals in the ^{19}F NMR, ^{1}H NMR, and $^{31}P\{^{1}H\}$NMR spectra. The target *bis* triflate complex could not be accessed through this route.

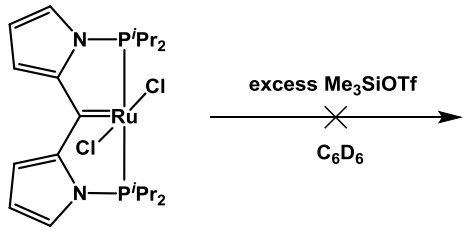

402

Scheme 4–3. Attempted synthesis of $(P_2C=)Ru(OTf)_2$ (**406**) by treatment of 402 with excess Me_3SiOTf.

4.2.3 Synthesis of d^6 ML_6 triflate complexes

4.2.3.1 Synthesis of *cis*–$(P_2C=)Ru(CO)(OTf)_2$ (407)

We sought to prepare the carbonyl adduct *cis*–$(P_2C=)Ru(CO)Cl_2$ (**404**)[153] in order to attempt chloride replacement using Me_3SiOTf. It was reasoned that the chloride *trans* to carbene should be more labile to abstraction given the strong *trans* influence exerted by the carbene (Scheme 4–4).

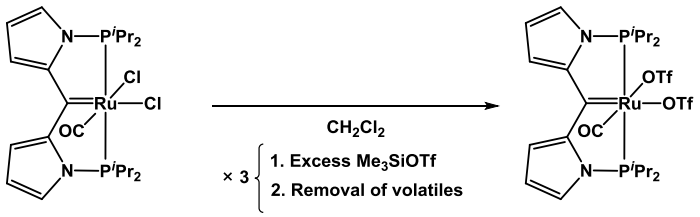

404 **407**

Scheme 4–4. Synthesis of *cis*–(P_2C=)Ru(CO)($OTf)_2$ (**407**) by treatment of **404** with excess Me_3SiOTf.

A solution of **404** in CH_2Cl_2 was treated with 20 equivalents of Me_3SiOTf, followed by removal of volatiles *in vacuo* to obtain a yellow powder. Analysis of the product by ^1H NMR revealed clean formation of a new compound that displayed C_S symmetry in solution, and a resonance at δ 226.4 ppm in the $^{13}C\{^1H\}$ NMR spectrum indicated that the Ru=$C_{carbene}$ double bond had been preserved. Two new signals were observed in the ^{19}F NMR spectrum at δ −78.1 and −79.0 ppm, with an integral ratio of 1:1. These chemical shifts seemed to suggest the possibility that one of the triflate ligands could be coordinated to the metal, with the other triflate being an outer sphere counter anion,[162a,b] although a few examples of ^{19}F NMR chemical shifts of δ −79.0 ppm for ruthenium–bound triflate can be found in the literature.[162a] We were able to ascertain, through an X–ray diffraction study, that the compound is correctly described by the formula *cis*–(P_2C=)Ru(CO)(κ^1–$OTf)_2$ (**407**), where both triflate ligands are κ^1–coordinated to ruthenium (Figure 4–7).

The structure of **407** displays an approximately octahedral geometry around ruthenium, with the two triflate ligands *cis* to each other. The distance Ru1—O4 (2.179(5) Å) compares

well to the analogous distance in Ru(dppe)$(CO)_2$(OTf) (2.182(4) Å),[163] while the Ru1–(O1–1) distance is slightly longer (2.240(5) Å), owing to the stronger *trans* influence of the carbene ligand compared to CO. On the basis of these metrics, it could be argued that the resonance at δ −79.0 ppm in the ^{19}F NMR could be assigned to the triflate ligand *trans* to carbene, and the downfield shift could be a result of a weaker interaction with ruthenium compared to the triflate trans to CO.

The Ru–$C_{carbene}$ double bond distance of 2.016(7) Å is longer than that reported for compound **401** (1.918(10) Å),[153] and this difference is statistically significant within experimental error ($\Delta > 2.56\times\sigma_\Delta$; Δ = bond length difference; σ = estimated standard deviation). This can be interpreted as the result of weak π–back donation into the carbene p–orbital from an electron–deficient metal center, due to the coordination of two weak π–donor ligands,[163] and one strong π–acceptor ligand. The more electron poor nature of **407** relative to the parent compound **404** is evidenced by its increased IR ν_{CO} stretching frequency of 1979 cm^{-1} *vs.* 1967 cm^{-1}.[163]

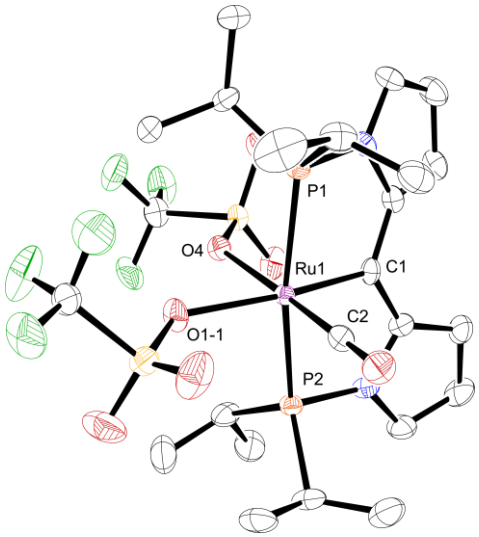

Figure 4–7. ORTEP diagram (50% probability ellipsoids) of *cis*–(P_2C=)Ru(CO)(κ^1–OTf)$_2$ (**407**) Selected atom labeling shown. Hydrogen atoms, and a disordered $CHCl_3$ solvent molecule were omitted for clarity. Selected bond distances (Å): Ru1–C1, 2.016(7); Ru1–C2, 1.843(8); Ru1–(O1–1), 2.240(5); Ru1–O4, 2.179(5); Ru1–P1, 2.392(2); Ru1–P2, 2.378(2); P1–Ru1–P2, 166.14(7); C(2)–Ru(1)–C(1), 90.6(3); C(2)–Ru(1)–O(4), 177.8(3); C(1)–Ru(1)–O(4), 91.6(3); O(4)–Ru(1)–(O1–1) 80.4(2); C(1)–Ru(1)–O11, 172.0(3).

4.2.4 Triflate complexes of κ^2 oxygen–based ligands

4.2.4.1 Synthesis of (P_2C=)Ru(acac)(OTf) (409)

(P_2C=)Ru(acac)(Cl) (**411**) was prepared by stirring a solution of **402** in toluene for 5 d in the presence of Na[acac]. Analysis of the ^{1}H NMR spectrum of the product revealed a compound that displayed C_S symmetry in solution. Incorporation of the acac ligand was confirmed by the presence of new resonances at δ 1.53 (s, 3H), 1.96 (s, 3H) and 5.23 (s, 1H) ppm. The characteristic downfield Ru–$C_{carbene}$ signal was observed at δ 265.6 (t, $^2J_{C-P}$ = 8.6 Hz) ppm in the $^{13}C\{^1H\}$ NMR spectrum. With this compound in hand, we explored the synthesis of (P_2C=)Ru(acac)(OTf) (**409**) by treatment of a solution of **411** in $CDCl_3$ with 2

equivalents of Me_3SiOTf. Analysis of the resulting reaction mixture by multinuclear NMR spectroscopy revealed that *ca.* 20% of a new product had formed, along with Me_3SiCl, which could be observed at δ 0.42 ppm. Removal of volatiles *in vacuo* and treatment with excess Me_3SiOTf two more times led to complete conversion. The new compound exhibited C_S symmetry in solution. In the ^1H NMR spectrum, all the resonances for the pincer and acac ligands could be accounted for, while a signal at δ −80.96 was observed in the ^{19}F NMR spectrum, revealing incorporation of a triflate group.

4.2.4.2 Attempted synthesis of $(P_2C=)Ru(OAc)(OTf)$ (408)

Substitution of chloride for triflate from compound **412** was attempted by treatment of a solution of $CDCl_3$ with 2 equivalents of Me_3SiOTf. Analysis of the ^1H NMR spectrum of the reaction mixture clearly revealed the formation of compound **402**, 1 equivalent of Me_3SiOAc, 1 equivalent of unreacted Me_3SiOTf, and a side product that was not identified (Figure 4–8). In the case of **412**, the κ^2 bidentate ligand is more prone to electrophilic removal than the acac ligand in **411**. It is conceivable that even though acetate is a bidentate chelating ligand, the 4–member chelate ring formed is more is strained, and therefore less stable than the 6–member ring formed by κ^2 coordination of acac. We surmise that electrophilic abstraction of acetate results in the formation of a putative species "$[(P_2C=)RuCl]^+$", which disproportionates into **402** and an unidentified compound.

*4.2.5 Triflate abstraction from **405***

We set out to investigate the possibility of forming the 4–coordinate, cationic, pincer–ligated ruthenium compound [(P_2C=)Ru(H)][WCA] (**413**) (WCA = Weakly Coordinating Anion; [$MeCB_{11}Cl_{11}$]$^-$ (**413a**), [B(3,5–$C_6H_3(CF_3)_2)_4$]$^-$ (**413b**) by removal of the weakly bound triflate from compound **405** by electrophilic abstraction with alkali metal salts of the corresponding WCA. A solution of **405** in the weakly coordinating solvent C_6D_5Br was treated with the sodium salts of **201** and [B(3,5–$C_6H_3(CF_3)_2)_4$]$^-$, resulting in darkening of the reaction mixture, and formation of a white solid, presumably NaOTf. Quantitative abstraction of the triflate ligand from **405** was confirmed by the absence of the triflate resonance in the region of δ −78 ppm in the ^{19}F NMR spectrum. Relevant features observed in the ^{1}H NMR spectrum, of both **413a** and **413b,** are the absence of agostic interactions, most likely as a result of solvent coordination. An upfield hydride resonance observed at δ −14.26 (t, $^2J_{H-P}$ = 23.1 Hz) is consistent with a hydride *trans* to an empty coordination site. Compounds **413a** and **413b** also appear to display C_S symmetry in solution (Figure 4–9), as three sets of methyl group resonances, and one set of overlapping methine resonances are observed for the $PCH(CH_3)_2$ resonances.

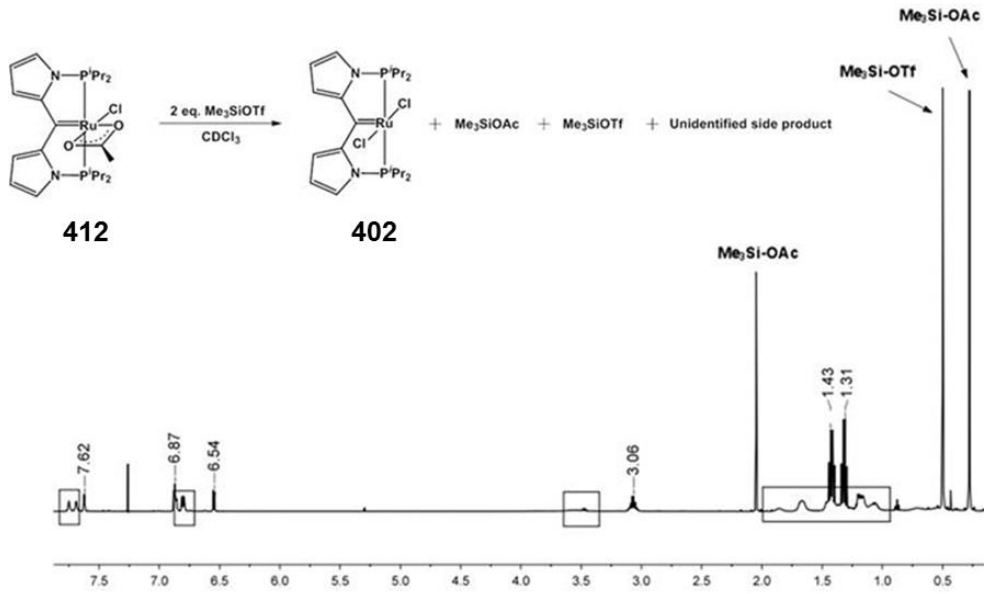

Figure 4–8. Attempted chloride substitution with triflate from (P_2C=)Ru(OAc)(Cl) (**412**) using Me_3SiOTf resulting in formation of (P_2C=)$RuCl_2$ (402), Me_3SiOAc and an unidentified product (highlighted in boxes).

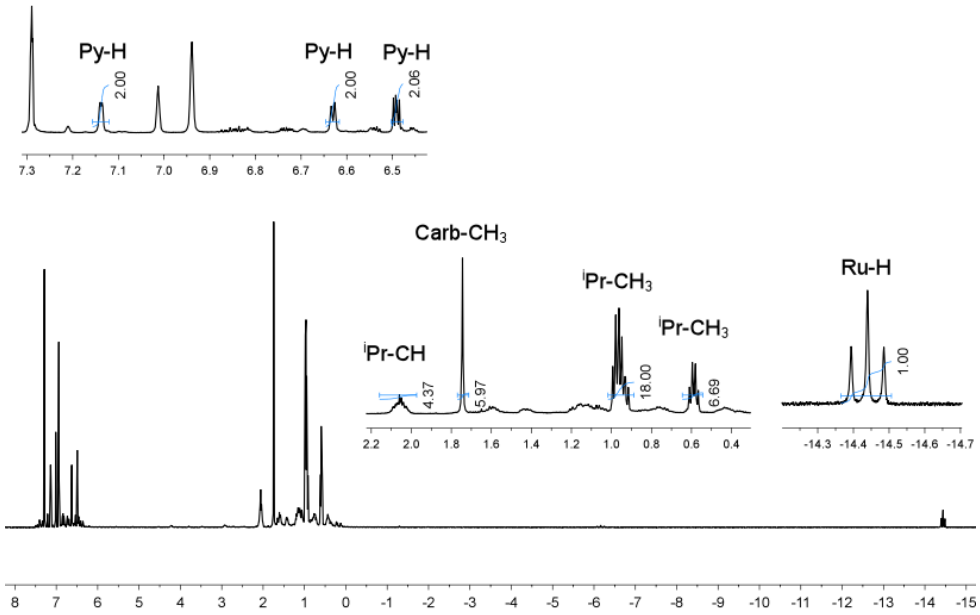

Figure 4–9. ^1H NMR spectrum (499.43 MHz) of 413a collected in C_6D_5Br. Residual *protio* solvent peaks observed at δ 6.93, 7.01, and 7.29 ppm.

Next, the thermal stability of compound **413b** formed *in situ* was examined by thermolysis of a solution of the compound in a 1:1 solvent mixture of toluene and 1,2–difluorobenzene. Analysis of the ^{1}H NMR spectrum of the product revealed that the formation of an η^6 arene adduct had taken place, yielding the 18–electron, three–legged piano–stool complex [$(P_2CH)Ru(\eta^6$–toluene)][B(3,5–$C_6H_3(CF_3)_2)_4$] (**414**), which is a well–known configuration for arene complexes of d^6 metals (Scheme 4–5).[164] The absence of a hydride resonance, and the appearance of new signals at δ 2.08 (s), 4.76 (s), 5.29 (d, *J* = 6.0 Hz), 5.83 (t, *J* = 6.0 Hz), and 6.07 (t, *J* = 6.1 Hz) in the ^{1}H NMR spectrum, and the absence of the characteristic downfield carbene resonance in the vicinity of the region around δ 250 ppm in the $^{13}C\{^{1}H\}$ NMR spectrum, was indicative of a 1,2–hydride shift to the carbene carbon on the ligand backbone. This assignment was confirmed by an X–ray diffraction study conducted on a single crystal of the compound (Figure 4–10). The environment around ruthenium is distorted away from the ideal three–legged piano stool geometry. The angles P2–Ru–C1, P1–Ru1–C1, and P1–Ru1–P2 deviate significantly from the ideal 90° value[165] as a result of the geometric constrictions imposed by the rigid ligand scaffold (Figure 4–10). Although not a common geometry for pincer ligands, this conformation is not unexpected because it is the direct result of the change in hybridization of the central carbon donor, from planar sp^2 to tetrahedral sp^3.

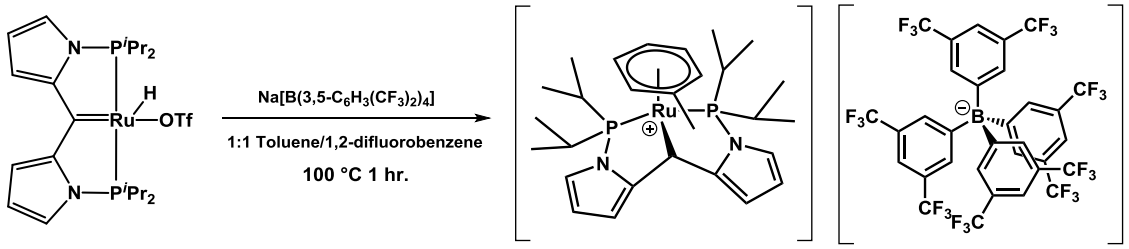

405 414

Scheme 4–5. Thermolysis after triflate abstraction from **405**, in a 1:1 solution of toluene and 1,2–difluorobenzene.

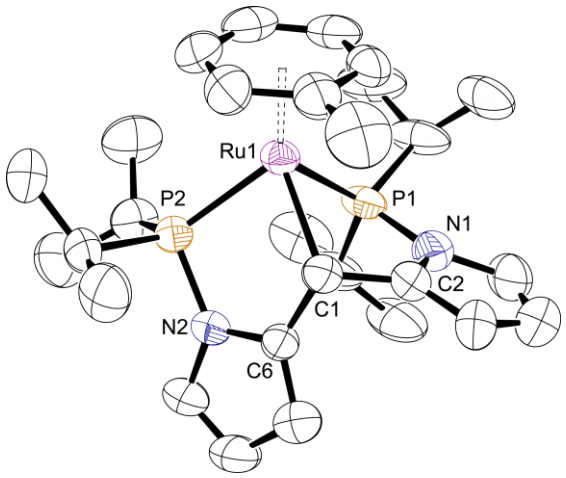

Figure 4–10. ORTEP diagram (50% probability ellipsoids) of [(P$_2$CH)Ru(η^6–toluene)][B(3,5–C$_6$H$_3$(CF$_3$)$_2$)$_4$] (**414**). Selected atom labeling shown. Hydrogen atoms and [B(3,5–C$_6$H$_3$(CF$_3$)$_2$)$_4$]$^-$ anion omitted for clarity. Selected bond distances (Å) and angles (deg): Ru1–C1, 2.175(5); Ru1–P1, 2.3516(13); Ru1–P2, 2.3018(14); P2–Ru–C1, 80.65(14); P1–Ru1–C1, 76.39(14); P1–Ru1–P2, 98.05(5).

4.3 Conclusion

The synthesis of a family of d^6 ML_5 and d^6 ML_6 ruthenium triflate complexes of the pincer $(P_2C=)Ru(L)_n$ architecture by ligand exchange using Me_3SiOTf was presented. This proved to be a good synthetic method for all the compounds except for **406** and **408**. Access to **406** through **402** through this method was not possible. We conjecture that Me_3SiOTf is not electrophilic enough to abstract chloride from **402**, which could potentially be a result of a stronger Ru–Cl bond with respect to the other Cl–containing $(P_2C=)Ru$ compounds used. This is not unexpected, given the mutually *trans* disposition of chloride in **402**, which is a weak *trans* influence donor.

The synthesis of **408** was hampered by electrophilic removal of OAc by Me_3SiOTf, in contrast to the acac–ligated **411**, where chloride substitution was achieved to yield **409**. This difference in reactivity may be attributed to the reduced stability provided by the more strained 4–member chelate ring of **412**.

Finally, triflate abstraction from **405** results in formation of a cationic species that, based on spectroscopic evidence, seems to be stabilized by solvent coordination. **405** can also form η^6 complexes with arenes, resulting in 1,2–hydride shift across Ru=C to form an 18–electron, piano stool complex.

4.4 Experimental details

4.4.1 General considerations

All operations were performed in a dry box filled with argon unless otherwise indicated. Ruthenium(III) chloride trihydrate was purchased from Johnson Matthey. α–Phellandrene, pyrrole, 1.3M ^{i}PrMgCl • LiCl in THF, and paraformaldehyde were purchased from Aldrich. Indium(III) chloride 99.999% was purchased from Strem, and was stored in a dry box filled with argon. Chlorodiisopropylphosphine was purchased from Dalchem and was used without further purification. [Ru(*p*–cymene)Cl_2]$_2$, **402** ,and **404** were prepared following literature procedures.[153,166] Hydrocarbon and ether solvents were dried over and distilled from Na/K/Ph_2CO/18–crown–6. Halogenated solvents were dried over, and vacuum transferred or distilled from calcium hydride for 48 h. and then. Solution NMR spectra were collected on Varian Inova 400 (^{1}H NMR, 399.52 MHz; ^{13}C NMR, 100.46 MHz; ^{31}P NMR, 161.73 MHz; ^{11}B NMR, 128.18 MHz) and Varian Inova 500 (^{1}H NMR, 499.43 MHz; ^{13}C NMR, 125.58 MHz; ^{31}P NMR, 202.27 MHz; ^{19}F NMR, 470.17 MHz), using deuterated solvents as indicated. ^{1}H NMR spectra were referenced to residual solvent peaks as follows: C_6D_5Br referenced to the most downfield resonance to δ 7.29 ppm. ^{13}C{^{1}H} NMR spectra were referenced as follows: C_6D_5Br referenced to the most upfield resonance to δ 122.25 ppm. ^{31}P NMR spectra were referenced to δ 0.0 ppm using H_3PO_4. ^{19}F NMR spectra were referenced to δ −78.5 ppm using neat F_3CCO_2H. Elemental analyses were performed by CALI Labs, Inc. (Parsippany, NJ, USA).

4.4.2 Synthetic procedures and characterization data

Synthesis of 401.[153] Bis(1–(diisopropylphosphino)–2–pyrrolyl)methane[153] (3.69 g, 9.74 mmol), [Ru(*p*–cymene)Cl_2]$_2$ (2.64 g, 4.87 mmol), dry triethyl amine (9.86 g, 9.74 mmol) and 50 mL of dry toluene were charged in a Schlenk flask equipped with a PTFE coated stir bar. A reflux condenser was assembled on top of the Schlenk flask and the contents were heated overnight to reflux temperature in a silicon oil bath, with a constant flow of argon through the top of the condenser. The next morning, the flask was removed from the oil bath and cooled to room temperature. The reflux condenser was then replaced with a glass stopper, and the atmosphere in the flask was replaced with H_2. The contents were stirred 1 h, at the end of which the flask was moved into an argon filled dry box. All volatiles were removed *in vacuo*, the solid was dissolved in toluene, filtered through a short path of silica gel and concentrated *in vacuo*. The compound was purified by crystallization by pentane diffusion into a concentrated toluene solution of the compound. Yield: 2.95 g (59%) ^{1}H NMR (499.43 MHz, C_6D_6) δ −15.41 (t, 1H, $^2J_{P-H}$ = 20.5 Hz, Ru–H), 0.97 (m, 12H, P(CH(CH_3)$_2$), 1.10 (dvt, app quartet, 6H, J_{H-P} = 8.0 Hz, J_{H-H} = 8.0 Hz, P(CH(CH_3)$_2$), 1.18 (dvt, 6H, app quartet, J_{H-P} = 8.0 Hz, J_{H-H} = 8.0 Hz, P(CH(CH_3)$_2$), 2.07 (m, 2H, P(CH(CH_3)$_2$), 2.73 (m, 2H, P(CH(CH_3)$_2$), 6.38 (m, 2H, py H), 6.72 (m, 2H, py H), 6.90 (m, 2H, py H). ^{31}P{^{1}H} NMR (202.27 MHz, C_6D_6) δ 121.01 (s, P^{i}Pr).

Synthesis of 405. Method 1. 410 (0.126 g, 256 μmol) and 5 mL of dry fluorobenzene were charged in a Schlenk flask equipped with a PTFE–lined stir bar. To this solution,

Me_3SiOTf (51 μL, 282 μmol) was added via Hamilton syringe in one portion. The reaction is quantitative and takes place within the time of mixing. Volatiles were removed *in vacuo* to obtain a golden–brown powder. Yield 0.15 g (95%). **Method 2. 401** (0.35 g, 680.9 μmol) and 20 mL of dry fluorobenzene were charged in a Schlenk flask. To the resulting solution, Me_3SiOTf (400 μL, 2.04 mmol) was added via Hamilton syringe in one portion and the contents were mixed thoroughly by swirling. The reaction is quantitative and takes place within the time of mixing. The volatiles were removed *in vacuo* to obtain a golden–brown powder. Yield: 0.36 g (98%). ^{1}H NMR (499.43 MHz, C_6D_6) δ– 16.44 (t, $^2J_{P-H}$ = 19.7 Hz, 1H, Ru–*H*), 0.91 (overlapping A_6BXY multiplets, 12H, P(CH(CH_3)$_2$), 1.05 (A_6BXY multiplet, calculated coupling constants (using MestReNova™ version 8.1.2): $\Delta\delta_{XY}$ = 0.01 ppm, $^2J_{X-Y}$ = 500.43 Hz, $^3J_{A-B}$ = 7.0 Hz, $^3J_{A-X}$ = 12.0 Hz, $^5J_{A-Y}$ = 0 Hz, 6H, P(CH(CH_3)$_2$), 1.20 (A_6BXY multiplet, calculated coupling constants (using MestReNova™ version 8.1.2): $\Delta\delta_{XY}$ = 0.001 ppm, $^2J_{X-Y}$ = 280 Hz, $^3J_{A-B}$ = 7.5 Hz, $^3J_{A-X}$ = 19.0 Hz, $^5J_{A-Y}$ = 0 Hz, 6H, P(CH(CH_3)$_2$), 2.13 (A_6*B*XY multiplet, 2H, P(C*H*(CH_3)$_2$), 2.94 (A_6*B*XY multiplet, calculated coupling constants (using MestReNova™ version 8.1.2): $\Delta\delta_{XY}$ = 0.01 ppm, $^2J_{X-Y}$ = 500 Hz, $^3J_{A-B}$ = 7.0 Hz, $^2J_{B-X}$ = 1.0 Hz, $^4J_{B-Y}$ = 5.0 Hz, 6H, P(CH(CH_3)$_2$), 6.30 (m, 2H, py H), 6.62 (m, 2H, py H), 6.85 (m, 2H, py H). ^{13}C{^{1}H} NMR (100.46 MHz, C_6D_6) δ 17.0 (t, *J* = 4.3 Hz, P(C*H*(CH_3)$_2$), 17.3 (s, P(CH(CH_3)$_2$), 17.4 (s, P(CH(CH_3)$_2$), 19.5 (t, *J* = 3.3 Hz, P(CH(CH_3)$_2$), 24.0 (s, P(CH(CH_3)$_2$), 26.5 (t, *J* = 9.7 Hz, P(C*H*(CH_3)$_2$), 28.2 (t, *J* = 8.9 Hz, P(C*H*(CH_3)$_2$), 101.3 (t, *J* = 4.0 Hz), 118.0 (s), 130.3 (t, *J* = 2.1 Hz), 159.6 (t, *J* = 13.9 Hz), 183.0 (s), 268.2 (t, $^2J_{C-P}$ = 8.5 Hz, Ru=C).

$^{31}P\{^{1}H\}$ NMR (202.28 MHz, C_6D_6) δ 123.4. ^{19}F NMR (470.17 MHz, C_6D_6) δ −77.2. Elemental analysis: Calculated (Found) C 42.10% (42.01%), H 5.62% (5.74%).

Attempted synthesis of (405) using AgOTf. AgOTf (10.0 mg, 38.9 μmol) was charged in a Schlenk flask equipped with a PTFE–lined stir bar and was suspended in *ca.* 5 mL of CH_2Cl_2. To this suspension, **401** (20.0 mg, 38.9 μmol) was added, and the mixture was stirred for 20 min, at which point a white precipitate of AgCl was observed. The volatiles were removed *in vacuo* to obtain a brown solid residue. This residue was extracted with C_6D_6, the solution was filtered through a fiberglass filter packed in a Pasteur pipette, and collected into a J. Young NMR tube. NMR spectroscopic analysis revealed formation, albeit not clean, of **405** as the major product. Multiple signals can be observed in the region around δ −78 ppm in the ^{19}F NMR spectrum. The aliphatic region of the ^{1}H NMR spectrum revealed multiple, intractable signals in the region between δ 0.5 and 1.7 ppm.

Attempted synthesis of 406. Compound **402** (0.046 g, 83.9 μmol) was charged in a J. Young NMR tube and was dissolved with *ca.* 500 μL of C_6D_6. To the resulting solution, Me_3SiOTf (100 μL, 517.4 μmol) was charged via Hamilton microliter syringe and mixed thoroughly by shaking the contents. By ^{19}F NMR only the $-CF_3$ resonance of unreacted Me_3SiOTf was observed. By ^{1}H and $^{31}P\{^{1}H\}$ NMR only unreacted **402** was observed.

Synthesis of 407. 404 (0.149 g, 259 μmol) was charged in a Schlenk flask, and dissolved in 20 mL of dry CH_2Cl_2. To this solution, Me_3SiOTf (900 μL, 5.17 mmol) was added in a single portion using a Hamilton microliter syringe, thoroughly mixed by swirling, and the volatiles were removed *in vacuo* to obtain a yellow–golden powder. Yield: 0.205 g (98%) ^{1}H NMR (499.43 MHz, C_6D_6) δ 0.80 (dvt, app quartet, 6H, J_{H-P} = 7.1 Hz, J_{H-H} = 7.1 Hz, P(CH(CH_3)$_2$), 0.94 (dvt, app quartet, 6H, J_{H-P} = 6.8 Hz, J_{H-H} = 6.8 Hz, P(CH(CH_3)$_2$), 1.46 (A_6BXY multiplet, calculated coupling constants (using MestReNova™ version 8.1.2): $\Delta\delta_{XY}$ = 0.01 ppm, $^2J_{X-Y}$ = 500.43 Hz, $^3J_{A-B}$ = 9.0 Hz, $^3J_{A-X}$ = 21.0 Hz, $^5J_{A-Y}$ = 0 Hz, 6H, P(CH(CH_3)$_2$), 1.63 (A_6BXY multiplet, calculated coupling constants (using MestReNova™ version 8.1.2): $\Delta\delta_{XY}$ = 0.01 ppm, $^2J_{X-Y}$ = 500 Hz, $^3J_{A-B}$ = 10.7 Hz, $^3J_{A-X}$ = 25.0 Hz, $^5J_{A-Y}$ = 0 Hz, 6H, P(CH(CH_3)$_2$), 2.42 (m, 2H, P(CH(CH$_3$)$_2$), 3.59 (m, 2H, P(CH(CH$_3$)$_2$), 6.21 (dd, 2H, *J* = 4.2 Hz, *J* = 2.5 Hz, py H), 6.69 (dd, 2H, *J* = 4.2 Hz, *J* = 1.0 Hz, py H), 6.86 (m, py H). ^{13}C{^{1}H} NMR (100.46 MHz, $CDCl_3$) δ 17.7 (t, *J* = 4.9 Hz), 18.2 (s), 18.3 (s), 18.5 (t, *J* = 5.1 Hz), 28.8 (t, *J* = 10.0 Hz), 29.9 (t, *J* = 7.2 Hz), 118.3 (t, *J* = 3.1 Hz), 122.5 (s), 155.1 (t, *J* = 9.8 Hz), 200.6 (t, *J* = 15.0 Hz), 226.4 (t, $^2J_{C-P}$ = 5.7 Hz, Ru=C). ^{31}P{^{1}H} NMR (202.28 MHz, $CDCl_3$) δ 116.4. ^{19}F NMR (470.17 MHz, $CDCl_3$) δ −78.1, −79.0. IR ν_{CO} (solid) = 1979 cm^{-1}.

Observation of 409. 411 (8.6 mg, 14.0 μmol) and *ca.* 600 μL of $CDCl_3$ were charged in a J.Young NMR tube. To the resulting solution, 40 μL of a 0.7 M solution of Me_3SiOTf in $CDCl_3$ (28.0 μmol) was added via syringe. The contents were thoroughly mixed by shaking, and the reaction mixture was analyzed by ^{1}H NMR, revealing *ca.* 20% of a new product.

Volatiles were removed *in vacuo*. The residue was dissolved in $CDCl_3$, and treated with neat Me_3SiOTf (76 μL, 420.6 μmol). This process was repeated once more. Analysis of the reaction mixture revealed that the previously observed new product was now the major product (> 90%). ^1H NMR (499.43 MHz, $CDCl_3$) δ 0.84 (dvt, app. quartet, 6H, J_{H-H}= 7.0 Hz, J_{H-P}= 7.0 Hz, P(CH(CH_3)$_2$), 1.11 (m, 6H, P(CH(CH_3)$_2$), 1.37 (m, 6H, P(CH(CH_3)$_2$), 1.40 (dvt, app. quartet, 6H, J_{H-H}= 6.5 Hz, J_{H-P}= 6.5 Hz, P(CH(CH_3)$_2$), 1.66 (s, 3H, acac –CH_3), 2.11 (s, 3H, acac–CH_3), 2.62 (m, 2H, P(C*H*(CH_3)$_2$), 3.02 (m, 2H, P(C*H*(CH_3)$_2$), 5.50 (s, 1H, acac–CH), 6.63 (dd, 2H, *J* = 3.8 Hz, *J* = 2.6 Hz), 7.03 (m, 2H, Py H), 7.66 (m, 2H, Py H). $^{31}P\{^1H\}$ (202.27 MHz, $CDCl_3$) δ 105.9. ^{19}F NMR (470.17 MHz, $CDCl_3$) δ 80.96.

Synthesis of 410. 401 (0.25 g, 486.4 μmol), NaOAc (0.477 g, 4.86 mmol), and dry fluorobenzene were charged in a Schlenk flask equipped with a PTFE–lined stir bar, and the reaction mixture was stirred overnight. The color of the solution changed slowly over time from wine red to brown. The resulting mixture was filtered through a short path of silica gel and dried *in vacuo*. This compound was purified by crystallization by diffusion of pentane into a solution of the compound in fluorobenzene. Yield: 0.096 g (35%) ^1H NMR (499.43 MHz, C_6D_6) δ −11.05 (t, 1H, $^2J_{P-H}$ = 20.3 Hz, Ru–*H*), 1.03 (dvt, app quartet, 6H, J_{H-P} = 7.3 Hz, J_{H-H} = 7.3 Hz, P(CH(CH_3)$_2$), 1.10 (dvt, app quartet, 6H, J_{H-P} = 6.9 Hz, J_{H-H} = 6.9 Hz, P(CH(CH_3)$_2$), 1.18 (m, 12H, P(CH(CH_3)$_2$), 1.97 (s, 3H, CH_3COORu), 2.06 (m, 2H, P(C*H*(CH_3)$_2$), 2.28 (hept, 2H, $^3J_{H-H}$ = 6.9 Hz, P(C*H*(CH_3)$_2$), 6.43 (m, 2H, py H), 6.65 (m, 2H, py H), 6.91 (m, 2H, py H). $^{13}C\{^1H\}$ NMR (125.58 MHz, C_6D_6) δ 17.2 (s), 17.4 (t, *J* = 3.8 Hz, P(CH(CH_3)$_2$), 17.9 (t, *J*

= 6.0 Hz, P(CH(CH_3)$_2$), 18.7 (t, *J* = 1.3 Hz, P(CH(CH_3)$_2$), 24.3 (s), 28.5 (t, *J* = 11.4 Hz, P(C*H*(CH$_3$)$_2$), 29.5 (t, *J* = 8.5 Hz, P(C*H*(CH$_3$)$_2$), 100.3 (t, *J* = 4.3 Hz), 117.7 (s), 126.7 (t, *J* = 2.3 Hz), 159.3 (t, *J* = 15.2 Hz), 180.6 (s), 256.8 (t, $^2J_{C-P}$ = 10.5 Hz, Ru=C). $^{31}P\{^1H\}$ NMR (202.28 MHz) δ 120.9. Elemental analysis: Calculated (Found) C 51.29% (51.52%), H 7.30% (7.21%).

Synthesis of 411. 402 (0.152 g, 277 μmol), NaAcac (0.371g, 3.04 mmol), and 10 mL of dry toluene were charged in a Schlenk flask equipped with a PTFE–coated stir bar. This mixture was stirred for 5d at room temperature. The slurry was filtered through Celite, and the filtrate dried *in vacuo* to obtain a dark solid residue, which was dissolved in CH_2Cl_2, filtered once more through Celite and dried *in vacuo*. The compound was purified by crystallization at–32 °C from a concentrated solution in pentane to obtain a purple solid. Yield: 0.121g (71%). ^1H NMR (399.52 MHz, C_6D_6) δ 0.81 (dvt, app quartet, 6H, J_{H-P} = 6.9 Hz, J_{H-H} = 6.9 Hz, P(CH(CH_3)$_2$), 1.00 (m, 6H, P(CH(CH_3)$_2$), 1.18 (dvt, app quartet, 6H, J_{H-P} = 7.0 Hz, J_{H-H} = 7.0 Hz, P(CH(CH_3)$_2$), 1.52 (m, 6H, P(CH(CH_3)$_2$), 1.53 (s, 3H, acac–CH_3), 1.96 (s, 3H, acac–CH_3), 2.25 (m, 2H, P(C*H*(CH$_3$)$_2$), 3.21 (m, 2H, P(C*H*(CH$_3$)$_2$), 5.23 (s, 3H, acac–C*H*), 6.43 (dd, 2H, *J* = 3.7 Hz, *J* = 2.7 Hz, py H), 6.88 (m, 2H, py H), 7.21 (m, 2H, py H). $^{13}C\{^1H\}$ NMR (100.46 MHz, C_6D_6) δ 17.4 (s), 17.5 (t, *J* = 5.1 Hz), 17.6 (s), 19.3 (t, *J* = 3.5 Hz), 26.9 (t, *J* = 9.2 Hz), 27.4 (t, *J* = 8.1 Hz), 27.8 (s), 28.1 (s), 100.0 (s), 102.1 (t, J = 3.9 Hz), 118.1 (s), 130.3 (t, *J* = 2.4 Hz), 161.0 (t, *J* = 13.4 Hz), 185.8 (s), 188.2(s), 265.6 (t, $^2J_{C-P}$ = 8.6 Hz, Ru=C). $^{31}P\{^1H\}$ NMR (161.73 MHz, C_6D_6) δ 103.3.

Synthesis of 412. 402 (0.206 g, 376 μmol), NaOAc (0.328 g, 4.00 mmol), and 20 mL of dry toluene were charged in a Schlenk flask equipped with a PTFE–lined stir bar. The reaction mixture was stirred for 4d at room temperature. The mixture was then filtered through a short path of silica gel and dried *in vacuo*. Yield: 0.178 g (83%) ^{1}H NMR (499.43 MHz, $CDCl_3$) δ 0.94 (dvt, app quartet, 6H, J_{H-P} = 7.2 Hz, J_{H-H} = 7.2 Hz, P(CH(*C*H_3)$_2$), 1.18 (dvt, app quartet, 6H, J_{H-P} = 7.2 Hz, J_{H-H} = 7.2 Hz, P(CH(*C*H_3)$_2$. A_3BXY multiplet, calculated coupling constants (using MestReNova™ version 8.1.2): $\Delta\delta_{X-Y}$ = 0.01 ppm, $^{3}J_{A-B}$ = 7 Hz, $^{3}J_{A-X}$ = 14 Hz, $^{2}J_{X-Y}$ = 500 Hz), 1.18 (dvt, app quartet, 6H, J_{H-P} = 7.5 Hz, J_{H-H} = 7.5 Hz, P(CH(*C*H_3)$_2$), 1.47 (dvt, app quartet, 6H, J_{H-P} = 7.1 Hz, J_{H-H} = 7.1 Hz, P(CH(*C*H_3)$_2$), 1.50 (dvt, app quartet, 6H, J_{H-P} = 8.4 Hz, J_{H-H} = 8.4 Hz, P(CH(*C*H_3)$_2$), 2.67 (m, 2H, P(*C*H(CH$_3$)$_2$), 3.11 (m, 2H, P(*C*H(CH$_3$)$_2$), 6.57 (m, py H), 6.83 (m, py H), 7.59 (m, py H). ^{13}C{^{1}H} NMR (100.46 MHz, C_6D_6) δ 17.0 (t, *J* = 4.3 Hz), 17.3 (s), 17.4 (s), 19.5 (t, *J* = 3.3 Hz), 24.0 (s), 26.5 (t, *J* = 9.6 Hz), 28.2 (t, J = 8.8 Hz), 101.3 (t, *J* = 4.0 Hz), 118.0 (s), 130.3, (t, J = 2.1 Hz), 160.7 (t, *J* = 13.9 Hz), 183.0 (s), 268.2 (t, *J* = 8.5 Hz, Ru=C). ^{31}P{^{1}H} NMR (161.73 MHz, C_6D_6) δ 104.8. Elemental analysis: Calculated (Found) C 48.40% (48.21%), H 6.44% (6.68%),.N 4.89% (5.07%)

Triflate abstraction from 405 (413a). 405 (7.2 mg, 23.9 μmol), **Na–201** (10.8 mg, 24.0 μmol), and *ca.* 700 μL of C_6D_5Br were charged in a J. Young NMR tube and the contents were shaken vigorously shaken. The solids were allowed to settle at the bottom of the tube, and NMR spectra were collected. Triflate ligand abstraction was confirmed by ^{19}F NMR spectroscopy, by the absence of the $-CF_3$ group resonance at δ –74.0 ppm. Attempted

crystallization by diffusion of pentane into a solution of this compound in 1,2–difluorobenzene, after evaporation of C_6D_5Br, resulted in the growth of a single crystal of [(P_2C=)Ru(H)(η^2–2–*trans*–pentene)][$MeCB_{11}Cl_{11}$] *(vide infra).* ^{1}H NMR (499.43 MHz, C_6D_5Br) δ −14.26 (t, 1H, $^2J_{H-P}$ = 23.1 Hz, Ru–*H*), 0.59 (dvt, app. quartet, 6H, J_{H-H} = 7.2 Hz, J_{H-P} = 7.2 Hz, P(CH(*CH*$_3$)$_2$), 0.96 (m, overlapping signals, 18H, P(CH(*CH*$_3$)$_2$), 1.74 (s, 3H, [*CH*$_3$–$CB_{11}Cl_{11}$]$^-$), 2.06 (m, 4H, P(*CH*(CH$_3$)$_2$), 6.49 (dd, 2H, *J* = 3.9, *J* = 2.6 Hz, Py H), 6.63 (d, 2H, *J* = 3.9 Hz, Py H), 7.14 (m, 2H, Py H). ^{31}P{^{1}H} NMR (202.27 MHz, C_6D_5Br) δ 135.06 (major). ^{19}F NMR (470.17 MHz, C_6D_5Br) δ 138.69 (residual 1,2–difluorobenzene).

Triflate abstraction from 405 (413b). 405 (0.04 g, 63.7 μmol), Na[B(3,5–$C_6H_3(CF_3)_2)_4$] (0.06 g, 67.7 μmol), and *ca.* 700 μL of C_6D_5Br were charged in a J. Young tube. The contents were vigorously shaken, and NMR spectra were collected. Triflate ligand abstraction was confirmed by ^{19}F NMR spectroscopy, by the absence of the triflate –CF_3 group resonance at δ –74.0 ppm. ^{1}H NMR (399.52 MHz, C_6D_5Br) δ −14.38 (t, 1H, $^2J_{H-P}$ = 22.4 Hz, Ru–*H*), 0.56 (dvt, app. quartet, 6H, J_{H-H} = 7.2 Hz, J_{H-P} = 7.2 Hz, P(CH(*CH*$_3$)$_2$), 0.93 (m, overlapping signals, 18H, P(CH(*CH*$_3$)$_2$), 2.01 (m, 4H, P(*CH*(CH$_3$)$_2$), 6.43 (dd, 2H, *J* = 3.9, *J* = 2.6 Hz, Py H), 6.60 (m, 2H, Py H), 7.09 (m, 2H, Py H). ^{31}P{^{1}H} NMR (161.73 MHz, C_6D_5Br) δ 122.60. ^{19}F NMR (470.17 MHz, C_6D_5Br) δ −63.41 (s, B(3,5–$C_6H_3(CF_3)_2)_4$)

[(P_2CH)Ru(η^6–toluene)][B(3,5–$C_6H_3(CF_3)_2)_4$] (414). 405 (5.0 mg, 8.0 μmol), Na[B(3,5–$C_6H_3(CF_3)_2)_4$] (8.6 mg, 9.6 μmol), and *ca.* 700 μL of a 1:1 solvent mixture of toluene–h_8 and

1,2–difluorobenzene were charged in a J. Young tube. The contents were shaken vigorously, the tube was then placed in an oil bath set to 100 °C for 1 h. The contents were transferred to a Schlenk flask and the volatiles were removed *in vacuo*. The residue was dissolved in $CDCl_3$ and NMR spectra were collected. ^{1}H NMR (499.43 MHz, $CDCl_3$) δ 1.09 (m, 6H, P(CH(*CH*$_3$)$_2$), 1.16(m, 6H, P(CH(*CH*$_3$)$_2$), 1.22 (m, 6H, P(CH(*CH*$_3$)$_2$), 1.33 (m, 6H, P(CH(*CH*$_3$)$_2$), 1.53 (m, 2H, P(CH(*CH*$_3$)$_2$), 2.09 (s, 3H, toluene–CH3), 2.75 (m, 2H, P(CH(*CH*$_3$)$_2$), 4.74 (s, 1H, Ru–CH), 5.30 (d, 2H, J_{H-H} = 6.0 Hz, toluene–CH), 5.81(m, 2H, Py H), 5.84 (t, J_{H-H} = 6.0 Hz, toluene–CH), 6.08 (t, J_{H-H} = 6.0 Hz, toluene–CH), 6.24 (t, *J* = 3.1 Hz, Py H), 6.58 (m, 2H, Py H), 7.54 (s, 4H, 3,5–$C_6H_3(CF_3)_2)_4$ *para*–CH), 7.71 (bs, 8H, 3,5–$C_6H_3(CF_3)_2)_4$ *ortho*–CH). ^{13}C{^{1}H} (125.58 MHz, $CDCl_3$) δ 17.7 (s), 19.2 (s), 19.6(m), 19.6 (s), 20.2 (m), 23.2 (t, *J* = 8.6 Hz), 31.9 (m), 34.3 (s), 88.3 (s), 89.7 (m), 94.4 (s), 105.2 (m), 115.5 (m), 117.1 (s), 117.6 (m), 118.18 (s), 121.4 (s), 123.6 (s), 127.8 (s), 129.1 (m, $^1J_{C-F}$ = 31.1 Hz, 3,5–$C_6H_3(CF_3)_2)_4$–*C*F_3), 135.0 (s), 137.7 (s), 150.8 (m), 161.8 (q, $^1J_{B-C}$ = 99.7 Hz, 3,5–$C_6H_3(CF_3)_2)_4$ *ipso* C). ^{31}P{^{1}H} NMR (202.27 MHz, $CDCl_3$) δ 125.5. ^{15}F NMR (470.17 MHz, $CDCl_3$) δ −63.05.

(^{Ph}P$_2$CH)Ru(μ–Cl)$_2$Ru(η^6–cymene)(Cl). Bis(2–(diisopropylphosphanyl)phenyl)methane[167] (0.409 g, 1.02 mmol), [Ru(*p*–cymene)Cl_2]$_2$ (0.313 g, 0.512 mmol), NEt_3 (1.0 g, 10.2 mmol), and 30 mL of dry toluene were charged in a Schlenk tube equipped with a PTFE–coated stir bar and a PTFE valve. The tube was placed in an oil bath and was heated to 130 °C overnight. The volatile components were removed *in vacuo* to obtain a dark, brick–red solid. The residue

was dissolved in dry toluene, and stirred in silica gel for 30 min. The slurry was filtered through a fritted funnel protected with Celite and the filtrate collected, concentrated *in vacuo*. The compound was purified by diffusion of pentane into a saturated solution in toluene at −32 °C. Yield: 0.192 g (27%) ^{1}H NMR (499.43 MHz, C_6D_6) δ 0.85 (m, 6H, P(CH(CH_3)$_2$), 1.04 (d, 6H, $^{3}J_{H-H}$ = 7.0 Hz, cymene–CH(CH_3)$_2$), 1.42 (dd, 6H, $^{3}J_{H-P}$ = 13.5 Hz, $^{3}J_{H-H}$ = 7.4 Hz, P(CH(CH_3)$_2$), 1.49 (dd, 6H, $^{3}J_{H-P}$ = 13.7 Hz, $^{3}J_{H-H}$ = 7.2 Hz, P(CH(CH_3)$_2$), 1.69 (1, 6H, J_{H-P} = 7.0 Hz, J_{H-H} = 7.0 Hz, P(CH(CH_3)$_2$), 1.71 (s, 3H, cymene–CH_3), 1.74 (m, 2H, P(CH(CH_3)$_2$), 2.86 (hept, 1H, $^{3}J_{H-H}$ = 7.0 Hz, cymene–C*H*(CH$_3$)$_2$), 2.74 (m, 2H, P(C*H*(CH$_3$)$_2$), 4.52 (d, 2H, $^{3}J_{H-H}$ = 5.9 Hz, cymene C_{ar}–H), 4.81 (d, 2H, $^{3}J_{H-H}$ = 5.9 Hz, cymene C_{ar}–H), 5.43 (s, 1H, Ru–CH(Ph)$_2$), 6.90 (t, 2H, *J* = 7.2 Hz, C_{ar}–H), 7.00 (t, 2H, *J* = 7.0 Hz, C_{ar}–H), 7.32 (t, 2H, *J* = 7.3 Hz, C_{ar}–H), 7.50 (d, 2H, *J* = 7.4 Hz, C_{ar}–H). ^{13}C{^{1}H} NMR (100.46 MHz, C_6D_6) δ 18.4 (s), 20.73 (filled–in doublet), 20.9 (filled–in doublet), 21.1 (s), 22.2 (s), 23.0 (broad), 27.8 (d, J_{P-C} = 21.3 Hz), 29.2 (d, J_{P-C} = 20.2 Hz), 31.0 (s), 43.5 (t, J_{P-C} = 5.4 Hz), 78.4 (d, J_{P-C} = 50.6 Hz), 94.1 (s), 99.6 (s), 123.4 (filled–in doublet), 143.9 (d, J_{P-C} = 38.3 Hz), 165.7 (d, J_{P-C} = 24.6 Hz). ^{31}P{^{1}H} NMR (202.27 MHz, C_6D_6) δ 85.3. Elemental analysis: Calculated (Found) C 49.91% (50.49%), H 6.10% (5.76%).

4.4.3 X–ray structural determinations

X–ray data collection, solution, and refinement for [(P$_2$C=)Ru(H)(η^2–2–*trans*–pentene)][MeCB$_{11}$Cl$_{11}$]. (Solved by Dr. Nattamai Bhuvanesh.) A Leica MZ 75 microscope was used to identify a suitable, orange block with very well defined faces with dimensions (max,

intermediate, and min) 0.720 mm × 0.154 mm × 0.075 mm from a representative sample of crystals of the same habit. The crystal mounted on a nylon loop was then placed in a cold nitrogen stream (Oxford) maintained at 110 K. A BRUKER APEX2 X–ray (three–circle) diffractometer was employed for crystal screening, unit cell determination, and data collection. The goniometer was controlled using the APEX2 software suite, v2008–6.0.[98] The sample was optically centered with the aid of a video camera such that no translations were observed as the crystal was rotated through all positions. The detector was set at 6.0 cm from the crystal sample (APEX2, 512 × 512 pixel). The X–ray radiation employed was generated from a Mo sealed X–ray tube (K_α = 0.70173Å with a potential of 40 kV and a current of 40 mA) fitted with a graphite monochromator in the parallel mode (175 mm collimator with 0.5 mm pinholes). Sixty data frames were taken at widths of 0.5°. These reflections were used in the auto–indexing procedure to determine the unit cell. A suitable cell was found and refined by nonlinear least squares and Bravais lattice procedures. The unit cell was verified by examination of the *h k l* overlays on several frames of data by comparing with both the orientation matrices. No super–cell or erroneous reflections were observed. After careful examination of the unit cell, a standard data collection procedure was initiated using omega scans. Integrated intensity information for each reflection was obtained by reduction of the data frames with the program APEX2.[98] The integration method employed a three dimensional profiling algorithm and all data were corrected for Lorentz and polarization factors, as well as for crystal decay effects. Finally the data was merged and scaled to produce a

suitable data set. The absorption correction program SADABS[99] was employed to correct the data for absorption effects.

Systematic reflection conditions and statistical tests of the data suggested the space group $P2_1/n$. A solution was obtained readily using SHELXTL (XS).[100] Idealized methyl groups were refined as rotating groups. Disordered carbon atoms around the olefinic double bond were refined with restrained distances set to sigma 0.005.

Hydrogen atoms were placed in idealized positions, and were set riding on the respective parent atoms. All non–hydrogen atoms were refined with anisotropic thermal parameters. The structure was refined (weighted least squares refinement on F^2) to convergence.[100,138] ORTEP–II was employed for the final data presentation and structure plots.[102]

Crystallographic information in the form of a CIF file for [(P_2C=)Ru(H)(η^2–2–*trans*–pentene)][$MeCB_{11}Cl_{11}$] is available in the form of a CIF file from the Cambridge Crystallographic Data Centre (CCDC 1019163). Crystallographic information is summarized in Table 4–2.

Table 4–2. Crystal data and structure refinement for [(P_2C=)Ru(H)(η^2–2–*trans*–pentene)][$MeCB_{11}Cl_{11}$].

Empirical formula	$C_{34}\ H_{51}\ B_{11}\ Cl_{11}\ F_2\ N_2\ P_2\ Ru$	
Formula weight	1197.63	
Temperature	110(2) K	
Wavelength	0.71073 Å	
Crystal system	Monoclinic	
Space group	$P2_1/n$	
Unit cell dimensions	a = 13.108(3) Å	α = 90°
	b = 11.571(3) Å	β = 100.197(2)°
	c = 34.449(8) Å	γ = 90°
Volume	5143(2) $Å^3$	
Z	4	
Density (calculated)	1.547 g cm^{-3}	
Absorption coefficient	0.977 mm^{-1}	
F(000)	2412.0	
Crystal size	0.720 × 0.154 × 0.075 mm^3	
Theta range for data collection	1.86 to 27.60°	
Index ranges	$-17 \le h \le 17, -115 \le k \le 15, -44 \le l \le 44$	
Reflections collected	44654	
Independent reflections	11697 [R(int) = 0.0573]	
Completeness to theta = 27.60°	98.0%	
Absorption correction	Semi–empirical from equivalents	
Max. and min. transmission	0.7456 and 0.6282	
Refinement method	Full–matrix least–squares on F^2	
Data / restraints / parameters	11697 / 4 / 598	
Goodness–of–fit on F^2	1.048	
Final R indices [$I > 2\sigma(I)$]	R_1 = 0.0467, wR_2 = 0.1076	
R indices (all data)	R_1 = 0.0748, wR_2 = 0.1197	
Largest diff. peak and hole	1.00 / −0.64 e.$Å^{-3}$	

X–ray data collection, solution , and refinement for 407. (Solved by Mr. Billy J. McCulloch). Crystals of **407** were grown from by pentane vapor diffusion into a solution of the compound in $CHCl_3$. An orange block of suitable size and quality (0.67 × 0.37 × 0.33 mm) was selected from a representative sample of crystals of the same habit using an optical microscope, mounted onto a nylon loop, and placed in a cold stream of nitrogen (110 K). Low–temperature X–ray data were obtained on a Bruker APEXII CCD based diffractometer (Mo sealed X–ray tube, K_α = 0.71073 Å). All diffractometer manipulations, including data collection, integration, and scaling were carried out using the Bruker APEX2 software.[98] An absorption correction was applied using SADABS.[99] The space group was determined on the basis of systematic absences and intensity statistics. The structure was solved by direct methods in the monoclinic $P2_1$ space group using SHELXS.[100] All non–hydrogen atoms were refined with anisotropic thermal parameters. Hydrogen atoms bound to carbon were placed in idealized positions and refined using a riding model. The chloroform solvent molecule and disordered triflate ligand were restrained using the SHELXL's RESI and SAME facilities. Disordered atoms in close proximity to each other (<0.9 Å) were restrained to have the same U_{ij} components with SIMU. The structure was found to be an inversion twin of statistically equal weight components; the Flack parameter refined to 0.54(5). The structure was brought to convergence by weighted full–matrix least–squares refinement on $|F|^2$. PLATON's ADDSYM and NEWSYM features were used to check for missed symmetry.[101] Structure manipulations were performed with the aid of shelXle.[168] ORTEP–II was employed for the final data presentation and structure plots.[102]

Crystallographic information for **407** is available in the form of a CIF file from the Cambridge Crystallographic Data Centre (CCDC 1021171). Crystallographic information is summarized on Table 4–3.

Table 4–3. Crystal data and structure refinement for **407.**

Empirical formula	$C_{25}\ H_{35}\ Cl_3\ F_6\ N_2\ O_7\ P_2\ Ru\ S_2$	
Formula weight	923.03	
Temperature	110(2) K	
Wavelength	0.71073 Å	
Crystal system	Monoclinic	
Space group	$P2_1$	
Unit cell dimensions	a = 9.3451(19) Å	α = 90°
	b = 14.922(3) Å	β = 96.50(3)°
	c = 13.263(3) Å	γ = 90°
Volume	1837.6(7) $Å^3$	
Z	2	
Density (calculated)	1.668 g cm^{-3}	
Absorption coefficient	0.919 mm^{-1}	
F(000)	932	
Crystal size	0.67 × 0.37 × 0.33 mm^3	
Theta range for data collection	2.062 to 27.542°	
Index ranges	$-12 \le h \le 12, -19 \le k \le 19, 0 \le l \le 17$	
Reflections collected	7705	
Independent reflections	7558 [R_{int} = 0.0421]	
Completeness to theta = 25.242°	98.8%	
Absorption correction	Semi–empirical from equivalents	
Max. and min. transmission	0.7456 and 0.5747	

Table 4–3. (Continued).

Refinement method	Full–matrix least–squares on F^2
Data / restraints / parameters	7558 / 86 / 534
Goodness–of–fit on F^2	0.948
Final R indices [$I > 2\sigma(I)$]	R_1 = 0.0498, wR_2 = 0.1348
R indices (all data)	R_1 = 0.0547, wR_2 = 0.1388
Largest diff. peak and hole	0.900 / −0.482 e.Å^{-3}

X–ray data collection, solution, and refinement for 414. (Solved by Dr. Nattamai Bhuvanesh). Single crystals of **414** were grown from a reaction mixture formed by treating 405 (0.020 g, 31.9 μmol) with Na[B(3,5–$C_6H_3(CF_3)_2)_4$] (0.034 g, 38.2 μmol) in *ca.* 700 μL of a 1:1 solvent mixture of toluene and 1,2–difluorobenzene, followed by thermolysis at 100 °C for 1h. The mixture was removed from the heat source, and the reaction mixture filtered through a fiberglass filter packed in a Pasteur pipette into a clean NMR tube. The crystals were grown under slow diffusion of pentane vapors into the reaction mixture. A Leica MZ 75 microscope was used to identify a suitable, light–orange block with very well defined faces with dimensions (max, intermediate, and min) 0.507 mm × 0.325 mm × 0.202 mm from a representative sample of crystals of the same habit. The crystal mounted on a nylon loop was then placed in a cold nitrogen stream (Oxford) maintained at 110 K. A BRUKER APEX2 X–ray (three–circle) diffractometer was employed for crystal screening, unit cell determination, and data collection. The goniometer was controlled using the APEX2 software suite, v2008–6.0.[98] The sample was optically centered with the aid of a video camera such that no

translations were observed as the crystal was rotated through all positions. The detector was set at 6.0 cm from the crystal sample (APEX2, 512 × 512 pixel). The X–ray radiation employed was generated from a Mo sealed X–ray tube (K_α = 0.70173 Å with a potential of 40 kV and a current of 40 mA) fitted with a graphite monochromator in the parallel mode (175 mm collimator with 0.5 mm pinholes). Sixty data frames were taken at widths of 0.5°. These reflections were used in the auto–indexing procedure to determine the unit cell. A suitable cell was found and refined by nonlinear least squares and Bravais lattice procedures. The unit cell was verified by examination of the *h k l* overlays on several frames of data by comparing with both the orientation matrices. No super–cell or erroneous reflections were observed. After careful examination of the unit cell, a standard data collection procedure was initiated using omega scans. Integrated intensity information for each reflection was obtained by reduction of the data frames with the program APEX2.[98] The integration method employed a three dimensional profiling algorithm and all data were corrected for Lorentz and polarization factors, as well as for crystal decay effects. Finally the data was merged and scaled to produce a suitable data set. The absorption correction program SADABS[99] was employed to correct the data for absorption effects.

Systematic reflection conditions and statistical tests of the data suggested the space group P1211. A solution was obtained readily using SHELXTL (XS).[100] Hydrogen atoms were placed in idealized positions and were set riding on the respective parent atoms. All non–hydrogen atoms were refined with anisotropic thermal parameters. The structure was refined (weighted least squares refinement on F^2) to convergence.[100,138] ORTEP–II was employed for the final

data presentation and structure plots.[102] Crystallographic information for **414** is available in the form of a CIF file (CCDC 1019162) from the Cambridge Crystallographic Data Centre. Crystallographic information is summarized in Table 4–4.

Table 4–4. Crystal data and structure refinement for **414.**

Empirical formula	$C_{60}\ H_{55}\ B\ Fl_{24}\ N_2\ P_2\ Ru$	
Formula weight	1433.92	
Temperature	110(2) K	
Wavelength	0.71073 Å	
Crystal system	Monoclinic	
Space group	$P12_11$	
Unit cell dimensions	a = 12.7135(13) Å	α= 90°
	b = 18.4476(18) Å	β= 92.521(4)°
	c = 13.2888(14) Å	γ = 90°
Volume	3113.7(6) $Å^3$	
Z	2	
Density (calculated)	1.5293 g cm^{-3}	
Absorption coefficient	0.415 mm^{-1}	
F(000)	1447.1	
Crystal size	0.507 × 0.325 × 0.202 mm^3	
Theta range for data collection	2.43 to 27.61°	
Index ranges	$-16 \le h \le 16, -23 \le k \le 24, -17 \le l \le 16$	
Reflections collected	37173	
Independent reflections	14156 [R_{int} = 0.0304]	
Completeness to theta = 27.61°	98.0%	

Table 4–4. (Continued).

Absorption correction	Semi–empirical from equivalents
Max. and min. transmission	0.7456 and 0.6860
Refinement method	Full–matrix least–squares on F^2
Data / restraints / parameters	14156 / 54 / 804
Goodness–of–fit on F^2	1.024
Final R indices [$I > 2\sigma(I)$]	R_1 = 0.0601, wR_2 = 0.1583
R indices (all data)	R_1 = 0.0736, wR_2 = 0.1705
Largest diff. peak and hole	0.78/−0.65 e.Å^{-3}

CHAPTER V

REACTIVITY OF NEUTRAL AND CATIONIC SYSTEMS OF A TANTALUM ALKYLIDYNE WITH INTERNAL AND TERMINAL ALKYNES

5.1 Introduction

Compounds with transition metal–carbon triple bonds (*i.e.*, M≡CR),[169] typically termed carbyne or alkylidyne complexes,[170,171] are of particular importance as intermediates and catalysts in the metathesis of carbon–carbon triple bonds.[172,173] They are most common in the chemistry of Mo and W (group 6),[174] which function as capable alkyne and nitrile metathesis catalysts.[175,176] Metal–carbon triple bonds are also well established for Re (group 7),[177,178] with some examples of alkyne metathesis,[179] as well as Ru[180] and Os[181] (group 8), while Rh and Ir (group 9)[182] offer only a few examples. Isolated compounds of metal–carbon triple bonds are unknown for metals of groups 3 and 4, and are rare for group 5. For purely hydrocarbyl CR ligands (alkylidynes) only one family of NacNac–based compounds is known for V,[183] none for Nb, and only the 1978 report[184] from the Schrock group describing Cp'Ta(≡CPh)(PMe_3)$_2$Cl (where Cp' = η^5–C_5H_5 or η^5–C_5Me_5) for Ta. The Lippard group reported a series of V, Nb, and Ta siloxycarbyne complexes containing M≡C$OSiX_3$ moieties that resulted from silylation of metal carbonylate anions.[185] Li and coworkers described Nb[186] and Ta[187] phosphoniomethylidynes with a M≡CPPh_3 substructure. Several bridging alkylidyne complexes are known in group 5, including homobimetallic dimetallacyclobutadienes,[188,189] and alkylidynes bridging between Ta and Li,[190] as well as Ta and Zn.[191]

We were intrigued by the scarcity of group 5 terminal alkylidynes, and by the fact that the existing examples have not been studied experimentally[192] in the context of alkyne metathesis. To the best of our knowledge, the only observation (*in situ*) of a [2+2] cycloaddition to give tantalacyclobutadiene comes from the report by Pasman *et al.*[193] in 1985 describing the conversion of trimetallic Ta_2Zn bridging alkylidyne to cyclopentadienyls in reactions with alkynes. In view of this, we decided to delve into the possible usefulness of Schrock's (η^5–C_5Me_5)Ta(≡CPh)(PMe_3)$_2$Cl (**501**) in alkyne metathesis reactions.[184] In light of our interest in highly reactive cations,[194] we speculated that abstraction of the chloride from it may lead to a more reactive complex.

5.2 Results and discussion

*5.2.1 Synthesis of (η^5–C_5Me_5)Ta(≡CPh)(PMe_3)$_2$Cl (**501**)*

Our synthesis of **501** largely followed the original procedure reported by Schrock (Scheme 5–1).[184] Abstraction of chloride was performed using excess of Na[BARF] (BARF = [B($C_6H_3(CF_3)_2)_4$]) which was dried following the Bergman procedure.[195] In some reactions, especially for the purposes of isolation of pure solids, we used equimolar amounts of **Na–108** or **Na–203**,[97] which can be safely dried by heating under vacuum. A 3:2 mixture of toluene–d_8 and *protio*–1,2–difluorobenzene (ODFB) was our solvent of choice for *in situ* NMR studies. This mixture provides a reasonable compromise in terms of cost, the ability to dissolve organometallic BARF or carborane salts, and the ability to collect quality ^{1}H NMR spectra (with the exception of the aromatic region).

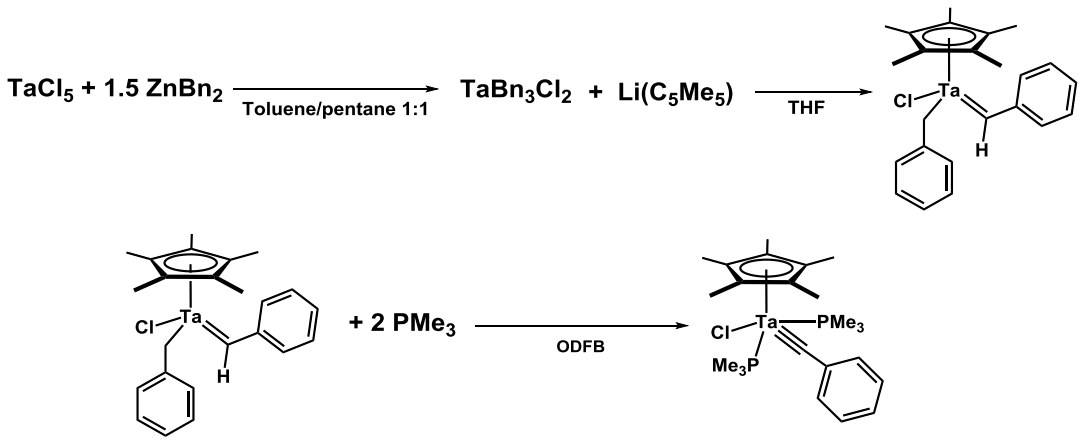

501

Scheme 5–1. Synthesis of $(\eta^5\text{–}C_5Me_5)Ta(\equiv CPh)(PMe_3)_2$ (**501**).[184]

*5.2.2 Analysis of the mixture of products from chloride abstraction from **501***

Treatment of **501** with 2.5 equivalents of Na[BARF] resulted in a mixture of four apparent products (Scheme 5–2). The same mixture of organometallic cations was observed when 1.0 equivalents of Na[BARF], **Na–108** or **Na–203** were used, along with the free anion resonances. We were able to identify the nature of three of the components of the mixture. One is the tris–phosphine complex $[(\eta^5\text{–}C_5Me_5)Ta(\equiv CPh)(PMe_3)_3]^+$ (**502**). This compound was isolated as a BARF salt in 84% yield in analytically pure form, from a reaction with three additional equivalents of PMe_3. In the $^{31}P\{^1H\}$ NMR spectrum of **502**, a doublet at δ −13.7 ppm and a triplet at δ −31.8 ppm ($^2J_{P\text{–}P}$ = 28.5 Hz) were observed, while the $^{13}C\{^1H\}$ NMR spectrum revealed a resonance at δ 365.6 ppm for the alkylidyne carbon (dt, $^2J_{C\text{–}P}$ = 29.9 Hz, $^2J_{C\text{–}P}$ = 9.2 Hz).

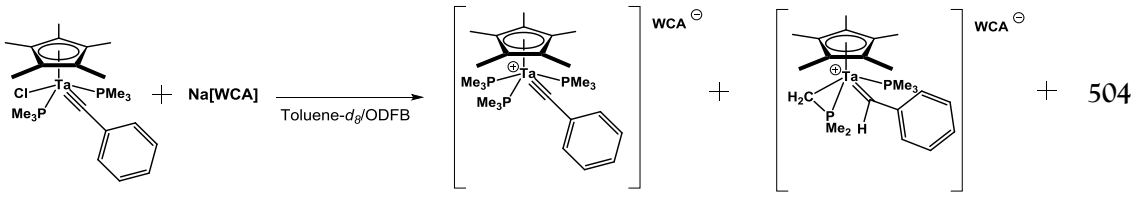

501 **502** **503–1, 503–2**

WCA = $[B(C_6H_3(CF_3)_2)_4]^-$(*a*); $[HCB_{11}Cl_{11}]^-$(*b*); $[n\text{–}BuCB_{11}Cl_{11}]^-$(*c*)

Scheme 5–2. Products of chloride abstraction from **501** using sodium salts of Weakly Coordinating Anions (WCA).

Two other components of the mixture appear to be isomers of the cyclometalated complex $[(\eta^5\text{–}C_5Me_5)Ta(=CHPh)(PMe_3)(CH_2PMe_2]^+$ (**503**), and are formed in a 1:1 ratio (compounds **503–1** and **503–2**). Each of the isomers displayed a pair of doublets in the $^{31}P\{^1H\}$ NMR spectrum, and the ^1H NMR spectra of the mixture contained resonances assignable to two sets of cyclometalated Me_2PCH_2 fragments, in addition to the corresponding non–activated PMe_3 and C_5Me_5 signals. Compounds **503–1a**/ **503–2a** originate from the net addition of a C—H bond in PMe_3 across the Ta≡C bond in the unobserved $[(\eta^5\text{–}C_5Me_5)Ta(\equiv CPh)(PMe_3)_2]^+$ cation. Compound **502a**, and the isomers **503–1a**/ **503–2a** are clearly related by equilibrium with PMe_3. Treatment of the mixture with excess PMe_3 at 40 °C overnight led to an increase in the content of **502**; *vice versa*, treatment of a pure sample of **502a** with 1.0 equivalents of $B(C_6F_5)_3$ to trap PMe_3 in the form of the highly insoluble adduct $Me_3P\text{—}B(C_6F_5)_3$, led to clean formation of a 1:1 mixture of the **503–1a**/ **503–2a** isomers exclusively. This demonstrates the facile reversibility of C—H bond activation by the tantalum—carbon triple bond under the reaction conditions.

We were not able to identify the fourth, minor component **504** (<2%) of the mixture corresponding to the singlet at *ca.* δ 0 ppm in the $^{31}P\{^{1}H\}$ NMR spectrum. Its content in the mixture was not affected by addition or removal of PMe_3. We considered whether it might be a product of adventitious hydrolysis, however, carefully measured addition of small quantities of water to a mixture of **502a**, **503–1a**, **503–2a**, and **504** did not result in increase of its content. The mass balance for the chloride abstraction reaction is not fully clear. Naturally, the phosphorus:tantalum (P:Ta) ratio of three for **502** and of two for **503** requires the formation of another co–product with a lower P:Ta ratio. It is possible that the unknown compound **504** contains only one phosphorus per tantalum, or else that formation of a small quantity of phosphine–free Ta complex(es) takes place. Chloride abstraction in the presence of mesitylene as an internal integration standard showed retention of C_5Me_5 and PMe_3 ^{1}H NMR resonance intensity in solution within the likely 10% error of measurement, but this margin of error may be enough to provide for the extra PMe_3 release needed to form **502**.

5.2.3 X–ray diffraction study of one of the isomers of 503

Our efforts to isolate **503–1**/**503–2** separately or as a pure isomeric mixture on a preparative scale have not been successful. However, we obtained an X–ray quality single crystal from the reaction of **501** with **Na–203**, and an X–ray diffraction study confirmed the proposed connectivity (Figure 5–1). The CH_2–P vector of the cyclometalated phosphine is in the same plane as the Ta–P bond to the unaffected PMe_3, with the CH_2 group tilted towards the C_5Me_5 ring. The two Ta–P distances are nearly the same and the Ta–CH_2 bond length of

2.262(2) Å is normal for a single Ta–C single bond. The overall geometry of the $Ta(CH_2PMe_2)$ fragment is very similar to that in $(Me_3P)_4W(CH_2PMe_2)(H)$ (Table 5–1 and 5–2).[196]

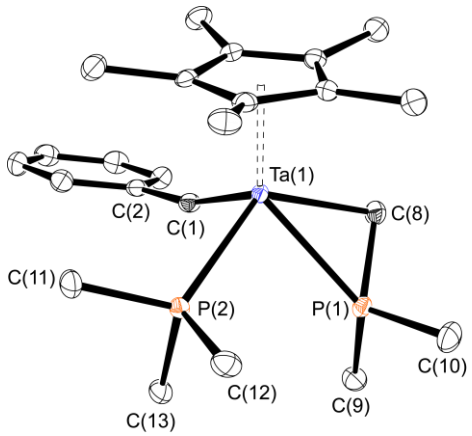

Figure 5–1. ORTEP diagram of one of the isomers of 503**c**. Thermal ellipsoids set to 50% probability. Hydrogen atoms and $[n\text{-BuCB}_{11}Cl_{11}]^-$ (**203**) anion omitted for clarity. Selected distances (Å) and angles (deg): Ta(1)–C(1) 1.918(2), C(1)–C(2) 1.463(3), Ta(1)–C(8) 2.262(2), Ta(1)–(P1) 2.5729(6), Ta(1)–(P2) 2.5680(6), P(1)–C(8) 1.762(2), P(1)–C(9) 1.808(2), P(1)–C(10) 1.817(2), P(2)–C(11) 1.819(2), P(2)–C(12) 1.821(2), P(2)–C(13) 1.820(2); Ta(1)–C(1)–C(2) 164.24(18), P(2)–Ta(1)–P(1) 82.065(19), C(8)–P(1)–Ta(1) 59.46(8), Ta(1)–P(1)–C(10) 126.48(9), Ta(1)–P(1)–C(9) 125.83(8), C(10)–P(1)–C(9) 106.96(12). Sum of angles around P(1) *ca.* 359°.

Table 5–1. Comparison of relevant interatomic distances (Å) of 503**c**, $(Me_3P)_4W(CH_2PMe_2)(H)$ (**505**),[196] and $(\eta^5\text{-}C_5Me_5)Ta(=CHCMe_3)(C_2H_4)(PMe_3)$ (**506**).[197]

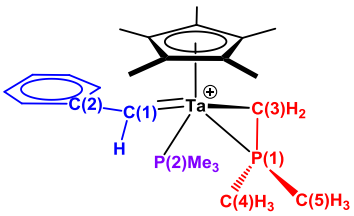

503
M = Ta

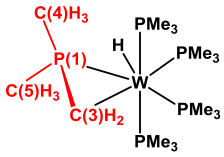

505
M = W

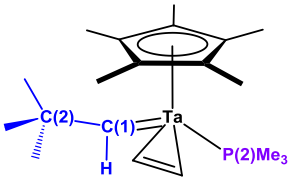

506
M = Ta

	Comparative distances (Å)		
Distance	(**503c**)	**506**	**505**
M–C(1)	1.918(2)	1.946(3)	–
M–P(2)	2.5680(4)	2.507(4)	2.448(1)
P(1)–C(3)	1.762(2)	–	1.760(6)
P(1)–C(4)	1.808(2)	–	1.849(6)
P(1)–C(5)	1.817(2)	–	1.840(6)

Table 5–2. Comparison of relevant interatomic angles (deg) of 503**c**, **505**,[196] and **506**.[197]

	Comparative angles (deg)		
Angle	(**503c**)	**506**	**505**
M–C(1)–C(2)	164.24(18)	170.0(2)	–
M–P(1)–C(4)	125.83(8)	–	129.9(2)
M–P(1)–C(5)	126.48(9)	–	130.2(2)
C(4)–P(1)–C(5)	106.96(12)	–	98.2(3)
Σ∠ around P(1)	*ca.* 359	–	*ca.* 358

The Ta=C bond length of 1.918(2) Å in the alkylidene fragment of **503** is at the shorter end of the Ta=C bond length range,[169] but is significantly longer than the 1.849(8) Å Ta≡C bond in **501**.[184] The Ta=C–C angle of *ca.* 164° is quite typical for agostic Ta alkylidenes.[184] The alkylidene formulation of **503–1**/**503–2** is further supported by the observation of two downfield resonances (δ 234.6 and 244.7 ppm) in the ^{13}C NMR spectrum of the reaction mixture showing low $^{1}J_{C-H}$ values of 76–77 Hz. The closest Ta structural analog of **503c** is $(\eta^5\text{-}C_5Me_5)Ta(=CHCMe_3)(C_2H_4)(PMe_3)$,[197] with the $Ta(C_2H_4)$ metallacyclopropane positioned very similarly to $Ta(CH_2PMe_2)$ in **503c**. The two isomers of **503c** are likely the result of a swapping of the positions between the PMe_2 and CH_2 coordinating groups in the cyclometalated unit. While we cannot rule out other possibilities, this explanation is consistent with the observation of markedly different $^{2}J_{P-P}$ values in **503–1**/**503–2** (14 and 54 Hz) in the $^{31}P\{^{1}H\}$ NMR spectrum. There is abundant precedent for addition of C–H bonds across metal–element multiple bonds.[198] The most closely related example is the chemistry of C–H bond activation by an unobserved Ti alkylidyne, extensively studied by the Mindiola group.[199]

5.2.4 Chloride abstraction from $(\eta^5\text{-}C_5H_5)Ta(\equiv CPh)(PMe_3)_2(Cl)$

The Cp analogue of **501**, $(\eta^5\text{-}C_5H_5)Ta(\equiv CPh)(PMe_3)_2(Cl)$ (**507**), underwent a transformation to an apparently analogous mixture upon treatment with Na[BARF], based on NMR spectroscopic data (Figure 5–2). We have not pursued full characterization or isolation

of Cp complexes. The details of the *in situ* observations are given in the experimental procedures section (page 161).

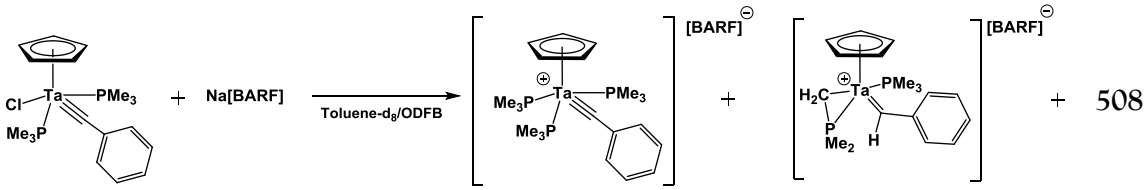

507 **509** **510–1, 510–2**

Figure 5–2. Chloride abstraction reaction from **507**.

5.2.5 Reactivity with alkynes

5.2.5.1 Reactivity of the mixture of 502, 503**–1, and** 503**–2 with alkynes**

We set out to examine reactions of the **502a**/ **503–1a**/ **503–2a** mixture with alkynes. Treatment of a mixture of **502b**/ **503–1b**/ **503–2b** with 3–hexyne resulted in a clean reaction, forming [(η^5–C_5Me_5)Ta(CPhCEtCEt)(PMe_3)][$HCB_{11}Cl_{11}$] (**511b**) in >95% purity (NMR evidence) *in situ* and in 68% isolated yield. In contrast, addition of diphenylacetylene gave no evidence of formation of a metallacycle. Treatment of **502a**/ **503–1a**/ **503–2a** with a mixture of 3–hexyne and diphenylacetylene gave only **511a**, with no evidence for a cross–metathesis product. The molecular structure of **511b** in the solid state was established by an X–ray diffraction study (Figure 5–3). While there are no other structurally characterized

tantalacyclobutadienes for comparison, the metrics of the TaC_3 ring in Figure 5–3 are similar to those observed in tungstacyclobutadiene $W(C^tBuCMeCMe)Cl_3$ (Table 5–3 (distances), and Table 5–4 (angles)).[204] **511** exhibits a geometry that is slightly distorted away from the ideal 3–legged piano stool configuration,[165] due to the geometric restrictions imposed by the planar tantalacyclobutadienes. The Ta–C(21) (1.948(4) Å) and Ta–C(11) (1.956(4) Å) distances are essentially equal, and are within the range of Ta–C double bonds,[184,200] while the distances C(21)–C(18) (1.481(5) Å) and C(11)–C(18) (1.461(5) Å) are also equal, and fall in between the typical range of C–C double bonds (1.330(3) Å in ethylene[201]), and single bonds (1.543 Å in ethane[202]).

In reactions with phenylacetylene, **502a**/ **503–1a**/ **503–2a** were completely consumed, and the dominant product appeared to be a tantalacyclobutadiene **[**(η^5–C_5Me_5)Ta($(CPh)_2CH$)(PMe_3)$_2$][BARF] (**512**) with an α–CH. Relevant NMR spectral features are three downfield resonances at δ 195.3, 2.03.5 and 215.4 ppm in the $^{13}C\{^1H\}$ NMR spectrum, and a doublet at δ 10.85 ppm (J_{H-P} = 11.7 Hz). An HMBC experiment revealed cross peaks between all these resonances, and a $^1J_{C-H}$ = 176.2 Hz between the ^{13}C signal at δ 195.3 ppm, and the ^1H signal at δ 10.85 ppm. Based on this information, these two resonances were assigned to the metallacyclic C–H, and the assignment was confirmed by an HSQC experiment. These key spectral features of **512** matched related literature compounds closely.[203] In contrast to **511a**, the product seemed to contain two PMe_3 ligands, based on the finding of two phosphine resonances in the aliphatic region of the ^1H NMR spectrum, which was confirmed in the $^{31}P\{^1H\}$ NMR spectrum, where two doublets could be found at δ 6.74

and −2.08 ppm (J_{P-P} = 4.9 Hz). We were not able to isolate **512** in pure form, in part because other minor products were present in the mixture.

A similar reaction between **502a**/ **503–1a**/ **503–2a** 1–hexyne also resulted in the formation of a metallacyclobutadiene, however, the $^{31}P\{^{1}H\}$ revealed that **502** and **504** were still present, while **503–1a**/ **503–2a** were consumed. In addition to that, four slightly broadened resonances were observed at δ 11.25, 7.86, −2.12 and −3.01 ppm all in a 1:1:1:1 ratio. Although we could not group the signals, it seems that two isomers had formed, each with two different PMe_3 ligands. The phosphine resonances could not be observed in the ^{1}H NMR due to broadening. Spectroscopic signature signals for a protiotantalacyclobutadiene were found in the ^{1}H NMR, where a signal at δ 10.63 ppm (J = 1.1 Hz), and in the $^{13}C\{^{1}H\}$ NMR spectrum at δ 240.7 and 229.7 ppm.

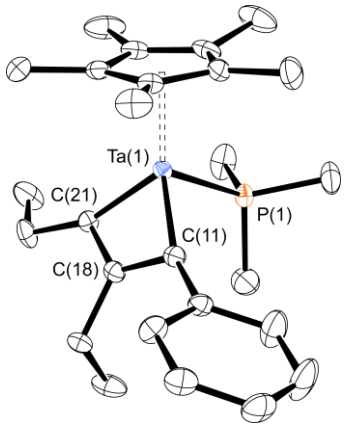

Figure 5–3. ORTEP diagram (50% probability ellipsoids) of one of the enantiomers of **(511b)** Selected atom labeling shown. Thermal ellipsoids set to 50% probability. Hydrogen atoms and $[HCB_{11}Cl_{11}]^{-}$ **(108)** anion omitted for clarity. Selected distances (Å) and angles (deg): Ta(1)–C(11) 1.956(4), Ta(1)–C(21) 1.948(4), Ta(1)–C(18) 2.179(3), C(11)–C(18) 1.461(5), C(18)–C(21) 1.481(5), Ta(1)–P(1) 2.5602(10), C(21)–Ta(1)–C(11) 82.51(15), C(21)–C(18)–C(11) 122.1(3).

Table 5–3. Comparison of relevant interatomic distances (Å) of **511b** and W(C^{t}BuCMeMe)Cl$_3$ (**513**).[204]

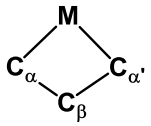

M = Ta (**511**); W (**513**)

	Comparative distances (Å)	
Distance	(**511b**)	513
M–C$_{\alpha}$'	1.956(4)	1.861(9)
M–C$_{\alpha}$	1.948(4)	1.864(8)
M–C$_{\beta}$	2.179(3)	2.115(8)
C$_{\alpha}$'–C$_{\beta}$	1.461(5)	1.455(13)
C$_{\alpha}$–C$_{\beta}$	1.481(5)	1.478(12)

Table 5–4. Comparison of relevant interatomic angles (deg) of **511b** and **513**.[204]

	Comparative angles (deg)	
Angle	(**511b**)	513
C$_{\alpha}$–M–C$_{\alpha}$'	82.51(15)	85.4(4)
C$_{\alpha}$–C$_{\beta}$–C$_{\alpha}$'	122.1(3)	118.9(8)

5.2.5.2 Reactivity of 501 with alkynes

Interestingly, abstraction of chloride is not required to activate **501** towards cycloaddition with alkynes. Treatment of solutions of **501** in toluene–d_8/1,2–orthodifluorobenzene with trimethylsilylacetylene and 3–hexyne, resulted in the formation of tantalacyclobutadiene complexes (η^5–C_5Me_5)Ta(CPhCHCSiMe$_3$)(Cl) (**514**), and (η^5–C_5Me_5)Ta(CPhCHCSiMe$_3$)(Cl) (**515**) (Scheme 5–3). Relevant features of the multinuclear NMR spectra of compound **514** are a set of three distinctive downfield resonances at δ 142.3, 146.5 ($^1J_{C-H}$ = 187.1 Hz),[203] and 207.8 ppm observed in the ^{13}C NMR spectrum (metallacyclic carbon atoms). These data are in the range for analogous tungstacyclobutadienes containing the C–H unit.[203] In the ^{1}H NMR spectrum, a new downfield resonance at δ 10.7 ppm appeared, and notably, no PMe$_3$ resonances were observed after workup. The loss of both PMe$_3$ ligands was confirmed by the absence of any signals in the ^{31}P{^{1}H} NMR spectrum after workup. Although we cannot ascertain the exact connectivity of the metallacyclic C–H group, we believe it is reasonable to propose that it is located in the α position of the TaC$_3$ ring, given the close similarity of the spectral data to that of related compounds of W,[203] and also because cycloadditions of bulky terminal alkynes to analogous tungsten alkylidynes appear to have a preference for that regiochemistry (Figure 5–4).[203]

The main features of the ^{1}H NMR spectrum of compound **515** are two different sets of ethyl group signals, with two distinct diastereotopic resonances for each CH$_2$ group, and also the absence of PMe$_3$ resonances, which was confirmed in the ^{31}P{^{1}H} NMR spectrum.

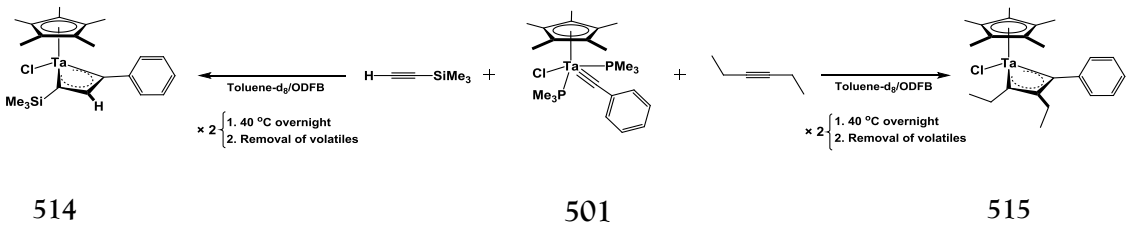

514 501 515

Scheme 5–3. Reactivity of **501** towards terminal and internal alkynes.

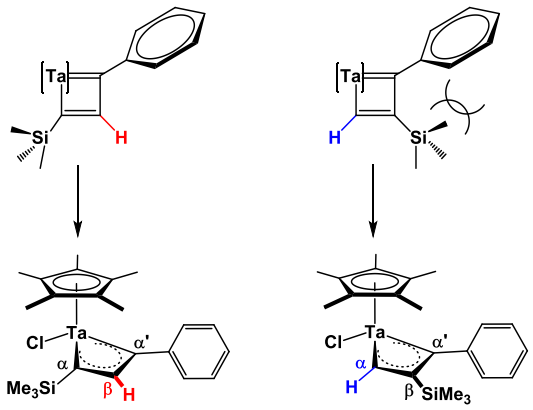

Figure 5–4. Steric interactions between the trimethylsilyl group and the phenyl group in the two possible isomers of **514**.

5.3 Conclusion

In summary, it has been demonstrated that removal of chloride from **501** resulted in facile and reversible C–H bond activation of the PMe_3 ligand, concomitant with protonation of the carbyne carbon, to yield the two isomeric, cationic alkylidenes **503–1** and **503–2** in a relative ratio very close to 1:1. Along with **503–1** and **503–2**, a relatively smaller amount of the tris–phosphine adduct **502**, and an unidentified side product **504** were observed consistently in all the experiments performed. Formation of **504** may be the result of PMe_3

ligand release, which is trapped by **503–1**/ **503–2** to form of **502**. Similar chemistry is observed when chloride is abstracted from the Cp analogue **507**.

Reactions of neutral **501**, and the mixture of cationic **503–1**, **503–2** and **502** resulted in formation of very stable, 14–electron, neutral and cationic metallacyclobutadienes respectively that did not show alkyne–metathesis reactivity.

5.4 Experimental details

5.4.1 General considerations

All operations were performed in a dry box filled with argon unless otherwise indicated. Tantalum(V) chloride (99.99%), zinc(II) chloride (99.99%), trimethylphosphine, lithium pentamethylcyclopentadienide and Na(C_5H_5) (THF solution) were purchased from Strem Chemicals and used as received. Benzylmagnesium chloride was purchased from Aldrich as a 1.0 M solution in diethyl ether. Hydrocarbon and ether solvents were dried over and distilled from Na/K/Ph_2CO/18–crown–6. Halogenated and toluene–d_8 solvents were dried over calcium hydride for 48 h. and then vacuum transferred. Na[B(3,5–$C_6H_3(CF_3)_2)_4$] was purchased from Matrix Scientific and dried *in vacuo* for 48 h at 100 °C in a Schlenk flask with a 24/40 joint in the presence of a vial containing P_2O_5.[195] **Me_3NH–108** and solvent–free **Na–203** salts were prepared following previously published procedures.[81,97] The organozinc and precursor organotantalum compounds were prepared according to previously published methods.[205-] Solution NMR spectra were collected on Varian Inova 300 (^{31}P NMR, 121.43 MHz), Varian Inova 399.52 (^{1}H NMR, 399.52 MHz; ^{13}C NMR, 100.46 MHz; ^{31}P NMR,

161.73 MHz; ^{11}B NMR, 128.18 MHz) and Varian Inova 500 (^{1}H NMR, 499.43 MHz; ^{13}C NMR, 125.58 MHz; ^{31}P NMR, 202.27 MHz; ^{19}F NMR, 470.17 MHz) and Bruker 500 cryoprobe (^{1}H NMR, 499.43 MHz; ^{13}C NMR, 125.58 MHz) spectrometers using deuterated solvents as indicated. ^{1}H NMR spectra were referenced to residual solvent peaks as follows: 3:2 solvent mixture of toluene–d_8/1,2–difluorobenzene referenced to the most upfield resonance to δ 2.08 ppm, C_6D_5Br referenced to the most downfield resonance to δ = 7.29 ppm. ^{13}C{^{1}H} NMR spectra were referenced as follows: 3:2 solvent mixture of toluene–d_8/1,2–difluorobenzene referenced to the most upfield resonance to δ 20.43 ppm, C_6D_5Br referenced to the most upfield resonance to δ 122.25 ppm. ^{31}P NMR and ^{11}B NMR spectra were referenced to δ 0.0 ppm using H_3PO_4 and $BF_3 \bullet OEt_2$ respectively. ^{19}F NMR spectra were referenced to δ −78.5 ppm using neat F_3CCO_2H. Elemental analyses were performed by CALI Labs, Inc. (Parsippany, NJ, USA).

5.4.2 Synthetic procedures and characterization data

5.4.2.1 Chloride abstraction reactions from 501

Chloride abstraction from 501 with Na[B(3,5–$C_6H_3(CF_3)_2)_4$]. **501** (40.0 mg, 77.0 μmol), Na[B(3,5–$C_6H_3(CF_3)_2)_4$] (170.0 mg, 191.0 μmol) and 700 μL of a 3:2 toluene–d_8/1,2–difluorobenzene solvent mixture were charged in a J. Young NMR tube and shaken vigorously for 1 min. A mixture of compounds can be observed by ^{1}H and ^{31}P{^{1}H} NMR spectroscopies, which is composed of two products of C–H bond activation of one of the $P(CH_3)_3$ ligands (compounds **503–1a** and **503–2a**). The exact structure of one of them was established by

X–ray diffractometry (*vide infra*). The ^{1}H NMR signals of these compounds (Figure 5–5) were were matched to their respective and $^{31}P\{^{1}H\}$ NMR resonances (Figure 5–6) by selective decoupling of ^{31}P signals from the ^{1}H NMR spectrum (Figure 5–7 and 5–8). The signals of **503–1a** and **503–2a** are highlighted in blue and red boxes respectively. Another component of the mixture is compound **502a**. Its $^{31}P\{^{1}H\}$ NMR signals are highlighted in yellow boxes. Finally, an unknown compound **(504)** can also be observed by $^{31}P\{^{1}H\}$ NMR spectroscopy (green box, Figure 5–6).

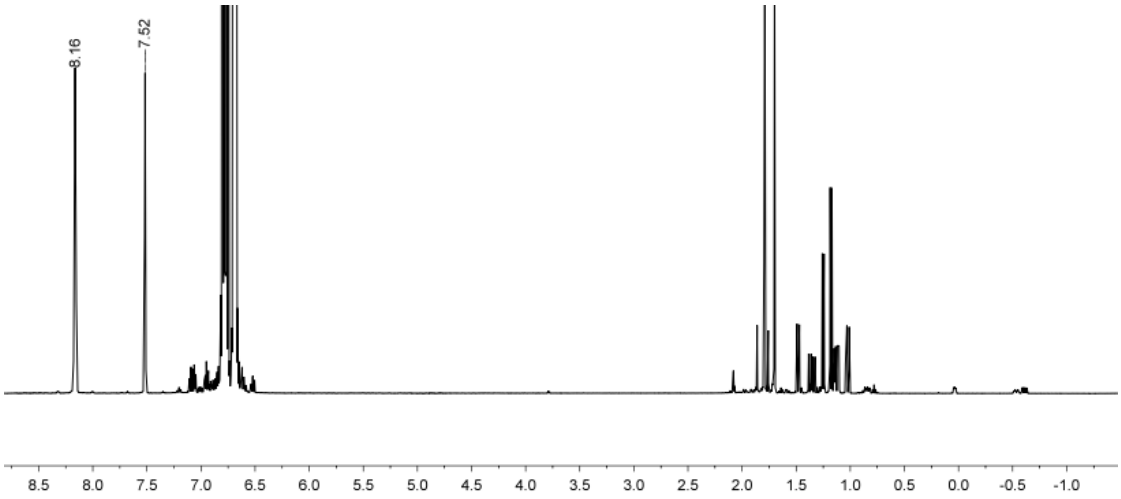

Figure 5–5. Full 1H NMR (499.43 MHz) spectrum of the reaction mixture resulting after treating **501** with 2.5 equivalents of $Na[B(3,5\text{–}C_6H_3(CF_3)_2)_4]$ in a 3:2 solvent mixture of toluene–d_8/1,2–difluorobenzene. Signals at δ 8.16 and δ 7.52 ppm correspond to the ortho and para hydrogen atoms on the $[B(3,5\text{–}C_6H_3(CF_3)_2)_4]^-$ anion respectively. Phenyl group resonances are obscured by solvent signals. *Protio* 1,2–difluorobenzene signals observed in the region between δ 6.5 and 7.0 ppm.

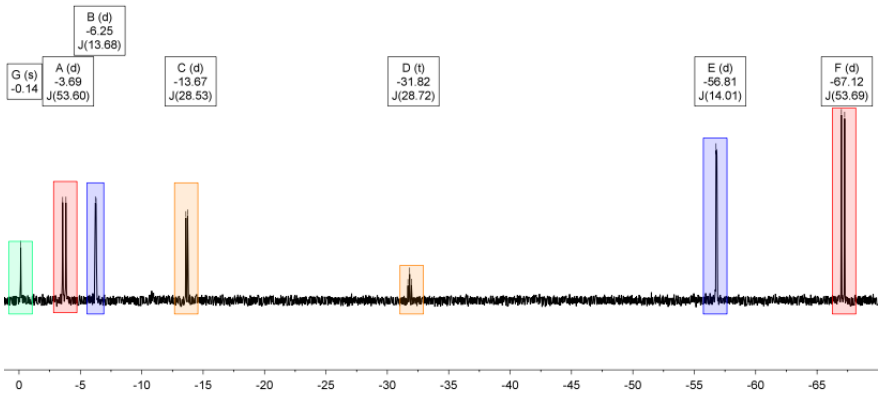

Figure 5–6. $^{31}P\{^{1}H\}$ NMR (202.27 MHz) spectrum of the reaction mixture resulting after treating **501** with 2.5 equivalents of Na[B(3,5-$C_6H_3(CF_3)_2)_4$] in a 3:2 solvent mixture of toluene-d_8/1,2-difluorobenzene. Signals highlighted in yellow, red, blue, and green boxes correspond to compounds **502a** at δ −13.67 and −31.82 ppm ($^{2}J_{P-P}$ = 28.7 Hz); 503–**1a** at δ −3.69 and −67.12 ($^{2}J_{P-P}$ = 53.6 Hz); 503–**2a** at δ −6.25 and −56.81 ($^{2}J_{P-P}$ = 14.0 Hz); **504** at *ca.* δ 0.0 ppm respectively.

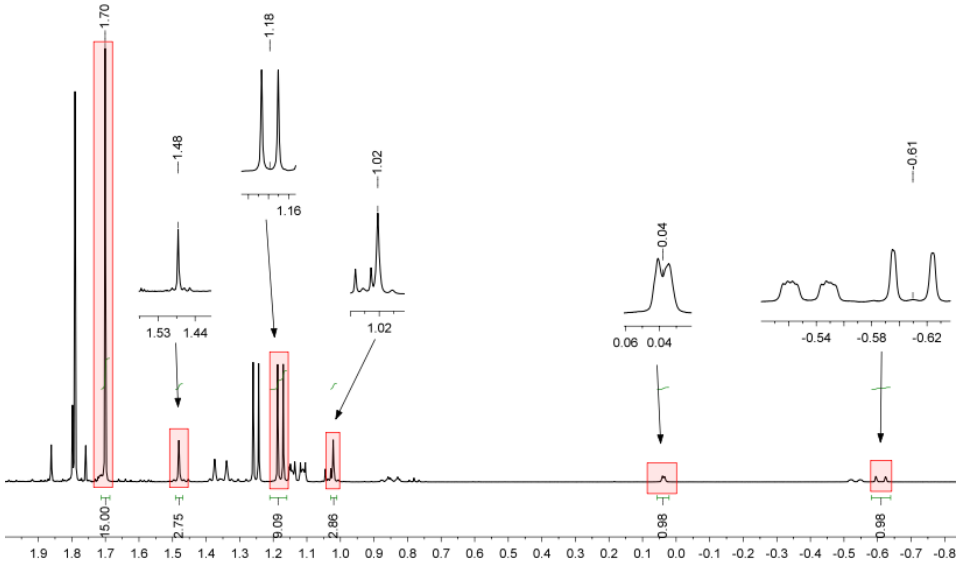

Figure 5–7. Aliphatic region of the ^{1}H NMR (499.43 MHz) spectrum, selectively decoupled from the ^{31}P NMR resonance at δ −67.12 ppm, of the reaction mixture resulting after treating **501** with 2.5 equivalents of Na[B(3,5-$C_6H_3(CF_3)_2)_4$] in a 3:2 solvent mixture of toluene-d_8/1,2-difluorobenzene. Signals highlighted in red boxes correspond to compound 503–**1a**. The decoupled ^{1}H NMR resonances, and the ^{31}P resonance at δ −67.12 ppm correspond to the cyclometalated PMe_3 ligand.

The assignment of the ^{1}H NMR signals for compounds **503–1a** and **503–2a** are shown in Figure 5–9 and 5–10 respectively.

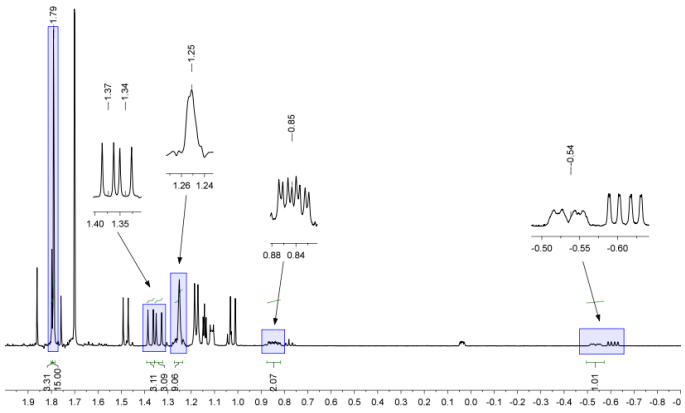

Figure 5–8. Aliphatic region of the ^{1}H NMR (499.43 MHz) spectrum, selectively decoupled from the ^{31}P NMR resonance at δ −6.25 ppm, of the reaction mixture resulting after treating **501** with 2.5 equivalents of Na[B(3,5–$C_6H_3(CF_3)_2)_4$] in a 3:2 solvent mixture of toluene–d_8/1,2–difluorobenzene. Signals highlighted in blue boxes correspond to compound **503–2a**. The decoupled ^{1}H NMR resonances, and the ^{31}P resonance at δ −6.25 ppm correspond to the non–cyclometalated PMe_3 ligand. Signal simplification of the ^{1}H NMR resonances at δ 0.85 and 0.54 ppm can be observed.

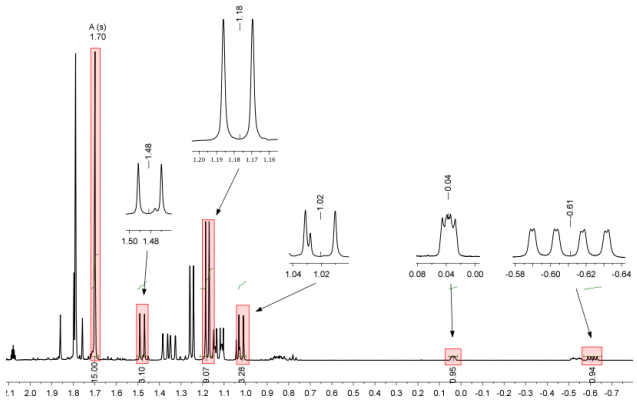

Figure 5–9. Aliphatic region of the ^{1}H NMR spectrum, selectively decoupled from the ^{31}P NMR resonance at δ −67.12 ppm, of the reaction mixture resulting after treating **501** with 2.5 equivalents of Na[B(3,5–$C_6H_3(CF_3)_2)_4$] in a 3:2 solvent mixture of toluene–d_8/1,2–difluorobenzene. Signals highlighted in red boxes correspond to compound **503–1a**. The decoupled ^{1}H NMR resonances, and the ^{31}P resonance at δ −67.12 ppm correspond to the cyclometalated PMe_3 ligand.

Cyclometalated compound 503–1a. ^{1}H NMR (499.43 MHz, toluene–d_8/1,2–difluorobenzene) δ 1.70 (s, 15H, Cp*–$(CH_3)_5$), 1.48 (d, 3H, $^{2}J_{H-P}$ = 10.9 Hz, activated $P(CH_3)_3$), 1.18 (d, 9H, $^{2}J_{H-P}$ = 8.3 Hz, non–activated $P(CH_3)_3$), 1.02 (d, 3H, $^{2}J_{H-P}$ = 10.5 Hz, activated $P(CH_3)_3$), 0.04 (m, 1H, activated $P(CH_3)_3$), −0.61 (ddd, 1H, *J* = 14.2 Hz, *J* = 6.7 Hz, *J* = 1.1 Hz, activated $P(CH_3)_3$). $^{31}P\{^{1}H\}$ NMR (202.27 MHz, toluene–d_8/1,2–difluorobenzene) δ −3.69 (d, $^{2}J_{P-P}$ = 53.6 Hz, activated $P(CH_3)_3$), −67.12 (d, $^{2}J_{P-P}$ = 53.7 Hz, non–activated $P(CH_3)_3$). ^{19}F NMR (470.17 MHz, toluene–d_8/1,2–difluorobenzene) δ −63.73 (C_{ar}–CF_3). $^{11}B\{^{1}H\}$ NMR (128.18 MHz, toluene–d_8/1,2–difluorobenzene) δ −6.4 (s, $[B(3,5\text{–}C_6H_3(CF_3)_2)_4]^-$).

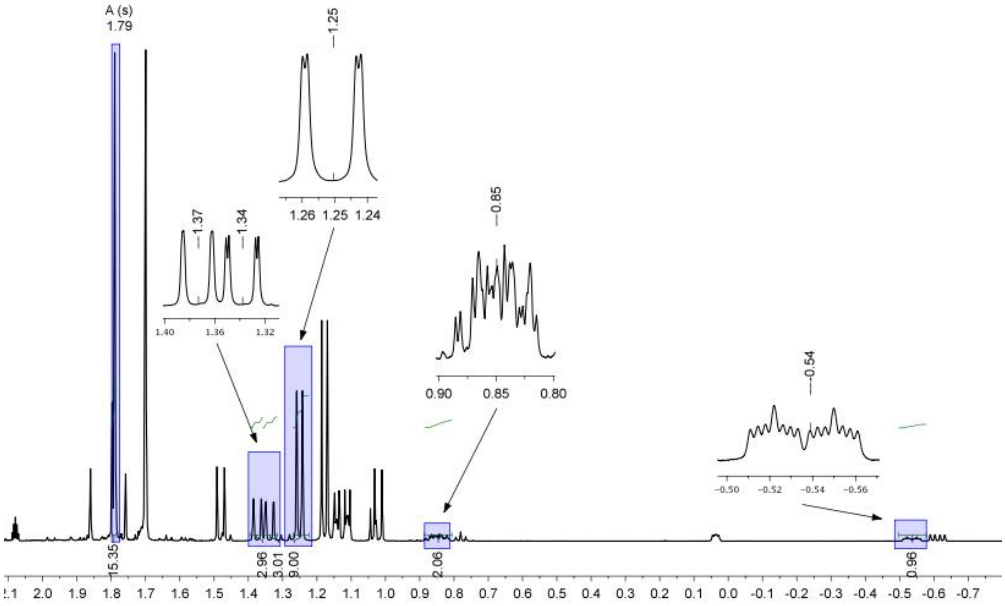

Figure 5–10. Aliphatic region of the ^{1}H NMR (499.43 MHz) spectrum of the reaction mixture resulting after treating **501** with 2.5 equivalents of $Na[B(3,5\text{–}C_6H_3(CF_3)_2)_4]$ in a 3:2 solvent mixture of toluene–d_8/1,2–difluorobenzene. Signals highlighted in blue boxes correspond to compound 503–**2a**.

Cyclometalated compound 503–2a. ^{1}H NMR (499.43 MHz, toluene–d_8/1,2–difluorobenzene) δ 1.79 (s, 15H, Cp*–(CH_3)$_5$), 1.37 (dd, 3H, J = 11.6 Hz, J = 0.9 Hz, activated P(CH_3)$_3$), 1.34 (dd, 3H, $^{2}J_{H-P}$ = 11.8 Hz, $^{4}J_{H-P}$ = 1.2 Hz, activated P(CH_3)$_3$),1.25 (dd, 9H, dd, $^{2}J_{H-P}$ = 8.2 Hz, $^{4}J_{H-P}$ = 0.8 Hz, non–activated P(CH_3)$_3$), 0.85 (m, 2H, activated P(CH_3)$_3$), −0.54 (dddd, 1H, J = 14.0 Hz, J = 5.6 Hz, J = 3.6 Hz, J = 1.8 Hz, activated P(CH_3)$_3$). ^{31}P{^{1}H} NMR (202.27 MHz, toluene–d_8/1,2–difluorobenzene) δ −6.25 (d, $^{2}J_{P-P}$ = 13.7 Hz, activated P(CH_3)$_3$), −56.81 (d, $^{2}J_{P-P}$ = 14.0 Hz, non–activated P(CH_3)$_3$). ^{19}F NMR (470.17 MHz, toluene–d_8/1,2–difluorobenzene) δ −63.73 ([B(C_6H_3(CF_3)$_2$)$_4$]$^-$) ^{11}B{^{1}H} NMR (128.18 MHz, toluene–d_8/1,2–difluorobenzene) δ −6.4 (s, [B(3,5–C_6H_3(CF_3)$_2$)$_4^-$]).

Chloride abstraction from 501 with 1.0 equivalents of Na[B(3,5–C_6H_3(CF_3)$_2$)$_4$]. 501 (32.0 mg, 54.0 μmol), Na[B(3,5–C_6H_3(CF_3)$_2$)$_4$] (49.0 g, 54.0 μmol) and 700 μL of a 3:2 toluene–d_8/1,2–difluorobenzene solvent mixture were charged in a J. Young NMR tube and shaken vigorously for 1 min. Solids were allowed to sediment and NMR spectra were collected (Figure 5–11, and 5–12). A mixture of compounds can be observed, as described above.

Chloride abstraction from 501 with 1.0 equivalent of Na–108. 501 (22.0 mg, 37.0 μmol), **Na–108** (20.0 mg, 37.0 μmol) and 700 μL of a 3:2 toluene–d_8/1,2–difluorobenzene solvent mixture were charged in a J. Young NMR tube and shaken vigorously for 1 min. Solids were allowed to sediment and NMR spectra were collected. A mixture of compounds

identical to that described above was observed by ^{1}H (Figure 5–13 and Figure 5–14), and $^{31}P\{^{1}H\}$ (Figure 5–15) NMR spectroscopies. The ^{13}C NMR spectrum of the reaction mixture revealed two downfield resonances, one at δ 234.6 (d, $^{1}J_{C-H_{\alpha}}$ = 77.6 Hz), and another at δ 244.7 (d, $^{1}J_{C-H_{\alpha}}$ = 76.6 Hz) ppm, consistent with the agostic, "distorted" Ta=CH moieties, one for each cyclometalated isomer **503**–1b, and **503**–2b (Figure 5–16). These resonances were not assigned to their respective isomers.

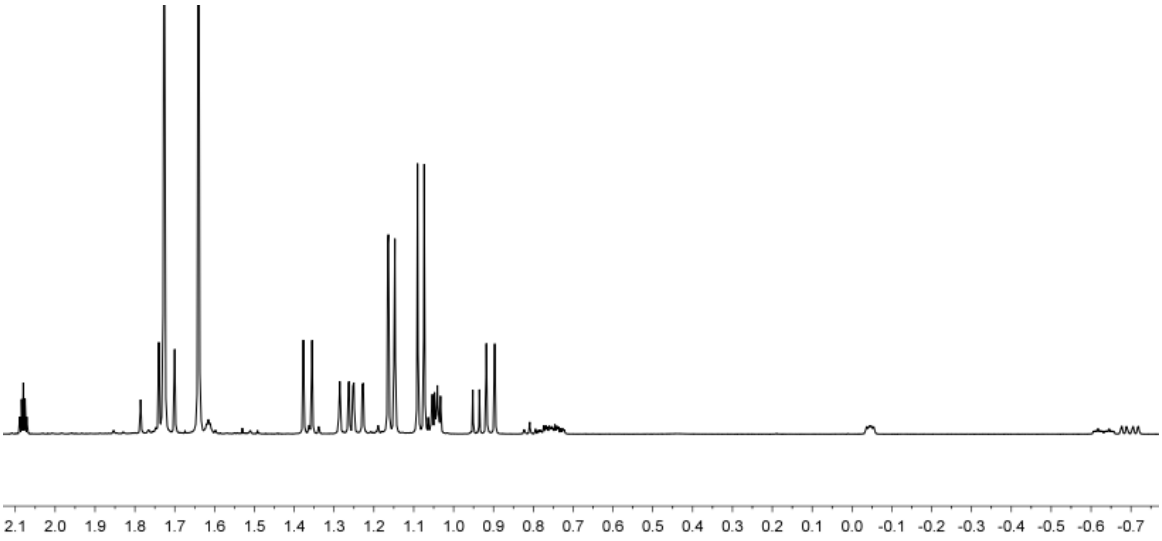

Figure 5–11. Aliphatic region of the ^{1}H NMR (499.43 MHz) spectrum of the reaction mixture resulting after treating **501** with 1.0 equivalent of $Na[B(3,5\text{–}C_6H_3(CF_3)_2)_4]$ in a 3:2 solvent mixture of toluene–d_8/1,2–difluorobenzene.

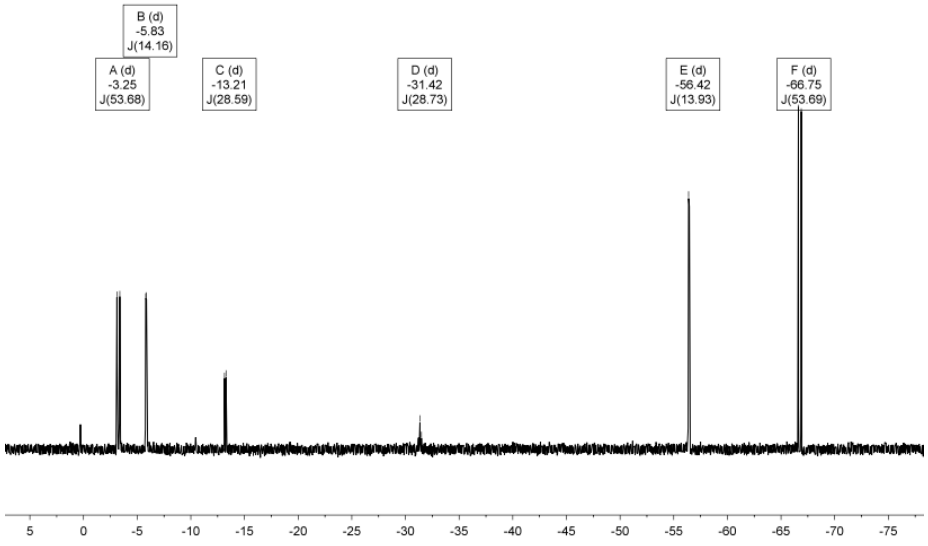

Figure 5–12. $^{31}P\{^{1}H\}$ NMR (202.27 MHz) spectrum of the reaction mixture resulting after treating **501** with 1.0 equivalents of $Na[B(3,5\text{–}C_6H_3(CF_3)_2)_4]$ in a 3:2 solvent mixture of toluene–d_8/1,2–difluorobenzene.

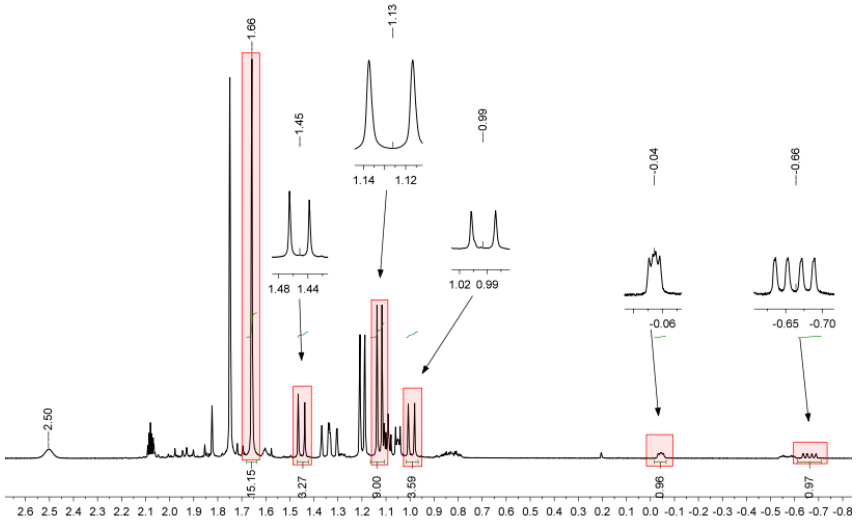

Figure 5–13. Aliphatic region of the ^{1}H NMR spectrum (399.52 MHz) of the reaction mixture resulting after treating **501** with 1.0 equivalents of **Na–108** in a 3:2 solvent mixture of toluene–d_8/1,2–difluorobenzene. Signals highlighted in blue boxes correspond to cyclometalated compound 503–**1b**. Signal at δ 2.50 ppm corresponds to **108**.

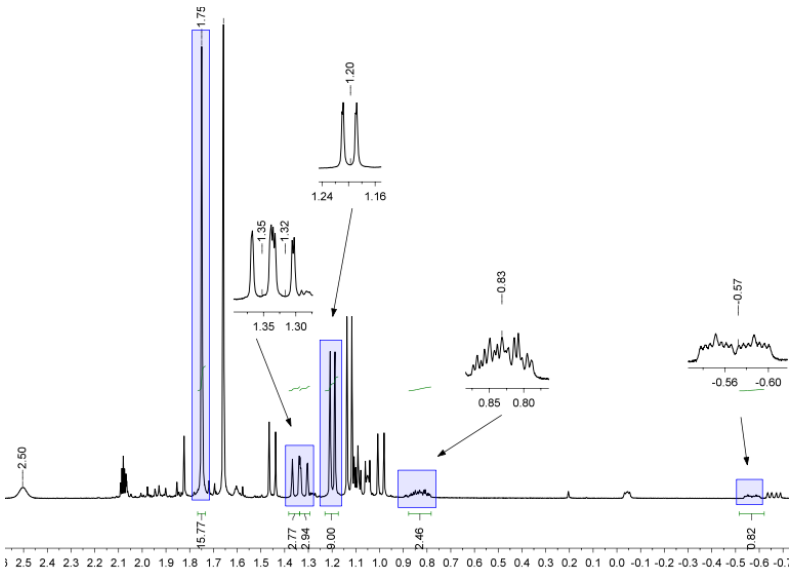

Figure 5–14. Aliphatic region of the ^{1}H NMR spectrum (399.52 MHz) of the reaction mixture resulting after treating **501** with 1.0 equivalents of **Na–108** in a 3:2 solvent mixture of toluene-d_8/1,2-difluorobenzene. Signals highlighted in blue boxes correspond to cyclometalated compound 503–**2b**. Signal at δ 2.50 ppm corresponds to **108**.

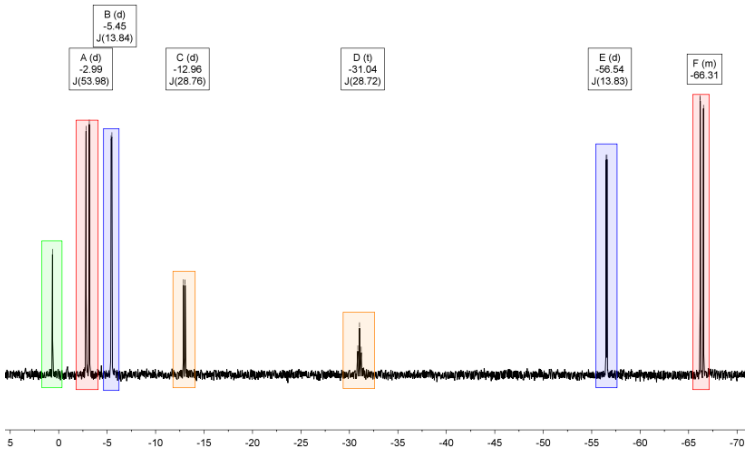

Figure 5–15. ^{31}P{^{1}H} NMR spectrum (161.73 MHz) of the reaction mixture resulting after treating **501** with 1.0 equivalents of **Na–108** in a 3:2 solvent mixture of toluene-d_8/1,2-difluorobenzene. Signals highlighted in blue, red, yellow and green boxes correspond respectively to compounds **502b** at δ −12.96 and −31.04 ppm ($^{2}J_{P-P}$ = 28.8 Hz); 503–**1b** at δ −2.99 and −66.31 ($^{2}J_{P-P}$ = 54.0 Hz); 503–**2b** at δ −5.45 and −56.54 ($^{2}J_{P-P}$ = 13.8 Hz); **504** at δ 0.64 respectively.

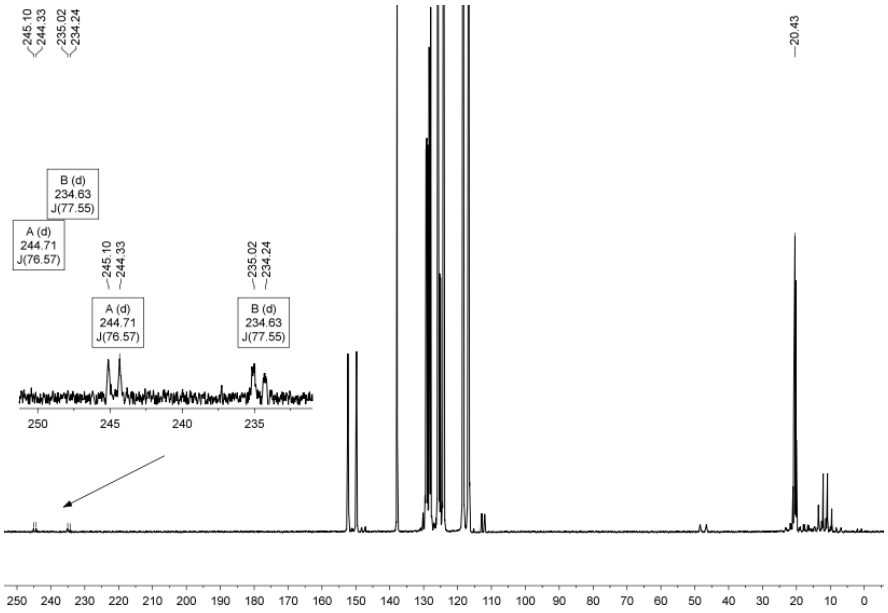

Figure 5–16. ^{13}C NMR spectrum (100.46 MHz) of the reaction mixture resulting after treating **501** with 1.0 equivalents of **Na–108** in a 3:2 solvent mixture of toluene–d_8/1,2–difluorobenzene. Two resonances at δ 234.6 (d, $^1J_{C-H_\alpha}$ = 77.6 Hz) and 244.7 (d, $^1J_{C-H_\alpha}$ = 76.6 Hz) ppm, consistent with agostic, "distorted" Ta=CH moieties.

Mass balance after chloride abstraction from 501. Compound **501** (26.0 mg, 45.0 μmol), $[P(C_6H_4)_4][B(3,5–C_6H_3(CF_3)_2)_4]$ (54.0 mg, 44.5 μmol), and $Na[B(3,5–C_6H_3(CF_3)_2)_4]$ (40.0 mg, 45.0 μmol) and 700 μL of a 3:2 toluene–d_8/1,2–difluorobenzene solvent mixture were charged in a J. Young NMR tube and shaken vigorously for 1 min. Solids were allowed to sediment and NMR spectra were collected (Figure 5–17). Once the spectra were collected, P(CH3)3 (15.0 μL, 135.6 μmol) was added, and spectra were collected again (Figure 5–18).

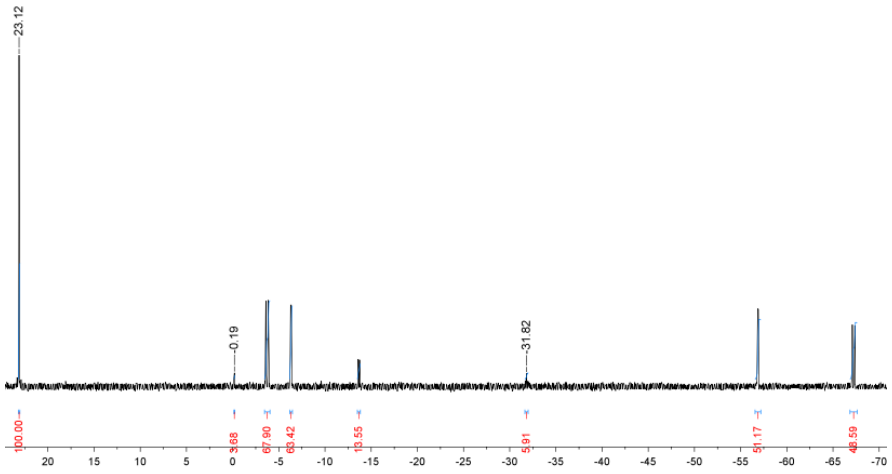

Figure 5–17. $^{31}P\{^{1}H\}$ NMR (202.27 MHz) spectrum of the reaction mixture obtained after treating **501** with 1.0 equivalents of $Na[B(3,5\text{–}C_6H_3(CF_3)_2)_4]$. Signal at δ 23.12 ppm corresponds to $[PPh_4]^+$, used as an integration standard. Signal at δ –0.19 ppm corresponds to **504**. Integral ratio $([PPh_4]^+)/(\mathbf{504})$ = 25.4.

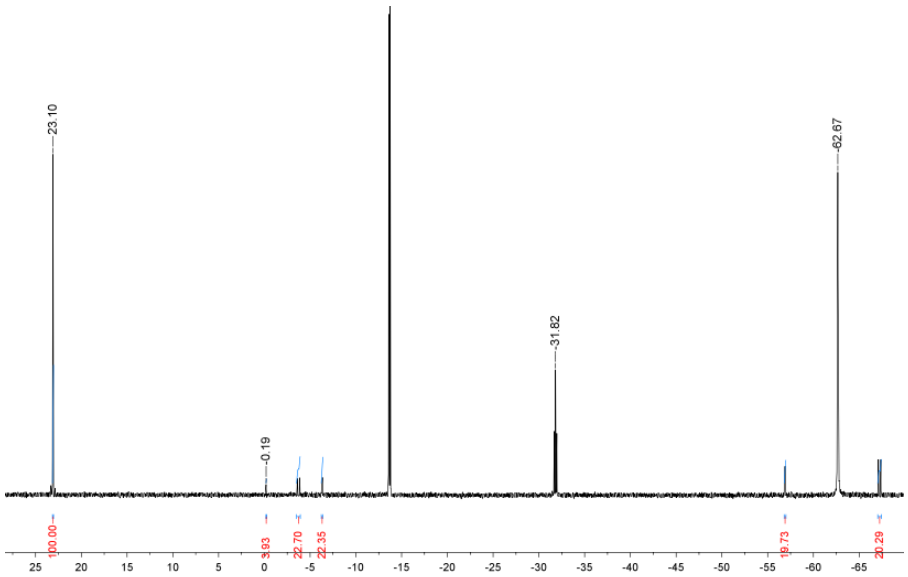

Figure 5–18. $^{31}P\{^{1}H\}$ NMR (202.27 MHz) spectrum of the reaction mixture obtained after adding excess PMe_3 to the reaction mixture shown in Figure 5–17. The intensity of the signal at δ –0.19 ppm did not change after addition of PMe_3, suggesting that its formation is not reversible. The signals corresponding to the cyclometalated compounds decreased in intensity, as they were trapped by PMe_3. Signal at δ –62.7 ppm corresponds to free excess PMe_3. Integral ratio $([PPh_4]^+)/(\mathbf{504})$ = 25.4.

5.4.2.2 Trapping of 503–1 and 503–2 with PMe_3 and abstraction of PMe_3 from 502

Trapping of 503a with PMe_3. 501 (118.0 mg, 198.7 μmol), $Na[B(3,5\text{–}C_6H_3(CF_3)_2)_4]$ (176.0 mg, 199.0 μmol) and 2.0 mL of a 3:2 toluene–d_8/1,2–difluorobenzene solvent mixture were charged in a round bottom flask equipped with a PTFE valve and a magnetic stir bar. The contents were stirred vigorously for 1 min. To this mixture, PMe_3 (60.0 μL, 58.0 mmol) was added in a single portion with a Hamilton syringe and the flask was placed overnight in an oil bath set to 45 °C. Volatiles were removed *in vacuo*, the residue was dissolved in fluorobenzene and filtered through a fritted funnel protected with Celite, and the mother liquor was concentrated to around 1.5 mL *in vacuo* and then transferred to a glass vial. This solution was layered with approximately 3 mL of toluene and placed in a freezer at −35 °C to obtain a large, amber–colored crystal. Yield: 0.25g (84%) ^{1}H NMR (499.43 MHz, toluene–d_8/1,2–difluorobenzene) δ 1.11 (filled–in doublet, 18H, *transoid* $P(CH_3)_3$), 1.14 (d, 9H, cis $P(CH_3)_3$), 1.79 (s, 15H, $C_5(CH_3)_5$). $^{31}P\{^1H\}$ NMR (202.27 MHz, toluene–d_8/1,2–difluorobenzene) δ −13.7 (d, $^2J_{P\text{–}P}$ = 28.5 Hz), −31.8 (t, $^2J_{P\text{–}P}$ = 28.5 Hz). $^{13}C\{^1H\}$ NMR (125.65 MHz, toluene–d_8/1,2–difluorobenzene) δ 12.7 (m, $P(CH_3)_3$), 22.4 (m, $P(CH_3)_3$), 111.9 (s, $C_5(CH_3)_5$) , 118.2 (s, $C_5(CH_3)_5$), 122.2 (–C_6H_5), 124.4 (–C_6H_5), 126.5 (–C_6H_5), 128.7 (–C_6H_5), 365.6 (dt, $^2J_{C\text{–}P}$ = 29.9 Hz, $^2J_{C\text{–}P}$ = 9.2 Hz, Ta≡C). ^{19}F NMR (125.65 MHz, toluene–d_8/1,2–difluorobenzene) δ −63.35 (s, $[B(3,5\text{–}C_6H_3(CF_3)_2)_4]$). Elemental analysis. Calculated for $C_{58}H_{59}BF_{24}P_3Ta$: C, 46.54%; H, 3.97%. Found: C, 46.50%; H, 4.00%.

Observation of loss of PMe_3 from 502a in solution. Pure **502a** (26.0 mg, 17.0 μmol) was charged in a J. Young NMR tube, and dissolved in *ca.* 700 μL of a solvent mixture of toluene–d_8/1,2–difluorobenzene 3:1 and a ^{1}H NMR spectrum was collected (Figure 5–19). It was observed, given the integral ratios of free PMe_3 and remaining compound **502** in solution, that loss of 1.0 equivalents of PMe_3 had taken place, concomitant with formation of the cyclometalated species **503–1a** and **503–2a**. To this mixture, excess PMe_3 (10.0 μL, 97.3 μmol) was added with a Hamilton microliter syringe in a single portion, the contents were thoroughly mixed and a ^{1}H NMR spectrum was collected (Figure 5–20). Mostly compound **502**, and excess PMe_3 could be observed. Broadening of the signal of free PMe_3, observed at δ 0.79 ppm, suggests rapid exchange in the NMR time scale.

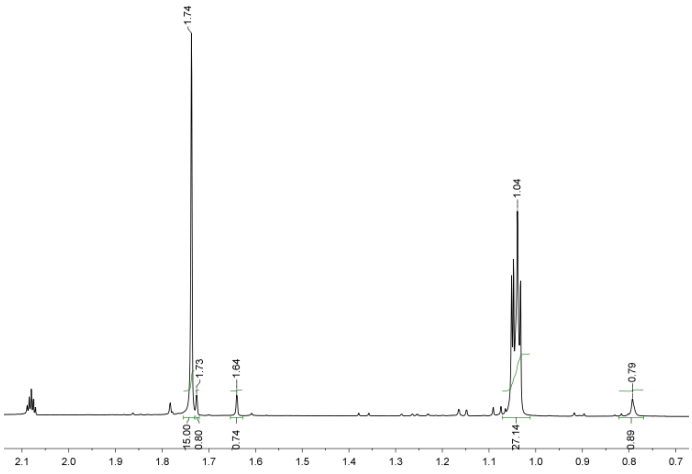

Figure 5–19. ^{1}H NMR spectrum (499.43 MHz) in a 3:2 solvent mixture of toluene–d_8/1,2–difluorobenzene of the isolated and crystallized **502a**. The resonance at δ 0.79 ppm corresponds to free PMe_3 that is lost when this compound goes in solution. The signals at δ1.64 and 1.73 ppm correspond to the Cp* resonances of compounds **503–1a** and **503–2a**. The ratio of integrals of these signals is consistent with the loss of 1.0 equivalents of PMe_3. (502a–Cp*)/(Free PMe_3) = 16.7.

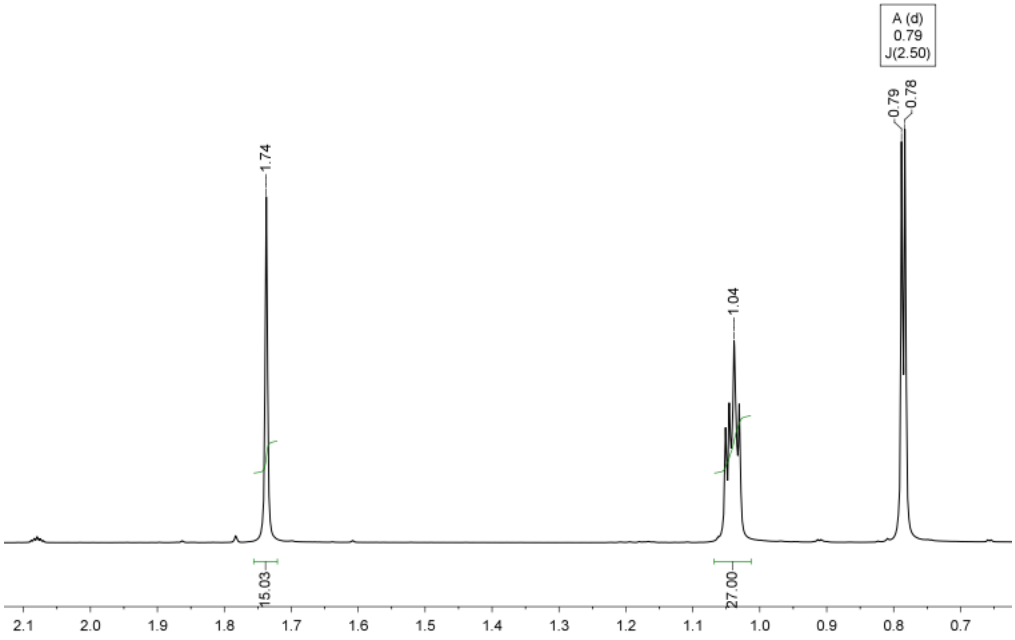

Figure 5–20. ^{1}H NMR spectrum (499.43 MHz) in a 3:2 solvent mixture of toluene–d_8/1,2–difluorobenzene of the same sample of **502a** (26.0 mg, 17.0 μmol) shown in Figure 5–19 after **Figure 5–20.** (Continued) addition of addition of a large excess of PMe_3 (10.0 μL, 97.3 μmol) at room temperature, displacing the equilibrium towards **502a**. The resonance at δ 0.79 ppm corresponds to free PMe_3.

Formation of 503–1a and 503–2a by abstraction of PMe_3 from 502a. Compound **502a** (13.4 mg, 9.0 μmol) was charged in a J. Young tube and was dissolved in *ca.* 700 μL of a 3:2 solvent mixture of toluene–d_8/1,2–difluorobenzene. To this solution, 40.0 μL (9.0 μmol) of a 44.8 mM solution of $B(C_6F_5)_3$ in 3:2 toluene–d_8/1,2–difluorobenzene were added via a Hamilton microliter syringe, with precipitation of the Me_3P–$B(C_6F_5)_3$ adduct observed a few seconds thereafter. NMR spectra were collected once all solid particles had sedimented. By $^{31}P\{^{1}H\}$ (202.27 MHz) NMR it can be observed quantitative formation of only the two sets of isomer resonances the products of PMe_3 cyclometalation at δ –6.21 and –56.81 ppm ($^{2}J_{P-P}$ =

13.9 Hz), and at δ –3.63 and –67.11 ppm ($^2J_{P-P}$ = 53.7 Hz). To the resulting mixture, an additional portion of 40 μL (9.0 μmol) of the 44.8 mM solution of $B(C_6F_5)_3$ was added, and NMR spectra were collected. No further changes to the mixture were observed by $^{31}P\{^1H\}$ (202.27 MHz) NMR spectroscopy.

5.4.2.3 Hydrolysis experiment

Attempted hydrolysis of a mixture of 502, 503.1, and 503.2. Compound **501** (50.8 mg, 85.7 μmol), $Na[HCB_{11}Cl_{11}]$ (50.5 mg, 91.8 μmol), and *ca.* 700 μL of a 3:2 solvent mixture of toluene–d_8/1,2–difluorobenzene were charged in a J. Young tube. The contents were shaken vigorously. To this mixture, increasing amounts of a saturated solution of water in 1,2–orthodifluorobenzene were added by subsequent additions to the reaction mixture via a Hamilton syringe, in the following order: **1.** 22.0 μL; **2.** 22.0 μL; **3.** 50.0 μL; **4.** 200.0 μL; **5.** 200.0 μL; **6.** 200.0 μL. Addition of water did not result in the production of **504** (Figure 5–21). Free PMe_3 can be observed at δ –62.5 ppm.

Treatment of a mixture of 502a, 503–1a, and 503–2a with 1–hexyne. 501 (0.029 g, 0.056 mmol), $Na[B(3,5\text{–}C_6H_3(CF_3)_2)_4]$ (0.120 g, 0.106 mmol) and a 3:2 solvent mixture of toluene–d_8/1,2–difluorobenzene were charged in a J. Young tube, and the contents vigorously shaken for 1 min. To this suspension, 1–hexyne (7.0 μL, 0.060 μmol) was added. The NMR tube was sealed and placed overnight in an oil bath set to 40 °C. Volatiles were removed *in vacuo*, redissolved in more toluene–d_8/1,2–difluorobenzene mixture and NMR spectra were

collected. The ^{1}H NMR spectrum revealed the formation of a mixture of compounds that included **502** and **504**, and at least four more products that could not be identified. In the ^{1}H NMR spectrum a signal at δ 10.85 (t, J = 1.2 Hz) ppm could be observed, while the ^{13}C{^{1}H} NMR spectrum revealed downfield signals at δ −240.9 and −229.7 ppm. These observations are consistent with the formation of a *protio* metallacyclobutadiene. The third metallacyclic resonance could not be distinguished from neighboring signals in the ^{13}C{^{1}H} NMR spectrum. No formation of diphenylacetylene (metathesis product) could be detected.

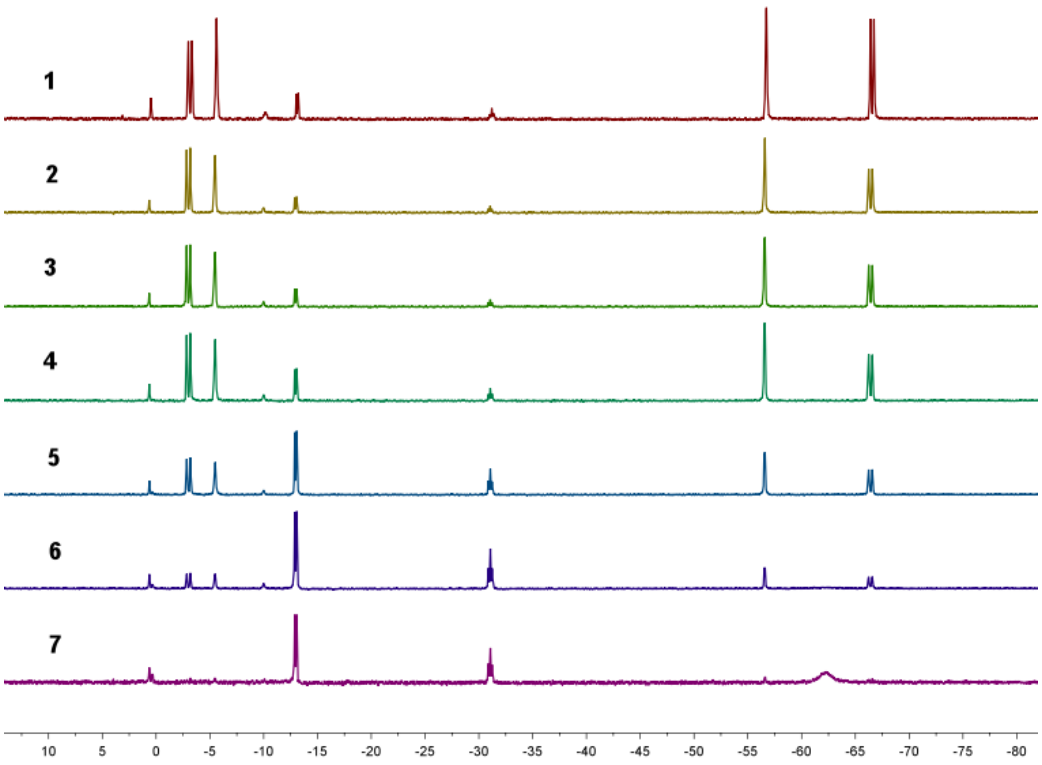

Figure 5–21. ^{31}P{^{1}H} NMR spectra (202.27 MHz) of the reaction mixture obtained after subsequent additions of a saturated solution of water in 1,2–difluorobenzene.

5.4.2.4 Cationic metallacyclobutadienes

Synthesis of 511b. Compound **501** (0.135 g, 0.258 mmol), **Na–108** (0.141 g, 0.258 mmol) and 5.0 mL of a 3:2 solvent mixture of toluene–d_8/1,2–difluorobenzene were charged in a Schlenk flask equipped with a stir bar. This mixture was stirred for 10 min. and at this point 3–hexyne (34.0 μL, 0.30 mmol) was added in a single portion using a Hamilton syringe. The flask was placed overnight in an oil bath set to 40 °C. Volatiles were removed *in vacuo* to obtain an oily residue that was dissolved in fluorobenzene, filtered through a fine fritted funnel protected with Celite. The filtrate was dried *in vacuo* to obtain a residue that was triturated in pentane and dried *in vacuo* to obtain a dark yellow–brown powder. Yield 0.19 g (68%) ^{1}H NMR (499.43 MHz, toluene–d_8/1,2–difluorobenzene) δ 0.75 (t, $^3J_{H-H}$ = 7.6 Hz, 3H, –CH_2–CH_3), 0.83 (d, $^2J_{P-H}$ = 9.3 Hz, 9H, P(CH_3)$_3$), 1.24 (t, $^3J_{H-H}$ = 7.4 Hz, 3H, –CH_2–CH_3), 1.69 (s, 15H, $C_5(CH_3)_5$), 2.47 (broad, 1H, $HCB_{11}Cl_{11}^-$), 3.06 (ABX$_3$ system, calculated coupling constants (using MestReNova™ version 8.1.2): $\Delta\nu_{A-B}$ = 6.9 Hz, $^2J_{AB}$ = −10.5 Hz, $^3J_{AM}$ = $^3J_{BM}$ = 7.7 Hz, J_{AX} = 3.6 Hz, J_{BX} = 2.5 Hz), 3.45 (ABM$_3$X system, calculated coupling constants (using MestReNova™ version 8.1.2): $\Delta\nu_{A-B}$ = 6.9 Hz, $^2J_{H-H}$ = −10.5 Hz, $^3J_{H-H}$ = 7.7 Hz, J_{H-P} = 3.6 Hz, J_{H-P} = 2.5 Hz, 2H, –CH_2–CH_3). ^{31}P{^{1}H} NMR (202.27 MHz, toluene–d_8/1,2–difluorobenzene) δ −2.81. ^{13}C{^{1}H} NMR (100.8 MHz, toluene–d_8/1,2–difluorobenzene) δ 10.9 (s, $C_5(CH_3)_5$), 14.2 (s, –CH_2–CH_3), 17.2 (d, $^1J_{C-P}$ = 31.4 Hz, P(CH_3)$_3$), 17.6 (s, –CH_2–CH_3), 27.1 (s, –CH_2–CH_3) 31.9 (–CH_2–CH_3), 47.5 (b, [$HCB_{11}Cl_{11}$]$^-$), 170.7 (s, metallayclic C), 236.2 (d, J_{C-P} = 3.7 Hz, metallacyclic C), 240.8 (d J_{C-P} = 2.9 Hz metallacyclic C). C(CH_3)$_5$ and–C_6H_5 signals obscured by residual solvent resonances.

Attempted cross–metathesis reaction between phenylacetylene and 3–hexyne in a mixture of 502, 503–1, and 503–2. Compound **501** (0.005 g, 0.01 mmol), Na[B(3,5–$C_6H_3(CF_3)_2)_4$] (0.009 mg, 0.01 mmol) and a 3:2 solvent mixture of toluene–d_8/1,2–difluorobenzene were charged in a J. Young tube, and the contents vigorously shaken for 1 min. To this suspension, 50.0 μL of a mixture of 3–hexyne and diphenylacetylene in toluene–d_8/1,2–difluorobenzene was added (22.0, and 25.0 μmol of each alkyne respectively), the tube was sealed and then placed for 7 h in an oil bath set to 50 °C. NMR spectra were collected after this period, revealing the formation of **511a** exclusively.

Treatment of a mixture of 502a, 503–1a, and 503–2a with phenylacetylene. Compound **501** (0.032 g, 0.054 mmol), Na[B(3,5–$C_6H_3(CF_3)_2)_4$] (0.049 g, 0.054 mmol) and a 3:2 solvent mixture of toluene–d_8/1,2–difluorobenzene were charged in a J. Young tube, and the contents vigorously shaken for 1 min. To this suspension, phenylacetylene (9.0 μL, 0.081 mmol) was added. The NMR tube was sealed and then placed in an oil bath set at 45 °C overnight. Volatiles were removed *in vacuo*, more solvent mixture and phenylacetylene (9.0 μL, 0.081 mmol) were added and the tube was placed overnight in the oil bath set at 45 °C. The next morning, NMR spectra were collected. The $^{31}P\{^1H\}$ NMR spectrum revealed the presence of a set of two doublets at δ 6.74 and δ −2.08 ppm with $^2J_{P-P}$ = 4.9 Hz, and a singlet at δ 2.24 ppm. Signals consistent with the formation of a protio metallacyclobutadiene can be observed by ^1H NMR at δ 10.85 ppm, and by $^{13}C\{^1H\}$ NMR spectroscopy at δ 194.8 ppm, 202.8 and 214.8 ppm. HMBC and HSQC NMR correlation experiments confirmed that

these atoms belong to the same structural unit (Figure 5–22). These spectral data are consistent with formation of a protiometallacyclobutadiene. Formation of the metathesis product (diphenylacetylene), could not be detected by NMR multinuclear spectroscopy, or GC–MS.

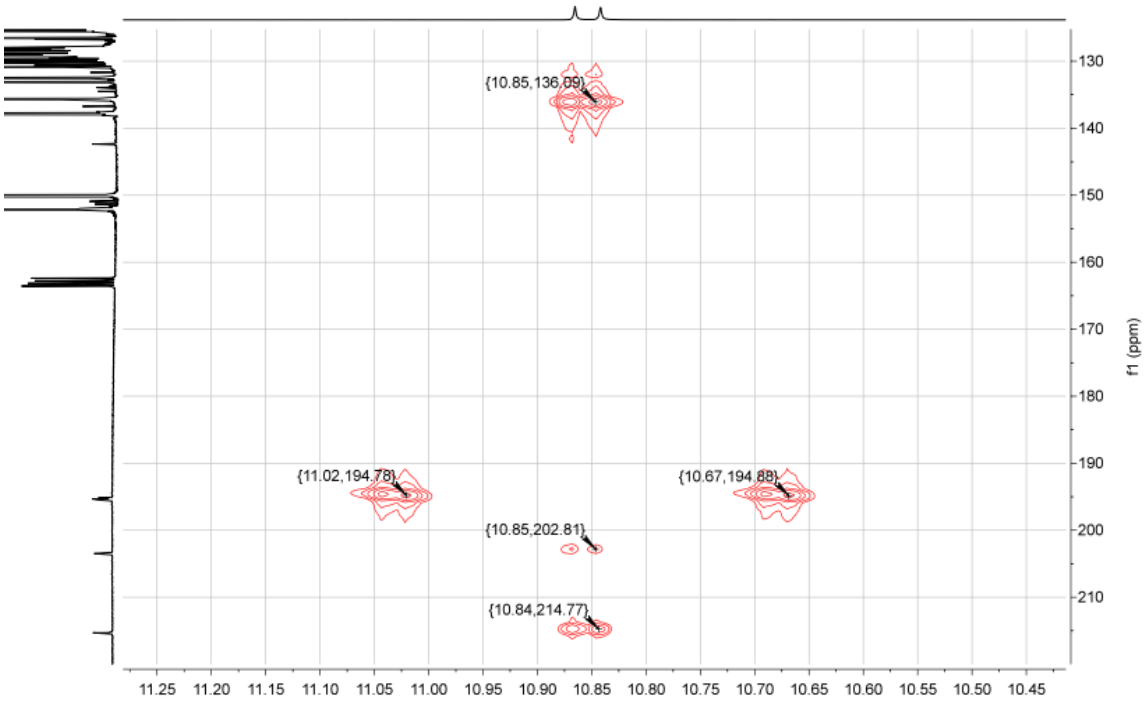

Figure 5–22. ^{1}H–^{13}C HMBC NMR spectrum in a 3:2 solvent mixture of toluene–d_8/1,2–difluorobenzene of the reaction mixture formed after treating **501** (0.032 g, 0.054 mmol) with Na[B(3,5–$C_6H_3(CF_3)_2)_4$] (0.049 g, 0.054 mmol) and phenylacetylene (9.0 μL, 0.081 mmol). The $^{1}J_{C\text{-}H_\alpha}$ = 176.2 Hz and $J_{P\text{-}H}$ = 11.6 Hz coupling constants can be observed. Correlation between all the metallacyclic carbon atoms (δ 194.8, 202.8, and 214.8 ppm), and the ^{1}H NMR resonance at δ 10.85 ppm can be observed, indicating that all four atoms belong to the same structural unit.

5.4.2.5 Other reactions with mixtures of 502, 503–1, and 503–2

Acetonitrile adduct of 503a. Compound **501** (0.020 g, 0.038 μmol), Na[B(3,5–$C_6H_3(CF_3)_2)_4$] (0.085 mg, 0.096 mmol) and a 3:2 solvent mixture of toluene–d_8/1,2–difluorobenzene were charged in a J. Young tube, and the contents vigorously shaken for 1 min. To this suspension, acetonitrile (5.0 μL, 0.077 μmol) was added using a Hamilton syringe. Formation of the corresponding cationic acetonitrile adduct was observed. ^{1}H NMR (399.52 MHz, toluene–d_8/1,2–difluorobenzene) δ 1.08 (filled–in doublet, 18H, P(CH_3)$_3$), 1.09 (s, 3H, NC–CH_3), 1.78 (s, 15H, C_5(CH_3)$_5$), 7.56 (s, [B(3,5–$C_6H_3(CF_3)_2)_4$]$^-$), 8.20 (s, [B(3,5–$C_6H_3(CF_3)_2)_4$]$^-$). ^{31}P{^{1}H} (121.42 MHz, toluene–d_8/1,2–difluorobenzene) δ 1.75 (s, *transoid* P(CH_3)$_3$). ^{19}F NMR, (470.17 MHz, toluene–d_8/1,2–difluorobenzene) δ −63.5 (s, –CF_3). ^{13}C{^{1}H} NMR (100.46 MHz, toluene–d_8/1,2–difluorobenzene) δ 361.0 (t, $^2J_{C-P}$ = 25.4 Hz, Ta≡C).

Treatment of a mixture of 502a, 503–1a, and 503–2a with *trans*–2–pentene. 501 (0.032 g, 0.062 mmol), Na[B(3,5–$C_6H_3(CF_3)_2)_4$] (0.136 g, 0.150 mmol) and a 3:2 solvent mixture of toluene–d_8/1,2–difluorobenzene were charged in a J. Young NMR tube, and the contents vigorously shaken for 1 min. To this suspension, *trans*–2–pentene (8.0 μL, 0.074 mmol) was added using a Hamilton syringe. The NMR tube was sealed and placed overnight in an oil bath set to 45 °C. Only the formation of a mixture of products from chloride abstraction is observed. There is no indication of formation of a metallacyclobutene, or coordination of the alkene to tantalum.

5.4.2.6 Neutral metallacyclobutadienes

Observation of 514. 501 (0.136 g, 0.260 mmol) and 5.0 mL of a 3:2 solvent mixture of toluene–d_8/1,2–difluorobenzene were charged in a Schlenk flask equipped with a stir bar. To this solution, trimethylsilyl acetylene (57.0 μL, 40.0 μmol) was added with a Hamilton syringe, and the flask was placed overnight in an oil bath set to 40 °C, then the volatiles were removed *in vacuo*. This procedure was repeated twice more to obtain a dark, thick oil that is very soluble in non–polar solvents. Yield: 0.108 g (*ca.* 70% purity by ^{1}H NMR spectroscopy). ^{1}H NMR (499.43 MHz, C_6D_6) δ 0.29 (t, $^2J_{Si-H}$ = 6.6 Hz, 9H, –Si(CH_3)$_3$), 1.88 (s, 15H, $C_5(CH_3)_5$), 6.96 (m, 1H, –C_6H_5), 7.26 (m, 2H, –C_6H_5), 7.33 (m, 2H, –C_6H_5), 10.7 (s, $^3J_{Si-H}$ = 7.6 Hz 1H, metallacyclic C–H). ^{13}C NMR (125.58 MHz, C_6D_6) δ1.9 (q, $^1J_{C-H}$ = 118.9 Hz, Si(CH_3)$_3$), 11.5 (q, $^1J_{C-H\alpha}$ = 127.5 Hz, $C_5(CH_3)_5$), 115.4 (s, $C_5(CH_3)_5$), 142.3 (s, metallacyclic $C_{\alpha'}$), 146.5 (d, $^1J_{C-H\alpha}$ = 187.1 Hz, metallacyclic C_β), 207.8 (s, metallacyclic C_α). The aromatic resonances overlapped with the residual solvent peaks.

Observation of 515. Compound **501** (0.040 g, 0.077 mmol) was charged in a J. Young NMR tube and dissolved in a 3:2 mixture of toluene-d_8/1,2-difluorobenzene. To this solution, 3–hexyne (9.0 μL, 0.080 mmol) was added using a Hamilton syringe. The NMR tube was placed overnight in a heat bath set to 40 °C. Volatiles were removed *in vacuo*, more toluene-d_8/1,2-difluorobenzene mixture and 9.0 μL of 3–hexyne were added. This process was repeated twice more. Formation of a neutral metallacyclobutadiene can be observed by ^{1}H NMR, with no cycloreversion to alkyne metathesis products. ^{1}H NMR (499.43 MHz, C_6D_6) δ

0.85 (t, $^3J_{H-H}$ = 7.5 Hz, 3H, –CH_2–CH_3), 1.41 (t, $^3J_{H-H}$ = 7.4 Hz, 3H, –CH_2–CH_3), 1.87 (s, 5H, $C_5(CH_3)_5$), 3.11 (ABX_3 system, calculated coupling constants (using MestReNova™ version 8.1.2): $^3J_{H-H}$ = 7.4 Hz, $^2J_{H-H}$ = −15.9 Hz, 1H, –CH_2–CH_3), 3.26 (ABX_3 system, calculated coupling constants (using MestReNova™ version 8.1.2): $^2J_{H-H}$ = −15.9 Hz, $^3J_{H-H}$ = 7.5 Hz, 1H, –CH_2–CH_3), 3.39 (ABX_3 system, calculated coupling constants (using MestReNova™ version 8.1.2): $^2J_{H-H}$ = −11.5 Hz, $^3J_{H-H}$ = 7.6 Hz, 1H, –CH_2–CH_3), 3.57 (ABX_3 system, calculated coupling constants (using MestReNova™ version 8.1.2): $^2J_{H-H}$ = −11.5 Hz, $^3J_{H-H}$ = 7.4 Hz, 1H, –CH_2–CH_3), 7.02 (tt, $^3J_{H-H}$ = 7.4 Hz, $^4J_{H-H}$ = 1.3 Hz, 1H, *para* C–H), 7.09 (dd, $^3J_{H-H}$ = 8.3 Hz, $^4J_{H-H}$ = 1.2 Hz, 1H, *ortho* C–H), 7.27 (dd, $^3J_{H-H}$ = 8.2 Hz, $^3J_{H-H}$ = 7.5 Hz, 1H, *meta* C–H).

^{1}H NMR (499.43 MHz, toluene-d_8/1,2-difluorobenzene) δ0.88 (t, 3H, $^3J_{H-H}$ = 7.5 Hz, –CH_2–CH_3), 1.35 (t, $^3J_{H-H}$ = 7.5 Hz, –CH_2–CH_3), 1.84 (s, 15H, C_5–$(CH_3)_5$), 3.13 (ABX_3 multiplet, 1H, –CH_2–CH_3), 3.29 (ABX_3 multiplet, 1H, –CH_2–CH_3), 3.42 (ABX_3 multiplet, 1H, –CH_2–CH_3), 3.59 (ABX_3 multiplet, 1H, –CH_2–CH_3). Aromatic resonances eclipsed by solvent signals.^{13}C{^{1}H} NMR (125.58 MHz, toluene-d_8/1,2-difluorobenzene) δ11.1 (s, C_5–$(CH_3)_5$), 14.8 (s, –CH_2–CH_3), 17.5 (s, –CH_2–CH_3), 25.3 (s, –CH_2–CH_3), 29.3 (s, –CH_2–CH_3), 114.4 (s, C_5–$(CH_3)_5$), 126.1 (s), 131.2 (s), 144.4 (s), 154.7 (s, TaC_3), 207.2 (s, TaC_3), 212.9 (TaC_3).

Treatment of 501 with diphenylacetylene. Compound **501** (0.027 g, 0.046 mmol) was charged in a J. Young NMR tube and dissolved in *ca.* 700 μL of a 3:2 mixture of toluene-d_8/1,2-difluorobenzene. To this solution, 27.5 μL of a 2.0 M solution of diphenyl acetylene in

toluene-d_8/1,2-difluorobenzene (0.055 mmol) were added using a Hamilton syringe. The NMR tube was placed overnight in a heat bath set to 40 °C. Volatiles were removed in vacuo and additional toluene-d_8/1,2-difluorobenzene mixture was added. This process was repeated twice more. There is no indication of formation of a metallacyclobutadiene, or coordination of diphenylacetylene to **501** by NMR spectroscopy. Only free, intact **501** was observed.

5.4.2.7 Chloride abstraction reactions from 507

Chloride abstraction from 507. Compound 507 (0.035 g, 0.067 mmol), Na[B(3,5–$C_6H_3(CF_3)_2)_4$] (0.150 g, 0.167 mmol) and a 3:2 solvent mixture of toluene–d_8/1,2–difluorobenzene were charged in a J. Young tube, and the contents vigorously shaken for 1 min. The ^{1}H NMR spectrum (Figure 5–24) revealed non–activated PMe_3 resonances in the region between δ 0.90 and and 1.05 ppm, and activated PMe_3 resonances in the region between −0.5 and 0.6 ppm. Signals in the region between δ 5.0 and 5.5 ppm correspond to overlapping Cp resonances that could not be assigned. The ^{31}P{^{1}H} spectrum revealed a mixture of compounds analogous to that obtained with the Cp* ligated metal system. This mixture is composed of two products of C−H bond activation of one of the PMe_3 ligands 510–1 (δ −2.57 (d) and −67.53 (d), ($^2J_{P-P}$ = 53.7 Hz)), and 510–2 (δ −6.47 (d) and −60.34 (d), ($^2J_{P-P}$ = 16.0 Hz)), a cationic trisphosphine compound 509 (δ −14.91 (d) and −30.96 ppm (t), ($^2J_{P-P}$ = 36.1 Hz)), and an unidentified compound 508 (δ 0.64 (s)).

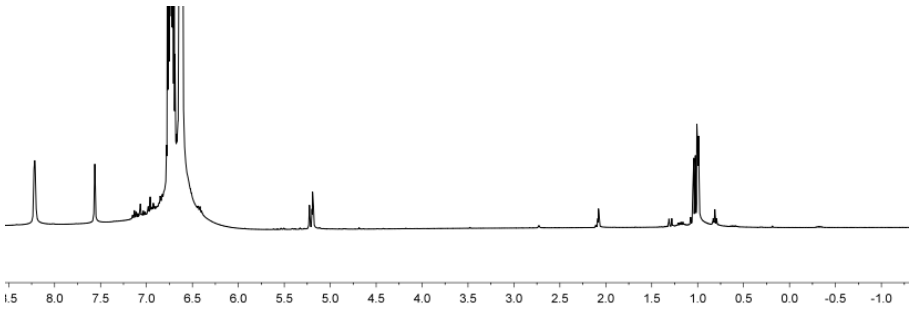

Figure 5–23. Full ^{1}H NMR spectrum (499.43 MHz) of the reaction mixture resulting after treating **507** with 2.5 equivalents of Na[B(3,5–$C_6H_3(CF_3)_2)_4$] in a 3:2 solvent mixture of toluene–d_8/1,2–difluorobenzene. *Protio* 1,2–dilfuorobenzene peak observed in the region betrween δ 6.5 and 7.0 ppm.

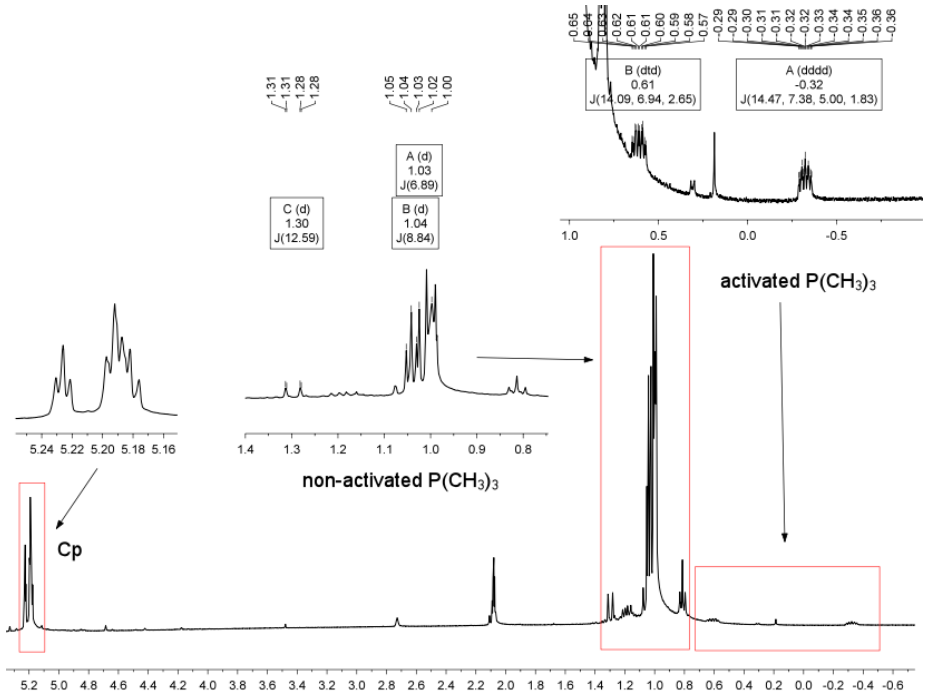

Figure 5–24. Olefinic and aliphatic regions of the ^{1}H NMR spectrum (499.43 MHz) of the reaction mixture resulting after treating **507** with 2.5 equivalents of Na[B(3,5–$C_6H_3(CF_3)_2)_4$] in a 3:2 solvent mixture of toluene–d_8/1,2–difluorobenzene.

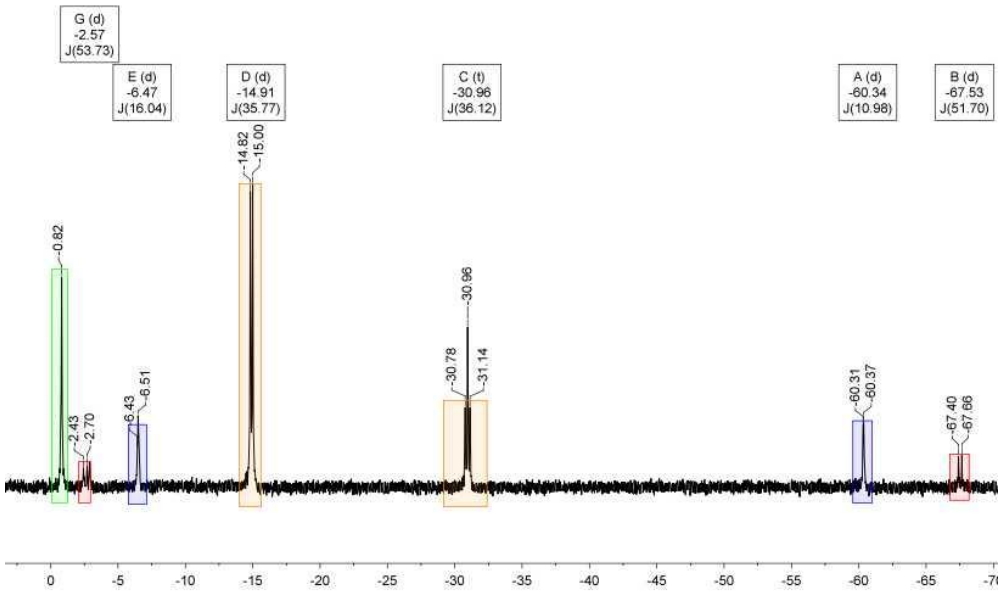

Figure 5–25. $^{31}P\{^{1}H\}$ NMR spectrum (202.27 MHz) of the reaction mixture resulting after treating **507** with 2.5 equivalents of $Na[B(3,5\text{–}C_6H_3(CF_3)_2)_4]$ in a 3:2 solvent mixture of toluene–d_8/1,2–difluorobenzene. Signals highlighted in yellow, red, blue, and green boxes correspond respectively to compounds **509** at δ −14.91 and −30.96 ppm ($^{2}J_{P\text{–}P}$ = 36.1 Hz); 510–1 at δ −2.57 and −67.53 ($^{2}J_{P\text{–}P}$ = 53.7 Hz); **510–2** at δ −6.47 and −60.34 ($^{2}J_{P\text{–}P}$ = 16.0 Hz); **508** at δ 0.64 respectively.

Trapping of 510–1 and 510–2 with PMe_3. **507** (0.032 g, 0.060 mmol), $Na[B(3,5\text{–}C_6H_3(CF_3)_2)_4]$ (0.151 g, 0.133 mmol) and 5 mL of a 3:2 solvent mixture of toluene–d_8/1,2–difluorobenzene were charged in a Schlenk flask and stirred for 30 min. PMe_3 (10.0 μL, 100.0 mmol) was then added and the contents stirred for additional 5 min. At this point, the suspension was filtered through a fine fritted funnel into another Schlenk flask and volatiles were removed *in vacuo*. The residue was dissolved in *ca.* 1.0 mL of a 3:2 solvent mixture of toluene–d_8/1,2–difluorobenzene and NMR spectra were collected. ^{1}H NMR (499.43 MHz,

toluene–d_8/1,2–difluorobenzene) δ 1.00 (filled–in–doublet, 18H, *transoid* P(*CH*$_3$)$_3$), 1.04 (d, 9H, *cisoid* P(*CH*$_3$)$_3$), 5.19 (dt, J_{H-P} = 2.2 Hz, J_{H-P} = 0.6 Hz, 5H, η^5–C_5H_5), aromatic signals obscured by the solvent. $^{31}P\{^1H\}$ NMR (161.73 MHz, toluene–d_8/1,2–difluorobenzene) δ −14.54 (d, $^2J_{P-P}$ = 36.2 Hz, *transoid* *P*(CH$_3$)$_3$), −30.65 ($^2J_{P-P}$ = 36.2 Hz, *cisoid* *P*(CH$_3$)$_3$).

5.4.3 X–ray structural determinations

X–Ray data collection, solution, and refinement for 503c. Single crystals of **503c** were grown from a reaction mixture formed by treating **501** (0.045 g, 86.3 μmol) with Na–203 (0.052 g, 86.3 μmol) in 700 μL of a 3:2 mixture of toluene–d_8/1,2–difluorobenzene. This mixture was shaken vigorously and filtered through a fiberglass filter packed in a Pasteur pipette into a clean NMR tube. The crystals were grown under slow diffusion of pentane vapors into the reaction mixture. A Leica MZ 75 microscope was used to identify a suitable orange blocks with very well defined faces with dimensions (max, intermediate, and min) 0.17 mm × 0.15 mm × 0.07 mm from a representative sample of crystals of the same habit. The crystal mounted on a nylon loop was then placed in a cold nitrogen stream (Oxford) maintained at 110 K. A BRUKER APEX2 X–ray (three–circle) diffractometer was employed for crystal screening, unit cell determination, and data collection. The goniometer was controlled using the APEX2 software suite, v2008–6.0.[98] The sample was optically centered with the aid of a video camera such that no translations were observed as the crystal was rotated through all positions. The detector was set at 6.0 cm from the crystal sample (APEX2, 512 × 512 pixel). The X–ray radiation employed was generated from a Mo sealed X–ray tube

(K_α = 0.70173Å with a potential of 40 kV and a current of 40 mA) fitted with a graphite monochromator in the parallel mode (175 mm collimator with 0.5 mm pinholes). All diffractometer manipulations, including data collection, integration and scaling were carried out using the Bruker APEXII software.[98] An absorption correction was applied using SADABS.[99] The structure was solved in the monoclinic C2/c space group using XS (incorporated in SHELXTL).[100] The solution was refined by full–matrix least squares on F^2. No additional symmetry was found using ADDSYMM incorporated into the PLATON program.[101] All non–hydrogen atoms were refined with anisotropic thermal parameters. All hydrogen atoms were placed in idealized positions and refined using a riding model. The structure was refined (weighted least squares refinement on F^2) and the final least–squares refinement converged to R_1 = 0.0221 ($I > 2\sigma(I)$, 9605 data) and wR_2 = 0.0486 (F^2, 10531 data, 489 parameters). ORTEP–II was employed for the final data presentation and structure plots.[102]

Crystallographic information in the form of a CIF file for **503c** (CCDC 943083) is available from the Cambridge Crystallographic Data Centre (www.ccdc.cam.ac.uk). Crystallographic information is summarized in Table 5–5.

Table 5–5. Crystal data and structure refinement for 503**c**.

Empirical formula	$C_{28}\,H_{47}\,B_{11}\,Cl_{11}\,P_2\,Ta$	
Formula weight	1135.40	
Temperature/K	110.15	
Crystal system	monoclinic	
Space group	C2/c	
Unit cell dimensions		
	a = 34.205(2) Å	α = 90°
	b = 8.6565(6) Å	β = 94.8310(10)°
	c = 31.071(2) Å	γ = 90°
Volume	9167.2(11) $Å^3$	
Z	8	
Density (calculated)	1.645 g cm^{-3}	
Absorption coefficient	3.133 mm^{-1}	
F(000)	4480.0	
Crystal size	0.169 × 0.154 × 0.069 mm^3	
Theta range for data collection	1.701 to 27.498°	
Index ranges	$-44 \le h \le 44$, $-11 \le k \le 11$, $-40 \le l \le 40$	
Reflections collected	48864	
Independent reflections	10531[R(int) =0.0333]	
Completeness to theta = 27.498°	100%	
Absorption correction	Semi–empirical from equivalents	
Data/restraints/parameters	10531/0/489	
Goodness–of–fit on F2	1.048	
Final R indexes [$I>2\sigma(I)$]	R_1 = 0.0221, wR_2 = 0.0472	
Final R indexes [all data]	R_1 = 0.0259, wR_2 = 0.0486	
Largest diff. peak/hole	1.08/−0.89 e $Å^{-3}$	

X–Ray data collection, solution, and refinement for 511b. (Solved by Dr. Nattamai Bhuvanesh). Single crystals of **511b** were grown under slow diffusion of pentane vapors into a solution of the compound in a 3:2 solvent mixture of toluene–d_8/1,2–difluorobenzene. A Leica MZ 75 microscope was used to identify a suitable orange block with very well defined faces with dimensions (max, intermediate, and min) 0.22 mm × 0.12 mm × 0.06 mm from a representative sample of crystals of the same habit. The crystal mounted on a nylon loop was then placed in a cold nitrogen stream (Oxford) maintained at 110 K. A BRUKER APEX2 X–ray (three–circle) diffractometer was employed for crystal screening, unit cell determination, and data collection. The goniometer was controlled using the APEX2 software suite, v2008–6.0.[98] The sample was optically centered with the aid of a video camera such that no translations were observed as the crystal was rotated through all positions. The detector was set at 6.0 cm from the crystal sample (APEX2, 512 × 512 pixel). The X–ray radiation employed was generated from a Mo sealed X–ray tube (K_α= 0.70173 Å with a potential of 40 kV and a current of 40 mA) fitted with a graphite monochromator in the parallel mode (175 mm collimator with 0.5 mm pinholes). Sixty data frames were taken at widths of 0.5°. These reflections were used in the auto–indexing procedure to determine the unit cell. A suitable cell was found and refined by nonlinear least squares and Bravais lattice procedures. The unit cell was verified by examination of the *h k l* overlays on several frames of data by comparing with both the orientation matrices. No super–cell or erroneous reflections were observed. After careful examination of the unit cell, a standard data collection procedure was initiated using omega scans. Integrated intensity information for each reflection was obtained by

reduction of the data frames with the program APEX2.[98] The integration method employed a three dimensional profiling algorithm and all data were corrected for Lorentz and polarization factors, as well as for crystal decay effects. Finally the data was merged and scaled to produce a suitable data set. The absorption correction program SADABS[99] was employed to correct the data for absorption effects. Systematic reflection conditions and statistical tests of the data suggested the space group *P*–1. A solution was obtained readily using SHELXTL (XS).[100] Hydrogen atoms were placed in idealized positions and were set riding on the respective parent atoms. All non–hydrogen atoms were refined with anisotropic thermal parameters. Absence of additional symmetry was confirmed using PLATON (ADDSYM).[101] A solvent molecule was found which suggested toluene as a possible solvent, however it was only partially occupied with disorder. Significantly short interactions between toluene (assumed) and the Ta complex did not favor toluene as solvent. Subsequently, PLATON[101] was used to SQUEEZE the solvent, which showed the presence of about 37 electrons for the solvent which, again, could not be accounted with toluene. For the final refinement the SQUEEZE'd data was used. The structure was refined (weighted least squares refinement on F^2) to convergence.[100,138] ORTEP–II was employed for the final data presentation and structure plots.[102] Crystallographic information in the form of a CIF file for **511b** (CCDC 965655) is available free of charge from the Cambridge Crystallographic Data Centre (www.ccdc.cam.ac.uk).Crystallographic information is summarized in Table 5–6.

Table 5–6. Crystal data and structure refinement for **511b**.

Empirical formula	$C_{27}\ H_{40}\ B_{11}\ Cl_{11}\ P\ Ta$	
Formula weight	1085.37	
Temperature	110(2) K	
Wavelength	0.71073 Å	
Crystal system	Triclinic	
Space group	P–1	
Unit cell dimensions	a = 9.2542(9) Å	α = 81.7560(10)°
	b = 15.4298(15) Å	β = 74.7910(10)°
	c = 17.0711(17) Å	γ = 84.2530(10)°
Volume	2322.9(4) $Å^3$	
Z	2	
Density (calculated)	1.552 g cm^{-3}	
Absorption coefficient	3.054 mm^{-1}	
F(000)	1064	
Crystal size	0.22 × 0.12 × 0.06 mm^3	
Theta range for data collection	1.71 to 27.50°.	
Index ranges	$-12 \le h \le 12, -20 \le k \le 19, -22 \le l \le 22$	
Reflections collected	25039	
Independent reflections	10429 [R(int) = 0.0328]	
Completeness to theta = 27.50°	98.0%	
Absorption correction	Semi–empirical from equivalents	
Max. and min. transmission	0.8380 and 0.5530	
Refinement method	Full–matrix least–squares on F^2	
Data / restraints / parameters	10429 / 0 / 470	
Goodness–of–fit on F^2	1.025	
Final R indices [$I > 2\sigma(I)$]	R_1 = 0.0330, wR_2 = 0.0944	
R indices (all data)	R_1 = 0.0354, wR_2 = 0.0957	
Largest diff. peak and hole	3.567 / −1.624 e.$Å^{-3}$	

CHAPTER VI

SUMMARY

A bench–top method for the synthesis of C–alkylated carborane anions of the type $[RCB_{11}Cl_{11}]^-$ (R = Me, Et, Pr, Bu, Hex) has been developed. These anions were isolated as the respective triethylammonium salts as analytically pure solids, in good yields. It has been demonstrated that salts of these C–alkylated carboranes are also capable of forming X–ray quality single crystals. As an example of this, compounds **207** and **503c** have been characterized structurally as the salts of the $[BuCB_{11}Cl_{11}]^-$ anion.

The synthesis and characterization of **302**, a zwitterionic construction with a carborane cage as the anionic component has been presented. This approach is conceptually related to the use of neutral carborane radical $MeCB_{11}Me_{11}$ as a one–electron oxidant that converts to a weakly coordinating anion upon accepting an electron. Metric parameters of **302** obtained through an X–ray structural study revealed the silylium–like nature of the cationic silicon atom, which is a result of weak coordination of one of the chlorine atoms on the *ortho* belt of the carborane cage. The metric data are similar to that of analogous, two–component silylium salts stabilized by weak coordination of halogenated carboranes. These findings were also in agreement with the observed ^{29}Si CP–MAS chemical shift of **302**, which is in the range expected for silylium–like cations stabilized by weak coordination. The retention of high electrophilic character was confirmed experimentally by the observation of chloride abstraction from $(CH_3)_3Cl$ to form $(\mathbf{CH_3})_3\mathbf{C}$**–303** at –70 °C in SO_2.

The synthesis of a family of d^6 ML_5 and d^6 ML_6 ruthenium triflate complexes of the pincer $(P_2C=)Ru(L)_n$ architecture by ligand exchange using Me_3SiOTf has been prepared, however, compounds except for **406** and **408** were not accessible through this method. We conjecture that Me_3SiOTf is not electrophilic enough to abstract chloride from **402** to form **406**, which could potentially be a result of a stronger Ru–Cl bond with respect to the other Cl–containing $(P_2C=)Ru$ compounds used. This is not unexpected, given the mutually *trans* disposition of chloride in **402**, which is a weak *trans* influence donor. The synthesis of **408** was hampered by electrophilic removal of OAc by Me_3SiOTf, in contrast to the acac–ligated **411**, where chloride substitution was achieved to yield **409**. This difference in reactivity may be attributed to the reduced stability provided by the more strained 4–member chelate ring of **412**. Triflate abstraction from **405** results in formation of a cationic species that, , seems to be stabilized by solvent coordination. **405** can also form η^6 complexes with arenes, resulting in 1,2–hydride shift across Ru=C to form an 18–electron, piano stool complex.

Finally, the competence of compound **501**, one of the very few examples of isolable terminal alkylidynes of early transition metals, as a viable alkyne metathesis catalyst was investigated. Treatment of **501** with 3–hexyne resulted in the formation of a stable, 14–electron tantalacyclobutadiene that did not show alkyne–metathesis reactivity. In addition to this, chloride abstraction from **501** was effected, in order to potentially enhance any reactivity towards alkynes. It has been demonstrated that removal of chloride from **501** results in reversible C–H bond activation of the PMe_3 ligand, and that this process is concomitant with protonation of the carbyne carbon affording two isomeric, cationic alkylidenes **503–1** and

503–2 in a relative ratio very close to 1:1. In addition, comparatively smaller amounts of the tris–phosphine adduct **502**, and an unidentified side product **504**, consistently formed in all the experiments performed. It can be speculated that formation of compound **504** could be the result of PMe_3 ligand release, which is trapped by **503–1**/ **503–2** to form of **502**. Similar chemistry is observed when chloride is abstracted from the Cp analogue **507**. Treatment of the the mixture of cationic **503–1**, **503–2** and **502** with terminal and internal alkynes resulted in the formation of very stable, 14–electron, neutral and cationic metallacyclobutadienes that did not show alkyne–metathesis reactivity.

REFERENCES

1. Pauling, L. *General Chemistry;* Dover Publications: New York, 1988; p 136.

2. (a) Hartwig, J. F. Metal–Ligand Complexes. *Organotransition Metal Chemistry: From Bonding to Catalysis;* University Science Books: Sausalito, CA, 2009; p13. (b) Crabtree, R. H. General Properties of Organometallic Complexes. *The Organometallic Chemistry of the Transition Metals*, 5th edition; Wiley: Hoboken, NJ, 2009; p 40.

3. Albright, T. A.; Burdett, J. K.; Whangbo, M. H. *Orbital Interactions in Chemistry;* Wiley: Hoboken, NJ, 1985; pp 277–394.

4. Crabtree, R. H. Oxidative Addition and Reductive Elimination. *The Organometallic Chemistry of the Transition Metals*, 5th edition; Wiley: Hoboken, NJ, 2009; p 153.

5. Hartwig, J. F. Reductive Elimination. *Organotransition Metal Chemistry: From Bonding to Catalysis;* University Science Books: Sausalito, CA, 2009; p324.

6. Hartwig, J. F. Elimination Reactions. *Organotransition Metal Chemistry: From Bonding to Catalysis;* University Science Books: Sausalito, CA, 2009; p399.

7. Karsch, H. H. *Chem. Ber.* **1977**, *110*, 2699.

8. Brookhart, M.; Green, M. L. H.; Parkin, G. *Proc. Natl. Acad. Sci. U.S.A.* **2007**, *104*, 6908.

9. Tomaszewski, R.; Hyla-Kryspin, I.; Mayne, C. L.; Arif, A. M.; Gleiter, R.; Ernst, R. D. *J. Am. Chem. Soc.* **1998**, *120*, 2959.

10. Hasegawa, M.; Segawa, Y.; Yamashita, M.; Nozaki, K. *Angew. Chem. Int. Ed.* **2012**, *51*, 6956.

11. (a) Evans, D. R.; Drovetskaya, T.; Bau, R.; Reed, C. A.; Boyd, P. D. W. *J. Am. Chem. Soc.* **1997**, *119*, 3633. (b) Bernskoetter, W. H.; Schauer, C. K.; Goldberg, K. I.; Brookhart, M. *Science* **2009**, *326*, 553. (c) Pike, S. D.; Thompson, A. L.; Algarra, A. G.; Apperley, D. C.; Macgregor, S. A.; Weller, A. S. *Science* **2012**, *337*, 1648.

12. Watson, L. A.; Ozerov, O. V.; Pink, M.; Caulton, K. G. *J. Am. Chem. Soc.* **2003**, *125*, 8426.

13. MacInnis, M. C.; McDonald, R.; Ferguson, M. J.; Tobisch, S.; Turculet, L. *J. Am. Chem. Soc.* **2011**, *133*, 13622.

14. Singh, A. K.; Levine, B. G.; Staples, R. J.; Odom, A. L. *Chem. Commun.* **2013**, *49*, 10799.

15. a) Dorta, R.; Stevens, E. D.; Nolan, S. P. *J. Am. Chem. Soc.* **2004**, *126*, 5054. b) Scott, N. M.; Dorta, R.; Stevens, E. D.; Correa, A.; Cavallo, L.; Nolan, S. P. *J. Am. Chem. Soc.* **2005**, *127*, 3516.

16. (a) Jordan, R. F.; Bajgur, C. S.; Willett, R.; Scott, B. *J. Am. Chem. Soc.* **1986**, *108*, 7410. (b) Taube, R.; Krukowka, L. *J. Organomet. Chem.* **1988**, *347*, C9. (c) Hlatky, G. G.; Turner, H. W.; Eckman, R. R. *J. Am. Chem. Soc.* **1989**, *111*, 2728.

17. Kaminsky, W.; Funck, A.; Hahnsen, H. *Dalton Trans.* **2009**, 8803.

18. Kaminsky, W.; Strübel, C. *J. Mol. Cat. A: Chem.* **1998**, *128*, 191.

19. Tritto, I.; Donetti, R.; Sacchi, M. C.; Locatelli, P.; Zannoni, G. *Macromolecules* **1997**, *30*, 1247.

20. Yang, X.; Stern, C.; Marks, T. J. *Organometallics* **1991**, *10*, 840.

21. Arndtsen, B. A.; Bergman, R. G. *Science* **1995**, *270*, 1970.

22. Douvris, C.; Reed, C. A. *Organometallics* **2008**, *27*, 807.

23. Douvris, C.; Ozerov, O. V. *Science* **2008**, *321*, 1188.

24. Yang, J.; Brookhart, M. *J. Am. Chem. Soc.* **2007**, *129*, 12656.

25. Rosenthal, M. R. *J. Chem. Ed.* **1973**, *50*, 331.

26. Wickenden, A. E.; Krause, R. A. *Inorg. Chem.* **1963**, *4*, 404.

27. Strauss, S. H. *Chem. Rev.* **1993**, *93*, 927.

28. Krossing, I.; Raabe, I. *Angew. Chem., Int. Ed.* **2004**, *43*, 2066.

29. Marks, T. J.; Seyam, A. M. *Inorg. Chem.* **1974**, *13*, 1624.

30. (a) Kubas, G. J. *J.Organomet. Chem.* **2001**, *635*, 37. (b) Heinekey, D. M.; Oldham, W. J. *Chem. Rev.***1993**, *93*, 913.

31. Brayshaw, S. K.; Sceats, E. L.; Green, J. C.; Weller, A. S. *Proc. Natl. Acad. Sci. U.S.A.* **2007**, *104*, 6921.

32. Nava, M.; Reed, C. A. *Organometallics* **2011**, *30*, 4798.

33. Ibad, M. F.; Langer, P.; Schulz, A.; Villinger, A. *J. Am. Chem. Soc.* **2011**, *133*, 21016.

34. Hoffmann, S. P.; Kato, T.; Tham, F. S.; Reed, C. A. *Chem. Commun.* **2006**, 767.

35. (a) Lehmann, M.; Schulz, A.; Villinger, A. *Angew. Chem., Int. Ed.* **2009**, *48*, 7444. (b) Schulz, A.; Thomas,J.; Villinger, A. *Chem. Commun. 2010*, **46**, 3696.

36. (a) Lambert, J. B.; Zhao, Y.; Wu, H.; Tse, W. C.; Kuhlmann, B. *J. Am. Chem. Soc.* **1999**, *121*, 5001. (b) Reed, C. A.; Xie, Z.; Bau, R.; Benesi, A. *Science* **1993**, *262*, 402. (c) Kim, K. C.; Reed, C. A.; Elliott, D. W.; Mueller, L. J.; Tham, F.; Lin, L.; Lambert, J. B. *Science* **2002**, *297*, 825.

37. (a) Bochmann, M.; Jagger, A. J.; Nicholls, J. C. *Angew. Chem. Int. Ed.* **1990**, *29*, 780. (b) Horton, A. D.; Frijns, J. H. G. *Angew. Chem. Int. Ed.* **1991**, *30*, 1152.

38. Nishida, H.; Takada, N.; Yoshimura, M. *Bull. Chem. Soc. Jpn.* **1984**, *57*, 2600.

39. Legzdins, P.; Martin, D. T. *Organometallics* **1983**, *2*, 1785.

40. Fachinetti, G.; Funaioli, T.; Zanazzi, P.F. *J. Chem. Soc., Chem. Commun.* **1988**, 1100.

41. Sacconi, L.; Mealli, C.; Gatteschi, D. *Inorg. Chem.* **1974**, *13*, 1985.

42. For examples of η^2 and η^3 coordination: (a) Solari, E.; Musso, F.; Gallo, E.; Floriani, C.; Re, N.; Chiesi-Villa, A.; Rizzoli, C. *Organometallics* **1995**, *14*, 2265. (b) Horton, A. D.; Frijns, J. H. G. *Angew. Chem. Int. Ed.* **1991**, *30*, 1152. Examples of η^6 coordination: (c) Albano, P.; Aresta, M.; Manassero, M. *Inorg. Chem.* **1980**, *19*, 1069. (d) Kruger, G. J.; du Preez, A. L.; Haines, R. J. *J. Chem. Soc., Dalton Trans.* **1974**, 1302. (e) Bochmann, M. *Angew. Chem. Int. Ed.* **1992**, *31*, 1181.

43. Chaplin, A. B.; Weller, A. S. *Eur. J. Inorg. Chem.* **2010**, *2010*, 5124.

44. Calderazzo, F.; Englert, U.; Pampaloni, G.; Rocchi, L. *Angew. Chem. Int. Ed.* **1992**, *31*, 1235.

45. Nishida, H.; Takada, N.; Yoshimura, M. *Bull. Chem. Soc. Jpn.* **1984**, *57*, 2600.

46. Geiger, W. E.; Barrière, F. *Acc. Chem. Res.* **2010**, *43*, 1030.

47. Kira, M.; Hino, T.; Sakurai, H. *J. Am. Chem. Soc.* **1992**, *114*, 6697.

48. Reed, C. A.; Fackler, N. L. P.; Kim, K. C.; Stasko, D.; Evans, D. R.; Boyd, P. D. W.; Rickard, C. E. F. *J. Am. Chem. Soc.* **1999**, *121*, 6314.

49. Kuprat, M.; Lehmann, M.; Schulz, A.; Villinger, A. *Organometallics* **2010**, *29*, 1421.

50. Reed, C. A. *Acc. Chem. Res.* **1998**, *31*, 133.

51. King, B. T.; Zharov, I.; Michl, J. *Chemical Innovation* **2001**, *31*, 23.

52. Tsang, C.-W.; Yang, Q.; Sze, E. T.-P.; Mak, T. C. W.; Chan, D. T. W.; Xie, Z. *Inorg. Chem.* **2000**, *39*, 5851.

53. Ivanov, S. V.; Rockwell, J. J.; Polyakov, O. G.; Gaudinski, C. M.; Anderson, O. P.; Solntsev K. A.; Strauss, S. H. *J. Am. Chem. Soc.* **1998**, *120*, 4224.

54. Jelínek, T.; Baldwin, P.; Scheidt, W. R.; Reed, C. A. *Inorg. Chem.* **1993**, *32*, 1982.

55. Kim, K. C.; Reed, C. A.; Elliott, D. W.; Mueller, L. J.; Tham, F.; Lin, L.; Lambert, J. B. *Science* **2002**, *297*, 825.

56. Xie, Z.; Manning, J.; Reed, R. W.; Mathur, R.; Boyd, P. D. W.; Benesi, A.; Reed, C. A. *J. Am. Chem. Soc.* **1996**, *118*, 2922.

57. Stasko, D.; Reed, C. A. *J. Am. Chem. Soc.* **2002**, *124*, 1148.

58. Kato, T.; Stoyanov, E.; Geier, J.; Grützmacher, H.; Reed, C. A. *J. Am.Chem. Soc.* **2004**, *126*, 12451.

59. Kato, T.; Reed, C. A. *Angewandte Chemie* **2004**, *116*, 2968.

60. (a) Nava, M.; Stoyanova, I. V.; Cummings, S.; Stoyanov, E. S.; Reed, C. A. *Angew. Chem. Int. Ed.* **2014**, *126*, 1149. (b) Juhasz, M.; Hoffmann, S.; Stoyanov, E. S.; Kim, K. C.; Reed C. A. *Angew. Chem. Int. Ed.* **2004**, *43*, 5352.

61. a) Barbarich, T. J.; Handy, S. T.; Miller, S. M.; Anderson, O. P.; Grieco, P. A.; Strauss, S. H. *Organometallics* **1996**, *15*, 3776. b) Krossing, I.; Reisinger, A. *Coord. Chem. Rev.* **2006**, *250*, 2721. c) Gonsior, M.; Krossing, I.; Müller, L.; Raabe, I.; Jansen, M.; van Wüllen, L. *Chem. Eur. J.* **2002**, *8*, 4475.

62. a) Van Seggen, D. M.; Hurlburt, P. K.; Noirot, M. D.; Anderson, O. P.; Strauss, S. H. *Inorg. Chem.* **1992**, *31*, 1423. b) Mercier, H. P. A.; Sanders, J. C. P.; Schrobilgen, G. J. *J. Am. Chem. Soc.* **1994**, *116*, 2921.

63. Morgan, M. M.; Marwitz, A. J. V.; Piers, W. E.; Parvez, M. *Organometallics* **2012**, *32*, 317.

64. Kira, M.; Hino, T.; Sakurai, H. *J. Am. Chem. Soc.* **1992**, *114*, 6697.

65. Reed, C. A. *Acc. Chem. Res.* **2010**, *43*, 121.

66. a) Leoni, P.; Aquilini, E.; Pasquali, M.; Marchetti, F.; Sabat, M. *J. Chem. Soc., Dalton Trans.* **1988**, 329. b) Schrock, R. R.; Sharp, P. R. *J. Am. Chem. Soc.* **1978**, *100*, 2389. c) Chien, J. C. W.; Tsai, W. M.; Rausch, M. D. *J. Am. Chem. Soc.* **1991**,*113*, 8570. d) Bodner, G. S.; Gladysz, J. A.; Nielsen, M. F.; Parker, V. D. *J. Am. Chem. Soc.* **1987**, *109*, 1757. e) Sanders, J. R. *J. Chem. Soc., Dalton Trans.* **1973**, 748.

67. Connelly, N. G.; Geiger, W. E. *Chem. Rev.* **1996**, *96*, 877.

68. a) Bochmann, M.; Dawson, D. M. *Angew. Chem. Int. Ed.* **1996**, *35*, 2226. b) Hill, G. S.; Rendina, L. M.; Puddephatt, R. J. *J. Chem. Soc., Dalton Trans.* **1996**, 1809. c) Yang, X.; Stern, C. L.; Marks, T. J. *J. Am. Chem. Soc.* **1991**, *113*, 3623.

69. Lambert, J. B.; Zhao, Y. *Angew. Chem. Int. Ed.* **1997**, *36*, 400.

70. Krossing, I.; Reisinger, A. *Coord. Chem. Rev.* **2006**, *250*, 2721.

71. Krossing, I.; Raabe, I. *Angew. Chem. Int. Ed.* **2004**, *43*, 2066.

72. Reed, C. A. *Acc. Chem. Res.* **1998**, *31*, 133.

73. Kim, K. C.; Reed, C. A.; Elliott, D. W.; Mueller, L. J.; Tham, F.; Lin, L.; Lambert, J. B. *Science* **2002**, *297*, 825.

74. Duttwyler, S.; Douvris, C.; Fackler, N. L. P.; Tham, F. S.; Reed, C. A.; Baldridge, K. K.; Siegel, J. S. *Angew. Chem. Int. Ed.* **2010**, *49*, 7519.

75. Reed, C. A. *Chem. Commun.* **2005**, 1669.

76. Kato, T.; Stoyanov, E.; Geier, J.; Grützmacher, H.; Reed, C. A. *J. Am. Chem. Soc.* **2004**, *126*, 12451.

77. Douvris, C.; Stoyanov, E. S.; Tham F. S.; Reed, C. A. *Chem.Commun.* **2007**, 1145.

78. Gu, W. X.; Haneline, M. R.; Douvris C.; Ozerov, O. V. *J. Am. Chem. Soc.* **2009**, *131*, 11203.

79. Douvris C.; Ozerov, O. V. *Science* **2008**, *321*, 1188.

80. Siegel, J. S.; Allemann, O.; Duttwyler, S.; Romanato P.; Baldridge, K. K. *Science* **2011**, *332*, 574.

81. Gu, W. X.; McCulloch, B. J.; Reibenspies J. H.; Ozerov, O. V. *Chem. Commun.* **2010**, *46*, 2820.

82. Xie, Z.; Tsang, C.–W.; Sze, E. T.–P.; Yang, Q.; Chan D. T. W.; Mak, T. C. W. *Inorg. Chem.* **1998**, *37*, 6444.

83. Xie, Z.; Tsang, C.–W.; Xue F.; Mak, T. C. W. *J. Organomet. Chem.* **1999**, *577*, 197.

84. Jelinek, T.; Baldwin, P.; Scheidt W. R.; Reed, C. A. *Inorg. Chem.* **1993**, *32*, 1982.

85. King, B. T.; Kör̈be, S.; Schreiber, P. J.; Clayton, J.; Němcová, A.; Havlas, Z.; Vyakaranam, K.; Fete, M. G.; Zharov, I.; Ceremuga J.; Michl, J. *J. Am. Chem. Soc.* **2007**, *129*, 12960.

86. Larsen, A. S.; Holbrey, J. D.; Tham F. S.; Reed, C. A. *J. Am. Chem. Soc.* **2000**, *122*, 7264.

87. Nava M. J.; Reed, C. A. *Inorg. Chem.* **2010**, *49*, 4726.

88. Ivanov, S. V.; Rockwell, J. J.; Polyakov, O. G.; Gaudinski, C. M.; Anderson, O. P.; Solntsev K. A.; Strauss, S. H. *J. Am. Chem. Soc.* **1998**, *120*, 4224.

89. Kuppers, T.; Bernhardt, E.; Eujen, R.; Willner, H.; Lehmann, C. W. *Angew. Chem. Int. Ed.* **2007**, *46*, 6346.

90. Huang, D. J.; Huffman, J. C.; Bollinger, J. C.; Eisenstein, O.; Caulton, K. G. *J. Am. Chem. Soc.* **1997**, *119*, 7398.

91. Perez, J.; Hevia, E.; Riera, V.; Miguel, D.; Kassel S.; Rheingold, A. *Inorg. Chem.* **2002**, *41*, 4673.

92. Xie, Z. W.; Jelinek, T.; Bau R.; Reed, C. A. *J. Am. Chem. Soc.* **1994**, *116*, 1907.

93. Hall Griffith E. A.; Amma, E. L. *J. Am. Chem. Soc.* **1974**, *96*, 743.

94. Xie, Z.; Wu, B. M.; Mak, T. C. W.; Manning J.; Reed, C. A. *J. Chem. Soc., Dalton Trans.* **1997**, 1213.

95. Bondi, A. *J. Phys. Chem.* **1964**, *68*, 441.

96. Hall Griffith E. A.; Amma, E. L. *J. Am. Chem. Soc.* **1974**, *96*, 743.

97. Ramírez–Contreras, R.; Ozerov, O. V. *Dalton Trans.* **2012**, *41*, 7842.

98. APEX2 "Program for Data Collection and Integration on Area Detectors" BRUKER AXS Inc., 5465 East Cheryl Parkway, Madison, WI 53711–5373 USA.

99. Sheldrick, G. M. "SADABS (version 2008/1): Program for Absorption Correction for Data from Area Detector Frames", University of Göttingen, Göttingen, Germany, 2008.

100. Sheldrick, G.M. *Acta Cryst.* **2008**, *A64*, 112.

101. (a) Spek, A. L. "PLATON, A Multipurpose Crystallographic Tool", Utrecht University, Utrecht, The Netherlands, 2006. (b) Speck, A. *J. Appl. Cryst.* **2003**, *36*, 7. (c) Spek, A. L. *Acta Cryst.* **1990**, *A46*, C34.

102. Johnson, C. K. *ORTEP-II: A FORTRAN Thermal-Ellipsoid Plot Program for Crystal Structure Illustration;* Report for Oak Ridge National Laboratory: Oak Ridge, TN, 1976.

103. Lambert, J. B.; Kania, L.; Zhang, S. *Chem. Rev.* **1995**, *95*, 1191.

104. Reed, C. A. *Acc. Chem. Res.* **1998**, *31*, 325.

105. Reed, C. A. *Acc. Chem. Res.* **2010**, *43*, 121.

106. Reed, C. A.; Xie, Z.; Bau, R.; Benesi, A. *Science* **1993**, *262*, 402.

107. Lambert, J. B.; Zhang, S. *J. Chem. Soc., Chem. Commun.* **1993**, 383.

108. Lambert, J. B.; Zhang, S.; Stern, C. L.; Huffman, J. C. *Science* **1993**, *260*, 1917.

109. Kim, K.–C.; Reed, C. A.; Elliott, D. W.; Mueller, L. J.; Tham, F.; Lin, L.; Lambert, J. B. *Science* **2002**, *297*, 825.

110. Krossing, I.; Raabe, I. *Angew. Chem. Int. Ed.* **2004**, *43*, 2066.

111. Körbe, S.; Schreiber, P. J.; Michl, J. *Chem. Rev.* **2006**, *106*, 5208.

112. Stoyanov, E. S.; Kim, K.–C.; Reed, C. A. *J. Am. Chem. Soc.* **2006**, *128*, 8500.

113. Schäfer, A.; Reißmann, M.; Schäfer, A.; Saak, W.; Haase, D.; Müller, T. *Angew. Chem. Int. Ed.* **2011**, *50*, 12636.

114. Xie, Z.; Manning, J.; Reed, R. W.; Mathur, R.; Boyd, P. D. W.; Benesi, A.; Reed, C. A. *J. Am. Chem. Soc.* **1996**, *118*, 2922.

115. Hoffmann, S. P.; Kato, T.; Tham, F. S.; Reed, C. A. *Chem. Commun.* **2006**, 767.

116. Ibad, M. F.; Langer, P.; Schulz, A.; Villinger, A. *J. Am. Chem. Soc.* **2011**, *133*, 21016.

117. Klare, H. F. T.; Oestreich, M. *Dalton Trans.* **2010**, *39*, 9176.

118. Douvris, C.; Ozerov, O. V. *Science* **2008**, *321*, 1188.

119. Allemann, O.; Duttwyler, S.; Romanato, P.; Baldridge, K. K.; Siegel, J. S. *Science* **2011**, *332*, 574.

120. Stoyanov, E. S.; Hoffmann, S. P.; Juhasz, M.; Reed, C. A. *J. Am. Chem. Soc.* **2006**, *128*, 3160.

121. Egbert, J. D.; Bullock, R. M.; Heinekey, D. M. *Organometallics* **2007**, *26*, 2291.

122. Erker, G. *Dalton Trans.* **2005**, 1883.

123. Piers, W. E.; Chivers, T. *Chem. Soc. Rev.* **1997**, *26*, 345.

124. Müller, L. O.; Himmel, D.; Stauffer, J.; Steinfeld, G.; Slattery, J.; Santiso–Quiñones, G.; Brecht, V.; Krossing, I. *Angew. Chem. Int. Ed.* **2008**, *47*, 7659.

125. Kraft, A.; Trapp, N.; Himmel, D.; Böhrer, H.; Schlüter, P.; Scherer, H.; Krossing, I. *Chem. Eur. J.* **2012**, *18*, 9371.

126. Ramírez–Contreras, R.; Bhuvanesh, N.; Zhou, J.; Ozerov, O. V. *Angew. Chem. Int. Ed.* **2013**, *52*, 10313.

127. Douvris, C.; Nagaraja, C. M.; Chen, C.–H.; Foxman, B. M.; Ozerov, O. V. *J. Am. Chem. Soc.* **2010**, 132, 4946.

128. Kim, K.-C.; Reed, C. A.; Elliott, D. W.; Mueller, L. J.; Tham, F.; Lin, L.; Lambert, J. B. *Science* **2002**, *297*, 825.

129. Küppers, T.; Bernhardt, E.; Eujen, R.; Willner, H.; Lehmann, C. W. *Angew. Chem. Int. Ed.* **2007**, *46*, 6346.

130. Kato, T.; Reed, C. A. *Angew. Chem. Int. Ed.* **2004**, *43*, 2908.

131. Scholz, F.; Himmel, D.; Scherer, H.; Krossing, I. *Chem. Eur. J.* **2013**, *19*, 109.

132. Allen, F. H.; Kennard, O.; Watson, D. G.; Brammer, L.; Orpen, A. G.; Taylor, R. In *International Tables of Crystallography*; Wilson, A. J. G., Ed.; Kluwer Academic Publishers: Dordrecht, 1992; Vol. C, pp 685.

133. Hollenstein, S.; Laube, T. *J. Am. Chem. Soc.* **1993**, *115*, 7240.

134. Zharov, I.; King, B. T.; Havlas, Z.; Pardi, A.; Michl, J. *J. Am. Chem. Soc.* **2000**, *122*, 10253.

135. Ingleson, M. J.; Mahon, M. F.; Weller, A. S. *Chem. Commun.* **2004**, 2398.

136. FRAMBO v. 4.1.05 "Program for Data Collection on Area Detectors" BRUKER–Nonius Inc., 5465 East Cheryl Parkway, Madison, WI 53711–5373 USA.

137. G. M. Sheldrick, "Cell_Now (version 2008/1): Program for Obtaining Unit Cell Constants from Single Crystal Data": University of Göttingen, Germany.

138. Dolomanov, O. V.; Bourhis, L. J.; Gildea, R. J.; Howard, J. A. K.; Puschman, H. *J. Appl. Cryst.* **2009**, *42*, 339.

139. Frisch, M. J.; Trucks, G. W.; Schlegel, H. B.; Scuseria, G. E.; Robb, M. A.; Cheeseman, J. R.; Scalmani, G.; Barone, V.; Mennucci, B.; Petersson, G. A.; Nakatsuji, H.; Caricato, M.; Li, X.; Hratchian, H. P.; Izmaylov, A. F.; Bloino, J.; Zheng, G.; Sonnenberg, J. L.; Hada, M.; Ehara, M.; Toyota, K.; Fukuda, R.; Hasegawa, J.; Ishida, M.; Nakajima, T.; Honda, Y.; Kitao, O.; Nakai, H.; Vreven, T.; Montgomery. Jr., J. A.; Peralta, J. E.; Ogliaro, F.; Bearpark, M.; Heyd, J. J.; Brothers, E.; Kudin, K. N.; Staroverov, V. N.; Kobayashi, R.; Normand, J.; Raghavachari, K.; Rendell, A.; Burant, J. C.; Iyengar, S. S.; Tomasi, J.; Cossi, M.; Rega, N.; Millam, N. J.; Klene, M.; Knox, J. E.; Cross, J. B.; Bakken, V.; Adamo, C.; Jaramillo, J.; Gomperts, R.; Stratmann, R. E.; Yazyev, O.; Austin, A. J.; Cammi, R.; Pomelli, C.; Ochterski, J. W.; Martin, R. L.; Morokuma, K.; Zakrzewski, V. G.; Voth, G. A.; Salvador, P.; Dannenberg, J. J.; Dapprich, S.; Daniels, A. D.; Farkas, Ö.; Foresman, J. B.; Ortiz, J. V.; Cioslowski, J.; Fox, D. J.; Revision B.01 ed.; Gaussian, Inc.: Wallingford, CT, 2009.

140. (a) Becke, A. D. *J. Chem. Phys.* **1993,** *98*, 5648. (b) Lee, C.; Yang, W.; Parr, R. D. *Phys. Rev. B* **1988,** *37*, 785. (c) Stephens, P. J.; Devlin, F. J.; Chabalowski, C. F.; Frisch, M. J. *J. Phys. Chem.* **1994,** *98*, 11623.

141. Seiji Iwasa, H. N. In *Acid Catalysis in Modern Organic Chemistry*; H. Yamamoto, K. I., Ed.; Wiley-VCH: Weinheim, 2008, p 859.

142. Hamashima, Y.; Hotta, D.; Umebayashi, N.; Tsuchiya, Y.; Suzuki, T.; Sodeoka, M. *Adv. Synth. Cat.* **2005**, *347*, 1576.

143. Dias, E. L.; Brookhart, M.; White, P. S. *Chem. Comm.* **2001**, 423.

144. Gutsulyak, D. V.; Nikonov, G. I. *Angew. Chem. Int. Ed.* **2010**, *49*, 7553.

145. Olson, A. S.; Seitz, W. J.; Hossain, M. M. *Tetrahedron Lett.* **1991**, *32*, 5299.

146. Kumagai, N.; Matsunaga, S.; Shibasaki, M. *J. Am. Chem. Soc.* **2004**, *126*, 13632.

147. Fan, L.; Ozerov, O. V. *Chem. Comm.* **2005**, 4450.

148. Faller, J. W.; Grimmond, B. J.; D'Alliessi, D. G. *J. Am. Chem. Soc.* **2001**, *123*, 2525.

149. Trnka, T. M.; Grubbs, R. H. *Acc. Chem. Res.* **2000**, *34*, 18. Sanford, M. S.; Ulman, M.; Grubbs, R. H. *J. Am. Chem. Soc.* **2001**, *123*, 749.

150. Love, J. A. *Nat. Chem.* **2010**, *2*, 524.

151. Beck, W.; Suenkel, K. *Chem. Rev.* **1988**, *88*, 1405.

152. van der Boom, M. E.; Milstein, D. *Chem. Rev.* **2003**, *103*, 1759.

153. Weng, W.; Parkin, S.; Ozerov, O. V. *Organometallics* **2006**, *25*, 5345.

154. Vaska, L.; DiLuzio, J.W. *J. Am. Chem. Soc.* **1961**, *83*, 2784.

155. (a) Poulton, J. T.; Hauger, B. E.; Kuhlman, R. L.; Caulton, K. G. *Inorg. Chem.* **1994**, *33*, 3325. (b) Esteruelas, M. A.; Oro, L. A.; Valero, C. *Organometallics* **1991**, *10*, 462.

156. Cheliatsidou, P.; White, D. F. S.; Slawin, A. M. Z.; Cole–Hamilton, D. J. *Dalton Trans.* **2008**, 2389.

157. Deng, H.; Yu, Z.; Dong, J.; Wu, S. *Organometallics* **2005**, *24*, 4110. Baratta, W.; Chelucci, G.; Gladiali, S.; Siega, K.; Toniutti, M.; Zanette, M.; Zangrando, E.; Rigo, P. *Angew. Chem. Int. Ed.* **2005**, *44*, 6214. Amoroso, D.; Jabri, A.; Yap, G. P. A.; Gusev, D. G.; dos Santos, E. N.; Fogg, D. E. *Organometallics* **2004**, *23*, 4047.

158. Pidcock, A. *Chem. Commun.* **1968**, 92.

159. Burling, S.; Haller, L. J. L.; Mas–Marza, E.; Moreno, A.; Macgregor, S. A.; Mahon, M. F.; Pregosin, P. S.; Whittlesey, M. K. *Chem. Eur. J.* **2009**, *15*, 10912.

160. Lee, J. H.; Caulton, K. G. *J. Organomet. Chem.* **2008**, *693*, 1664.

161. Weng, W. New designs of rigid pincer ligands (PNP and PCP) and their transition metal complexes in the context of formation of M=C (M–carbene) moiety, strong bond activation (C–H, N–C, C–Cl) and catalysis. PhD. Thesis, Brandeis University, February 2007.

162. (a) Ontko, A. C.; Houlis, J. F.; Schnabel, R. C.; Roddick, D. M.; Fong, T. P.; Lough, A. J.; Morris, R. H. *Organometallics* **1998**, *17*, 5467. (b) Hayashida, T.; Kondo, H.; Terasawa, J.–i.; Kirchner, K.; Sunada, Y.; Nagashima, H. *J. Organomet. Chem.* **2007**, *692*, 382.

163. Mahon, M. F.; Whittlesey, M. K.; Wood, P. T. *Organometallics* **1999**, *18*, 4068.

164. (a) Crabtree, R. H. Complexes of π–bound ligands. In *The Organometallic Chemistry of the Transition Metals*, 5th edition; Wiley: Hoboken, NJ, 2009; p 136. (b) Elschenbroich, C. *Organometallics*, 3rd edition; Wiley–VCH Verlag. KGaA, Weinheim, Germany, 2006; p 540.

165. Bailey, M. F.; Dahl, L. F. *Inorg. Chem.* **1965**, *4*, 1314.

166. Bennett, M. A.; Huang, T.–N.; Matheson, T. W.; Smith, A. K.; Ittel, S.; Nickerson, W. (η^6–hexamethylbenzene)ruthenium complexes. In *Inorganic Syntheses*; Fackler, J. P. Jr., Ed.; John Wiley & Sons, Inc.: Hoboken, NJ, USA, 1982; Vol. 21, p 74.

167. Burford, R. J.; Piers, W. E.; Parvez, M. *Organometallics* **2012**, *31*, 2949.

168. Hübschle, C.B.; Sheldrick, G.M. *J. Appl. Cryst.* **2011**, *44*, 1281–1284.

169. Schrock, R. R. *Chem. Rev.* **2002**, *102*, 145.

170. Fischer, H.; Hofmann, P.; Kreißl, F. R.; Schrock, R. R.; Schubert, U.; Weiss, K. *Carbyne Complexes*; Verlagsgesellschaft, Weinheim/VCH PubIishers, New York, 1988; 235 p.

171. Schrock, R. R. *J. Chem. Soc., Dalton Trans.* **2001**, 2541.

172. Fürstner, A. *Angew. Chem. Int. Ed.* **2013**, *52*, 2794.

173. Schrock, R. R.; Czekelius, C. *Adv. Synth. Catal.* **2007**, *349*, 55.

174. Schrock, R. R. *Acc. Chem. Res.* **1986**, *19*, 342.

175. Schrock, R. R. *Angew. Chem. Int. Ed.* **2006**, *45*, 3748.

176. Geyer, A. M.; Wiedner, E. S.; Gary, J. B.; Gdula, R. L.; Kuhlmann, N. C.; Johnson, M. J. A.; Dunietz, B. D.; Kampf, J. W. *J. Am. Chem. Soc.* **2008**, *130*, 8984.

177. Toreki, R.; Vaughan, G. A.; Schrock, R. R.; Davis, W. M. *J. Am. Chem. Soc.* **1993**, *115*, 127.

178. Ozerov, O. V.; Watson, L. A.; Pink, M.; Caulton, K. G. *J. Am. Chem. Soc.* 2007, 129, 6003.

179. Schrock, R. R.; Weinstock, I. A.; Horton, A. D.; Liu, A. H.; Schofield, M. H. *J. Am. Chem. Soc.* **1988**, *110*, 2686.

180. (a) Caskey, S. R.; Stewart, M. H.; Ahn, Y. J.; Johnson, M. J. A.; Rowsell, J. L. C.; Kampf, J. W. *Organometallics* **2007**, *26*, 1912. (b) Shao, M.; Zheng, L.; Qiao, W.; Wang, J.; Wang, J. *Adv. Synth. Catal.* **2012**, *354*, 2743.

181. Jia, G. *Coord. Chem. Rev.* **2007**, *251*, 2167

182. Luecke, H. F.; Bergman, R. G. *J. Am. Chem. Soc.* **1998**, *120*, 11008.

183. (a) Basuli, F.; Bailey, B. C.; Brown, D.; Tomaszewski, T.; Huffman, J. C.; Baik, M. H.; Mindiola, D. J. *J. Am. Chem. Soc.* **2004**, *126*, 10506. (b) Adhikari, D.; Basuli, F.; Orlando, J. H.; Gao, X.; Huffman, J. C.; Pink, M.; Mindiola, D. J. *Organometallics* **2009**, *28*, 4115.

184. McLain, S. J.; Wood, C. D.; Messerle, L. W.; Schrock, R. R.; Hollander, F. J.; Youngs, W. J.; Churchill, M. R. *J. Am. Chem. Soc.* **1978**, *100*, 5962.

185. (a) Protasiewicz, J. D.; Lippard, S. J. *J. Am. Chem. Soc.* **1991**, *113*, 6564. (b) Protasiewicz, J. D.; Bronk, B. S.; Masschelein, A.; Lippard, S. J. *Organometallics* **1994**, *13*, 1300. (c) Vrtis, R. N.; Rao, C. P.; Warner, S.; Lippard, S. J. *J. Am. Chem. Soc.* **1988**, *110*, 2669. (d) Vrtis, R. N.; Liu, S.; Rao, C. P.; Bott, S. G.; Lippard, S. J. *Organometallics* **1991**, *10*, 275.

186. Li, X.; Sun. H.; Harms, K.; Sundermeyer, J. *Organometallics* **2005**, *24*, 4699.

187. (a) Nazhen Liu, N.; Zhu, G.; Sun, H.; Li, X. *Inorg. Chem. Commun.* **2013**, *27*, 36. (b) Li, X.; Wang, A.; Wang, L.; Sun, H.; Harms, K.; Sundermeyer, J. *Organometallics* **2007**, *26*, 1411.

188. (a) Gambarotta, S.; Edema, J. J. H.; Minhas, R. K. *J. Chem Soc., Chem. Commun.* **1993**, 1503. (b) Shaver, M. P.; Johnson, S. A.; Fryzuk, M. D. *Can. J. Chem.* **2005**, *83*, 652.

189. (a) Riley, P. N.; Profilet,R. D.; Fanwick, P. E.; Rothwell, I. P. *Organometallics* **1996**, *15*, 5502. (c) Riley, P. N.; Thorn, M. G.; Vilardo, J. S.; Lockwood, M. A.; Fanwick, P. E.; Rothwell, I. P. *Organometallics* **1999**, *18*, 3016. (d) Fanwick, P. E.; Ogilvy, A. E.; Rothwell, I. P. *Organometallics* **1987**, *6*, 73.

190. Guggenberger, L. J.; Schrock, R. R. *J. Am. Chem. Soc.* **1975**, *97*, 2935.

191. (a) Rietveld, M. H. P.; Lohner, P.; Nijkamp, M. G.; Grove, D. M.; Veldman, N.; Spek, A. L.; Pfeffer, M.; van Koten, G. *Chem. Eur. J.* **1997**, *3*, 817. (b) Abbenhuis, H. C. L.; Feiken, N.; Henk F. Haarman, H. F.; Grove, D. M.; Horn, E.; Spek, A. L.; Pfeffer, M.; van Koten, G. *Organometallics* **1993**, *12*, 2227.

192. Suresh, C.; Frenking, G. *Organometallics* **2012**, *31*, 7171.

193. van der Heijden, H.; Gal, A. W. Pasman, P. *Organometallics* **1985**, *4,* 1847.

194. (a) DeMott, J. C.; Bhuvanesh, N.; Ozerov, O. V. *Chem. Sci*. **2013**, *4*, 642. (b) Douvris, C.; Nagaraja, C. M.; Chen, C.–H.; Foxman, B. M.; Ozerov, O. V. *J. Am. Chem. Soc*. **2010**, *132*, 4946.

195. Yakelis, N. A.; Bergman, R. G. *Organometallics* **2005**, *24*, 3579.

196. Gibson, V. C.; Graimann, C. E.; Hare, P. M.; Green, M. L. H.; Bandy, J. A.; Grebenik, P. D.; Prout, K. *J. Chem. Soc., Dalton Trans.* **1985**, 2025.

197. Schultz, A. J.; Brown, R. K.; Williams, J. M.; Schrock, R. R. *J. Am. Chem. Soc.* **1981**, *103*, 169.

198. (a) Schafer, D. F.; Wolczanski, P. T.; Lobkovsky, E. B. *Organometallics* **2011**, *30*, 6518. (b) Schafer, D. F.; Wolczanski, P. T.; Lobkovsky, E. B. *Organometallics* **2011**, *30*, 6539. (c) Cundari, T. R.; Klinckman, T. R.; Wolczanski, P. T. *J. Am. Chem. Soc.* **2002**, *124*, 1481. (d) Schaller, C. P.; Cummins, C. C.; Wolczanski, P. T. *J. Am. Chem. Soc.* **1996**, *118*, 591. (e) Schaller, C. P.; Wolczanski, P. T. *Inorg. Chem.* **1993**, *32*, 131. (f) Baillie, R. A.; Legzdins, P. *Acc. Chem. Res.* **2013**, *47*, 330. (g) Lefèvre, G. P.; Baillie, R. A.; Fabulyak, D.; Legzdins, P. *Organometallics* **2013**, *32*, 5561.

199. Bailey, B. C.; Fan, H.; Huffman, J. C.; Baik, M.–H.; Mindiola, D. J. *J. Am. Chem. Soc.* **2007**, *129*, 8781.

200. Churchill, M. R.; Hollander, F. J. *Inorg. Chem.* **1978**, *17*, 1957.

201. Bartell, L. S.; Bonham, R. A. *J. Chem. Phys.* **1957**, *27*, 1414.

202. Hansen, G. E.; Dennison, D. M. *J. Chem. Phys.* **1952**, *20*, 313.

203. Freudenberger, J. H.; Schrock, R. R. *Organometallics* **1986**, *5*, 1411.

204. Edwards, D. S.; Schrock, R. R. *J. Am. Chem. Soc.* **1982**, *104*, 6808.

205. McLain, S. J.; Wood, C. D.; Messerle, L. W.; Schrock, R. R.; Hollander, F. J.; Youngs, W. J.; Churchill, M. R. *J. Am. Chem. Soc.* **1978**, *100*, 5962.

206. (a) Messerle, L. W.; Jennische, P.; Schrock, R. R.; Stucky, G. *J. Am. Chem. Soc.* **1980**, *102*, 6744. (b) Schrock, R. R. *J. Organomet. Chem.* **1976**, *122*, 209.

APPENDIX A

SYNTHESIS OF *N*–(2–((2–(DIISOPROPYLPHOSPHINO–4–METHYLPHENYL)AMINO)–5–METHYLBENZYL)–2,4,6–TRIMETHYLANILINE PROTO LIGAND (PNN)

A.1 Experimental details

A.1.1 General considerations

All operations were performed in a dry box filled with argon, or using Schlenk techniques unless otherwise indicated. 4–4'–Dimethyldiphenylamine, diisopropyl chlorophosphine, *n*–butyllithium solution in hexanes, lithium aluminum, hydride, acetic acid, and N–bromosuccinimide were purchased from commercial sources. Mesitylamine and dimethylformamide were purchased from commercial sources, dried over CaH_2 and distilled under argon prior to use. Hydrocarbon and ether solvents were dried over and distilled from Na/K/Ph_2CO/18–crown–6. Halogenated solvents were dried over, and vacuum transferred or distilled from calcium hydride for 48 h. and then. Solution NMR spectra were collected on Varian Inova 400 (^{1}H NMR, 399.52 MHz; ^{13}C NMR, 100.46 MHz; ^{31}P NMR, 161.73 MHz; ^{11}B NMR, 128.18 MHz) and Varian Inova 500 (^{1}H NMR, 499.43 MHz; ^{13}C NMR, 125.58 MHz; ^{31}P NMR, 202.27 MHz; ^{19}F NMR, 470.17 MHz), using deuterated solvents as indicated. ^{1}H NMR spectra were referenced to residual solvent peaks ^{31}P NMR spectra were referenced to δ 0.0 ppm using H_3PO_4. Elemental analyses were performed by CALI Labs, Inc. (Parsippany, NJ, USA).

A.1.2 Synthetic procedures and characterization data

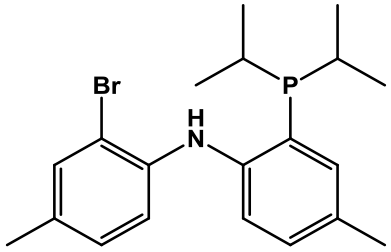

A01

Synthesis of A01. (Prepared according to literature procedures)[1] Bis(2–bromo–4–methylphenyl)amine (8.0 g, 22.5 mmol) and 70 mL of diethyl ether were charged in a 250 mL three–neck flask and equipped with a PTFE–lined stir bar. A hose adaptor equipped with a glass stopcock and two addition funnels were assembled on top of the flask. One of the addition funnels was charged with 10 mL of diethyl ether and a 2.5 M solution of *n*–butyllithium in hexanes (18.0 mL, 45.1 mmol). The other addition funnel was charged with 10 mL of diethyl ether and diisopropyl chlorophosphine (3.6 mL, 22.5 mmol). The flask was placed in a cold bath and cooled to −40 °C. The *n*–butyllithium solution was added dropwise over a period of 30 min. The reaction mixture turns yellow over the course of the addition. Once addition was complete, the mixture was allowed to warm up to room temperature over 1 h, obtaining a yellow solution with a white precipitate. Once this temperature was reached, the reaction mixture was stirred for further 15 min. The reaction mixture was cooled down to

1. Herbert, D. E.; Ozerov, O. V. *Organometallics* **2011**, *30*, 6641.

0 °C, then diisopropyl chlorophosphine was added dropwise over 10 min. Once the addition was complete, the flask was removed from the cooling bath, and slowly the yellow suspension turned into a deep orange suspension. The two addition funnels were replaced with glass stoppers and the contents were stirred overnight at room temperature. The next day, the mixture was quenched with 10 mL of a 1:1 mixture of ethanol/water and this mixture was stirred for 1 h. The orange suspension turns into a yellow solution. Volatiles are removed *in vacuo* to obtain a clear yellow solid residue that was extracted with pentane and filtered through Celite. The faint green mother liquor was concentrated *in vacuo* and placed in a freezer at −30 °C to obtain copious precipitation of a white, free flowing powdery solid. Yield: 5.8 g (66%) ^{1}H NMR (499.43 MHz, CD_2Cl_2) (Figure A–1) δ 0.95 (dd, 6H, $^{3}J_{P-H}$ = 11.9 Hz, $^{3}J_{H-H}$ = 6.9 Hz, PCH(CH_3)$_2$), 1.11 (dd, 6H, $^{3}J_{P-H}$ = 15.6 Hz, $^{3}J_{H-H}$ = 7.0 Hz, PCH(CH_3)$_2$), 2.14 (hd, 2H, $^{3}J_{H-H}$ = 7.0 Hz, $^{3}J_{P-H}$ = 2.1 Hz, P*C*H(CH_3)$_2$), 2.27 (S, 3H, *p*–toluidine backbone *para* −CH_3), 2.27 (s, 3H, *p*–toluidine backbone *para* −CH_3), 6.98 (d, 1H, J_{H-H} = 8.2 Hz, aromatic –CH), 7.09 (d, 1H, J_{H-H} = 8.2 Hz, aromatic –CH) 7.11–1.17 (overlapping signals, 3H, aromatic –CH), 7.20 (dq, J_{H-H} = 1.5 Hz, J_{H-H} = 0.7 Hz, aromatic –CH), 7.38 (s, 1H, NH). ^{31}P{^{1}H} NMR (202.27 MHz, CD_2Cl_2) δ −11.2 (*P*CH(CH_3)$_2$).

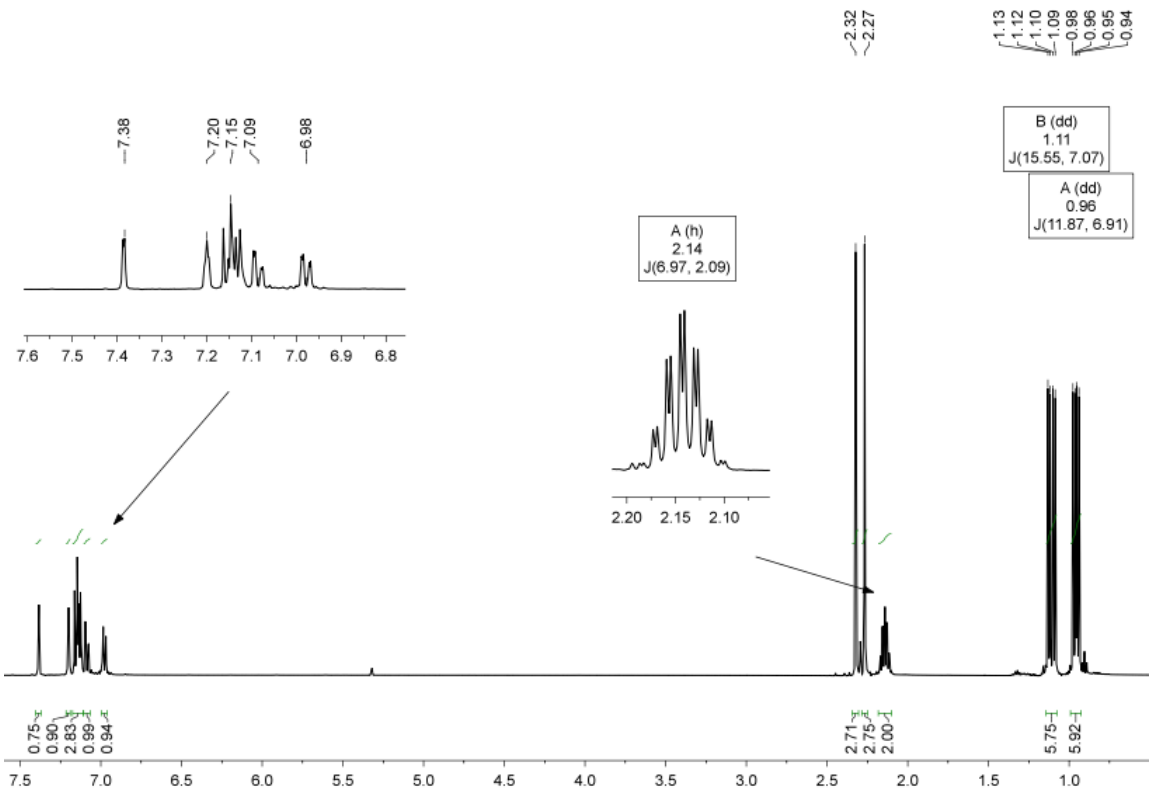

Figure A–1. ^{1}H NMR (499.43 MHz, CD_2Cl_2) of **A01**.

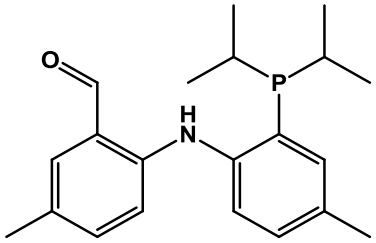

A02

Large scale synthesis of A02. (Modified from literature procedures)[1] **A01** (8.00 g, 20.3 mmol) was charged in a Schlenk flask equipped with a PTFE coated stir bar and 120 mL of

dry diethyl ether were added. On top of the flask, an addition funnel was assembled and charged with 10 mL of pentane and a 2.5 M solution of *n*–butyllithium in hexanes (18.0 mL, 45.1 mmol). The flask was connected to a Schlenk line and kept under a positive pressure of argon for the whole procedure, it was then placed in an acetone/dry ice cooling bath set to −35 °C. It was observed that some of the starting material precipitates out of solution. Following this, *n*–butyllithium was added to the solution drop wise over 15 min. Once the addition was complete, the flask was removed from the cooling bath and the reaction mixture was stirred at room temperature for 1.5 h, at the end of which period an intensely yellow colored solution was obtained. At this point the addition funnel was removed and replaced with a rubber septum, and the flask was placed once again in an acetone/dry ice bath set to −35 °C. Next, dimethylformamide (8.0 mL, 101.5 mmol) was added drop wise via syringe over 5 min to obtain a clear yellow suspension almost immediately. Once the addition was completed, the flask was removed from the cooling bath, the rubber septum replaced with a glass stopper and the reaction was stirred overnight at room temperature. The next morning the suspension had developed an intense neon orange color. The target product is air stable and the following procedures were carried out without the presence of an argon atmosphere. The reaction mixture was quenched with 20 mL of a 1:1 methanol/water mixture, turning into a clear yellow solution immediately. This mixture was stirred for 10 min and then volatiles were removed to dryness *in vacuo* to obtain a bright yellow solid. This solid was resuspended in *ca.* 20 mL of hexanes and recovered by filtration through a fine–fritted funnel. The compound contains a small amount (*ca.* 6%) of an impurity that was not

identified, and was used without further purification for the following steps. If additional purification is required, flash chromatography can be performed using neat ethyl acetated as the eluent. Yield: 5.6 g (75%) ^{1}H NMR (499.43 MHz, CD_2Cl_2) (Figure A–2 through A–4) δ 0.92 (dd, 6H, $^{3}J_{P-H}$ = 11.6 Hz, $^{3}J_{H-H}$ = 6.9 Hz, PCH(CH_3)$_2$), 1.06 (dd, 6H, $^{3}J_{P-H}$ = 15.1 Hz, $^{3}J_{P-H}$ = 7.0 Hz, PCH(CH_3)$_2$), 2.14 (hd, 2H, $^{3}J_{P-H}$ = 6.9 Hz, $^{3}J_{P-H}$ = 1.1 Hz, PC*H*(CH_3)$_2$), 2.28 (s, 3H, *p*–toluidine backbone *para* –CH_3), 2.36 (s, 3H, *p*–toluidine backbone *para* –CH_3), 6.97 (d, 1H, *J* = 8.6 Hz, aromatic –CH), 7.14 (ddd, 2H, *J* = 8.2, 5.8, 2.2 Hz, aromatic –CH), 7.26 (t, 1H, J = 2.1 Hz, aromatic –CH), 7.30 (dd, 1H, *J* = 8.1, 4.1 Hz, aromatic –CH), 7.35 (d, 1H, *J* = 1.8 Hz, aromatic –CH), 9.87 (s, 1H, –CHO), 10.00 (bs, 1H, NH). ^{31}P{^{1}H} NMR (202.27 MHz, CD_2Cl_2) δ –8.1 (*P*CH(CH_3)$_2$).

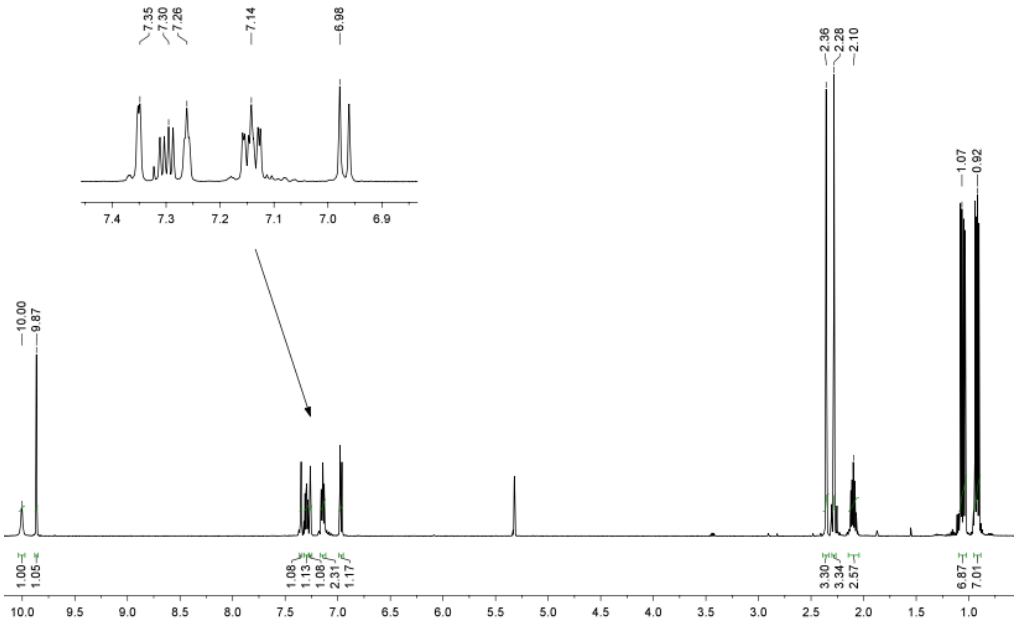

Figure A–2. ^{1}H NMR (499.43 MHz, CD_2Cl_2) of **A02** without purification by flash chromatography.

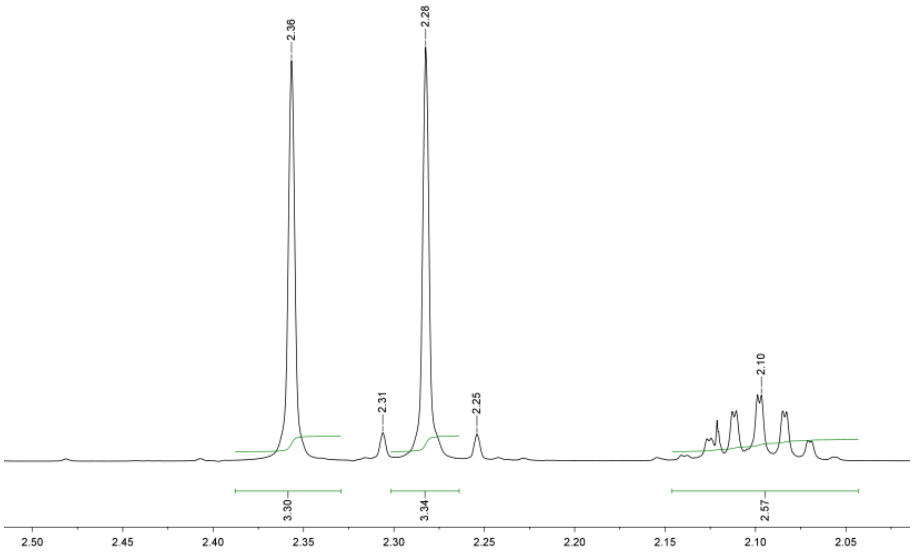

Figure A–3. ^{1}H NMR (499.43 MHz, CD_2Cl_2) of **A02** without purification by flash chromatography. Close up of the aliphatic region showing the presence of *ca.* 6% of an impurity that was not identified at δ 2.25 and 2.31 ppm.

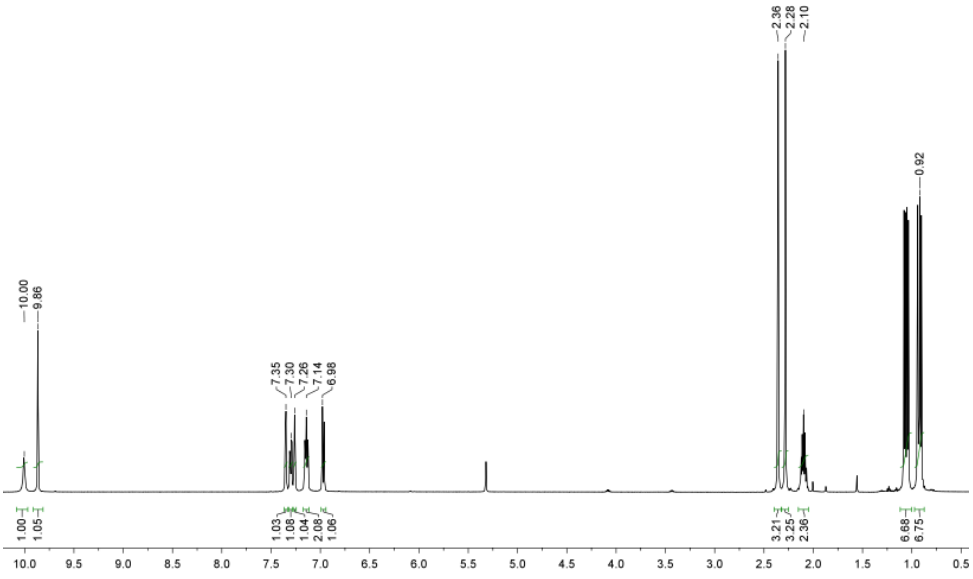

Figure A–4. ^{1}H NMR (499.43 MHz, CD_2Cl_2) of **A02** after purification by flash chromatography. Peak at δ 1.5 ppm corresponds to residual water present in the solvent.

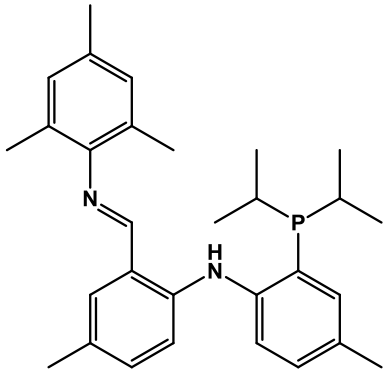

A03

Synthesis of A03. A02 (3.50 g, 10.3 mmol) used without further purification, mesitylamine (1.95 g, 14.4 mmol), acetic acid (0.062g, 1.03 mmol) and 100 mL of dry benzene were charged in a Schlenk flask equipped with a PTFE coated stir bar, and a Dean–Stark azeotropic distillation apparatus was assembled on top. This mixture was placed in an oil bath and heated to reflux temperature for 7 d with a constant flow of argon at the top of the condenser. Volatiles were removed *in vacuo*, the residue was dissolved in approximately 80 mL of pentane and filtered through a short path of silica gel to obtain a yellow solution that was concentrated *in vacuo* until a thick syrup was obtained. This concentrate was placed overnight in a freezer set to −30 °C to obtain a yellow solid that was pure by NMR. Yield: 2.4 g (51%) ^{1}H NMR (499.43 MHz, C_6D_6) (Figure A–5) δ 0.88 (dd, 6H, $^{3}J_{P-H}$ = 11.6 Hz, $^{3}J_{H-H}$ = 6.9 Hz, PCH(C*H*$_3$)$_2$), 1.04 (dd, 6H, $^{3}J_{P-H}$ = 14.8 Hz, $^{3}J_{P-H}$ = 7.0 Hz, PCH(C*H*$_3$)$_2$), 1.99 (hd, 2H, $^{3}J_{P-H}$ = 7.0 Hz, $^{3}J_{P-H}$ = 1.8 Hz, PC*H*(CH$_3$)$_2$), 2.10 (s, 3H, *p*–toluidine backbone *para* −CH$_3$), 2.16 (s, 3H, mesityl *para* −CH$_3$), 2.19 (s, 3H, *p*–toluidine backbone *para* −CH$_3$), 2.28 (s, 6H, mesityl *ortho* −CH$_3$), 6.85 (s, 2H, mesityl *meta* −CH), 6.87 (m, 1H, aromatic −CH), 6.90 (m, 1H, aromatic −CH), 7.28 (t, 1H, *J* = 2.8 Hz, aromatic −CH), 7.31 (d, 1H, *J* = 8.3 Hz, aromatic

−CH), 7.49 (dd, 1H, *J* = 8.2, 3.9 Hz, aromatic −CH), 8.08 (s, 1H, C*H*=NMes), 11.33 (s, 1H, NH). $^{31}P\{^{1}H\}$ NMR (202.27 MHz, C_6D_6) δ −5.8 (*P*CH(CH_3)$_2$).

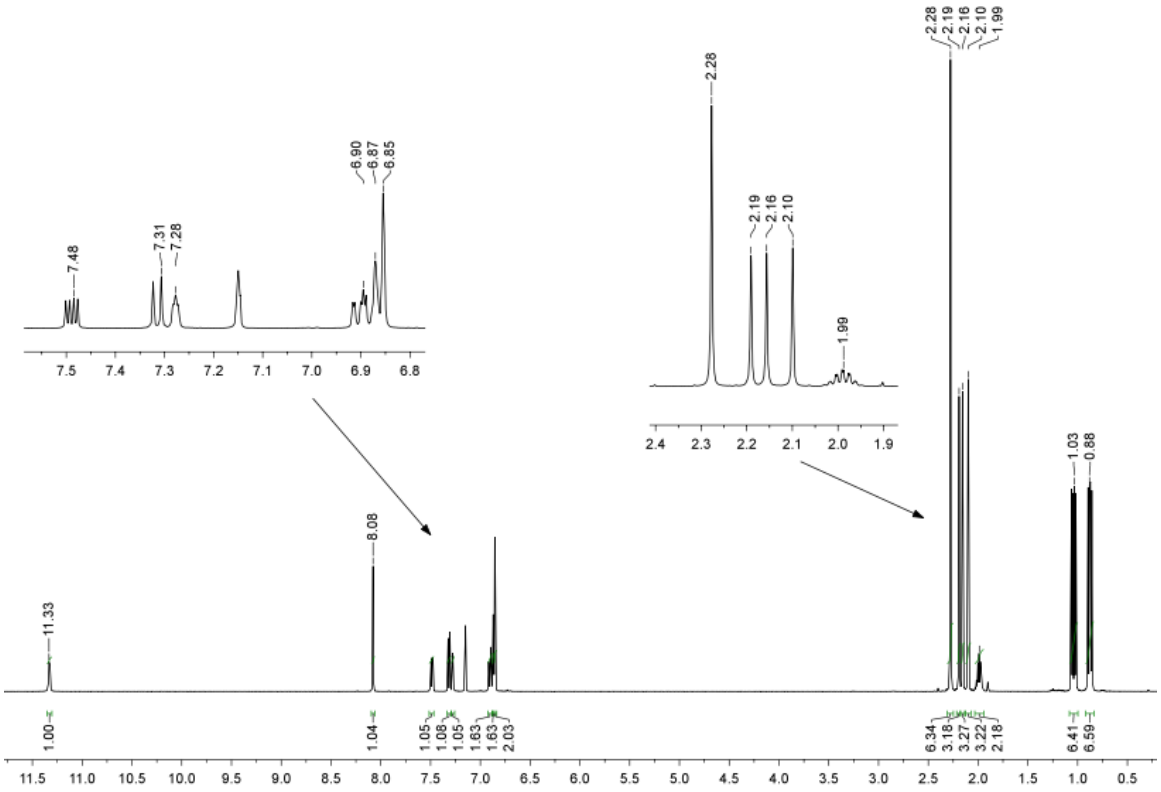

Figure A–5. ^{1}H NMR spectrum (499.43 MHz, C_6D_6) of **A03**.

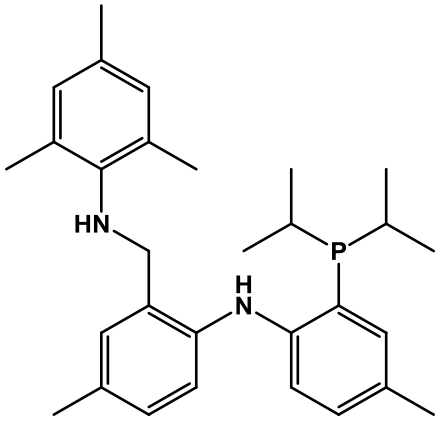

PNN

Synthesis of PNN. A03 (0.2 g, 0.436 mol), lithium aluminum hydride (0.017 g, 0.436 mol) and 10 mL of dry toluene were charged in a culture tube equipped with a PTFE–coated stir bar. The cap was screwed tightly and sealed to the tube on the outside with a layer of PTFE tape and one layer of electrical tape. The sealed culture tube was placed in an oil bath and heated overnight to reflux temperature with vigorous stirring. Within 1 h the yellow color of the suspension had turned into an intense neon orange color. The next morning it was observed that the suspension had turned white. The following operations were carried out without protection of an argon atmosphere. The cap was removed and reaction was quenched with 1 mL of a 1.74 M solution of water in THF. The resulting suspension was filtered through a short path of silica gel and the filtrate dried *in vacuo* to obtain a white solid. The product was dissolved in the minimum amount of hexanes and the solution placed overnight in a freezer set to −30 °C to obtain a white, crystalline solid that was pure by NMR. Yield ^{1}H NMR (499.43 MHz, C_6D_6) (Figure A–6) δ 0.97 (dd, 6H, $^{3}J_{P-H}$ = 11.6 Hz, $^{3}J_{H-H}$ = 6.9 Hz, PCH(C*H*$_3$)$_2$), 1.06 (dd, 6H, $^{3}J_{P-H}$ = 15.3 Hz, $^{3}J_{P-H}$ = 7.0 Hz, PCH(C*j*H$_3$)$_2$), 1.95 (hd, 2H, $^{3}J_{P-H}$ =

7.0 Hz, $^{3}J_{P-H}$ = 1.8 Hz, PC*H*$(CH_3)_2$), 2.14 (s, 3H, *p*–toluidine backbone *para* –CH_3), 2.15 (s, 3H, mesityl *para* –CH_3), 2.20 (s, 3H, *p*–toluidine backbone *para* –CH_3), 2.24 (s, 6H, mesityl *ortho* –CH_3), 3.07 (t, 1H, $^{3}J_{H-H}$ = 6.7 Hz, benzylic NH), 4.06 (d, 2H, $^{3}J_{H-H}$ = 6.7 Hz, N–CH_2–Ar), 6.76 (s, 2H, mesityl *meta* –CH), 6.92 (ddd, 2H, *J* = 6.9, 6.1, 1.8 Hz, aromatic –CH), 7.05 (d, 1H, *J* = 1.5 Hz, aromatic –CH), 7.19 (t, 1H, *J* = 2.3 Hz, aromatic –CH), 7.28 (dd, 1H, *J* = 8.3, 4.7 Hz, aromatic –CH), 7.38 (d, 1H, *J* = 8.1, aromatic –CH), 8.16 (d, 1H, *J* = 9.5 Hz, aromatic NH). $^{31}P\{^{1}H\}$ NMR (202.27 MHz, C_6D_6) δ –14.5 (*P*CH$(CH_3)_2$). $^{13}C\{^{1}H\}$ NMR (126 MHz, C_6D_6) δ 148.51, 148.35, 144.09, 141.85, 133.69, 131.95, 131.47, 131.00, 130.86, 130.51, 129.91, 129.32, 128.90, 128.06, 122.55, 122.42, 118.94, 118.38, 51.81, 23.32, 20.97, 20.85, 20.82, 20.46, 20.31, 19.06, 18.99.

Elemental analysis. Calculated for $C_{30}H_{41}N_2P$: C, 78.22%; H, 8.97%. Found: C, 78.21%; H, 8.98%.

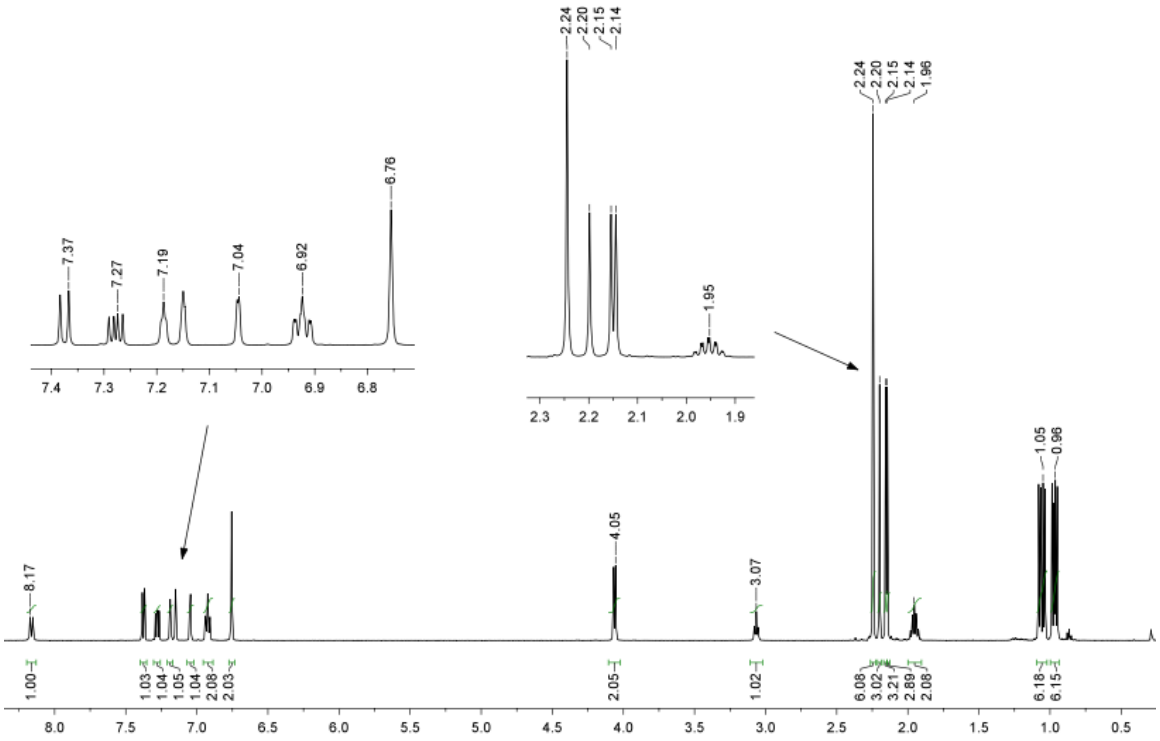

Figure A–6. ^{1}H NMR spectrum (499.43 MHz, C_6D_6) of **PNN**.